Functional perspectives on the evolution of argasid tick salivary gland protein superfamilies

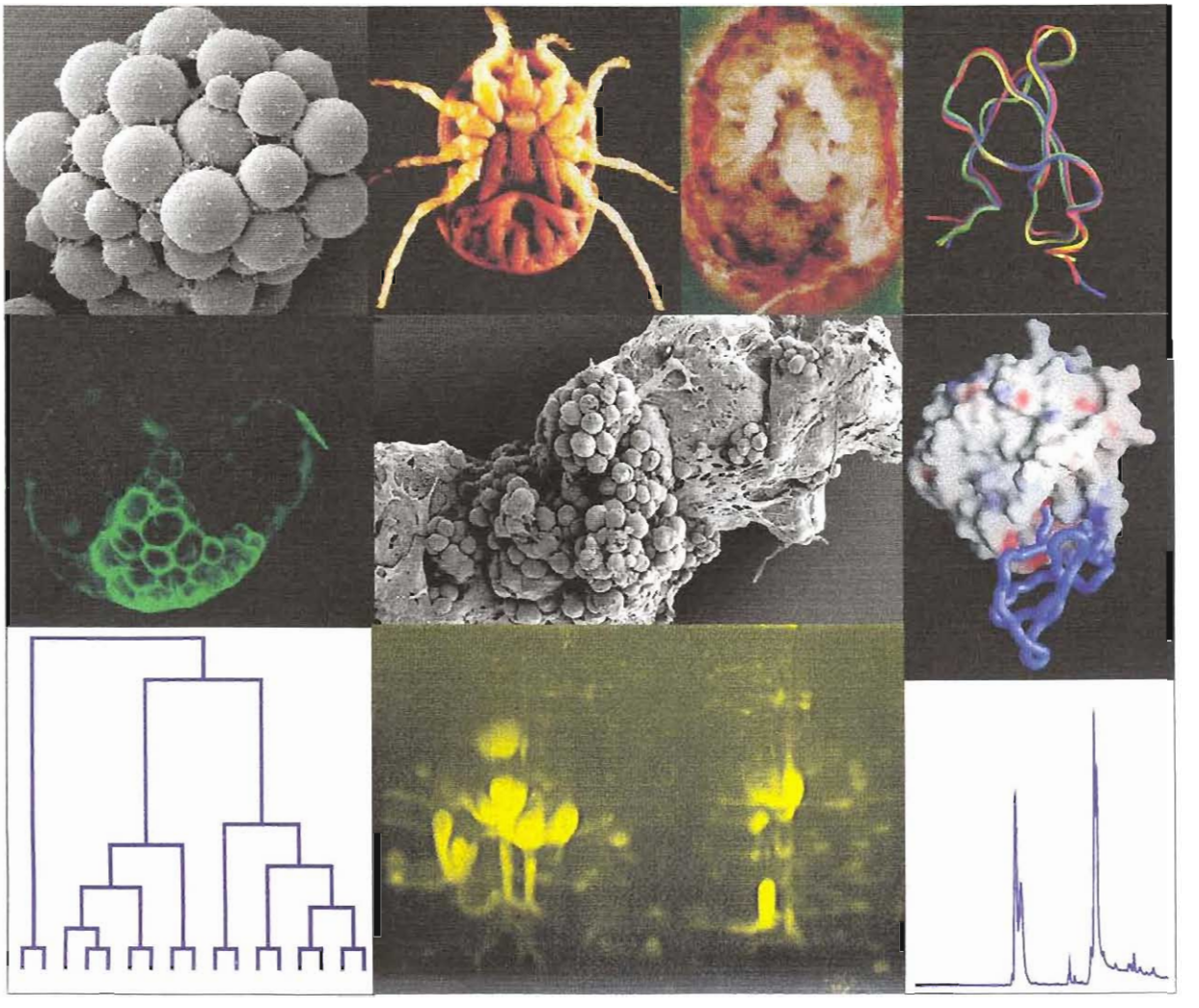

Functional perspectives on the evolution of argasid tick salivary gland protein superfamilies

by

Barend Johannes Mans

Submitted in fulfillment of the degree

Philosophiae Doctor

Department of Biochemistry

Faculty of Natural and Agricultural Sciences

University of Pretoria

June 2002

CONTENTS

List of Figures

List of Tables

Abbreviations

AA	arachidonic acid
ADP	adenosine diphosphate
ADS	antibody dilution solution
AEHPLC	anion exchange HPLC
ATP	adenosine triphosphate
BAPNA	N-α-benzoyl-L-arginine-4-nitranilide
BLAST	basic local alignment search tool
BMTI	*Boophilus microplus* trypsin inhibitor
BPTI	bovine/basic pancreatic trypsin inhibitor
BSA	bovine serum albumin
CEC	cation exchange chromatography
CI	collagen specific inhibitor
COX	cyclo oxygenase
CTI	C-terminal domain of the soft tick thrombin inhibitors
DAG	diacyl glycerol
DAB	3,3' diaminobenzidine
DMEM	Dulbecco's modified Eagle's medium
DMSO	dimethyl sulfoxide
DTT	dithiothreitol
DEPC	diethyl pyrocarbonate
EDTA	ethylene diamine tetra-acetic acid
EGTA	ethylene-bis(oxyethylene nitrilo) tetra-acetic acid
ELISA	enzyme linked immunosorbent assay
ER	endoplasmic reticulum
ESMS	electrospray mass spectrometry
FAP	focal adhesion point
FCS	fetal calf serum
FXaI	fXa inhibitors
GdCl	guanidinium chloride
GSP	gene specific primer
HIHPLC	hydrophobic interaction HPLC
HPLC	high performance liquid chromatography
IP_3	inositol triphosphate
IPTG	isopropyl β-D-thiogalactopyranoside
ISG	immature secretory granule

MALDI-TOF-MS	matrix assisted laser desorption ionization time of flight mass spectrometry
MOPS	3-(N-morpholino)propane sulphonic acid
MSA	methanesulfonic acid
NJ	neighbor joining
4-NPGB	p-nitrophenyl-p'-guanidinobenzoate
NTI	N-terminal domain of the soft tick thrombin inhibitors
OrnGD	Ornatin-glycine-aspartic acid
PAF	platelet activating factor
PAGE	poly-acrylamide gel electrophoresis
PAI	platelet aggregation inhibitors
PBS	phosphate buffered saline
PDB	protein databank
PG	prostaglandin
PGD_2	prostaglandin D2
PGI_2	prostglandin I2
PKC	protein kinase C
PLC	phospholipase C
RGD	arginine-glycine-aspartic acid
RMSD	root mean square deviation
RNAse	ribonucleic acid hydrolase
RPHPLC	reversed phase HPLC
SCR	structural conserved region
SCOP	structural classification of proteins
SD	standard deviation
SDS	sodium dodecyl sulphate
SEHPLC	size exclusion HPLC
SEM	scanning electron microscopy
SGE	salivary gland extract
SGS	salivary gland secretion
TAE	Tris-acetate-EDTA
TAI	tick adhesion inhibitor
TCH	thiocarbohydrazide
TEM	transmission electron microscopy
TEMED	N,N,N',N'-tetramethyl-ethylenediamine
TFPI	tissue factor pathway inhibitor

TGN	trans-Golg
TRAP	thrombin receptor activating peptide
Tris	tris(hydroxymethyl) aminomethane
Tricine	N-[Tris(hydroymethyl) methyl] glycine
TSGP	tick salivary gland proteins
TXA_2	thromboxane A2
4-VP	4-vinyl pyridine
vWf	von Willebrandt's factor
UPGMA	unweighted pair group method with arithmetic mean
UTR	untranslated region
X-gal	5-bromo-4-chloro-3-indolyl β-D-galacto-pyranoside

Professor Albert Neitz, who started tick research in this department. Without the research that he has done himself or has supervised over several decades, this thesis would not have been possible. Thank you for your never-ending support, the encouragement and freedom you gave me to pursue whatever avenue I thought worthwhile. For this I will be forever, grateful.

Professor Abraham Louw, you were always there to talk to about research and life. Your criticism and ideas improved the quality of my research.

Professor Lewis Coons, who took a complete stranger into his house and showed me the true spirit of America. Your insight into tick biology was truly a revelation and a fountain for the growth of new ideas. The use of your EM equipment and confocal microscope was truly appreciated.

Prof. Wolf Brandt, for the use of his N-terminal sequencing equipment and MALDI-TOF-MS.

Prof. Chris Steinmann, for his assistance with electro-cardiology and heart perfusion experiments. Thank you for the keen interest you took in our project.

Dr. Marthinus van der Merwe from the electrospray mass spectrometry unit at the University of Stellenbosch who performed the ESMS analysis.

Dr. Fourie Joubert, who introduced me to bio-informatical methods.

Mr. Nic Taljaard who performed many, many amino acid analyses during the course of this study, without ever complaining. Without your help, this study would have been much more difficult.

Mrs. Sandra van Wyngaardt who have always listened to me and assisted in numerous experiments over the years.

Mr. Jacobus Venter, my friend as well as colleague, without whom I would not have been able to perform most of the experiment's that required live animals.

Mrs. Renate Filter, for the superb nucleotide sequencing facility that is maintained at the University of Pretoria.

The Laboratory for Microscopy and Microanalysis at the University of Pretoria, for the use of their equipment and their professional expertise in the use of electron microscopical methodologies.

To my wife Janet, for your love and understanding, when I was more at the lab than at home. Your support and interest have truly made a difference during this time.

My family who were always supportive during this time of study. Thank you for enduring me during this period.

The Lord GOD, who created this world through his WORD. For the mysteries that we can investigate, for those precious few moments when we discover HIS divine grace in the molecules we study, for the opportunity to contemplate briefly the wonderful life locked up in nature.

Thesis title: Functional perspectives on the evolution of argasid tick salivary gland protein superfamilies

Student: B.J. Mans

Promoters: Prof. A.W.H. Neitz, Prof. A.I. Louw and Dr. A.R.M. Gaspar

Department: Biochemistry

Degree: Philosophia Doctor

Ticks evolved an obligate, hematophagous lifestyle approximately 120 million years ago while the vertebrate hemostatic system has existed for at least 400 million years. This implies that ticks adapted to an established and efficient hemostatic system. Adaptation to a new environment at a molecular level implies the gain of new protein functions. Mechanisms for the acquisition of new protein functions include gene duplication and subsequent gain/loss of protein function. This predicts the presence of multi-gene or protein families. The present study investigated the adaptation of ticks to a blood-feeding environment through the use of such multi-gene families present in the salivary gland proteins of the soft tick *Ornithodoros savignyi*.

In this study, a family of platelet aggregation inhibitors named savignygrins was characterized. These savignygrins for which gene duplication was indicated inhibit platelet aggregation induced by various agonists, disaggregate aggregated platelets and inhibit the binding of the monoclonal antibody P2 to integrin $\alpha_{IIb}\beta_3$ and $\alpha_{IIb}\beta_3$ to fibrinogen. This indicates that the savignygrins target the fibrinogen receptor, which was confirmed by sequence identity to disagregin, a fibrinogen receptor antagonist from the closely related tick specie *Ornithodoros moubata*. Savignygrin, however, differs from disagregin due to the presence of the integrin recognition motif RGD.

The thrombin inhibitor savignin was cloned and sequenced. Savignin consists of two BPTI-Kunitz domains. Homology modeling using the structure of ornithodorin, a thrombin inhibitor from *O. moubata*, shows similar mechanisms of inhibition. This

includes targeting of thrombin's active site with its N-terminal BPTI-domain and thrombin's fibrinogen recognition exosite with its C-terminal domain.

Protein fold prediction as well as phylogenetic analysis indicated that the savignygrins share the BPTI-fold with thrombin and fXa inhibitors previously described for the *Ornithodoros* genus. A model of protein evolution for the tick BPTI-inhibitors is proposed that indicates a sequential evolution of inhibition of the substrate recognition capability of thrombin (targeting of the fibrinogen binding exosite), its catalytic capability (targeting of the active site), the catalytic capability of fXa (similar to that of thrombin) and platelet aggregation. This model accounts for the different inhibitory mechanisms of the tick anti-coagulants relative to that of the canonical BPTI-family. The unique presentation mode of the RGD motif on the BPTI substrate-presenting loop of the platelet aggregation inhibitors is also explained.

Four highly abundant proteins (TSGPs) of the lipocalin family were characterized. It was proposed that these proteins function during salivary gland granule biogenesis. TSGP2 and TSGP4 were also identified as toxins that affect the cardiac system. In contrast to savignygrin and apyrase, which localizes to two specific salivary granule types, the TSGPs localize to all the different granule types identified in the salivary glands. Localization studies also indicate that instead of the previously described three granular cell types in soft tick salivary glands, there are five. Phylogenetic analysis of the tick lipocalins indicates a series of gene duplication events and subsequent gain/loss of protein function. The absence of the toxins in the salivary glands of *O. moubata* suggests that the toxins as well as the non-toxic TSGP3 might be recent gene duplications that occurred after the divergence of these two tick species.

OPSOMMING

Titel van tesis:	Functional perspectives on the evolution of argasid tick salivary gland protein superfamilies
Promoters:	Prof. A.W.H. Neitz, Prof. A.I. Louw en Dr. A.R.M. Gaspar
Departement:	Biochemie
Graad:	Philosophia Doctor

Bosluise het 'n verpligte bloedvoedende lewenstyl ongeveer 120 miljoen jaar gelede ontwikkel. Werweldiere se hemostatiese sisteem bestaan al ongeveer 400 miljoen jaar. Bosluise moes dus by 'n bestaande en hoogs ontwikkelde hemostatiese sisteem aanpas. Aanpassing op molekulêre vlak impliseer die ontwikkeling van nuwe proteïen funksie. Meganismes vir die ontwikkeling van nuwe proteïen funksie sluit geen duplikasie en die daaropvlogende wins/verlies van proteïen funksie in. Dit voorspel die bestaan van multi-geen of proteïen families. Die huidige studie ondersoek die aanpassing van bosluise by 'n bloedvoedende lewenstyl deur gebruik te maak van multi-geen families teenwoordig in die speekselkliere van die sagte bosluis *Ornithodoros savignyi*.

'n Familie van bloedplaatjie aggregasie inhibitore is gekarakteriseer. Geen duplikasie kon aangetoon word. Bloedplaatjie aggregasie deur verskeie agoniste sowel as binding van die monoklonale teenliggaam P2 aan die integrien $\alpha_{IIb}\beta_3$ en $\alpha_{IIb}\beta_3$ aan fibrinogeen is deur savignygrin voorkom. Dit identifiseer die fibrinogeen reseptor as teiken van savignygrin. Identiteit aan die fibrinogeen reseptor antagonis disagregien bevestig die hipotese. Savignygrin verskil egter van disagregin a.g.v. die teenwoordigheid van die integrien herkennings motief, RGD.

Die trombien inhibitor, savignin se geen volgorde is bepaal deur klonering. Savignin bestaan uit twee Kunitz-BPTI domeine. 'n Struktuur model gegrond op ornithodorin , 'n trombien inhibitor van *O. moubata,* voorspel soortgelyke inhibitor meganismes. Dit sluit die teikening van trombien se aktiewe setel deur die N-terminale BPTI-domein en die fibrinogeen herkennings setel deur die C-terminale BPTI-domein in.

Proteïen-vou voorspelling en filogenetiese analise dui aan dat savignygrin die BPTI-vou deel saam met die trombien en fXa inhibitore geidentifiseer in the genus *Ornithodoros*. 'n Model vir die opeenvolgende onwikkeling van die bosluis BPTI-inhibitor funksie word voorgestel. Dit sluit in die teiken van trombien se substraat herkennings setel, trombien se aktiewe sentrum, fXa se aktiewe setel en bloedplaatjie aggregasie. Die model verklaar die uiteenlopende inhibisie meganismes van the bosluis BPTI-inhibitore ten opsigte van die kanonikale BPTI-inhibitore. Die unieke presentering van die RGD motief op die BPTI-substraat herkennings lus word ook verklaar.

Vier van die mees volopste speekselklier proteïene (TSGPs) wat deel is van die lipokalien familie is gekarakteriseer. 'n Funksie in die biogenese van speekselklier granules is voorgestel. TSGP2 en TSGP4 is ook as toksiene aangedui wat die hart aantas. In teenstelling met savignyrin en apirase wat in slegs twee granule tipes gevind word, word die TSGPs in al die granule sel tipes gevind. In plaas van die oorspronklike drie granule seltipes van sagte bosluise, is vyf aangedui. Filogenetiese analise van die lipokaliene dui 'n reeks geen duplikasies aan met dienooreenkomstige wins/verlies van funksie. Die afwesigheid van die toksiene in die speekselklier ekstrakte van *O. moubata* dui ook aan dat die toksiene sowel as die nie-toksiese TSGP3 geen duplikasies mag wees wat plaasgevind het na die spesiasie van die twee bosluis spesies.

Chapter 1: Evolution of hematophagy in ticks

1.1.1 Ticks as a relevant problem

Man as manager of a variety of livestock has a moral responsibility to protect the animals under his care against damage caused by ectoparasites. Ticks are the most important ectoparasites in medical, veterinary and economical terms. Ticks transmit the highest number of pathogenic organisms that can kill and harm the host. These include anaplasmosis (*Boophilus* spp), babesiosis (*Boophilus* spp), cowdriosis (*Amblyomma* spp) and theileriosis (*Hyalomma truncatum*) (de Castro and Newson, 1993; Munderloh and Kurtti, 1995). Tick paralysis (Gothe and Neitz, 1991) and toxicoses (Gothe, 1999) also have significant impacts on lifestock mortality.

Although being obligate parasites, ticks are non-permanent feeders that can survive without their host for extended periods of time. Like predators, ticks are only in contact with their host for the short time during which they feed. For fast feeding ticks (Argasidae or soft ticks) this could be less than an hour and for slow feeders (Ixodidae or hard ticks) up to nine or ten days (Sauer *et al.* 1995). In many argasid and some ixodid species, new stages of development take place away from the host and after each molting stage a new host is found (Balashov, 1972). This relieves much of the burden other permanent parasites face, which have to depend on the host's fitness and viability for their own survival. This adaptation of ticks to survive away from their host also led to ticks being more aggressive than ectoparasites living permanently on their host (Lehmann, 1993). Due to this lack of dependence of ticks on host fitness, the tick burden itself can severely affect the host.

Natural infestations may involve thousands of ticks per animal. Anemia that follows from infestation can be severe. Salivary gland toxins secreted can cause loss of appetite which can aggrevate the anemia. This leads to fatigue and a weakened immune system. Even small numbers of ticks can have an impact on host fitness, especially in young animals (de Castro and Newson, 1993). It has been reported that calves infested with an average of 40 ticks gained 37 kg less in body mass than control calves (Kaufman, 1989). Wounds inflicted by ticks as well as skin damage due to scratching can lead to

secondary infections through miasis-producing flies. Other consequences include hair and weight loss, that leads to a decrease in the quality of hides and wool and reduced milk and meat production, respectively (de Castro and Newson, 1993).

Combined, these factors have a great economic impact on agriculture. In 1984, the United Nations Food and Agriculture Organization estimated an annual global loss of seven billion US dollars due to tick infestation and tick-borne diseases. This amount has increased even more in recent years (Sauer *et al.* 1995).

1.1.2 Tick control

Conventional methods of tick control make use of chemical acaricides, normally applied on the host through dipping or spraying practices. Although intensive use can be beneficial over a short period of time, it soon leads to the loss of protective immunity against ticks, due to acaricide resistance. Interruption in tick control programs also leaves livestock vulnerable to major outbreaks of tick-borne diseases or the build up of tick populations (de Castro and Newson, 1993). The increasing cost of development of new chemicals and residual contamination of meat and milk are other major drawbacks to this approach (de Castro and Newson, 1993). Pathogens are also becoming resistant to drugs directed against them and there is even emergence of new pathogenic strains (Wikel, 1996).

Anti-tick vaccines represent one of the most promising alternatives to chemical control (Willadsen, 2001). They have the advantage of target specificity, environmental safety, lack of human health risk and ease of administration and cost (Wikel, 1996). Cross reactivity between antigens of different species is an important consideration in the development of vaccines (Crause *et al.* 1994). This could be exploited as cross protection has been observed between different Ixodidae species (Opdebeeck, 1994; de Vos *et al.* 2001). One of the problems inherent in the strategy of vaccination against ticks is the inefficient or even non-existent anti-tick immunity in natural hosts (de Castro and Newson, 1993). This is attributed to either evasion of the host's immune system or its direct suppression (Sauer *et al.* 1995).

Two main strategies for vaccination development have been focused on, those based on the modulation of the host's immunocompetence and those that make use of novel antigens (Opdebeeck, 1994). The focus in the former is on the salivary secretions of the tick during feeding, as the saliva contains biologically active compounds necessary for suppression of the host's immune system (Sauer *et al.* 1995). The latter focus on those antigens that do not normally come into contact with the host's immune system and are appropriately called concealed antigens (Alger and Cabrera, 1972).

1.1.3 Concealed antigens as vaccine targets

The advantage of concealed antigens is that it bypasses the immune evasion response (Kaufman, 1989). It would be unlikely that the host have developed immune tolerance with respect to these antigens as opposed to those from the salivary glands. Concealed antigens include those from the midgut, which are involved in blood digestion, hemolymph, reproductive organs and synganglion. The different internal organs are validated as targets by the fact that ticks have an open circulatory system and that the host's immunoglobulins can pass through the gut barrier and retain their specificity (Opdebeeck, 1994; Munderloh and Kurtti, 1995). The efficacy of concealed antigens as vaccine targets was indicated by a reduced number of feeding ticks, reduced engorged body weights, increased feeding times, diminished production of ova and a decreased tick fecundity (Sauer *et al.* 1995). It was found that damage to the tick's midgut leads to leakage of host blood into the hemocoel. This is due to anti-midgut antibodies as well as the presence of host basophils, eosinophils and macrophages in the digestive tract of the tick (Opdebeeck *et al.* 1988). A recombinant midgut membrane protein (Bm86 from *Boophilus microplus*) has recently been expressed in a baculovirus system. Vaccination with this protein gave effective protection for cattle in the field as well as in pens with reduced tick reproductive capacity of 77% (Opdebeeck, 1994). This was also the first commercial available tick vaccine and it was recently shown that cross species protection could be attained using this vaccine (Willadsen *et al.* 1995; de Vos *et al.* 2001; Willadsen, 2001).

1.1.4 Exposed antigens as vaccine targets

Tick antigens that normally do invoke an immune response in the host enter through salivary secretions (Kaufman, 1989). The first anti-tick vaccine strategy was based on salivary gland extracts (Trager, 1939). This vaccine worked well in the laboratory setting, but poorly in the field. Some authors have argued that on principle a salivary gland derived antigen would be of limited value (Kaufman, 1989) and that ectoparasites and their hosts adapt in a complementary manner to reduce provocation of antagonistic reactions such as immune and pathogenic responses (Opdebeeck, 1994). Salivary gland secretions do however, perform a main function in the disarmament of the anti-hemostatic and inflammatory reactions of the host. Saliva is also the main vehicle for transmission of tick-borne pathogens, although pathogens may also be transmitted from the gut, as ticks do regurgitate bloodmeals (Munderloh and Kurtti, 1995). It was shown that immunosuppression of the host by tick saliva promotes both blood meal aquisition and the effective transmission of pathogens. Immunity to tick salivary gland extracts could have a protective effect against disease transmission and as such is worth investigating (Sauer *et al.* 1995).

Elevated immune responses against exposed antigens may circumvent immunosuppression (Opdebeeck, 1994). Artificial induced immunity with sufficient magnitude against the components which play a role in immunosuppression, could break immune system subversion. This could contribute significantly to the success of a multivalent vaccine. Advantages of using salivary gland extracts is that exposure to natural infestation has the capacity to boost vaccine immunity (Janse van Vuuren *et al.* 1992). It could also stimulate naturally acquired resistance mediated through reponses to antigens found in tick saliva. On the other hand, immediate or delayed hypersensitivity could occur on repeated exposure to salivary gland antigens. These should be screened for allergens and this necessitates the requirement for purified components (Opdebeeck, 1994). During feeding there is also the expression of numerous other proteins in the salivary glands of ixodids which have important functions in the feeding process and thus provide a new array of possible immunogens (Wikel, 1996). Despite arguments against the use of exposed antigens, a number of successes have been attained. These include vaccination stategies against *Ripicephalus appendiculatus* (Shapiro, Bascher

and Dobbelaere, 1987) and *Hyalomma anatolicum anatolicum* (Banerjee, Momin and Samantaray, 1990). In a recent study the vaccinal value of novel and salivary gland extracts were investigated for the argasid ticks *Ornithodoros moubata* and *Ornithodoros erraticus*. It was found that the immune response against salivary gland extract was much higher than the response toward novel antigens from the gut, ovaries or synganglion. Vaccination with salivary gland extracts also provided protection in swine against tick infestation (Astigarraga *et al.* 1996).

A combined approach of novel as well as exposed antigen vaccines may be the best strategy to follow. Molecular engineered vaccines containing immunogenic parts of both exposed and concealed antigens may be an exciting alternative to conventional approaches (Opdebeeck, 1994). For rational vaccine design a thorough knowledge of the properties of potential vaccine targets is needed. This necessitates a deeper understanding of tick-host interactions, which is at the heart a question of how ticks adapted to their blood-feeding environment.

1.2.1 Evolution of hematophagy

Hemostasis is an efficient defense mechanism that prevents blood-loss through an open wound. The vertebrate hemostatic system originated approximately 400 million years ago (MYA) (Doolittle and Feng, 1987). In contrast, hematophagy (blood-feeding behaviour) evolved independently at least six times in the approximately 15000 species and 400 genera of the hematophagous arthropods (Table 1.1) (Ribeiro, 1995). Many arthropods evolved blood-feeding capabilities during the Cretaceous and Jurassic Era's, (145-65 MYA) (Balashov, 1984). Adaptation of hematophagous arthropods to a blood-feeding environment thus entailed specific adaptation to an efficient existing hemostatic system. Elucidation of the evolutionary mechanisms of blood-feeding arthropods could further our understanding of the evolution of complex systems as is exhibited at the blood-feeding interface, as well as allow the development of new control strategies based on novel as well as shared mechanisms. The subject investigated in this thesis is the adaptation of ticks to a blood-feeding environment, with specific reference to salivary gland proteins.

Table 1.1: Arthropods that evolved hematophagy independently. Orders or genera suggested to have evolved blood-feeding behaviour independently are shown in bold. Adapted from Ribeiro (1995).

Insect or arachnid order	Family (common name)	Genera	Species
Diptera	Sandflies	6	70
	Blackflies	24	1571
	Horseflies	5	4400
	Tsetse flies	1	23
	Stable flies	3	50
	Mosquitoes	36	3450
Hemiptera	Bedbugs	23	91
	Bat bugs	5	32
	Kissing bugs	14	118
Anoplura	Lice	42	490
Siphonaptera	Fleas	239	2500
Acari	Soft ticks	3	178
	Hard ticks	12	657
Total number		417	14595

1.2.2 The Ixodida or ticks

Ticks are obligate hematophagous organisms and the most important ectoparasites of domestic animals. The Ixodida comprises three families (Fig. 1.1), the **Ixodidae** or hard ticks (Scutum present, short in female, long in male, capitulum at anterior of body in all stages), **Argasidae** or soft ticks (Scutum absent, capitulum on underside of body in nymphs and adults, anterior in larvae) and **Nuttalliellidae** that is monotypic (Hoogstraal, 1956). The Ixodida are part of the Phylum Arthropoda and group with the spiders, scorpions, whip-scorpions, sun spiders, harvestmen, hooded tick spiders and false scorpions in the Class Arachnida. Ticks are a small group of a much larger group of mites that group in the subclass Acari, more specifically in the superorder Parasitiformes. Parasitiformes are characterized by the presence of free coxae, a ventral anal opening covered by plates, a hypostome and a sclerotized ring surrounding the capitulum. Actinochitin is absent on the setae, distinguishing them from the other superorder Acariformes.

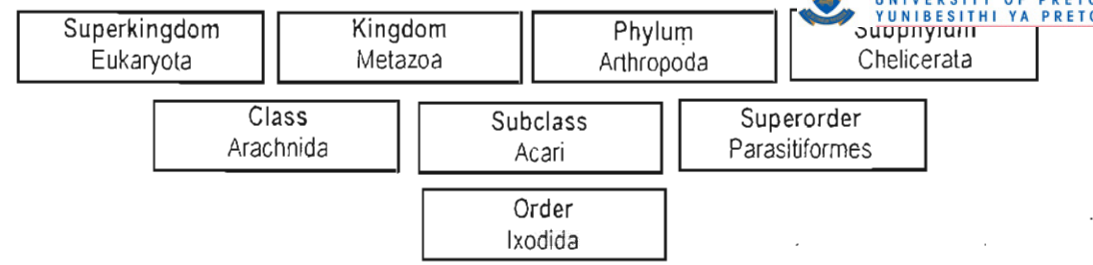

Family			
Ixodidae		Argasidae	Nuttalliellidae
Amblyomma (102)	*Anocentor* (1)	*Antricola* (14)	*Nuttalliella namaqua*
Aponomma (24)	*Anomalohimalaya* (1)	*Argas* (61)	
Boophilus (5)	*Cosmiomma* (1)	*Nothoaspis* (1)	
Dermacentor (32)	*Haemaphysalis* (150)	*Ornithodoros* (103)	
Hyalomma (25)	*Ixodes* (234)	*Otobius* (2)	
Margaropus (3)	*Nosomma* (1)		
Rhipicentor (2)	*Rhipicephalus* (76)		

Fig. 1.1: Hierarchy of the Ixodida. Approximate number of species is indicated in brackets next to the genus name (Personal communication, Dr. Lance Durden, 50th Annual Acarology Summer Program, Ohio State University, 2000).

1.2.3 The origin of ticks

Ticks were considered to be of the earlier lineages of terrestrial arachnids, with proposed origins in the Devonian (350-400 MYA) (Oliver, 1989), late Silurian (400 MYA) (Lindquist, 1984), late Permian (Hoogstraal and Aeschlimann, 1982) and late Paleozoic or early Mesozoic (225 MYA) (Hoogstraal, 1985; Balashov, 1989, 1994). These estimations were based on the assumptions that the most primitive group of ticks are associated with the most primitive group of hosts, and that ticks must have arisen approximately at the same time as their particular host group. It has been proposed that ticks originated more recently in the early Cretaceous (Fillipova, 1977) or late Cretaceous (120 MYA) (Klompen *et al.* 1996). The latter is based on comparison of the distribution of ixodids worldwide, where some of the presumably basal lineages are exclusively Australian and suggests a major role of Australia in the evolution of ixodids. The late Cretaceous was the last time that Australia was part of Gondwanaland and indicates that this period played an important role in the origin of the Australian lineages, and by extension the entire tick family (Klompen *et al.* 2000). This period also

saw the emergence of mammals and was closely followed by dinosaur extinction (65 MYA). This provokes tantalizing suggestions that ticks evolved at the dawn of the emergence of mammals.

1.2.4 Tick fossil records

Ixodid fossils were found in Baltic amber (*Ixodes succineus*, 30-40 MYA), Oligocene deposits (*Ixodes tertiarius*, 30 MYA), Dominican amber (*Amblyomma testudinis*, *Ornithodoros antiquus*, 30-40 MYA) and in the ear of a woolly rhinoceros (*Dermacentor reticulates*, 1-3 MYA (Scudder, 1885; Weidner, 1964; Lane and Poinar, 1986; Poinar, 1995). The oldest fossil to date is an argasid (*Carios jerseyi*) found in New Jersey amber, 90-94 MYA(Klompen and Grimaldi, 2001). If ticks originated 120 MYA, they already speciated by ~92 MYA into the main tick families, as well as argasid genus level.

1.2.5 Speciation of ticks

Phylogenetic analysis using 16S RNA placed the Argasinae basal to the Ixodidae, suggesting that ixodids were derived from an Argas-like ancestor (Black and Piesman, 1994). Phylogenetic analysis also suggested that Argasidae were paraphyletic (Crampton, McKay and Barker, 1996). However, re-analysis of ixodid and argasid relationships, using 18S RNA indicated strong support for the monophyly of Argasidae and Ixodidae (Black, Klompen and Keirans, 1997). It also placed Argasinae and Ornithodorinae as single monophyletic groups, respectively, inside the Argasidae, which is concurrent with original morphologically based phylogenies (Hoogstraal and Aeschlimann, 1982). The question raised here is whether ticks adapted to blood-feeding environment before or after speciation of the main tick families?

1.2.6 Ticks were free-living scavengers

Holothyrida forms with the Ixodida and Mesostigmata the Order Parasitiformes (Evans 1992). Phylogenetic analysis indicates that the Holothyrida rather than Mesostigmata are a sister-group to ticks (Dobson and Barker, 1999). It is of interest that the holothyrida are distributed only in areas that were part of Gondwanaland, which corresponds with the current ideas on tick origins (Klompen *et al.* 2000). Holothyrida is

a group of free-living mites, which mainly live on body fluids of dead organisms. It has been suggested that ticks shared this same trait before adaptation to a blood-feeding environment (Walter and Proctor, 1998).

1.2.7 Questions regarding tick evolution

The preceding sections lead to the following questions:

1) What was the nature of the ancestral tick before adaptation to a blood-feeding environment (i.e. which anti-hemostatic strategies were present or evolved *de novo*)?
2) Did ticks evolve anti-hemostatic strategies before or after divergence into the main tick families (i.e. did ticks evolve anti-hemostatic strategies more than once independently)?
3) How did ticks acquire novel anti-hemostatic strategies (i.e. what were the evolutionary mechanisms by which ticks adapted to an already present and complex hemostatic system)?
4) What was the driving force behind the evolution of hematophagy in ticks?

The answers to these questions can only be contemplated by a clear understanding of tick-host interactions: the interface where adaptation originated.

1.3.1 Tick-host interactions

To acquire a blood meal, ticks need to penetrate the host's skin and damage enough blood vessels for the release of blood. The depth of penetration and feeding time depends on the type of tick. Slow and fast feeding ticks have different mouthparts that cause different degrees of damage to the host (Binnington and Kemp, 1980). In ixodid ticks (slow feeders) the lesion develops gradually with the formation of a hematoma. It has been proposed that the main damage at the feeding lesion is caused by neutrophils attracted to the feeding site where they degranulate and cause inflammation (Ribeiro, 1987). Argasids feed rapidly with deep penetration of the host's skin and cause considerable damage. Bloodloss can still occur long after a tick has stopped feeding (Binnington and Kemp, 1980).

During probing for blood, capillary and small blood vessels are lacerated, host cells are ruptured and hemorrhage occurs. This increases the blood volume at the site of feeding and leads to activation of the host's defence mechanisms which include the hemostatic (blood coagulation and platelet aggregation) and the immune system (Ribeiro, 1987). Platelet aggregation represents the most immediate defence and is sufficient to arrest blood flow from small vessels (Law, Ribeiro and Wells, 1992). It is possible that platelet aggregation directed the evolution of the salivary gland proteins of all blood sucking arthropods to a greater extent than did blood coagulation (Ribeiro, 1987). Coagulation may thus be of lesser significance in the host's defence against blood sucking arthropods. It may play a more important role during the ingestion of the blood meal and it was suggested that anti-coagulant inhibitors from ticks have their main function in the gut where they serve to keep the blood in a fluid form (Bowman *et al.* 1997).

1.3.2 Platelet aggregation and its role in hemostasis

Platelet aggregation is essential for hemostasis (the cessation of bloodflow from a damaged vessel wall) by means of blood coagulation and formation of a fibrin clot that serves as a plug (Dam-Mieras and Muller, 1986). The whole blood coagulation cascade depends on a negatively charged membrane surface where the different serine proteases involved in the cascade can dock to be sequentially activated (Esmon, 1995). Normally the outer membranes of cells are depleted of negatively charged phospholipids. Platelets provide this membrane surface by the translocation of phosphatidyl serine from its inner to outer membrane during platelet activation and aggregation. Clotting proteins (fVII, fX and prothrombin) subsequently bind to the membrane through a Ca^{2+} bridge by means of the modified amino acid γ-carboxyglutamate (Gla) and are thus targeted and localized to the site of damage (Tans and Rosing, 1986).

1.3.3 Collagen and its role in hemostasis

Damage to the blood vessel wall exposes the collagen containing subendothelial layer. Collagen binds the plasma protein, von Willebrandt's factor (vWf), which changes conformation and activates platelets by binding to a specific vWf receptor (glycoprotein Ib) or to the main integrin involved in aggregation, $\alpha_{IIb}\beta_3$ (Hawiger, 1992). This restricts platelets to the site of injury and prevents thrombosis by localization of the clotting

cascade. Collagen also activates factor XII, the initiator of the intrinsic pathway of the blood-clotting cascade (Zwaal, Bevers and Comfrius, 1986).

1.3.4 Platelet activation

Unactivated platelets are discoid and smooth and upon activation change to a spherical shape with numerous pseudopods. Activated platelets secrete their granule contents and eventually aggregate to form a platelet plug. Platelets can be activated by a variety of compounds (ADP, collagen, thrombin, thromboxane A_2, epinephrine, platelet activating factor, thrombospondin) which binds to specific membrane receptors present on the platelet surface. Activation is mediated by signal transduction of the different receptors which activates either the cyclo-oxygenase or phospholipase C pathway, or inhibits adenylate cyclase (Fig. 1.2).

1.3.5 Inhibition of adenylate cyclase

Epinephrine, thrombin and ADP bind to Gi-coupled receptors, and prevent the synthesis of cAMP through inhibition of adenylate cyclase. Raised cAMP levels lower the intra-platelet free calcium levels necessary for shape change and granule secretion. Modulation of cAMP levels thus aid in platelet activation, although it does not cause platelet shape change.

1.3.6 The cyclo-oxygenase pathway

Collagen, epinephrine and thrombin receptors are all linked to G-proteins that activate phospholipase A_2, which cleaves phosphatidyl inositol and phosphatidyl choline to produce arachidonic acid. Cyclo-oxygenase then converts arachidonic acid to thromboxane A_2 (TXA_2) which is a platelet agonist as well as a vasoconstrictor. Overall, agonists exclusive to this pathway does not cause primary aggregation, but rather activation of platelets by TXA_2 and subsequent activation and aggregation via the PLC pathway.

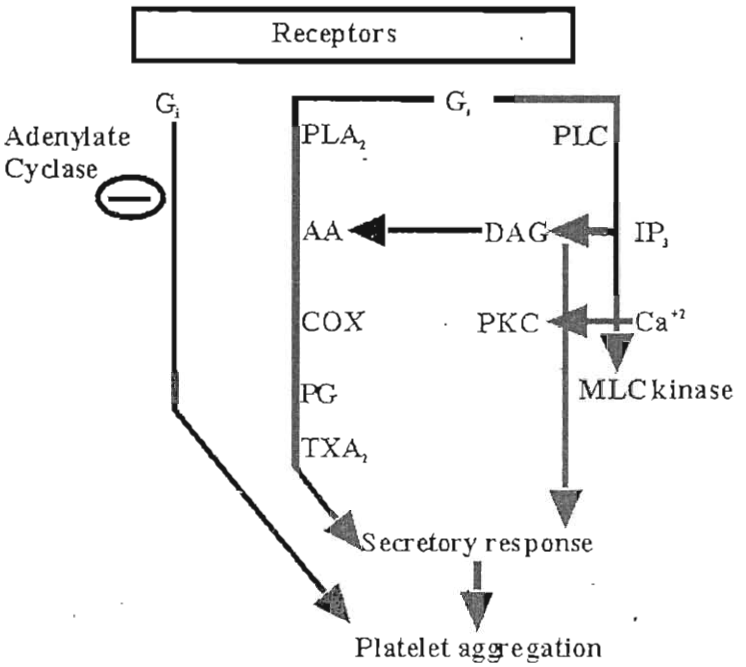

Fig. 1.2: Platelet activation mechanisms. Binding of different agonists to their specific receptors activates phospholipase A_2 (PLA_2) or phopholipase C (PLC) or inhibits adenylate cyclase. Arachidonic acid (AA) released by PLA_2 is converted to prostaglandins (PG) by cyclo-oxygenase (COX) with subequent conversion to thromboxane A_2 (TXA_2). PLC releases diacylglycerol (DAG) and inositol-1,4,5-trisphosphate (IP_3) from the platelet inner membrane. IP_3 induces release of Ca^{2+} from the dense tubular system and calcium activates myosin light chain kinase (MLC kinase), which phosphorylates myosin, leading to shape change. DAG in the presence of calcium activates protein kinase C (PKC), which phosphorylates a number of platelet proteins, leading to secretion of granules. Inhibition of adenylate cyclase leads to a relaxed control of intracellular calcium concentration, which promotes those processes activated by calcium (Hawiger, 1989).

1.3.7 The phospholipase C pathway (PLC)

Thrombin, ADP, PAF and TXA_2 receptors are linked to G-proteins that activate PLC leading to the formation of diacylglycerol (DAG) and inositol trisphosphate (IP_3) through hydrolysis of phosphatidyl inositol diphosphate. DAG in the presence of calcium activates phosphokinase C (PKC) causing degranulation of platelets. IP_3 releases Ca^{2+} from the dense tubular system and this activates myosin light chain kinase resulting in the phosphorylation of myosin (Hawiger, 1989). Activated myosin binds actin to form the actomyosin cytoskeleton which facilitates shape change and formation of focal adhesion points (FAP). These FAPs form on the ends of philopodia and consist of a multi-protein integrin $\alpha_{IIb}\beta_3$ complex (Jamaluddin, 1991). Due to multiple phosphorylation events in the

multi-protein complex, $\alpha_{IIb}\beta_3$ undergoes a conformational change, with exposure of a fibrinogen-binding site and subsequent platelet aggregation through linkage of platelets by fibrinogen (Clark *et al.* 1994). Fibrinogen binds to $\alpha_{IIb}\beta_3$ through two RGD integrin recognition motifs on its α-chain and one non-RGD containing sequence on its γ-chain (Hawiger and Timmons, 1992).

1.3.8 Secretion of granule components

Various biologically active compounds stored in α- and dense-granules are secreted during activation, which in turn, activate other platelets and induce inflammation (Table 1.2). Compounds of special interest for tick biology include ADP, which activates platelets and ATP, which causes mast cell degranulation and neutrophil aggregation. This leads to local inflammation and vasoconstriction (Ribeiro, 1989). Serotonin and thromboxane A_2 stimulate vasoconstriction, while serotonin also promotes vascular permeability for the infiltration of mast cells and macrophages (Bloom and Thomas, 1987).

Table 1.2: Biologically active compounds secreted by activated platelets. Adapted from Jamaluddin (1991).

Granule	Contents	Effect on hemostasis
Dense granules	ADP	Activates platelets
	ATP	Inflammation
	Ca^{2+}	Shape change of platelets
	Serotonin	Vasoconstriction and vascular permeability
α-granules	VWf	Binds platelets to collagen
	Fibrinogen	Platelet aggregation
	Fibronectin	Cell adhesion
	Plasminogen	Precursor of plasmin
	Thrombospondin	Activates coagulation
	Kininogen	Coagulation factor
	fV	Coagulation factor
	$\alpha_{IIb}\beta_3$	Platelet aggregation

1.3.9 Blood coagulation

The intrinsic pathway of blood coagulation starts with collagen-induced activation of fXII which activates fXI as well as kallikrein. Kallikrein cleaves a precursor to form bradikinin, a peptide causing inflammation, the sensation of pain and irritation (Ribeiro, 1989). The extrinsic pathway starts with the release of thromboplastin (tissue factor) from damaged endothelial cells, which activates factor VII (Fig. 1.3) (Bevers, Comfrius and Zwaal, 1993). Both pathways eventually coalesce in the formation of factor Xa which in turn

produces thrombin. Fibrinogen is then cleaved by thrombin to fibrin which forms a network, the main constituent of the blood clot together with platelets and erythrocytes (Jackson and Nemerson, 1980).

These events ultimately lead to edema, one of the signs many tick-resistant hosts display. Edema and associated irritation lead to host grooming, an important factor in the reduction of the tick burden (Wikel, 1996).

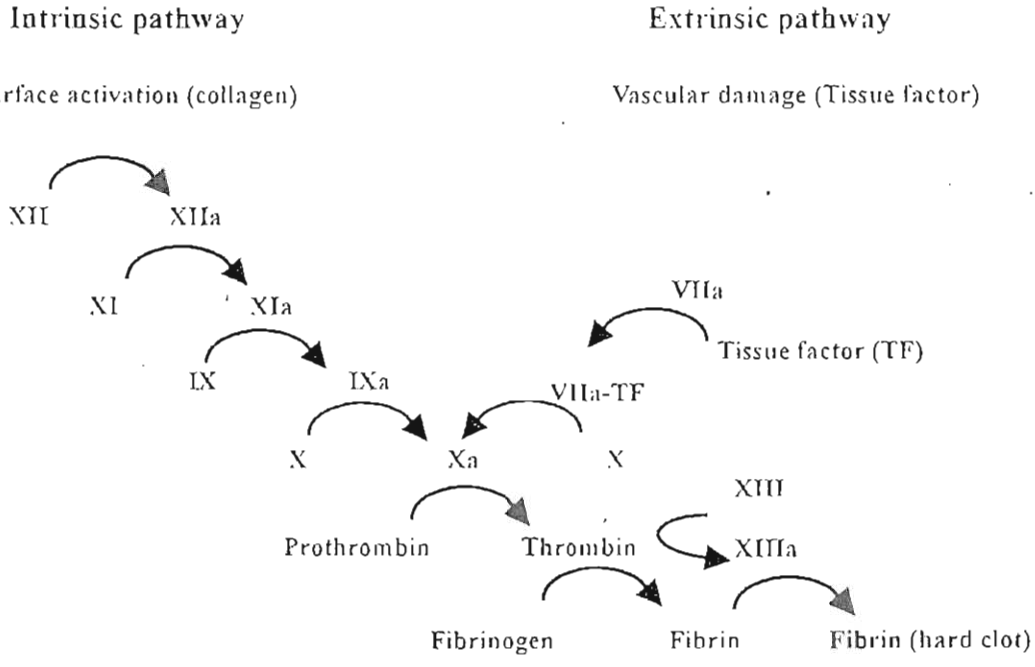

Fig. 1.3: The blood coagulation cascade. The intrinsic pathway is initiated by the binding of fXII to a negatively charged surface like collagen and is then activated by kallikrein. fXIIa then activates fXI as well as prekallikrein. This leads to eventual activation of fX. The extrinsic pathway is activated by trauma that releases tissue factor. This binds to fVIIa, that is activated by thrombin and together activates fX. Prothrombin is activated to thrombin by fXa which cleaves fibrinogen to fibrin that forms a network. Thrombin also activates fXIIIa which stabilizes the fibrin clot by crosslinkage. Adapted from Bloom and Thomas (1987).

1.4.1 Anti-hemostatic components produced by ticks

Ticks manage to down regulate the complex host immune and hemostatic mechanisms through secretion of bio-active components with a range of pharmacological properties which ease the burden of obtaining a bloodmeal.

1.4.2 Immunomodulatory components in tick saliva

Tick saliva contains prostaglandin E_2 (PGE_2) which promotes vasodilation, inhibits platelet aggregation, mast cell degranulation and T-lymphocyte activation. PGE_2 has been identified in the saliva of *Ixodes scapularis*, *Amblyomma americanum* and *B. microplus* (Dickinson *et al.* 1976; Ribeiro *et al.* 1985; Ribeiro, Makoul and Robinson, 1988; Ribeiro *et al.* 1992; Bowman *et al.* 1995). This alone counteracts a whole range of the host's defences. Anti-histamine is also present which prevents inflammation. Histamine-binding proteins that sequestrate histamine from the feeding-site have been identified in *R. appendiculatus* (Paesen *et al.* 1999; Paesen *et al.* 2000). The saliva of *I. scapularis* contain a carboxypeptidase activity which cleaves bradykinin and thus prevents irritation and pain (Ribeiro *et al.* 1985; Ribeiro and Mather, 1998). An anti-complement protein from the tick *I. scapularis* that inhibits erythrocyte lysis by human serum, has also been described (Valenzuela *et al.* 2000).

1.4.3 Blood clotting inhibitors from ticks

Numerous inhibitors for the different serine proteases involved in the clotting cascade have been described for hard and soft ticks (Table 1.2). Inhibitors of fV and fVII have been described for the hard tick *Dermacentor andersoni* (Gordon and Allen, 1991). Thrombin and fXa inhibitors have been described in a variety of hard ticks (Table 1.3). Tick anticoagulant peptide (TAP) and fXaI (factor Xa inhibitors) as well as ornithodorin and savignin (thrombin inhibitors) have been described for the soft ticks *O. moubata* and *Ornithodoros savignyi*, respectively (Waxman *et al.* 1990; Gaspar *et al.* 1996; Joubert *et al.* 1998; van de Locht *et al.* 1996; Nienaber, Gaspar and Neitz 1999; Mans, Louw and Neitz, 2002a).

Fibrinogen which serves as the connective link during platelet aggregation and which is the precursor for the fibrin network is also under attack during feeding. A fibrinogenolytic enzyme has been identified in the soft tick *O. savignyi* (Mahlaku, Gaspar and Neitz, 2000). Other enzymes present in the saliva of argasid ticks are the elastases and hyaluronidases (Neitz and Vermeulen, 1987). The function of these enzymes may be to assist in the enlargement of the feeding lesion through degradation of the extracellular-matrix, thus shortening the feeding time and promoting the formation of a hematoma (Kaufman, 1989).

Table 1.3: Anticoagulants from ticks. Adapted from Bowman *et al.* (1997).

Species	Source	Target	Mr (kDa)	Reference
R. appendiculatus	Salivary gland	fXa	65	Limo *et al.* 1991
H. truncatum	Salivary gland	fXa	17	Joubert *et al.* 1995
H. dromedarii	Nymphs	fXa	12, 16	Ibrahim *et al.* 2001
O. moubata	Whole tick	fXa	7	Waxman *et al.* 1990
O. moubata	Salivary gland	Thrombin	12	van de Locht *et al.* 1996
O. savignyi	Salivary gland	fXa	7	Gaspar *et al.* 1996; Joubert *et al.* 1998
O. savignyi	Salivary gland	Thrombin	12	Nienaber *et al.* 1999; Mans *et al.* 2002a
B. microplus	Salivary gland	fXa and thrombin	NA	Anastopoulos *et al.* 1991
B microplus	Whole larvae	Kallikrein	10, 18	Tanaka *et al.* 1999
B. microplus	Saliva	Thrombin	60	Horn *et al.* 2000
I. holocyclus	Salivary gland	fXa and thrombin	NA	Anastopoulos *et al.* 1991
H. longicornis	Salivary gland	fXa and thrombin	NA	Anastopoulos *et al.* 1991
A. americanum	Salivary gland	fXa and thrombin	NA	Zhu *et al.* 1997
I. ricinus	Whole tick	Thrombin	7	Hoffmann *et al.* 1991
D. andersoni	Salivary gland	fV and fVII	NA	Gordon and Allen, 1991

1.4.4 Platelet aggregation inhibitors from ticks

Moubatin, an inhibitor of collagen induced platelet aggregation has been identified in *O. moubata*, while tick adhesion inhibitor (TAI), inhibits the adhesion of platelets to matrix collagen (Waxman and Connolly, 1993; Karczewski *et al.* 1995). The thrombin inhibitors involved in the inhibition of the coagulation cascade also serve to inhibit thrombin-induced platelet aggregation (Nienaber, Gaspar and Neitz, 1999). Binding of fibrinogen to integrin $\alpha_{IIb}\beta_3$ are also inhibited by the RGD-containing inhibitors variabilin from *Dermacentor variabilis* and savignygrin from *O. savignyi*, as well as the RGD lacking inhibitor, disagregin from *O. moubata* (Karczewski, Endris and Connolly, 1994; Wang *et al.* 1996; Mans, Louw and Neitz, 2002b). Apyrase, an ATP-diphosphohydrolase enzyme inhibits platelet aggregation through hydrolysis of ADP (Law, Ribeiro and Wells, 1992). Apyrase activity has been found in the salivary gland extracts or saliva of *I. scapularis* and *O. moubata* and *O. savignyi* (Ribeiro *et al.* 1985; Ribeiro, Endris and Endris, 1991; Mans *et al.* 1998a; Mans *et al.* 1998b). It was also shown that apyrase could play a role in the disaggregation of aggregated platelets, which could serve an important function in dissolving platelet aggregates, during feeding (Mans *et al.* 2000). Apyrase activity appears

however, to be absent from the saliva of *A. americanum* (Bowman *et al.* 1997). PGI_2, PGD_2 and PGE_2 inhibit platelet aggregation by preventing ADP secretion during platelet activation (Ribeiro, Makoul and Robinson, 1988; Bowman *et al.* 1995, Aljamali *et al.* 2002). The various platelet aggregation inhibitors are summarized in Table 1.4.

Table 1.4: Platelet aggregation inhibitors from ticks. Adapted from Bowman *et al.* (1997).

Species	Compound	Target	Mr (kDa)	Reference
O. moubata	Apyrase	ADP	NA	Ribeiro *et al.* 1991
O. moubata	Moubatin	Collagen	17	Waxman and Connolly, 1993
O. moubata	TAI	Collagen	15	Karczewski *et al.* 1995
O. moubata	Disagregin	$\alpha_{IIb}\beta_3$	6	Karczewski *et al.* 1994
O. savignyi	Apyrase	ADP	67	Mans *et al.* 1998, 2000
O. savignyi	Savignygrin	$\alpha_{IIb}\beta_3$	7	Mans *et al.* 2002b
D. variabilis	Variabilin	$\alpha_{IIb}\beta_3$	5	Wang *et al.* 1996
I. dammini	PGI_2	PGI_2-receptor	NA	Ribeiro *et al.* 1988
A. americanum	PGD_2	PGI_2/D_2-receptor	NA	Bowman *et al.* 1995
A. americanum	PGE_2	PGE_2-receptor	NA	Aljamali *et al.* 2002

It is clear that there were a definite selective pressure on ticks to adapt to a blood-feeding environment and that an impressive array of anti-hemostatic components were evolved by ticks. The study of these salivary gland components could aid the understanding of the mechanisms that ticks evolved during their adaptation to a blood-feeding environment.

1.5.1 Argasidae as models of a primitive ancestor

The Argasidae are generally considered to be more primitive than the Ixodidae, by morphological, developmental and physiological criteria. The prototype ixodid ancestor is thus considered to be argasid-like (Oliver, 1989). Ixodids spend more time on the host, during which extensive changes take place in the salivary glands, while general argasid salivary gland structure is considered to be less complex than that of ixodids (Sauer *et al.* 1995). The study of argasid salivary gland biology is thus a good place to start when investigating tick adaptation to a blood feeding environment and the possible state of a primitive ancestor.

1.5.2 *Ornithodoros savignyi* as a model of argasid biology

Harry Hoogstraal penned the behaviour of the sand tampan in classic prose: "*at the Khartoum qaurantine one may see a long, seething line of thousands of hungry tampans helplessly confined to the shade of a row of acacia trees. A few yards away, separated only by the hot, nine o'clock sun, newly arrived cattle tied to a post fence tempt the tampans to cross the glaring strip. The next morning, in the coolness of seven o'clock, those tampans under the trees are all blood bloated and resting comfortably in the sand, others dragging back from their hosts across the now nonexistent barrier, and the legs of the cattle are beaded with yet other podshaped ticks taking their fill of blood in a regular line just above the hoof.*" (Hoogstraal, 1956). The ferociousness of these ticks can be attested by personal experience. Using the dry ice collection method to lure these tick from their hiding places, we were surrounded by ticks in a twenty meter radius around the dry ice container (Nevill, 1964). Ticks were running crazily this way and that way, seeking animals they could scent, in a futile attempt to be there first (personal observation, Upington, Western Cape Province, 1995). *O. savignyi* is of local economic importance in that it kills many domestic animals, especially young calves and lambs. Originally, the consensus was that these ticks kill their hosts through exsanguination, but it was later shown that death is caused by a toxin which may cause serious allergic reactions in humans (Howell, Neitz and Potgieter, 1975).

These ticks are relatively easily obtainable and they require little care and their salivary glands are of managable size. *O. savignyi* has a uniform integument which folds in on itself and allows the tick to obtain a large quantity of blood in a short feeding time (15-30 minutes). Males are smaller than females and lack the large genital opening that identify females (Fig. 1.4). *O. savignyi* is diploid (2n = 20), with the presence of sex-chromosomes, XY and XX for males and females, respectively (Howell, 1966a).

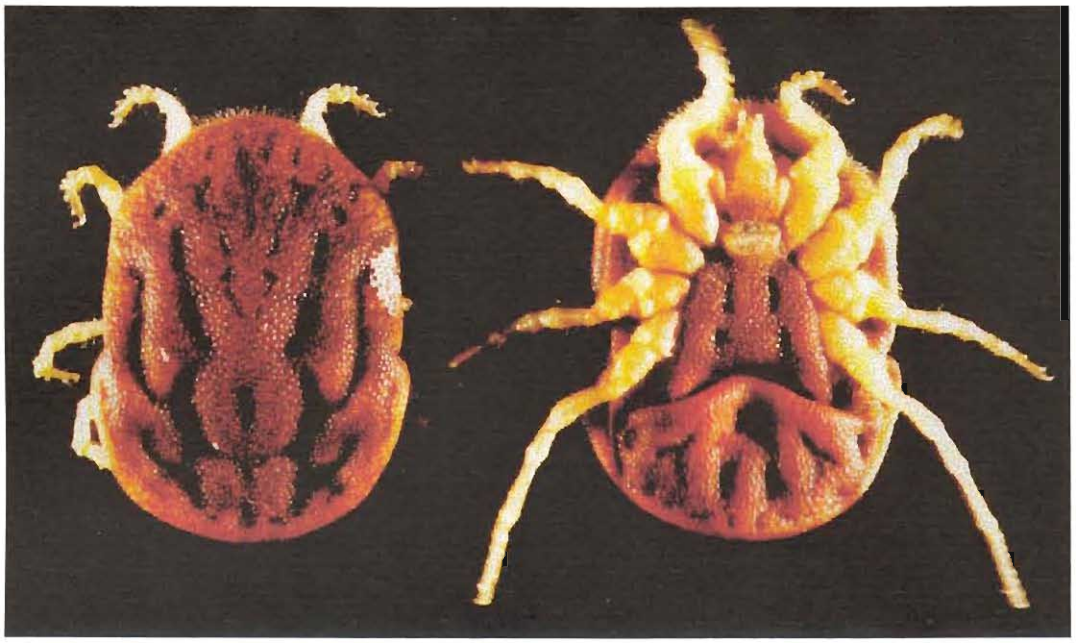

Fig. 1.4: External anatomy of a female *O. savignyi*. Note the folded integument, position of the capitulum and genital opening (Photograph:B.J Mans, 1996).

1.5.3 The relationship between *O. savignyi* and *O. moubata*

Extensive studies on anti-hemostatic components from the tick *O. moubata* have been conducted. A study of a closely related tick, like *O. savignyi*, could thus prove useful to gain comparative data, as there are few notable differences between these species. Morphologically they are similar, although *O. savignyi* has two pairs of eyes situated in its supracoxal folds, which is lacking in *O. moubata*. While *O. savignyi* burrows in sandy areas, *O. moubata* is endophilous (nest-dwelling). During its lifetime *O. moubata* is generally confined to a limited set of hosts that inhabit their burrow. *O. savignyi* is more predatory and will feed on any mammal in its proximity (Hoogstraal, 1956). *O. moubata* transmits *Borrelia duttoni*, which causes relapsing fever in humans and also transmits, african swine fever virus. In contrast, no pathogenic organisms have as yet been found associated with *O. savignyi*, although natural infection with Borrelia spirochetes have been reported (Helmy, 2000). *O. savignyi* do however, secrete toxic substances that can be lethal, especially in young animals. One adult tick or the salivary gland extract equivalent to half of a salivary gland can kill an adult mouse (20g) within 20 minutes (Mans *et al.* 2001, Mans *et al.* 2002). *O. moubata* however, does not secrete any toxins, exemplified by the feeding of 5 adult females, 10 males and 100 nymphs on an adult mouse to generate an immune response (Astigarraga *et al.* 1997).

1.5.4 Distribution of *O. savignyi*

O. savignyi is distributed through the North Western parts of South Africa and are also found in Egypt, Arabia, Ethiopia, Kenya and Zimbabwe (Paton and Evans, 1929). It lives in sandy regions where it resides below sand near trees, corrals and other places likely to attract animals. It has been reported that the incidence of these ticks has risen in regions where soil is more rocky as in kraals, which is probably due to attraction by domestic animals (Howell, Neitz and Potgieter, 1975).

1.5.5 Control of *O. savignyi*

The use of acaricides to control these ticks is limited due to the nature of their distribution over a large area and the fact that they do not reside on the host. Places where the soil has been treated with chemicals are avoided by these ticks. They can survive without feeding for up to five years, which makes starvation a null option. These ticks can have a lifespan of up to 15-20 years if they only feed occasionally (every 5-6 years) (Astigarraga *et al.* 1996). Long term biological control of these ticks would thus be a viable option.

1.5.6 Bio-active components from *O. savignyi*

O. savignyi is a rich source of bio-active components. An acidic toxin has been previously isolated and characterized in terms of its Mr (15400 Da), pI (5.01) (Neitz, Howell and Potgieter, 1969) and N-terminal amino acid sequence (Neitz *et al.* 1983). Re-purification confirmed the toxicity of this acidic toxin as well as a closely homologous non-toxin and the presence of yet another basic toxic activity (Mans *et al.* 2001). These proteins together with another highly abundant protein have been cloned and sequenced and shown to be part of the lipocalin family. It has also been suggested that these proteins could be involved in granule biogenesis (Mans *et al.* 2001). The toxins affect the cardio-vascular system rather than the nervous system, as is found in paralysis ticks (Mans *et al.* 2002). A factor Xa inhibitor has been identified, purified, characterized on kinetic level and has been cloned and expressed (Gaspar, Crause and Neitz, 1995; Gaspar *et al.* 1996; Joubert *et al.* 1998). Savignin, a thrombin inhibitor has been purified, kinetically characterized, cloned, sequenced and a molecular model has been proposed (Nienaber, Gaspar and Neitz, 1999; Mans, Louw and Neitz, 2002a). Apyrase, a ATP-diphosphohydrolase enzyme and platelet

aggregation inhibitor has been identified, purified, kinetically characterized and its disaggregation effect on aggregated platelets have been described (Mans *et al.* 1998a, Mans *et al.* 1998b, Mans *et al.* 2000). The savignygrins, a set of four platelet aggregation inhibitors proposed to target the platelet fibrinogen receptor, have been purified, characterized, cloned, sequenced, expressed and their relationship to the fXa and thrombin inhibitors elucidated (Mans, Louw and Neitz, 2002b; Mans, Louw and Neitz, 2002c).

1.6.1 Molecular evolution as mechanism of adaptation to a blood-feeding environment

Intrinsic to the word 'adaptation' is the notion of change, and applied to novel environments, the idea of acquisition of novel properties or functions. In biochemical terms, the study of the adaptation of organisms lies in the realm of molecular and protein evolution. As such adaptation entails the acquisition of novel protein functions. Several different modes for the acquisition of new protein function exist. An organism can utilize an existing function in a new way, for example, if apyrase had an intracellular function in the endoplasmic reticulum or Golgi-apparatus (Gao, Kaigorodov and Jigami, 1999; Zhong and Guidotti, 1999) and it acquires the signals for extracellular export, it might now also be involved in the regulation of platelet aggregation. Alternatively, a protein can through mutation acquire a novel function while still retaining its old function. This is referred to as gene sharing and such "moonlighting" proteins with multiple functions are discovered frequently (Jeffery, 1999). It has been estimated that there exists approximately a 1000-7000 different protein folds or topologies (Chothia, 1992; Orengo, Jones and Thornton, 1994). It has been predicted that there are at least 1709, 6241, 13601, 18424 and 40580 protein coding sequences in *Haemophilus*, yeast, fly, worm and human genomes (Rubin *et al.* 2000; Li *et al.* 2001). It should thus be clear that protein folds are utilized for more than one function. The problem that arises though, is how do new functions evolve from old folds? Protein function tends to be conserved, so that except for the case of gene sharing, proteins would not lose their original function to gain a new function. This phenomenon is referred to as purifying or negative selection in that any mutation that would be deleterious for protein function would be removed from the population. The answer to this lies in gene duplication, the single most important event in the generation of new protein functions (Ohno, 1970).

1.6.2 Gene duplication and the acquisition of novel protein function

Genes can be duplicated via unequal crossing-over during recombination, polyploidy (duplication of whole genomes), non-homologous chromosomal breakage and reunion or transposition (Maeda and Smithies, 1986). It has been estimated that gene duplication is a very common event during adaptive radiation (Ohno, 1970). In this regard, it has been estimated that there are at least 284, 1858, 8971, 5536 and 4519-15121 duplicated genes in the genomes of *Haemophilus*, yeast, fly, worm and humans, respectively (Rubin *et al.* 2000; Li *et al.* 2001). Gene duplication rates of 0.02-0.2 genes per million years have been estimated for different species, so that at least 50% of all genes in a genome are expected to duplicate and increase in frequency at least once every 35-350 million years. With a genome size of 15000 genes it can be expected that at least 60-600 duplicate genes arise in a pair of sister taxa per million years (Lynch and Conery, 2000). When genes duplicate and retain their original function, a whole set of the same genes form a multigene family that leads to expression of highly abundant proteins (such as histones) or high-level transcription (such as rRNAs). However, gene duplicates are normally functionally redundant at the time of origin and there are several possible outcomes for the evolution of such duplicate genes:

A) The vast majority of duplicated genes are silenced by deleterious mutations and the time it takes to silence a gene is considered to be relatively short (a few million years or less). B) Mutations in regulatory areas of the gene could lead to unique expression patterns in different tissues, where such a protein can acquire new functions due to a novel environment. C) During the acquisition of randomly sustained mutations, a duplicated redundant gene might acquire a novel, beneficial function that becomes fixed due to natural selection (Lynch and Conery, 2000).

The latter mode of functional acquisition has been described as the mutation during non-functionality model (MDN). It has been argued that this model is flawed and not supported by current evidence on gene duplication. It has been predicted that duplicated genes would be subjected to purifying selection, so that the "redundant" gene retains its function. In this case the rate of synonymous substitution always exceed that of non-synonymous substitution (Hughes, 1994). In order for new functions to evolve, positive selection would be needed so that the rate of non-synonymous to synonymous

substitution would be higher. It is expected that diversifying selection would operate shortly after gene duplication but would cease once a new function has evolved so that the genes would be subjected again to purifying selection. New models to account for the evolution of protein functions have been proposed:

A) New functions might first evolve (gene sharing) before the duplication event, as this would allow genes to each retain a function after duplication. A period of non-functionality as described for the MDN model is thus not required. Genes that do duplicate, which code for only one function, and are not subjected to purifying selection would thus be rapidly non-functionalized and become pseudogenes. B) A gene can also duplicate and insert into another gene sequence or be fused at the start or end of an existing gene. Hetero-multimeric proteins can form in this way, so that different functional domains are linked. Conversely, an internal-tandem duplication can lead to a homo-dimeric protein that contains two of the same structural domains. The duplicated domains can then either retain the same function or one domain can acquire a new one, leading to a multi-functional protein. Even here the protein that acquires the new function is postulated to go through a period of gene sharing. Gene duplication from individual domains can now take place to give single domain proteins with novel functions (Hughes, 1994). In these models positive Darwinian selection plays an important role in the evolution of novel protein functions. While this seems to contradict the now common accepted neutral theory of evolution, i.e. that random fixation of selectively neutral mutations is the predominant mode of evolution at molecular level (Kimura, 1983), there is really no contradiction, as the cases where duplicate genes assume separate functions will be in the minority of all gene duplications.

1.6.3 Orthologous genes

When a speciation event takes place, so that the same gene is now found in two distinct species, such "duplicated" genes are called orthologous genes. Orthologous genes represent the same phylogeny as is found for the organisms and can thus be used to construct species trees (Fitch, 2000). Proteins coded for by orthologous genes generally retain the same function and conserved structure. Due to functional constraints the ratio of nonsynonymous to synonymous substitution is usually a constant, low value. Identities in amino acid sequences of orthologous proteins are a good indication of

regions critical for structure or function. Functions for novel proteins that can be shown to be orthologs can thus be predicted with great confidence (Patthy, 1999).

1.6.4 Paralogous genes

Genes that duplicate and diverge in the same organism are called paralogous genes. Mixing of orthologous and paralogous genes can lead to a phylogenetic tree that has the correct sequence phylogeny, but does not indicate species phylogeny (Fitch, 2000). Generally paralogous genes change over time so that the encoded proteins have different functions although the same structural protein fold is retained. Residues that are essential for structure will be conserved, so that those regions that show marked differences are possible indications of new functional properties. Depending on the degree of divergence, paralogous proteins might have novel functions, while still retaining the original function. Predicting functions for novel paralogous proteins can be difficult and caution should be exercised when using homology to infer function. Because paralogous proteins generally diverge it can be difficult to detect distant homology with current homology-based methods and knowledge-based techniques might be needed to detect biological significant similarities (Patthy, 1999). Closely linked paralogous genes with significant similarity in sequence can undergo recombination, so that these genes evolve in a concerted fashion. This normally occurs close to the origin of duplication and ensures that divergence is slowed down, which reduces the chances for acquisition of new functions, but also protects redundant copies from rapid non-functionalization (Patthy, 1999). Paralogous genes in one species may thus share greater similarity than orthologous genes from different species, thereby complicating studies into the evolutionary relationships between proteins (Maeda and Smithies, 1986).

1.6.5 Alleles

Organisms that have more than one set of homologous chromosomes (diploid or polyploid) carry the same gene at the same chromosomal locus. If these genes differ due to mutation events, they are referred to as alleles. Due to sexual recombination, a population can consist of individuals that are either homozygous (same allele for a gene) or heterozygous (different alleles for a gene). The frequency of alleles in a

population is an indication of the polymorphism of such a population. When one allele is exclusively expressed in a heterozygous individual, such an allele is dominant, while the other non-expressed allele is recessive (Page and Holmes, 2000). If both alleles are expressed they are co-dominant. Depending on the frequency of different alleles in a population, protein isoforms that represent different alleles present in the population can be expected. Such isoforms can be encountered during a protein purification procedure so that care should be exercised when gene duplication events are considered.

1.6.6 Homology and analogy

Paralogous and orthologous genes are homologous. Homology indicates that two genes/proteins have descended from a common ancestor. In contrast, analogy indicates two genes that have descended convergently from unrelated ancestors. Two orthologous genes can independently attain a new function through divergence and as such be genetically homologous, but functionally analogous (Fitch, 2000). Homology is a term and the correct terminology to use when comparing protein sequences is to refer to percentage identity or similarity and not to percentage homology.

1.6.7 Detecting homology

Detecting homology is crucial when establishing the origins of novel protein function and when elucidating evolutionary adaptive mechanisms. Several criteria have been used to test whether two proteins are derived from a common ancestor: 1) similar DNA or protein sequences, 2) similar 3-D structures, 3) similar functions or protein-protein interactions. The criteria are in order of decreasing strength. If criterion 1 holds, the rest usually follows because similar sequences adopt similar structures and functions (Matthews *et al.* 1981). While this is the general case, care should be taken when inferring homology, as non-homologous proteins might either display similar functions or structures and cannot be considered to be strong evidence for homology on their own (Murzin, 1998). It should be clear that this problem is further compounded by the existence of paralogous proteins that have similar structures, but dissimilar functions.

1.6.8 Detecting homology by immunological means

The use of cross-reactivity between homologous proteins is an established method used to indicate sequence similarity and homology (Wilson, Carlson and White, 1977). It has been shown that the level of antigenic cross-reactivity correlate with the degree of similarity between two sequences (Van Regenmortel, Joisson and Wetter, 1993; Prager and Wilson, 1993). Immunological methods used to detect homology include microcomplement fixation, ELISA, immunoblotting and precipitin techniques. Microcomplement fixation can generally detect sequence identity above 70%, while ELISA and immunoblotting can detect sequence similarity between 30-40%, which is approximately the cut-off value for most orthologous proteins (Van Regenmortel *et al.* 1993). Care should however, be taken due to the fact that similar antigenic epitopes might occur in unrelated proteins. In this regard, immunoblotting after gel electrophoresis has the added advantage of identifying antigens also by their molecular masses and due to SDS and heat induced unfolding only sequence specific epitopes are detected and not conformational epitopes, that might be mimicked in various different sequences.

1.6.9 Detecting homology by database search

Pairwise alignments are normally used to determine the extent of identity or similarity between two proteins. To find similar proteins in the existing databases (SWISS-PROT or GenBank), a search tool such as BLAST (basic local alignment search tool) can be used, which employs a heuristic algorithm that can detect relationships between sequences which share only isolated regions of similarity (Altschul, 1990). Sequence databases are updated almost daily and share the sequence data submitted with other databases, so that they are in essence redundant and only differ in the way of annotation. Due to the size of sequence space, a sequence with significant similarity can be safely assumed to be a result of homology (Gogarten and Olendzenski, 1999). Problems arise in the "twilight zone" when sequence identity or similarity (20-35% sequence identity) is so low that alignment methods fail to indicate homology. Methods generally indicate homology above 30% sequence identity, while below 25% identity less than 10% are assigned homologous. However, the "more similar than identical" rule can be used to identify homologous proteins that fall into this area of false-positives and false-

negatives. Proteins that are homologous, normally have a higher similarity than identity, while the similarity and identity of non-homologous proteins does not significantly differ (Rost, 1999).

1.6.10 Detecting homology with multiple sequence alignment and phylogenetic analysis

Multiple alignments can be used to detect more distant relationships between proteins and possible motifs involved in structure or function. Used in conjunction with phylogenetic analysis this is a powerful method to investigate evolutionary relationships between homologous proteins. Closely linked to multiple alignment is the use of phylogenetic analysis to investigate possible evolutionary relationships between proteins. Thus, even if proteins are highly divergent, phylogenetic analysis can be used to infer homology.

1.6.11 Structure as means of detecting homology

Because structure evolves more slowly than sequence, protein structure is generally conserved even for highly divergent proteins. Assigning structures or folds to novel proteins by methods such as fold recognition by threading or molecular modeling can be valuable aids in detecting distant homology. The chances of finding a correct structure or fold is quite good, since the number of different protein-folds is limited and will improve as more protein structures are solved in the near future (Chothia and Lesk, 1986). However, the physico-chemical constraints of protein folding probably limited the number of protein folds in nature, so that different evolutionary families with unrelated functions can share a common structure. Consequently structural similarity do not necessarily imply homology (Todd, Orengo and Thornton, 1999). The same argument is valid for similar functions, but unrelated structure, so that structure as well as function should be considered when used to infer homology (Murzin, 1998). It has been shown that most similar structure pairs have less than 12% pairwise sequence identity, while the average sequence identity centered around 8%, which is comparable to sequence identities of unrelated proteins. In this "midnight zone", proteins could be similar due to convergent or divergent evolution. The levels of significant sequence identity and similarity that can be used to infer structural similarity depend on the alignment length of two sequences (Rost, 1997). Normally the longer the protein, the

lower the percentage identity that implies identical structure. The higher the percentage identity, the smaller would be the root mean square deviation (rmsd) of the coordinates of two structures. As a rule of thumb, RMSD values can be predicted for different levels of sequence identities: 80% (0.5-1.0Å), 40% (1.0-1.5 Å) and 20% (1.5-2.0 Å). Presently molecular modeling of novel sequences using known three-dimensional structures to obtain a structure model, can only be attained at higher than 25% sequence identity and structural models derived from lower identities should be treated with due caution if no other methods to detect homology are successful.

1.7 Aim of thesis

This thesis aims to look at adaptation of ticks to a blood feeding environment, in the light of gene duplication and gain/loss of protein function. Two protein families have been investigated. One concerns a family of platelet and blood coagulation inhibitors that possess the bovine pancreatic trypsin inhibitor fold (Part 1). The other family of proteins form part of the lipocalin family, which have diverse functions in the host, although evidence is presented of a universal function in tick salivary glands (Part 2).

PART 1

Evolution of soft tick anti-hemostatic factors of the BPTI-like superfamily

The subsequent three chapters discuss the characterization of the platelet aggregation inhibitor savignygrin and its relation to the BPTI-like anti-coagulants from the same tick species.

Chapter 2 focuses on the identification, cloning and sequence determination of the savignygrins, which exist as four conformational isoforms of which two are encoded by different genes. These proteins are shown to be homologous to disagregin, a platelet aggregation inhibitor previously described for *O. moubata*. The savignygrins possess a RGD motif that is absent in *O. moubata*.

Chapter 3 considers the cloning and molecular modeling of savignin, a thrombin inhibitor previously described for the tick *O. savignyi*. This inhibitor is shown to be homologous to ornithodorin, the thrombin inhibitor of *O. moubata*, for which a three-dimensional structure was described. Similar mechanisms of inhibition are predicted for these inhibitors. In addition, association between the separate domains of savignin is proposed, suggesting a dissociation step during binding to thrombin.

Chapter 4 investigates the evolutionary relationship between the platelet aggregation, thrombin and fXa inhibitors from *O. moubata* and *O. savignyi*. A model for the evolution of the respective inhibitor functions from a common ancestor is proposed and it is shown that savignygrin possesses a BPTI-like fold. The implications of this protein fold for the mechanism of action of savignygrin is considered and it is suggested that the RGD motif as well as downstream acidic residues are involved in integrin recognition.

Chapter 2: Characterization of savignygrin, a platelet aggregation inhibitor from the soft tick, *Ornithodoros savignyi* *

*Part of the work presented in this chapter has been accepted for publication in The Journal of Biological Chemistry (Mans, Louw and Neitz, 2002b).

2.1.1 Introduction: Integrins

Integrins are a family of adhesion receptors that propitiate cell-cell and cell-matrix interactions. Numerous physiological processes like hemostasis (receptors involved in platelet interaction with damaged vessel walls and platelet aggregation), fertilization (adhesion of sperm and oocyte), neuron-neuron interaction and inflammation (accumulation of leukocytes at affected sites) are mediated by integrins (Clemetson, 1998). The functional receptor is expressed as a transmembrane hetero-dimer assembled from various combinations of the 17α and 8β sub-units identified to date, forming the more than 20 current family members (Longhurst and Jennings, 1998; Plow *et al.* 2000). Integrins have different ligand specificities ($\alpha_2\beta_1$-collagen, $\alpha_5\beta_1$-fibronectin, $\alpha_6\beta_1$-laminin, $\alpha_v\beta_3$-vitronectin and $\alpha_{IIb}\beta_3$-fibrinogen), the latter which can also recognize fibronectin, vitronectin and von Willebrands factor. Most ligands recognized by integrins possess the recognition motif Arg-Gly-Asp (RGD) (Ruoslahti and Pierschbacher, 1987). Some ligands may also contain other sequences recognized by integrins, like the dodecapeptide sequence HHLGGAKQAGDV contained in the γ-chain of fibrinogen that binds to $\alpha_{IIb}\beta_3$ (Andrieux *et al.* 1989).

2.1.2 $\alpha_{IIb}\beta_3$ as model integrin

$\alpha_{IIb}\beta_3$ (GPIIbIIIa) is the most thoroughly characterized integrin and is the major integrin of platelets and the only adhesion receptor capable of mediating platelet aggregation by binding of fibrinogen or von Willebrands factor (Calvete, 1994; Calvete, 1995; Shattil *et al.* 1997; Plow *et al.* 2000; Plow *et al.* 2001). On resting platelets $\alpha_{IIb}\beta_3$ exists in an inactive conformation that binds irreversibly to the γ-chain C-terminal dodecapeptide (HHLGGAKQAGDV) of immobilized fibrinogen (Calvete, 1995). The unactivated form also has a ligand-binding site accessible to small molecules that contain RGD, KGD, RYD or OrnGD motifs, that are presented on mobile recognition loops protruding 14-17Å from the protein core (Calvete, 1995). The ligand-binding site can

also be reached by RGD-peptides that extend 11-32Å from the surface of polyacronitrile beads (Beer, Springer and Kohler, 1992). These results suggest that the binding-pocket in unactivated $\alpha_{IIb}\beta_3$ may resemble a narrow cavity buried 10-20Å below the protein surface (Calvete, 1995). Upon platelet activation by various agonists, $\alpha_{IIb}\beta_3$ undergoes a conformational change that allows binding of macromolecules containing the RGD-motif (Fig. 2.1). The ligand-binding site is probably discontinous and is formed by both α_{IIb} and β_3 subunits. It is speculated that there could be a divalent cation (Ca^{2+} ?) binding site inside the ligand-binding site that interacts with ligands containing aspartic acid residues, such as contained in the RGD motif (Calvete, 1994; Plow *et al.* 2000). A ternary complex between RGD ligand and the receptor-bound divalent cation may be formed, until stabilization of the RGD-integrin interaction, whereupon the divalent cation is displaced (D'Souza *et al.* 1994). Investigations into the secondary structure of the RGD motif using GRGDSP peptides predict that it occurs as a highly ordered and unusual structure that exhibits a double β-bend nature, which could provide the necessary conformational restraints to bind to cell-surface adhesion receptors (Reed *et al.* 1988).

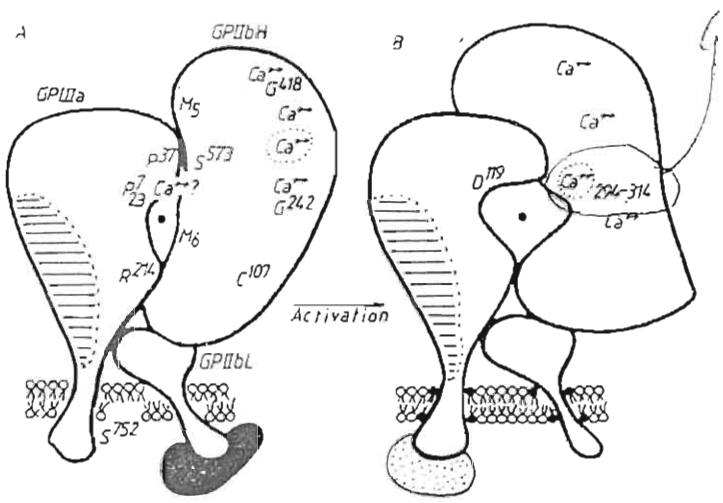

Fig. 2.1: Activation dependent conformational change of $\alpha_{IIb}\beta_3$. The buried ligand-binding site of $\alpha_{IIb}\beta_3$ in resting platelets (A), are exposed after platelet activation (B). The ligand-binding site as well as the putative cation-binding site is indicated by the dot. The circled Ca^{++} site around 294-314 indicates the binding site for the γ-chain fibrinogen C-terminal peptide. Adapted from Calvete (1994, 1995).

2.1.3 Snake venom disintegrins as platelet aggregation inhibitors

Inhibitors specific for integrins are useful for the study of integrin function and for the development of pharmaceutical compounds. The disintegrins identified in snake venom are the most extensively characterized $\alpha_{IIb}\beta_3$ antagonists. Their function is the maintenance of hemorrhage through inhibition of platelet aggregation, mediated by interaction with $\alpha_{IIb}\beta_3$, thereby preventing fibrinogen binding (Huang, 1998). Disintegrins are a family of low molecular weight (5400-9000 Da) proteins that contain the RGD motif, except for barbourin (Scarborough *et al.* 1991). Most disintegrins inhibit platelet aggregation with IC_{50} values 3000-30 000 times lower (nM range) than the tetra peptide RGDS (μM range) (Gould *et al.* 1990). The three dimensional structures (Fig. 2.2) of the *Viperidae* (viper) snake venom disintegrins echistatin, kistrin, flavoridin, dendroaspin (mambin) from *Elapidae* (mamba) and the leech derived decorsin show no classical secondary structure (Adler *et al.* 1991; Saudek, Atkinson and Pelton, 1991; Senn and Klauss, 1993; Krezel *et al.* 1994; Sutcliffe *et al.* 1994), but rather a dense core, consisting of β-turns kept intact by disulphide bonds, with a protruding hairpin-loop region that presents the RGD motif (Huang, 1998).

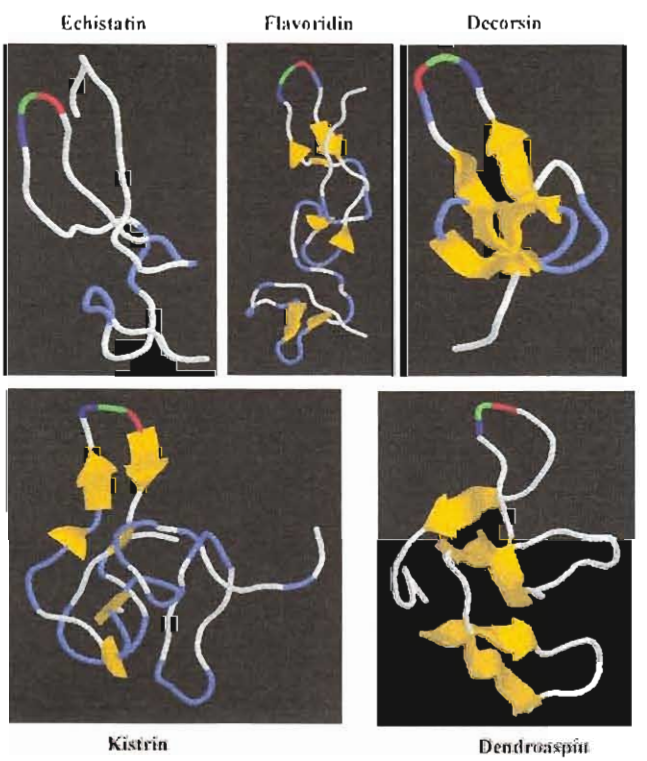

Fig. 2.2: Three-dimensional structures of $\alpha_{IIb}\beta_3$ antagonists. Antagonists from the *Viperidea* (echistatin, kistrin, flavoridin) and *Elapidae* (dendroaspin) snake venoms and leech-derived decorsin. The RGD sequence is colored in blue (Arg), green (Gly) and red (Asp), respectively.

The spatial configuration of the RGD motif at the end of the loop and the flanking sequences have been found to be important contributors to specificity for different integrins (Gould *et al.* 1990; Scarborough *et al.* 1993). The structural differences between the different snake venom inhibitors emphasize that their inhibitory activities are solely determined by the appropriate presentation of the RGD sequence (McDowell *et al.* 1992).

Disintegrins are classified as a protein family based on alignment of sequences by conserved cysteines (Huang, 1998). Only a certain set of proteins from the *Viperidiae* snake family fall in this rigid classification scheme (Fig. 2.3). *Elapidae* snake venom-derived (mambin), leech-derived (decorsin and ornatin) and tick-derived (variabilin and disagregin) inhibitors do not fall into this aligned family (Huang, 1998; Wang *et al.* 1996; Karczewski, Endris and Connolly, 1994). It can be expected that more diversification of this classification scheme will follow as more non-snake derived inhibitors are identified.

Fig. 2.3: Amino acid sequences of different $\alpha_{IIb}\beta_3$ antagonists. Disintegrins from the *Viperidae* family are similar, while dendroaspin from *Elapidae* snake venom have a totally different sequence and conformation. Leech-derived decorsin and ornatin shows similarity, while both tick-derived inhibitors (disagregin and variabilin) are unique. RGD sequences are boxed in grey and cysteines are shown in bold. Adapted from Huang, 1998.

2.1.4 Tick-derived $\alpha_{IIb}\beta_3$ antagonists

No homology exists between the tick-derived $\alpha_{IIb}\beta_3$ antagonists. Variabilin, from the hard tick, *Dermacentor variables*, contains a RGD motif, not flanked by cysteine residues, while disagregin from the soft tick *Ornithodoros moubata*, contains no RGD sequence (Wang *et al.* 1996). Disagregin does however, inhibit the binding of the RGD containing peptide echistatin, which suggests that its binding site could be in close proximity to the RGD-binding site on $\alpha_{IIb}\beta_3$. In addition, the γ-fibrinogen sequence HHLGGAKQAGDV competes with its binding to soluble $\alpha_{IIb}\beta_3$, indicating an inhibition mechanism distinct from the disintegrins as well as possible multiple binding sites (Karczewski, Endris and Connolly, 1994; Karczewski and Connolly, 1997). It has not been determined whether the RED sequence of disagregin, might play a role in its mechanism of action. Closely related homologues could thus provide important information on its mechanism of action if conserved regions necessary for function can be identified. With this in mind, a homologue (designated savignygrin) from the tick, *O. savignyi* was purified.

2.2 Materials and methods

2.2.1 Chemicals used

All materials were of analytical grade and deionized water was used in all experiments. Tris(hydroxymethyl) aminomethane (Tris), NaCl, ascorbic acid, ethylene diamine tetra-acetic acid (EDTA), $HgCl_2$, sodium azide, methanol, acetic acid, glycine, ammonium persulphate and N,N,N',N'-tetramethyl-ethylenediamine (TEMED) were obtained from Merck, Darmstadt, Germany. $CaCl_2$, $MgCl_2$, ethylene-bis(oxyethylene nitrilo) tetra-acetic acid (EGTA) was from BDH Chemicals Ltd. Poole, England. ADP-di(monocyclohexylammonium) salt, diethyl pyrocarbonate (DEPC), dithiothreitol (DTT), fibrinogen, p-nitrophenol and tris(hydroxymethyl) aminomethane (tricine) were obtained from Sigma Chemical Co., USA). Human $\alpha_{IIb}\beta_3$, α-thrombin, activated fXa and plasmin were obtained from Enzyme Research Laboratories, Inc. (South Bend, OR, USA). Microtitre plates were obtained from Bibby Sterilin, UK. Low molecular weight marker proteins were purchased from Pharmacia, USA and acrylamide, bisacrylamide, sodium dodecyl sulphate (SDS) from BDH Laboratory Supplies LTD., England. Coomassie Brilliant Blue was obtained from Bio-Rad Laboratories, USA and the Protein Assay Kit from Pierce, USA. Primers used were synthesized by GIBCO BRL

Custom Primers (Life Technologies) or Integrated DNA Technologies and resuspended at 100 pmole/μl in 20% acetonitrile and stored at –20 °C. Final concentrations were confirmed by spectrophotometric measurement at 260 nm. Isopropyl β-D-thiogalactopyranoside (IPTG), 5-bromo-4-chloro-3-indolyl β-D-galacto-pyranoside (X-gal) and RNAse were obtained from Roche Diagnostics. Yeast extract and tryptone were purchased from Oxoid Ltd. (Basingstoke, Hampshire, England).

2.2.2 Collection of ticks and preparation of salivary gland extract (SGE)

Ticks were collected from the North Western Province area of South Africa by sifting of sand. The salivary glands were obtained by dissection (Mans *et al.* 1998a). Female ticks were embedded in molten wax with their dorsal parts visible. The integument was then removed by lateral dissection of the cuticle with a #11 scalpel under a 0.9% NaCl solution using a binocular stereomicroscope (10x magnification). Salivary glands were removed with fine forceps, frozen in liquid nitrogen and stored at -70 °C. A stock solution of salivary gland extract was prepared by resuspension of 12 salivary glands in 500 μl buffer solution (20 mM Tris-HCl, 0.15M NaCl pH 7.6 at 25 °C). Resuspended glands were sonified with a Branson sonifier cell disrupter B-30 (Branson Sonic Power Co.) for 3x6 pulses at 30% duty cycle and an output control of 3, while keeping the solution on ice. Extracts were centrifuged in a microfuge (10 000xg for 5 min) and the supernatant used for further studies.

2.2.3 Measuring platelet aggregation using an aggregometer

Platelet aggregation studies using an aggregometer were performed as described (Mans *et al.* 1998a) to monitor inhibition of platelet aggregation induced by ADP (10 μM), collagen (40 μg, Diagnostica Stago), thrombin receptor activating peptide (TRAP, 50 μM, Sigma) and epinephrine (10 μM, Dioagnostica Stago). Aggregation of platelets was monitored using the photometric method of Born and Cross (1963). Fresh blood was collected in Vacutainer tubes containing a citrated buffer solution (0.109 M), from human donors using no substances known to inhibit platelet aggregation, such as alcohol, garlic and aspirin for at least two weeks prior to donation. Platelet rich plasma (PRP) was prepared by centrifugation (170xg for 10 min) and plasma was collected in plastic tubes. Platelet poor plasma was prepared by further centrifugation of the remaining blood from the platelet rich plasma at 2700xg for 15 min. Platelet rich plasma

was diluted to a final count of 300 x 10^9 l^{-1} using a Coulter counter. Savignygrins (20 μl at indicated concentrations) or 20 μl saline solution as control were pre-incubated with 400 μl of the diluted platelet rich plasma for 5 minutes to monitor for spontaneous aggregation. Platelet poor plasma (PPP) was set at 100% transmission and PRP at 0% transmission. Aggregation was then induced by adding 20 μl of different agonists to the PRP.

2.2.4 Disaggregation of aggregated platelets by savignygrin

It has been shown that apyrase can disaggregate aggregated platelets (Mans *et al.* 2000). To investigate whether the savignygrins could have a disaggregation effect on aggregated platelets, platelets were aggregated with 10 μM ADP for 4 minutes before their addition (41 μM final concentration). Platelets were allowed to disaggregate for a further 4 minutes. As controls, platelets were also incubated with savignygrin without addition of ADP or before addition of ADP. Platelets were also analyzed with or without the addition of ADP in the absence of savignygrin. All preparations were incubated for 8 minutes. Further analyses were conducted using electronmicroscopy (Mans *et al.* 2000).

2.2.5 Electron microscopical analysis of platelet disaggregation by savignygrin

Platelets were collected by centrifugation in 0.1% glutaraldehyde (0.075M phosphate buffer pH 7.5) before fixing in 1% glutaraldehyde (phosphate buffer) for 2 hours. Platelets were secondary fixed in OsO_4 before sequential dehydration in ethanol. For scanning electron microscopy (SEM), platelets were critical point dried and gold sputter coated before viewing in a JEOL 840 SEM (WD 16 mm, 5 keV, 4000X magnification). For transmission electron microscopy (TEM), platelets were infiltrated with Quetol resin and 100 nm thick sections were prepared using a microtome. Sections were contrasted with lead citrate and uranyl acetate before viewing with a Philips 301 TEM.

2.2.6 Platelet aggregation assay using a micro-plate method

For monitoring of anti-platelet activity during purification and also for IC_{50} determination of ADP-induced platelet aggregation, a microplate assay was used (Bednar *et al.* 1995). PRP was prepared as described and 100 μl was used per

microplate well. Savignygrins or saline (10 μl of indicated concentrations) were added and left to incubate for 3 minutes before addition of 10 μl ADP (10 μM final concentration). Aggregation was allowed to proceed for 10 minutes, before absorbance was measured at 620 nm in a microplate reader (Titertek). Platelet suspensions were stirred with a Titertek® microplate shaker (Flow Laboratories) set at a speed of 5 during the expreriment.

2.2.7 Inhibition of binding between monoclonal antibody P2 (α-CD41) and platelets by savignygrin

Monoclonal antibody P2 has been shown to interact specifically with α_{IIb} (CD41) of the intact $\alpha_{IIb}\beta_3$ complex (McGregor *et al.* 1983). Inhibition of P2 binding to platelets was assayed using flow cytometry (Liu *et al.* 1994). Platelet poor plasma (PPP) was prepared and used to dilute platelet rich plasma (PRP) to a count of $300x10^9$ platelets/liter. PRP (20 μl), savignygrin (20 μl, at various concentrations) and 150 μl Tyrode buffer (0.4 mM NaH_2PO_4, 0.4 mM NaCl, 136.9 mM NaCl, 2.7 mM KCl, 11.9 mM $NaHCO_3$, 0.5 mM $CaCl_2$, pH7.4, 3.5 mg/ml BSA) were incubated for 30 minutes at room temperature in the presence or absence of ADP (20 μM final concentration). P2-FITC conjugated mAb (10 μl, Immunotech, Coulter) was added and incubated for 30 minutes at room temperature. The unfixed platelet solution (120000 platelets/10μl) was diluted to 500 μl with Tyrode buffer before analysis with an Epics2 flow cytometer (Coulter Electronics, Inc.) by measurement of 10000 events. Fluorescent measurement was gated to count intact, non-aggregated platelets (3-5 μm diameter). Three separate experiments were used to determine the mean fluorescence.

2.2.8 Inhibition of $\alpha_{IIb}\beta_3$ binding to immobilized fibrinogen by savignygrin

The binding of $\alpha_{IIb}\beta_3$ to fibrinogen was performed as described (Seymour *et al.* 1990). ELISA plates were coated overnight with 100 μl fibrinogen (10μg/ml in 20 mM Tris-HCl, pH 8.5) before blocking with 100 μl block buffer (20 mM Tris-HCl, pH 7.4, 0.12 M NaCl, 2 mM $CaCl_2$, 0.05% Tween 20, 0.5% BSA) for 1 hour. Wells were washed 3X with 100 μl block buffer before 50 μl of savignygrin (at various concentrations) were added to each well followed immediately by 50 μl of purified $\alpha_{IIb}\beta_3$ (40 μg/ml, Enzyme Research Laboratories). ELISA plates were incubated for 2 hours before washing wells

with block buffer (3X) and incubating wells for 1 hour with 100 µl P2-FITC (50X dilution from stock), followed by washing 3X with block buffer. Block buffer (100 µl) was added to wells and fluorescence measured using a Fluoroscan Ascent FL (Thermo Labsystems) with excitation at 485 nm and emission at 438 nm. Background was subtracted using wells with no $\alpha_{IIb}\beta_3$.

2.2.9 Inhibition of osteosarcoma cell adhesion by savignygrin

The specificity of the savignygrins for integrins was investigated using the osteosarcoma cell line MG-63, known to express the integrin $\alpha_v\beta_3$ which binds to vitronectin and fibrinogen (Stuiver, Ruggerri and Smith, 1996). Adhesion studies were perfomed as described (Wang *et al.* 1996). Cells were cultured in 90% Dulbecco's modified Eagle's medium (DMEM), supplemented with 2 mM L-glutamine and 10% heat inactivated fetal calf serum (FCS). Cells at 60% confluence were trypsinized (0.25% trypsin, 3 mm EDTA in phosphate buffered saline) at 37°C, 4 min, before neutralization with DMEM/FCS. Cells were pelleted at 120xg (5 min), resuspended in DMEM/FCS and were incubated at 37°C (30 min) before centrifugation (120xg, 5 min). Cells were then suspended in serum free DMEM at $2x10^5$ cells/ml and incubated with various concentrations of savignygrin for 30 min at 37°C. This mixture (100 µl) was added to ELISA plate wells pre-coated overnight with 1µg/ml vitronectin (Sigma Co., USA) or fibrinogen (Sigma Co., USA) and incubated for 2 hours at 37 °C. Wells were washed 3X with wash buffer (20 mM Tris-HCl, pH 7.4, 2 mM $CaCl_2$, 0.12M NaCl) before staining with 0.1% bromophenol blue in 1% acetic acid for 1 hour. Wells were then washed 3X with 1% acetic acid before air drying. Bromophenol blue was eluted with 100 µl buffer (50 mM Tris-HCl, pH 9.2) before absorbance was measured at 595 nm.

2.2.10 Inhibition of platelet adhesion to fibrinogen

Adhesion of platelets to fibrinogen was performed as described previously (Keller *et al.* 1992). The same coating procedures for fibrinogen (section 2.2.9) were followed, but 100 µl PRP ($2-3X10^8$ platelets/ml) was added to wells. Savignygrin (10 µl at various concentrations) was added and platelets were incubated for 2 hours at room temperature. Wells were washed with block buffer before lysis with reaction buffer (20

mM citrate, pH 5.5, 0.1% Triton X-100, 10 mM p-nitrophenol). The reaction was allowed to proceed at room temperature and absorbance was measured at 340 nm in a microplate reader (Titertek) every hour, until an adequate reading was obtained.

2.2.11 Temperature stability of savignygrin

Savignygrin (14 μg protein in 300 μl 20 mM Tris, 0.15M NaCl, pH 7.4) was incubated at 94 °C for different time periods and immediately placed on ice for 10 minutes before centrifugation (14000xg for 15 minutes at room temperature), followed by measurement of platelet aggregation inhibitory activity. Activity was measured relative to untreated inhibitor.

2.2.12 High performance liquid chromatography (HPLC)

Beckman instrumentation was used for all HPLC work, which consists of two pumps (module 110B), an analog interface for control of solvent delivery from the pumps (module 406), a UV detector (module 166) and a Beckman 340 organiser with injector. This hardware was controlled using Beckman System Gold software (1987).

2.2.13 Size exclusion HPLC (SEHPLC)

Salivary gland extract (40 salivary glands, ~1600 μg protein) were prepared, filtered through a 0.22 μm filter (Millex GV4, Millipore Corporation, USA) and applied to a size exclusion column ($G2000SW_{XL}$, 7.8mm x 30 cm, TosoHaas, USA). Isocratic conditions (20 mM TrisHCl, 0.15 M NaCl pH 7.6, flow speed: 1 ml/min, A_{280}) were used during SEHPLC. Prior to application onto the size exclusion column, buffers were filtered through 0.22 μm membranes (Millipore Corporation, USA). The column was calibrated using molecular mass markers and a physiological saline buffer (20 mM Tris-HCl, 0.15 M NaCl, pH 7.6) for elution. Molecular mass markers used were aldolase (158 kDa, 0.1 mg/ml), bovine serum albumin (BSA) (67 kDa, 0.1 mg/ml), ovalbumin (43 kDa, 0.1 mg/ml), chymotrypsin (25 kDa, 0.05 mg/ml) and ribonuclease (13.5 kDa, 0.1 mg/ml). Markers were obtained from Pharmacia. SGE was applied to the column and 1 ml fractions were collected and assayed for platelet aggregation inhibitory activity.

2.2.14 Anion exchange HPLC (AEHPLC)

Fractions from SEHPLC were dialyzed against water (Slide-A-Lyzer cassettes, 10kDa molecular weight cutoff, Pierce) for two hours prior to application onto an anion exchange column (DEAE-5PW, 7.5 mm x 7.5 cm, TosoHaas). Proteins were fractionated using a gradient system (flowspeed: 1ml/min, A_{280}) with buffer A (20 mM Tris-HCl, pH 7.6) and buffer B (20 mM Tris-HCl, 1 M NaCl, pH 7.6) as set out in Table 3.3. Proteins with known iso-electric points were used as standard markers. These were, apo-transferrin (pI~5.9, 1mg/ml), β-lactoglobulin (pI~5.14, 1 mg/ml) and chicken egg ovalbumin (pI~4.6, 1 mg/ml) obtained from Sigma, USA. Fractions (1 ml) were collected and assayed for enzyme activity.

Table 2.1: Flow conditions used during AEHPLC.

Time (min.)	Flow (ml/min.)	% Buffer B	Duration (min.)
0	1	0	5
5	1	60	21
26	1	100	10
36	1	0	0.5
36.5	1	0	10
46.5	END		

2.2.15 Reversed phase HPLC (RPHPLC)

Fractions from AEHPLC were desalted and fractionated using RPHPLC (Jupiter 5μ C5 300 Å, 4.6 mm x 25 cm, Phenomenex, USA, flowspeed: 1ml/min, A_{280} or A_{230}). Elution was achieved with a gradient of buffer A (0.1% TFA, 0.1% acetonitrile) and buffer B (0.1% TFA, 60% acetonitrile) from 0-100% over 60 minutes. Peaks collected were dried in a vacuum concentrator (Bachoffer), rechromatographed on AEHPLC and desalted with RPHPLC.

Table 2.2: Flow conditions used during RPHPLC.

Time (min.)	Flow (ml/min.)	% Buffer B	Duration (min.)
0	1	0	5
5	1	100	60
60	1	100	10
70	1	0	0.5
70.5	1	0	10
80.5	END		

2.2.16 Quantitation of proteins

Total protein of SGE was determined with the method of Bradford (1976), using the Pierce Coomassie Protein Assay kit (Pierce, USA). BSA was used as standard reference protein. Standard protein or sample (150 μl) were pipetted into a microtitre plate well and 150 μl of the Coomassie Protein Assay Reagent added. The microplate was shaken for 10 minutes before reading the absorbance at 620 nm with a SLT 340 ATC scanner (SLT Labinstruments). Determinations were performed in triplicate. Purified proteins were quantitated using amino acid analysis.

2.2.17 Amino acid analysis

Amino acid analysis was performed according to the PICO-TAG method (Bidlingmeyer, Steven and Tarvin, 1984). Protein was dried in pyrolized hydrolysis tubes (PICO.TAG system) and placed in a larger glass vessel that contained 200 μl of 6M HCl, 7% thioglycolic acid solution and flushed with N_2 and evacuated prior to incubation at 110 °C for 24 hours. After hydrolysis the amino acids were extracted three times from the membranes using 50 μl of 30% methanol, 0.1 M HCl while drying the extracts each time under vacuum. Derivatization of the amino acids was performed by adding 10 μl of a 2:2:1 mixture of methanol: water: triethylamine which was then dried again under vacuum before adding 20 μl of a mixture of 7:1:1:1 methanol: water: triethylamine: phenylisothiocyanate (PITC). This was left at room temperature for 20 minutes before the unreacted PITC was removed under continuous vacuum for 1 hour. Standard PITC-amino acid mixture (Waters) or samples were solubilized in 200 μl 10% Na_2HPO_4, 5% acetonitrile buffer and the pH was adjusted to 7.4 with 10% H_3PO_4. Samples were filtered through a 0.45 μm membrane before 20 μl of standard or sample was injected onto the column. A reversed phased column (PICO-TAG, 3.9 mm x 150 mm,Waters) was used for the separation of the amino acids with 0.14 M sodium acetate, pH 5.7 for Buffer A and 60% acetonitrile for Buffer B. Gradient elution was used as set out in Table 3.4 and elution was monitored at 254 nm. The results were analyzed using Beckman System Gold software.

Table 2.3: HPLC gradient conditions for amino acid analysis.

Time (min.)	Flow (ml/min.)	% Buffer B	Duration (min.)
0	1	10	10
10	1	51	0.5
10.5	1	100	2.2
12.7	1.5	100	0.5
13.2	1.5	10	7.5
20.7	END		

2.2.18 Total cysteine determination by performic acid oxidation

Performic acid was prepared by adding H_2O_2 (10 µl) to formic acid (90 µl) and incubating the mixture at room temperature for 1 hour with regular vortexing. Protein samples (pyrolized tubes) and performic acid were then incubated on ice (30 min). Performic acid (20 µl) was added to each sample, mixed thoroughly and incubated for 16 hours at 4 °C. Octanol (20 µl) was added, followed by addition of HBr (7.5 µl), a vortex step and incubation on ice (30 min). The samples were evaporated under nitrogen gas and normal amino acid analysis procedures described above were then followed.

2.2.19 Alkylation of cysteines with 4-vinyl pyridine (4-VP)

Inhibitor (250 pmole) was denatured with 8M guanidinium chloride (GdCl, 250 µl) for 2 hours in the presence or absence of 4% DTT, before addition of 2 µl 4-VP (Sigma, St. Louis, MO, USA). Mixtures were incubated for 2 hours and alkylated protein was desalted using RPHPLC and vacuum dried before amino acid analysis, activity measurements and N-terminal sequence determination.

2.2.20 Tryptophan determination by methanesulfonic acid (MSA) hydrolysis

MSA (20 µl, 4M containing 0.2% w/v tryptamine HCl) was added to protein in pyrolyzed hydrolysis tubes. The tubes were added to a larger vessel containing water (100 µl) and evacuated. Hydrolysis was performed at 110 °C (24 hours). After hydrolysis the vial was cooled to room temperature and the MSA neutralized with 4 M KOH (22 µl), before drying under vacuum. Amino acids were extracted, derivatized and identified as described in section 2.2.13.

2.2.21 N-terminal sequence analysis

N-terminal sequence analysis of ~1 nmole alkylated protein was performed in a gas phase amino acid sequencer (Hewick *et al.* 1981) modified as described (Brandt *et al.* 1984), at the sequence facility of Prof. W.F. Brandt (Department of Biochemistry, University of Cape Town).

2.2.22 Tricine sodium dodecyl sulphate polyacrylamide gel electrophoresis (SDS-PAGE)

Purified proteins were analyzed using a tricine SDS-PAGE system (Schägger and von Jagow, 1987) that is suitable for resolution of proteins in the range of 1-100 kDa. A 16.5%T, 3%C separating gel (1 M Tris-HCl, 0.1% SDS, pH 8.45) and a 4%T, 3%C stacking gel (0.75 M Tris-HCl, 0.075% SDS, pH 8.45) were prepared from acrylamide (48% acrylamide/ 1.5% N', N'-methylene bisacrylamide) and electrophoresis buffer (3M Tris-HCl, pH 8.45, 0.3%SDS) stock solutions. These solutions were degassed for 30 minutes and polymerized by addition of 50 μl of 10% ammonium persulphate and 5 μl of TEMED.

Protein was diluted 1:4 in reducing buffer (0.06 M Tris-HCl, pH 6.8, 2% SDS (w/v), 0.1% glycerol (v/v), 0.05% β-mercaptoethanol (v/v) and 0.025% bromophenol blue (w/v) and boiled at 94 °C for 4 minutes. Low molecular mass and peptide mass markers were used for mass determination. The low molecular mass markers were phosphorylase b (94 kDa), BSA (67 kDa), ovalbumin (43 kDa), carbonic anhydrase (30 kDa), trypsin inhibitor (20 kDa) and α-lactoalbumin (14.5 kDa). Peptide mass markers are fragments from a cyanogen bromide digestion of myoglobin to give a ladder of masses as indicated in results. Electrophoresis was carried out with anodal buffer (0.2M Tris-HCl, pH 8.9) and cathodal buffer (0.1M Tris-HCl, 0.1M Tricine, 0.1% SDS, pH~8.2 with no adjusting of pH) using a Biometra electrophoresis system (Biometra, GmbH) with an initial voltage of 60 V for 45 minutes and then a voltage of 100 V until the bromophenol blue front reached the bottom of the gel.

2.2.23 Staining of SDS-PAGE gels

Savignygrins eluted from the gel under non-reducing conditions and normal methanol (40%), acetic acid (10%) fixation. Gels were thus fixed by washing steps in several

fixatives (Phoeling and Neuhoff, 1981). Solution A (30% methanol, 3.4% sulphosalicylic acid di-hydrate, 5.7% trichloroacteic acid): 15 min, solution B (50% methanol, 0.12% acetic acid): 30 min, solution C (5% methanol): 2 X 15 min, solution D (10% glutardialdehyde): 30 min, solution C: 3 X 30 min. Proteins were visualized by staining in 0.1% Coomassie Brilliant Blue (40% methanol, 10% acetic acid) and were destained in an excess of destaining solution (50% methanol, 10% acetic acid).

2.2.24 Tricine SDS-PAGE in the presence of urea

Unfolding of inhibitors in the presence of urea was investigated by including 8 M urea in the tricine separating gel, or by using a gradient of 0-8 M urea perpendicular to the direction of electrophoresis (Goldenberg and Creighton, 1984).

2.2.25 Electrospray mass spectrometry (ESMS)

Molecular masses of the native or alkylated inhibitors were determined using electrospray mass spectrometry (ESMS) by Dr. M.J. van der Merwe (Department of Biochemistry, University of Stellenbosch). A VG Micromass Quattro triple quadropole mass spectrometer equipped with an electrospray ionisation source was used (Micromass, UK). Capillary voltage (3.5 kV) was applied in the positive mode with source temperature 80 °C, cone voltage 70 V and skimmer lens at 5 V. Proteins (~300 pmoles) were dissolved in 50% acetonitrile/0.1% formic acid (100 µl) and injected (10 µl) into a stream of 50% acetonitrile at flow speed of 10 µl/min, supplied from a LKB/Pharmacia 2249 gradient pump. Data was aquired in the continuum mode, scanning from m/z 500-2000 at 100 amu/second. Horse heart myoglobin was used to calibrate the instrument before analysis.

2.2.26 Peptide mapping using matrix assisted laser desorption ionisation time of flight mass spectrometry (MALDI-TOF-MS)

Peptide mapping was performed at the mass spectrometry unit (Department of Biochemistry University of Cape Town). Protein (10 µg) was digested with trypsin (1:10) for 4 hours at 37 °C in digestion buffer (100 mM sodium carbonate pH 8.2, 2mM $CaCl_2$). Digested protein (5 pmole) was crystallized in an equal volume of α-cyano-4-hydroxycinnamic acid matrix before analysis with a DE-PRO MALDI-TOF (Perseptive

Biosystems, USA) mass spectrometer with a laser intensity of 1200, accelerating voltage (20000), grid voltage (91-92%) and guide wire voltage (0.1%) using a linear flight path. The spectrometer was calibrated using a calibration mixture of external standards and forty to sixty scans were averaged.

2.2.27 Origins of (+) and (-) forms: alleles or gene duplicates

The possibility that the (+)/(-) forms might be alleles was considered. To test this hypothesis, SGE from twenty individuals were heat treated (60°C, 10 minutes), before separation with RPHPLC. Savignygrin fractions were analyzed using non-reducing tricine SDS-PAGE.

2.2.28 Total RNA purification

Whole nymphae (0.2g) were ground up in the presence of liquid nitrogen, while salivary glands (120 glands) from female *O. savignyi* ticks were dissected as described previously and immediately transferred to 750 µl of TRI-REAGENT® (Molecular Research Center, INC). Total RNA was isolated according to the manufacturer's instructions. The RNA was dissolved in FORMAzol® (Molecular Research Center, INC) and stored at –20 °C. The purity of the RNA was determined by measurement of the 260/280 nm ratio which gave values of 1.24-1.29 for salivary gland preparations and 1.53-1.65 for mouse lung preparations. RNA quality was assessed by electrophoresis on a 1% agarose gel prepared in 40 mM MOPS, 10 mM sodium acetate, 1 mM EDTA, 18 % formaldehyde (Sigma) and DEPC treated ddH_2O. RNA samples were prepared in 40 mM MOPS, 10 mM sodium acetate, 1 mM EDTA, 20% formaldehyde, deionized formamide (Gibco, BRL) in DEPC treated, double distilled deionized water. Electrophoresis was conducted at 70 V for 30 minutes. RNA was quantified by spectrophotometric measurement at 260 nm, which gave a final concentration of 80 µg/ 20 µl for salivary glands, 106 µg/ 20µl for nymph and 93 µg/ 20 µl for mouse lung.

2.2.29 cDNA synthesis from total RNA

Single-stranded cDNA, was prepared using Superscript™ II (Life Technologies) and the anchor-dT primer (Table 2.4) (Joubert *et al.* 1998). Total RNA (0.5 µl – 2 µg) in 7.5µl DEPC treated H_2O was denatured at 70 °C for 3 minutes and snap cooled on ice. Five pmoles anchor-dT primer (1 µl), 3 µl DTT (0.1 M), 200 units of Superscript™ II

(1μl), 4μl 5X first strand buffer (250 mM Tris-HCl, 375 mM KCl, 15 mM $MgCl_2$, pH 8.3) was added and incubated at 42 °C for 60 minutes before inactivation at 70 °C (2min). Single-stranded cDNA was stored at –20 °C until used. Double stranded full-length cDNA was prepared with the Marathon cDNA amplification kit (ClonTech) according to the manufacturers instructions. Total RNA (4 μg) was used for synthesis and first strand cDNA was synthesized with the anchor primer (10 pmole) described above.

2.2.30 Rapid amplification of 3' cDNA ends (3'RACE)

To obtain the coding gene and 3' untranslated region (3' UTR) a degenerate primer (GrinA) was designed from the first seven amino-acids (YQPECLE) obtained by Edman degradation, using the program OLIGO Version 4.0 (National Biosciences, Hamel, USA) (Rychlick and Rhoades, 1989). Single-stranded cDNA (0.5 μl of the previously described single strand cDNA stock), GrinA (100 pmole- 1 μl), anchor primer (5 pmole – 1 μl), 5μl 10X PCR buffer (100 mM Tris-HCl, 500 mM KCl, pH 8.3), 4 μl $MgCl_2$ (2 mM final concentration) and 4 μl dNTP's (200 μM final concentration) were adjusted to 40 μl with H_2O. cDNA was denatured at 94 °C (3 minutes) and then cooled to 80 °C after which 0.5 μl TaKaRa Taq™ (5U/μl, TAKARA Biotechnology) diluted in 10 μl H_2O was added. Amplification consisted of 34 cycles of DNA denaturation (94 °C, 30s), annealing (55 °C, 30s) and extension (72 °C, 2 minutes), followed by a final extension (72 °C, 7 minutes). All amplification procedures were conducted in a Gene Amp® PCR System 9700 (Perkin Elmer Applied Biosystems).

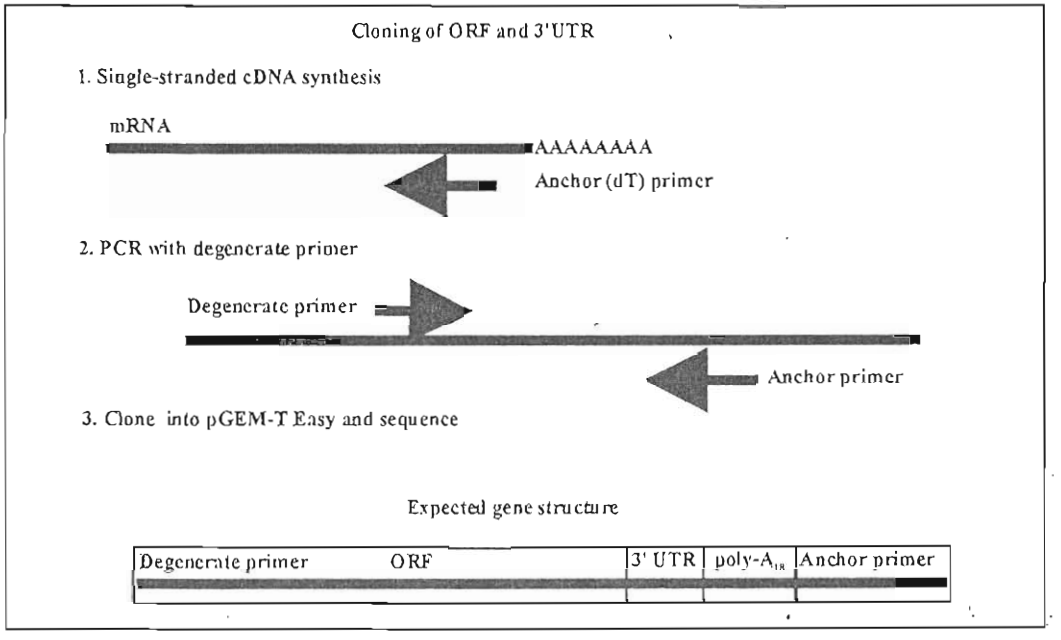

Fig. 2.4: Cloning strategy to obtain ORF and 3'UTR. (1) Single standed cDNA was synthesized with a anchor (dT) primer. (2) A degenerate primer and a anchor primer was used to amplify the product of interest. (3) The product was cloned into the pGEM T-Easy vector and sequenced. Indicated is the expected gene structure obtained with this method.

2.2.31 Rapid amplification of 5' cDNA ends (5'RACE)

To obtain the 5' UTR and signal peptide sequence a gene specific primer (GrinA1RB: ACT ATT TCC GTT CTG AAG) complementary to the coding sequence of the last six amino acids of savignygrin (KKACGNA) was designed. Double-stranded full-length cDNA (1 μl of a 50X dilution of cDNA stock solution), GrinA1RB (5 pmoles), and AP2 (5 pmoles, Clontech Marathon kit) were used for amplification. All other amplification conditions were identical to that of the 3' RACE.

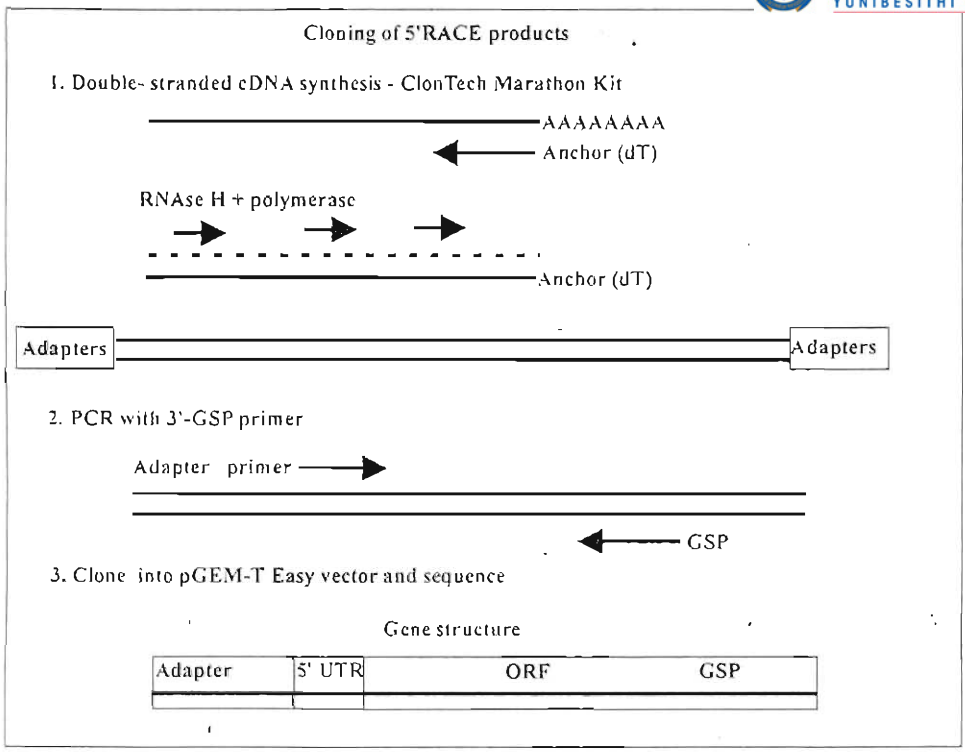

Fig. 2.5: Cloning strategy to obtain 5'UTR and ORF. (1) Double-standed cDNA was synthesized by first-strand cDNA synthesis from total RNA with an anchor (dT) primer, followed by second-strand cDNA synthesis with RNAse H and polymerase. Adapter primers were then ligated to the ends of the double-stranded cDNA. (2) A primer specific for the 3'end of the ORF (GSP) and a adapter primer were used to amplify the product of interest. (3) The product was cloned into the pGEM T-Easy vector and sequenced. Indicated is the expected gene structure obtained with this method.

2.2.32 Cloning of low-molecular mass savignygrin inhibitor

During the characterization of savignygrin two isoforms were observed. ESMS indicated that one had a slightly higher molecular mass (6966 Da, designated the high mass inhibitor) than the other (6808 Da, designated the low mass inhibitor). 3' RACE with the degenerate primer produced the high mass inhibitor only. A single colony obtained from the 5' RACE gave a sequence that differered at a single nucleotide (R52G). To determine whether this might be the low mass form a primer (GrinAB: ACT ATT TCC GTT CTG AAG) was designed with the single nucleotide differerence at the 3' end and 3' RACE was performed as described. A product was obtained that showed both R52G and N60G differences with the high mass inhibitor sequence. To confirm this difference a GSP (LMMprime: TGT ACC TCT CCT TGA AC) was designed in the 3'UTR where differences were observed with the high mass inhibitor sequence. 5'

RACE was performed with the GSP to obtain the full-lenght low mass inhibitor sequence.

2.2.33 Analysis of PCR products

Amplified products were analyzed by electrophoresis (68 Volts ~ 1.5 hours) using a 2% analytical grade agarose (Promega, Wisconsin, USA) gel with TAE (0.04 M Tris-acetate, 0.001 M EDTA) as running buffer in a minigel apparatus (Biometra, GmbH).

2.2.34 Quantitation of DNA

DNA was quantitated by visual comparison to known concentrations of 100 bp ladder markers (Promega, Wisconsin, USA).

2.2.35 Elution of RACE products from agarose gels

Amplified products were extracted from agarose gels with the silica elution method (Boyle and Lew, 1995). RACE products were excised from gels and gel pieces were dissolved in 1 ml NaI (0.9g/ml) at 55 °C. DNA was adsorbed on 5μl silica (100 mg/ml) (Sigma, USA) by incubation for 30 minutes on ice. Silica was washed 2X with wash buffer (10 mM Tris-HCl, 50 mM NaCl, 2.5 mM EDTA, pH 7.5 and 50% v/v ethanol) by centrifugation (30s in a microfuge). DNA was eluted with 10 μl 1mM Tris-HCl, pH 8.0 at 60 °C (5 minutes). Yield was determined by comparison with known concentrations of 100 bp ladder electrophoresis markers (Promega, Wisconsin, USA).

2.2.36 Purification of PCR products

For certain applications PCR products were purified using the High Pure PCR Product Purification Kit (Roche Molecular Biochemicals). PCR product (100 μl) was added to 500 μl binding buffer (3M guanidine-thiocyanate, 10 mM Tris-HCl, 5% ethanol (v/v), pH 6.6) before addition to High Pure filter tubes. Tubes were centrifuged for 1 minute at 12000xg and the flow through discarded. Filters were washed with 500μl wash buffer (2 mM Tris-HCl, 20 mM NaCl, 20% ethanol (v/v), pH 7.5) by centrifugation (12000xg, 1 minute), followed by another wash with 200μl wash buffer. PCR product was eluted with 100μl elution buffer (1 mM Tris-HCl, pH 8.5).

2.2.37 A/T cloning of RACE products into pGEM T-Easy

DNA product (3:1 insert to vector ratio) was ligated into the pGEM®-T Easy Vector (1µl ~ 50 ng) using A/T cloning at 4 °C (16-48 hours) with 1µl T4 ligase and 5µl 2X buffer of the pGEM®-T Easy Vector System I (Promega, Wisconsin, USA). T4 ligase was inactivated at 70 °C prior to transformation of competent cells. The products of at least three PCR reactions were cloned and at least 3 different clones of each PCR product cloned were sequenced from both up-and down stream ends.

2.2.38 Preparation of competent cells

Competent SURE (Stratagene, La Jolla, CA, USA) *E. coli* cells were prepared using the calcium/manganese-based method (Hanahan *et al.* 1991). Bacteria were grown overnight on M9 minimal medium agar (0.05 M Na_2HPO_4-$2H_2O$, 0.02 M KH_2PO_4, 8 mM NaCl, 0.02 M NH_4Cl, 2 mM $MgSO_4$, 0.01M D-glucose, 0.1 mM $CaCl_2$, 1 mM thiamine hydrochloride, 1.5% agar (w/v), pH 7.4). Colonies were plated onto LB plates (1% tryptone, 0.5% yeast extract, 1% NaCl, pH 7.5, 1.5% (w/v) agar with 12.5 µg/ml tetracycline) and grown overnight at 30 °C. Several colonies were suspended in SOB medium (2% tryptone, 0.5% yeast extract, 10 mM NaCl, 2.5 mM KCl, pH 7.0) by vortexing and inoculated into 50 ml SOB medium. Cells were grown at 30 °C with shaking (250xg) until OD_{600}~0.3 after which the cells were pelleted by centrifugation (10000xg, 15 min at 4 °C). The supernatant was discarded and the pellet suspended in 16.6 ml CCMB 80 medium (80 mM $CaCl_2$-2H2O, 20 mM $MnCl_2$-4H2O, 10 mM $MgCl_2$-$6H_2O$, 10 mM K-acetate, 10% glycerol, pH 6.4) and incubated on ice for 20 min. Cells were pelleted by centrifugation (10000xg, 10 min at 4 °C) and the supernatant discarded. The pellet was suspended in 4.1 ml CCMB 80 medium, aliquoted and stored at –70 °C.

2.2.39 Transformation of SURE *E. coli* cells

Transformation of competent cells was performed according to the heat-shock method (Sambrook *et al.* 1989). Transformation of cells with ligated plasmid was performed by preincubation of 100 µl cells (OD_{600} ~ 0.3) with plasmid at 4 °C (30 minutes), heat shock at 42 °C (60s) and incubation at 4 °C (3 minutes) before growing cells in SOC medium (2% tryptone, 0.5% yeast extract, 10 mM NaCl, 2.5 mM KCl, 50 mM D-

glucose, pH 7.1) for 1 hour before plating 100 µl of transformed cells onto 1.5% agar that contained 50 µg/ml ampicillin, 40 µl/plate X-gal (20 mg/ml DMSO) (Roche) and 4 µl/plate IPTG (400 mM) (Roche Diagnostics). Postitive colonies were selected using blue-white selection with conventional minipreps of plasmids and restriction enzyme digestion (Eco RI) of plasmid to identify inserts with the correct size.

2.2.40 Screening for recombinant clones

Blue/white selection is based on the fact that the β-galactamase gene is disrupted during insertion of foreign DNA into the multiple cloning site of the pGEM T-Easy vector. Vector that ligated without foreign DNA produces β-galactamase under induction of IPTG and hydrolyses X-galactose which then forms a blue colored product that yields blue colonies. When the gene for β-galactamase is disrupted, no hydrolysis of X-galactose occurs, which yields white colonies. White colonies were inoculated into 3 ml LB broth (10 µg/ml ampicillin) and grown for 16 hours at 30 °C.

2.2.41 Miniprep of plasmids

Cells from positive colonies (1 ml culture) were collected by centrifugation (12000xg, 1 min) in a microfuge and resuspended in 100 µl miniprep solution 1 (25 mM Tris-HCl, 50 mM glucose, 10 mM EDTA, pH 8.0). Miniprep solution 2 (150 µl, 0.2M NaOH, 1% SDS) were added and the solution were mixed by gentle inversion before incubation on ice (5 min) to lyse the cells. Ice cold miniprep solution 3 (250 µl, 3M potassium acetate, pH 4.2) was added and the solution was mixed by gentle inversion and incubated on ice (5 min) before centrifugation (12000xg, 5 min) in a microfuge to precipitate chromosomal DNA. Absolute ethanol (1 ml) was added to the supernatant and incubated at room temperature (10 min) before centrifugation (12000xg, 15 min) in a microfuge to precipitate plasmids. The supernatant was discarded and the pelleted plasmid was washed with 70% ethanol (1 ml) and again centrifuged. The supernatant was discarded and the pellet dried using the Bachoffer vacuum concentrator (5 min). Pellets were dissolved in 30 µl water (20 µg RNAse) and 8 µl were digested with 1 µl EcoRI (10U) in digestion buffer (90mM Tris-HCl, 10 mM $MgCl_2$, 50 mM NaCl, pH 7.5) for 2 hours before agarose gel analysis. Of those recombinant plasmids that showed

the correct insert size, the remaining 2 ml of culture was used for high pure plasmid purification for sequencing.

2.2.42 High pure plasmid isolation

Plasmids were purified for sequencing with the high pure plasmid purification kit (Roche Diagnostics). Cells (2 ml culture) were collected with centrifugation (12000xg, 1 min) in a microfuge and suspended in 250 µl suspension buffer (50 mM Tris-HCl, 10 mM EDTA, pH 8.0 at 25 °C, 0.1mg/ml RNAse). Cells were lyzed with 250 µl lysis buffer (0.2M NaOH, 1%SDS) by gentle inversion and incubation at room temperature (5 min) before addition of 350 µl binding buffer (4 M guanidine hydrochloride, 0.5M potassium acetate, pH 4.2). The solution was mixed by gentle inversion and incubated on ice (5 min) to precipitate chromosomal DNA. Chromosomal DNA was removed by centrifugation (12000xg, 10 min) and the supernatant added to a High Pure filter tube, which has a glass fibre filter for specific binding of plasmid DNA in the presence of chaotropic salts. The solution was centrifuged (12000xg, 1 min) and the flow through discarded before addition of 700 µl wash buffer II (2 mM Tris-HCl, 20 mM NaCl, 80% ethanol, pH 7.5) and recentrifugation (12000xg, 1 min). After another dry centrifugation (12000g, 1 min) to remove all ethanol, the High Pure filter tube was transferred to a new collection tube and plasmid was eluted with 100 µl of elution buffer (1 mM Tris-HCl, pH 8.5).

2.2.43 Sequencing of recombinant pGEM T-Easy plasmids

Sequencing was performed using the Big Dye Sequencing Kit (Perkin Elmer, Foster City) on an ABI Prism 377 DNA sequencer (Perkin Elmer Applied Biosystems, California, USA) according to the manufacturers instructions using 2 µl ready reaction mixture, 3 µl 5X buffer (400 mM Tris-HCl, 10 mM $MgCl_2$, pH 9.0), 1 µl primer (3.2 pmoles of upstream T7 or downstream SP6 promoter primers respectively), plasmid (150-250 ng) and water to a final volume of 20 µl. Cycle sequencing was performed using 25 cycles of denaturation (96 °C, 10s), annealing (50 °C, 5s) and extension (60 °C, 4 min). Big Dye products were precipitated with 64% ethanol (final volume 100 µl) for 30 minutes and pelleted by centrifugation (12000xg, 25 minutes). Pellets were washed with 70% ethanol and dried on a vacuum concentrator (Bachoffer) for 7

minutes. The pellet was suspended in 3 μl loading dye (5:1 ratio of deionized formamide: 25 mM EDTA, pH 8.0 and blue dextran, 30 mg/ml). Samples were denatured at 95 °C (2 min), snapcooled on ice and analyzed on a 36 cm gel according to the ABI Prism 377 Genetic Analyser User's Manual. At least 3 different clones were sequenced for each fragment and each clone was sequenced with both primers. Sequences obtained were analyzed using the Staden package. DNA and deduced protein sequences were analyzed using BLAST (Altschul *et al.* 1990) and alignments were performed with ClustalX (Jeanmougin *et al.* 1998). Protein molecular mass, amino acid composition and theoretical tryptic digests of the deduced sequence were determined with the PAWS program (http://www.proteometrics.com/software/paws.htm).

2.2.44 Primers used during study

Primers used for the cloning and sequencing of the various proteins described in this study are indicated in Table 2.4.

Table 2.4: Primers used in study

Name	Primer sequence	Chapter
General		
Anchor-dT	GCT ATC ATT ACC ACA ACA CTC T_{18}VN	2, 3, 7
Anchor	GCT ATC ATT ACC ACA ACA CTC	2,3, 7
AP2	AAC TCA CTA TAG GGC TCG AGC GGC	2, 3, 7
T7Seq	TAA TAC GAC TCA CTA TAG GG	2, 3, 7
SP6Seq	ATT TAG GTG ACA CTA TAG	2, 3, 7
Savignygrin		
GrinA	TAY CAR CCN GAR TGY YTI G	2
GrinA1RB	GGA TCC TCA CGC ATT TCC GCA TGC CTT CTT	2
GrinAB	ACT ATT TCC GCT CTG AAG	2
GrinA1F	CAT ATG TAC CAA CCC GAG TGC CTG GAG	2
LMMprime	TGT ACC TCT CCT TGA AC	2
Savignin		
ThrombA	YTN AAY GTI MGI TGY AAY AA	3
Thromb C1	CTC GAG TTC CAT TGA AAC GCC ACA	3
TSGP's		
TOC	TTY CCI ACI GAY GCN TA	7
TOE	TTY CCI ACI GAR GCN TA	7
C1T2	CTA GCA GTC CTT GTC TT	7
NTC1	GTT CCA ACA TCC ACA TG	7
TOKS1	GCN AAY GAY GTI TGG AAY GT	7
C1T1	CTA CGG AAC TCT GCA GCC TT	7
20kD	GGI CCI GAY GGI TGY GT	7
20kDC1	GTG TAG GGG ATG GGG CCA	7

2.3 Results

2.3.1 Purification of the savignygrins

Inhibition of ADP-induced platelet aggregation was used as a measure of activity during purification. Size exclusion chromatography was used as a first step in the purification procedure (Fig. 2.6a). Inhibition of platelet aggregation was observed across the whole protein spectrum and could be ascribed to the presence of apyrase activity in the high molecular mass region (500-20 kDa) as described previously (Mans *et al.* 1998b). Heat inactivation of apyrase shifted the inhibition pattern to the low molecular mass region (<20kDa). Fractionation of the size exclusion fractions on the anion exchange column indicated inhibitory activity over a broad range (10-13 min) at an approximate iso-electric point range of 5-6 (Fig. 2.6b). Reversed phase chromatography separated the inhibitory activity into two distinct peaks designated A and B (Fig. 2.6c). ESMS analysis showed that both peaks contained a high (6966 Da) and low (6808 Da) molecular mass species (results not shown). Separation of these species were attempted with rechromatography using AEHPLC (Fig 2.6d). Both peaks A and B separated into two peaks, indicating two species that differ in charge with approximate iso-electric points of 5.9 and 5.5, respectively. These peaks were designated A+, A-, B+ and B- on the basis of charge (as observed on AEHPLC) and hydrophobicity (as observed on RPHPLC). These different species were then desalted using RPHPLC (Fig. 2.6e and 2.6f). The yields obtained for three different separations were 45±15 μg, 37±9μg, 27±9μg and 27±9μg for the different forms (A+, A-, B+ and B-), respectively. This corresponds to approximately 1-3% of the total soluble salivary gland protein for each isoform.

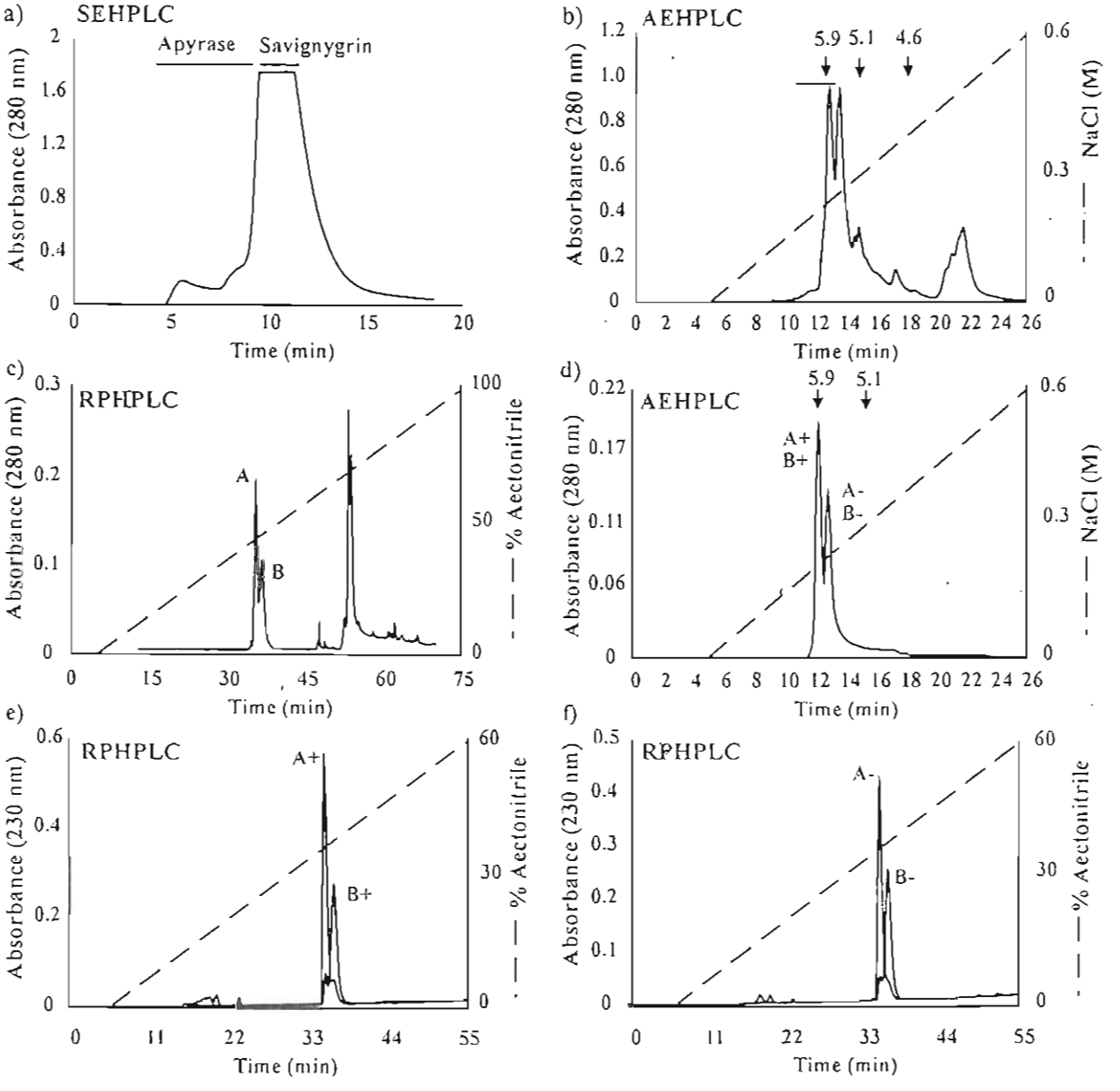

Fig. 2.6: Purification of savignygrin. (a) SEHPLC of tick salivary gland extract. Lines indicate apyrase activity and fractions pooled for AEHPLC (savignygrin). (b) AEHPLC of the fractions obtained after SEHPLC. The line indicates the region of platelet aggregation inhibitory activity and also those fractions pooled for RPHPLC. Relative iso-electric points are indicated with arrows. (c) RPHPLC of fractions with inhibitory activity obtained from AEHPLC. Inhibitory activity was observed in two peaks assigned A and B. (d) Rechromatography of fractions A and B on AEHPLC. The chromatograms of A and B are superimposed and peaks collected are indicated as A+, A-, B+ and B-. (e) Rechromatography of fractions A+ and B+ with RPHPLC. Chromatograms are superimposed. (f) Rechromatography of fractions A- and B- with RPHPLC. Chromatograms are superimposed.

2.3.2 Tricine SDS-PAGE analysis of the savignygrins

Tricine SDS-PAGE analysis was used to determine the purity of the inhibitors and to investigate their behaviour under reducing as well as non-reducing conditions (Fig. 2.7a). Reducing conditions indicated that the isoforms were pure with a relative Mr of 6.3 kDa for all four. Non-reducing conditions showed a reduction in electrophoretic mobilities for the different inhibitors. The A+ form migrated at ~15 kDa and the B+ form at ~12 kDa. The minus forms had surprisingly an even lower mobility with A- at ~32 kDa and B- at ~30 kDa. This indicates that disulphide bonds may play an important role in the maintenance of conformation and that the different inhibitors have distinct conformations. Lack of unfolding and reduced SDS binding could account for the lower mobilities. Electrophoresis in the presence of urea was thus investigated (Fig. 2.7b). In the presence of 8M urea the reduced inhibitors had a slight decrease (~2kDa) in electrophoretic mobility, indicating that reduced forms still bind SDS in the presence of urea. The non-reduced (+) forms however, showed a significant decrease in mobility.

This indicated unfolding by urea (increasing the hydrodynamic volume). By using a urea gradient (0-8M) perpendicular to the direction of electrophoresis the unfolding kinetics of a protein can be observed (Goldenberg and Creighton, 1984). Unfolding kinetics suggest that the (-) forms are already in an unfolded form due to the little change in mobility across the gradient, while the plus forms are unfolded to a greater extent (Fig. 2.7c). These results suggested that the (-) forms are less stable than the (+) forms and correlates with the finding that the (-) forms were less stable than the (+) forms when their temperature stability was measured (Fig. 2.7d). Although, all four inhibitors were extremely stable (retaining >50% activity after 3 hours of boiling at 94 °C), the (-) forms were slightly less stable and probably unfold more easily under the extreme conditions of boiling in the presence of SDS as was performed for electrophoretic analysis. There were no marked inflection points for the inhibitors that would indicate a rapid transition from a folded to unfolded state. There is rather a gradual decrease in electrophoretic mobility with increased urea concentration, indicating slow unfolding of a very stable conformation (Goldenberg and Creighton, 1984). This is most possibly due to a dense core structure kept intact by disulphide bonds, which is inaccessible to SDS. These

proteins would hence have a lower SDS:protein ratio and migrate to a greater extent on intrinsic charge.

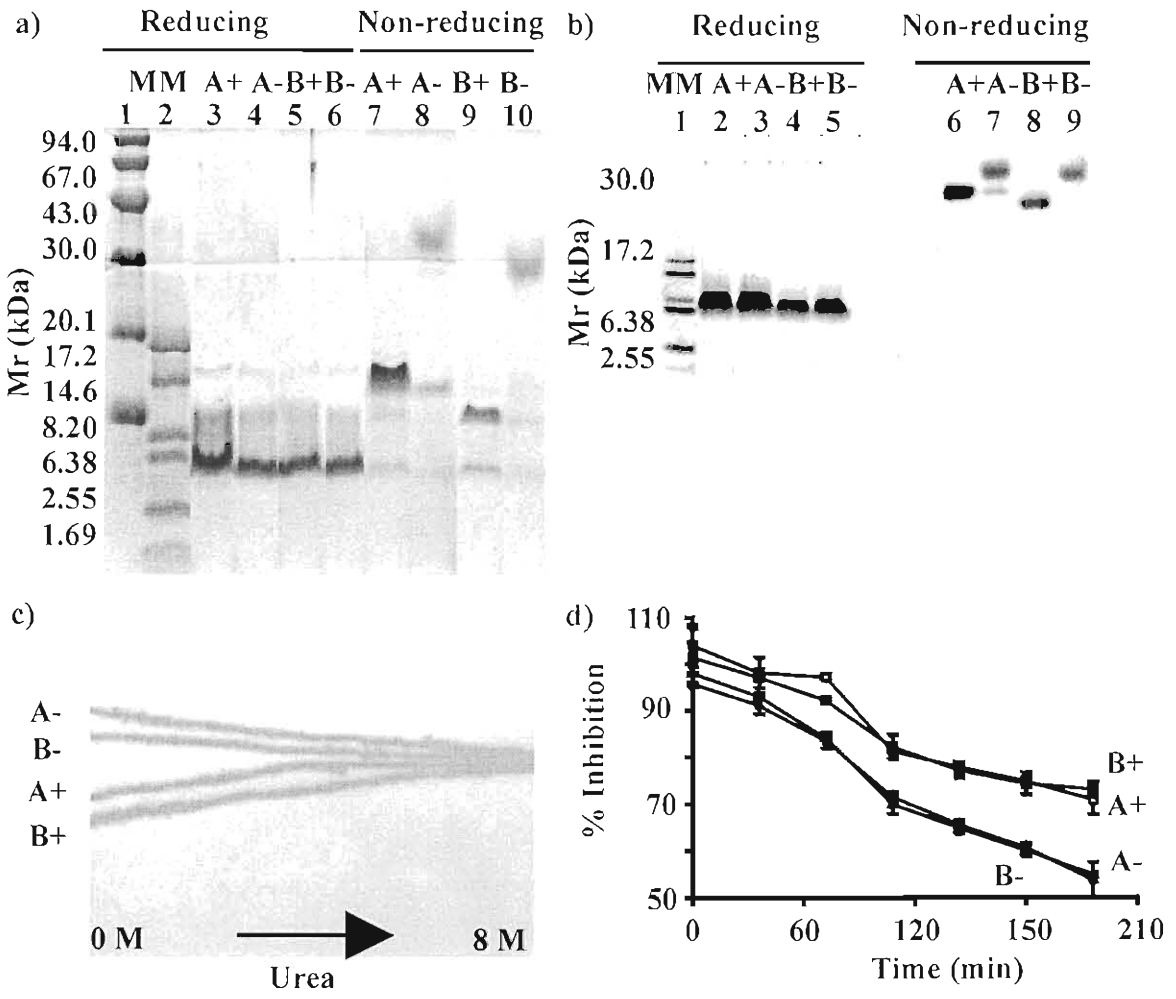

Fig. 2.7: Electrophoretic analysis of the savignygrins. (a) Tricine SDS-PAGE analysis of the savignygrins. Lane 1 indicates low molecular mass markers. Lane 2 indicates peptide molecular mass markers. Lane 3 to 6 shows electrophoresis under reducing conditions for A+, A-, B+ and B-, respectively. Lane 7-10 shows electrophoresis under non-reducing conditions for A+, A-, B+ and B-, respectively. (b) Tricine SDS-PAGE in the presence of 8M urea. Lane 1 shows peptide molecular mass markers. Lane 2-5 indicate inhibitors (A+, A-, B+ and B-, respectively) under reducing conditions. Lanes 6-9 show inhibitors (A+, A-, B+ and B-, respectively) under non-reducing conditions. (c) Tricine SDS-PAGE analysis under non-reducing conditions, with a 0-8 M urea gradient perpendicular to the direction of electrophoresis. (d) Temperature stability of the savignygrins. Inhibitors were incubated at 94 °C for the indicated time periods before activity was determined.

2.3.3 Electrospray mass spectrometry of the savignygrins

ESMS of the different forms shows that the (+) forms have the same molecular mass (6966 Da), while the (-) forms also have the same mass (6808Da), but are 158 Da smaller (Fig. 2.8). These masses correlate well with those obtained by SDS-PAGE under reducing conditions. The spectra show the M^{5+} to M^{8+} ion species for all four forms. The maximum number of positive charges correspond well with amino acid analysis and sequence data which indicate nine lysine and arginine residues (Fig. 2.10).

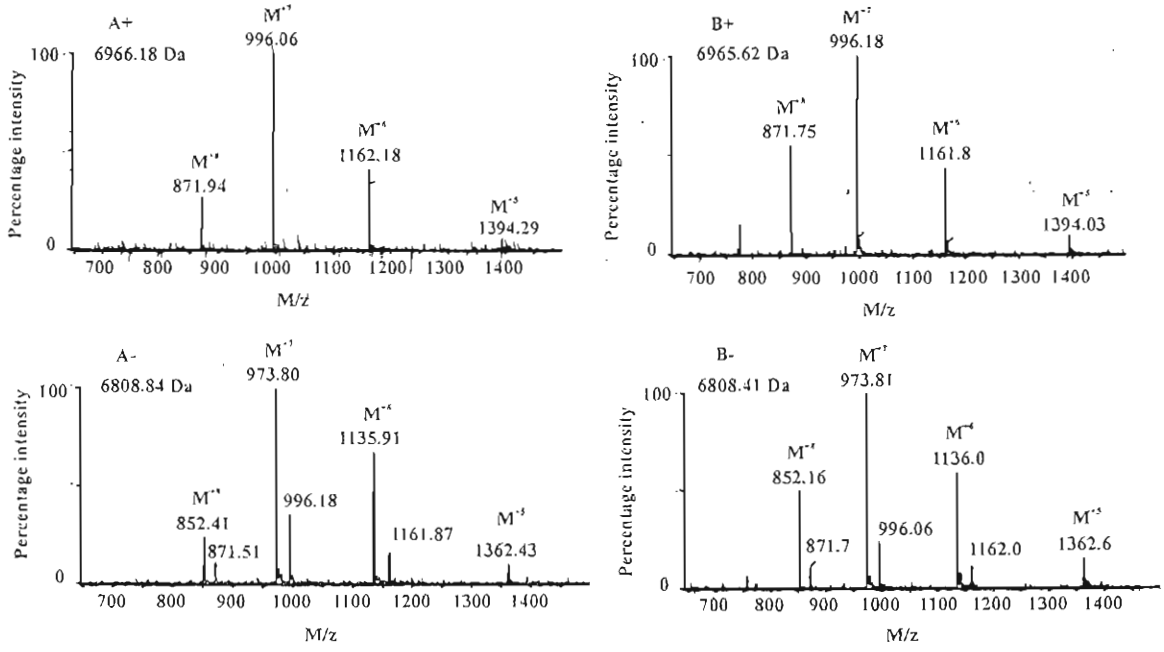

Fig. 2.8: Electrospray mass spectrometry analysis of the savignygrins. The M^{+5}, M^{+6}, M^{+7} and M^{+8} protonated species of each inhibitor is shown. Molecular masses obtained after deconvolusion of the respective spectra are included in each figure.

2.3.4 Peptide mass fingerprinting of the savignygrins

Peptide maps of the different inhibitors obtained by trypsin digestion and analyzed by MALDI-TOF-MS, was essentially the same (Fig. 2.9). These results indicate that the amino acid sequences are similar. No difference could be observed that could account for the discrepancy between the (+) and (-) forms.

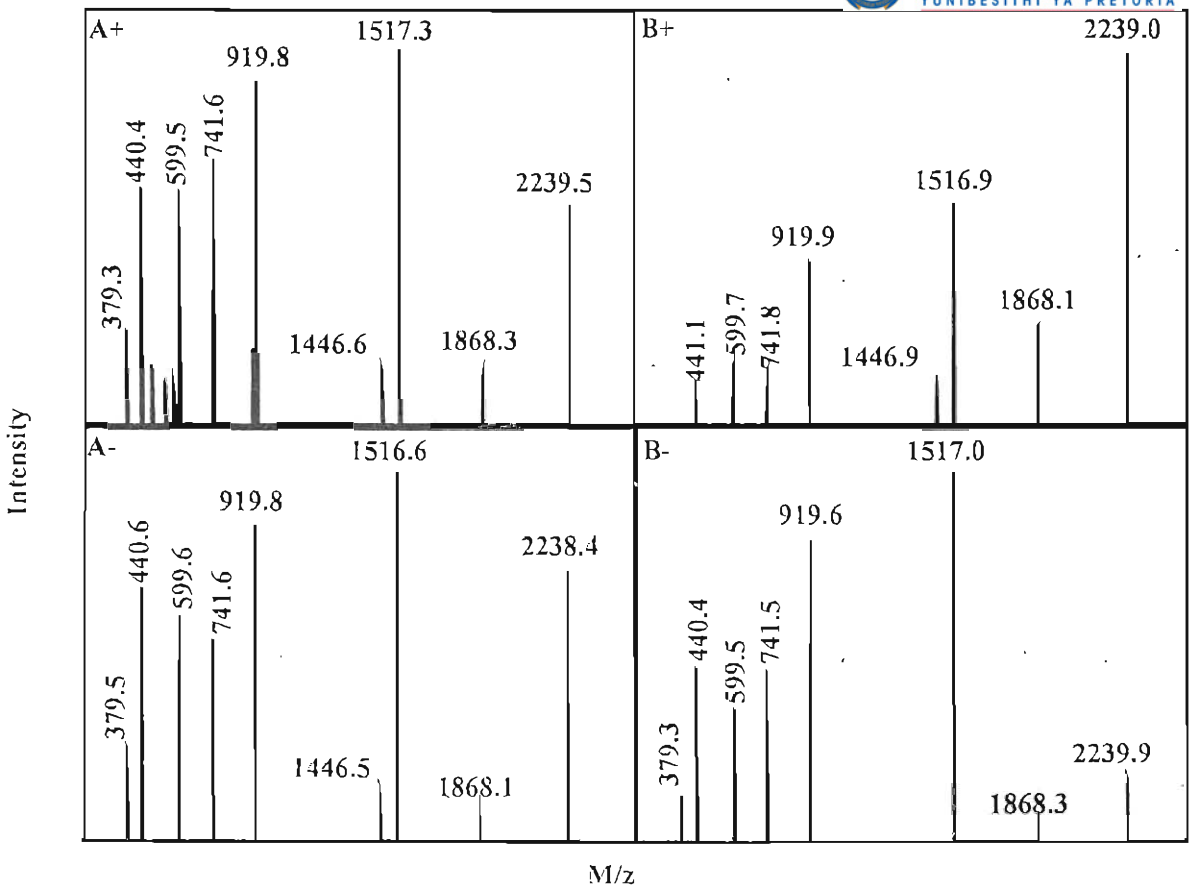

Fig. 2.9: Peptide molecular mass fingerprint analysis of the savignygrins. MALDI-TOF-MS spectra of tryptic digests of the A+, B+, A- and B- forms. Masses obtained for the fragments are indicated.

2.3.5 Amino acid analysis of the savignygrins

Amino acid analysis indicated that the overall compositions of the different inhibitors are similar (Fig. 2.10). No isoleucine or valine was detected, not even after hydrolysis up to 72 hours (results not shown). From these data the percentage of hydrophobic amino acids (using Ala, Leu and Phe) are approximately 13%. Performic acid oxidation, alkylation of cysteines with 4-vinylpyridine and ESMS of the alkylated forms (results not shown) all confirmed that 6 cysteines are present.

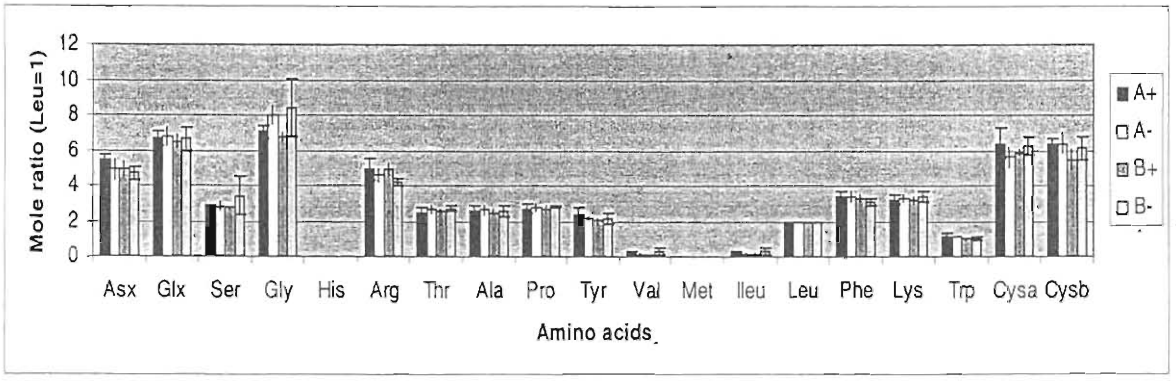

Fig. 2.10: Amino acid analysis of savignygrins. Indicated are mole ratios of amino acids relative to Leu for the different inhibitors. Cysa indicates performic acid oxidation and cysb alkylation with 4-vinylpyridine. SD is for three individual determinations.

2.3.6 Determination of disulphide content of the savignygrins

By using 4-vinylpyridine in the presence or absence of DTT, the existence of any free sulphydryl groups can be indicated. No alkylated cysteines were detected in the absence of DTT implying that all the cysteines are involved in disulphide bonds (Fig. 2.11).

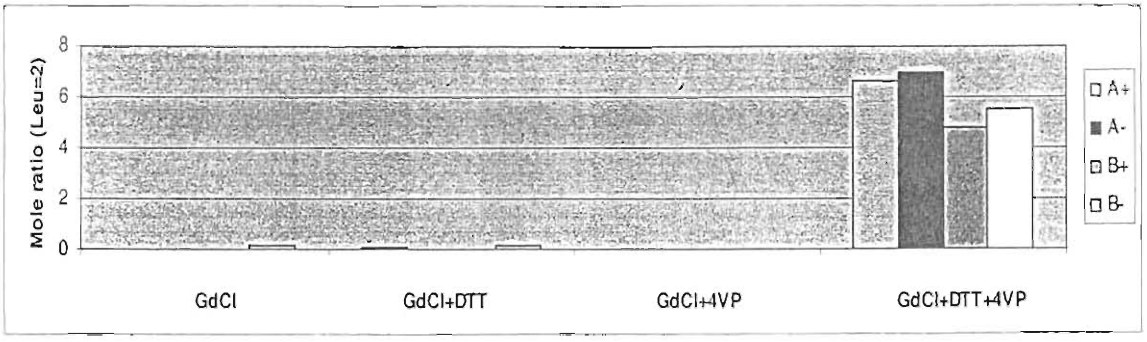

Fig. 2.11: Determination of the disulphide content of the savignygrins. Savignygrins were alkylated in the presence or absence of a reducing agent (DTT). Indicated are results obtained from amino acid analysis of savignygrins that were denatured (GdCl), denatured and reduced (GdCl+DTT), denatured and alkylated (GdCl+4VP) and denatured, reduced and alkylated (GdCl+DTT+4VP).

2.3.7 Disulphide bonds and their relevance for activity

Alkylation with 4-VP in the presence of DTT, or reduction with DTT alone, abolished inhibitory activity completely (Fig. 2.12), indicating that disulphide bonds are essential for the maintenance of activity.

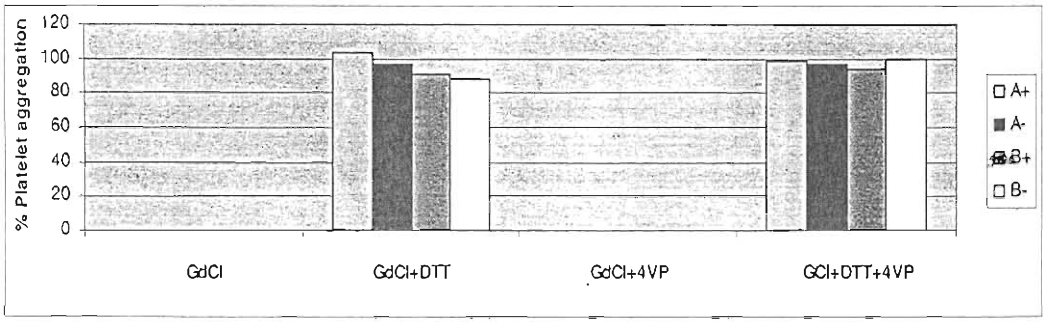

Fig. 2.12: The effect of disulphide bonds on activity of the savignygrins. Activity of savignygrins that were denatured (GdCl), denatured and reduced (GdCl+DTT), denatured and alkylated (GdCl+4VP) and denatured, reduced and alkylated (GdCl+DTT+4VP). A final concentration of 300 nM for the savignygrins was used for activity measurements. All values were calculated with respect to a control sample that was not treated in any way.

2.3.8 Biological activity of the savignygrins

All four inhibitors inhibited platelet aggregation induced by ADP, collagen, TRAP and epinephrine while platelets aggregated with ADP were also disaggregated (Fig. 2.13a). An IC_{50} of approximately 130 nM was determined for all four inhibitors (Fig. 2.13b). This is well in the range of the disintegrin inhibitors and close to that of disagregin (104 nM) (Gould *et al.* 1990; Karczewski, Endris and Connolly, 1994). A decrease in transmittance observed with added inhibitor indicates activation of platelets and concomitant shape change to the spherical form (Fig. 2.12a). This suggests post-activation inhibition at the level of the platelet integrin $\alpha_{IIb}\beta_3$. To investigate this further, platelets treated with savignygrin were analyzed using electron microscopy.

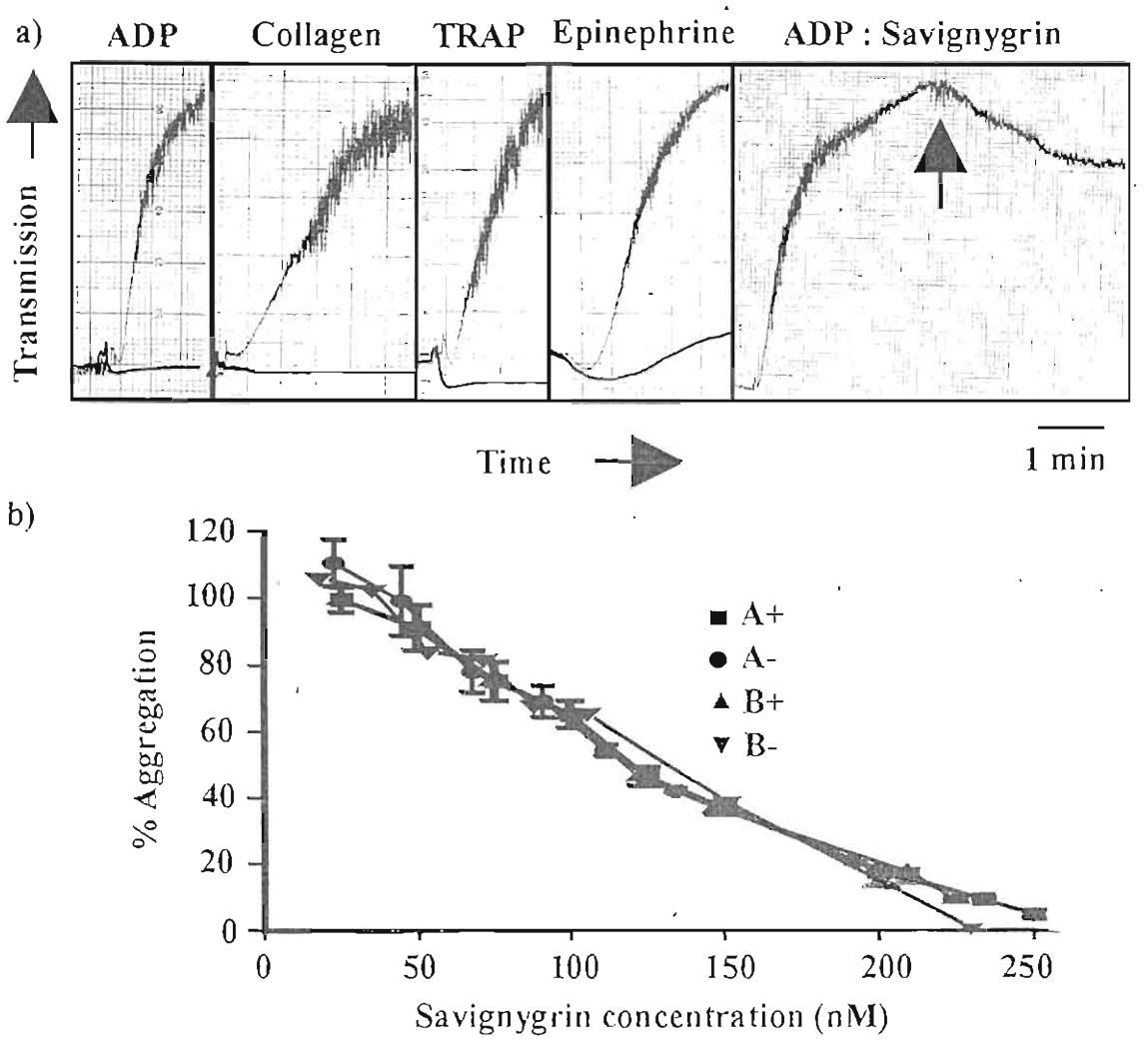

Fig. 2.13: Inhibition of platelet aggregation induced by various agonists by savignygrin. ADP (10 μM), collagen (2 μg), TRAP (50 μM) and epinephrine (10 μM) were used to induce platelet aggregation. Platelet rich plasma was incubated with savignygrin (300 nM final concentration, black tracings). Controls were incubated with saline (grey tracings). Platelet aggregation is indicated by an increase in transmission. Similar tracings were observed for all the different isoforms.

2.3.9 The influence of savignygrin on platelet shape change

Platelets used as negative control show a discoid (resting) shape with their granules intact (2.14a). Platelets aggregated with ADP show a fused state and secretion of granules (Fig. 2.14b). Platelets incubated with savignygrin, without ADP-induced activation, retain the discoid form associated with non-activated platelets and retain their granules (Fig. 2.14c). Platelets incubated with savignygrin and ADP possess an activated, spherical form and

retain their granules (Fig. 2.14d). Platelets aggregated with ADP and disaggregated with savignygrin possess the same shape as for those incubated with savignygrin and ADP but show a higher degree of dilatory open canaliculary system and show signs of degranulation (Fig. 2.14e). This is in contrast to results previously obtained for apyrase, which showed that removal of ADP leads to disaggregation but also signal transduction that manifests as reversible shape change (Mans *et al.* 2000). Platelets rather exhibited a similar shape as was found for platelets disaggregated with plasmin, a fibrino-(geno)-lytic enzyme, that severed the fibrinogen link between platelets, but had no signal transducing effect on platelets. These results are concurrent with targeting by savignygrin of the fibrinogen receptor that allows activation and degranulation of platelets, but inhibits fibrinogen binding, with no further effect on platelet signal transduction as observed for apyrase.

2.3.10 Targeting of $\alpha_{IIb}\beta_3$ by savignygrin

To test the possibility that $\alpha_{IIb}\beta_3$ is targeted, inhibition of binding of αCD41 (P2-FITC) to platelets and purified $\alpha_{IIb}\beta_3$ to immobilized fibrinogen was tested. Binding of P2-FITC to platelets was inhibited in a concentration dependent manner, both in the presence and absence of ADP (IC_{50}~15 μM) (Fig. 2.15a). Inhibition in the absence of ADP, indicate that the savignygrins can bind to resting $\alpha_{IIb}\beta_3$. Inhibition in the presence of ADP is much less than in the absence, suggesting that more competition exists between the antibody and the inhibitor. Furthermore, adhesion of $\alpha_{IIb}\beta_3$ to fibrinogen was inhibited with an IC_{50} ~3 nM (Fig. 2.15b). This is comparable with that of variabilin (9nM) (Wang *et al.* 1996) and decorsin (1.5nM) (Seymour *et al.* 1990). Taken together these results indicate the targeting of $\alpha_{IIb}\beta_3$ by the savignygrins.

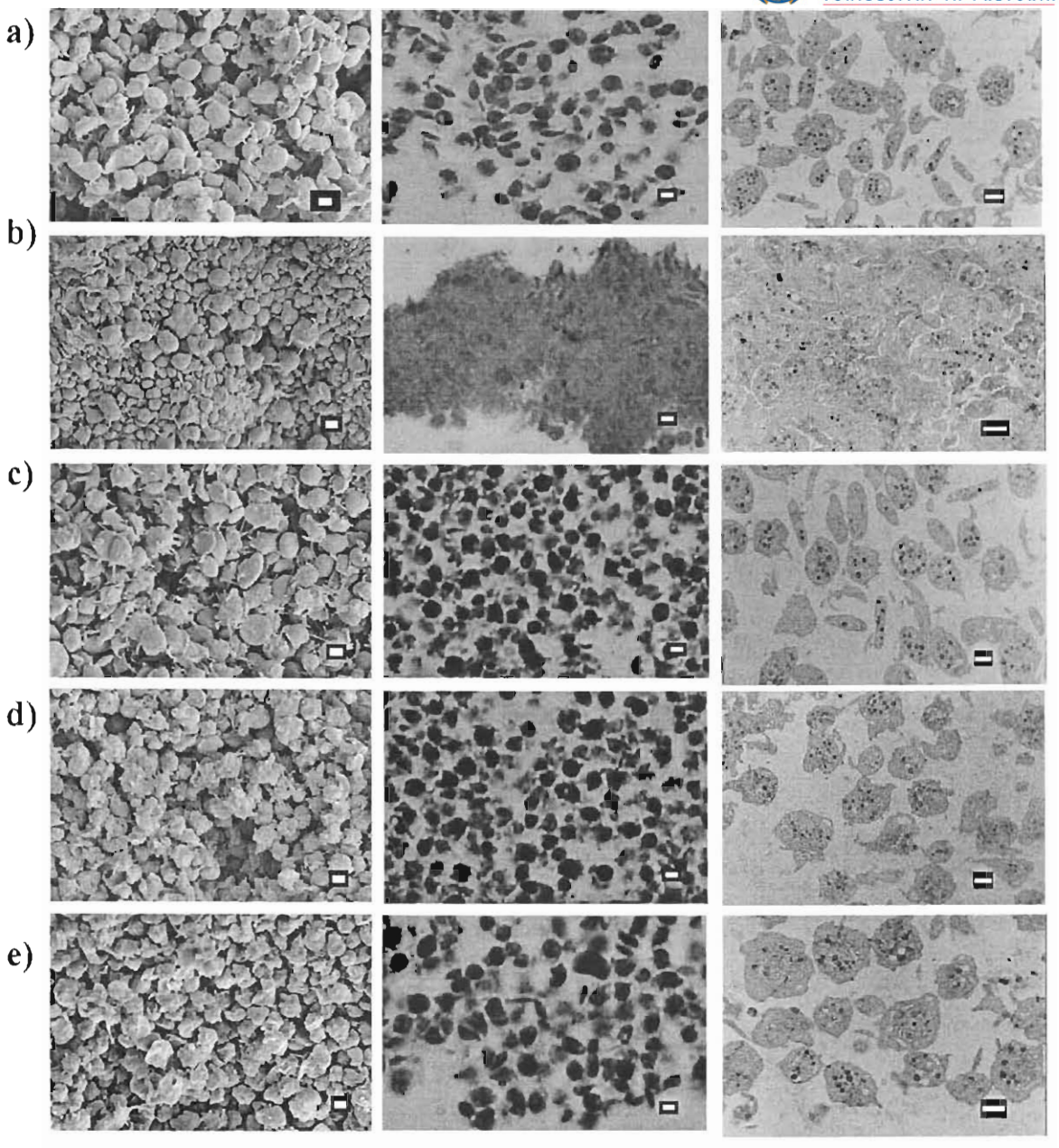

Fig. 2.14: The disaggregation effect of savignygrin on aggregated platelets. (a) Platelets without addition of any compounds. (b) Platelets aggregated with ADP (10 μM final concentration). (c) Platelets incubated with savignygrin. (d) Platelets incubated with savignygrin before addition of ADP (10 μM final concentration). (e) Platelets aggregated with ADP for 4 minutes and disaggregated with savignygrin. Scale bar = 1μm.

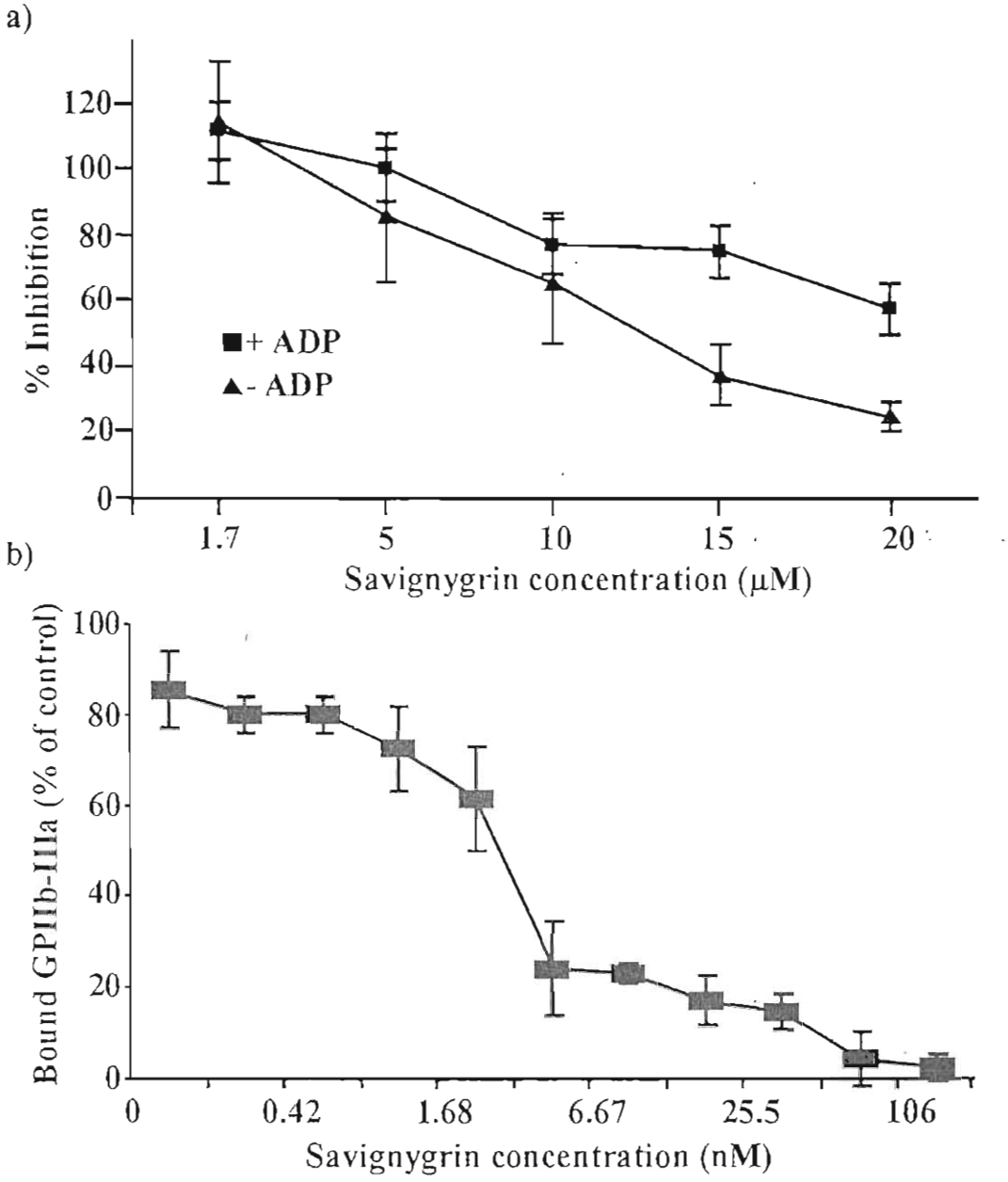

Fig. 2.15: Targeting of $\alpha_{IIb}\beta_3$ by savignygrin. (a) Inhibition of αCD41-FITC binding to platelets. Platelets were incubated with savignygrin, at various concentrations in the presence or absence of ADP, before incubation with αCD41-FITC. SD is for triplicate values. (b) Inhibition of the binding of purified $\alpha_{IIb}\beta_3$ to immobilized fibrinogen. $\alpha_{IIb}\beta_3$ was incubated with various concentrations of savignygrin before addition to fibrinogen. Values indicated are SD for triplicate values.

2.3.11 Integrin specificity of savignygrin

The integrin $\alpha_v\beta_3$ recognizes most ligands, such as vitronectin and fibrinogen that bind to $\alpha_{IIb}\beta_3$ (Plow *et al.* 2000). No inhibition of osteosarcoma cell adhesion to vitronectin or fibrinogen by savignygrin was observed, not even at a concentration of 10μM, although adhesion of platelets to fibrinogen was inhibited at concentrations of 20 nM (5% of control) (Fig. 2.16). This suggests that savignygrin is specific for $\alpha_{IIb}\beta_3$.

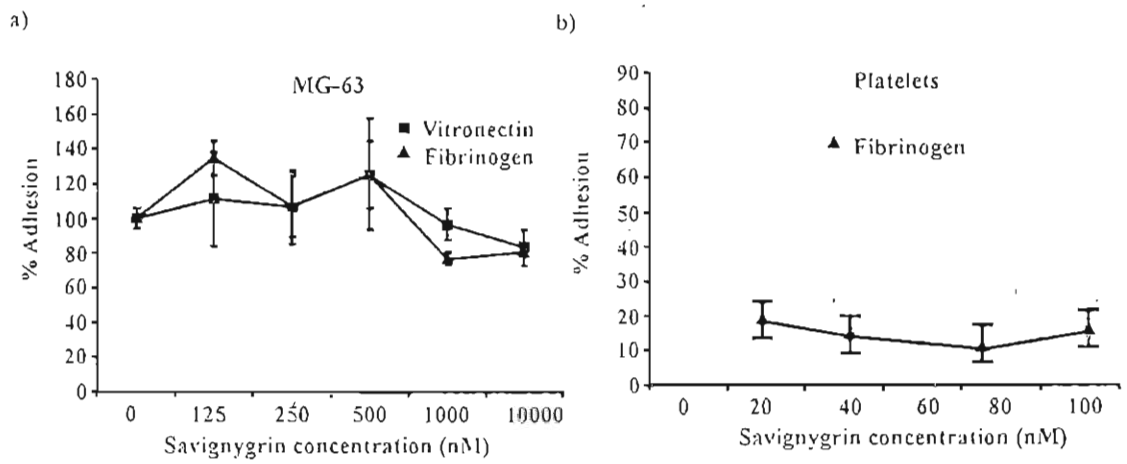

Fig. 2.16: Integrin specificity of the savignygrins. a) Adhesion of osteosarcoma cells to vitronectin and fibrinogen in the presence of savignygrin. b) Adhesion of platelets to fibrinogen in the presence of savignygrin. SD are for values in triplicate.

2.3.12 N-terminal amino acid sequence determination of the savignygrins

N-terminal amino acid sequence determination of the inhibitors shows that they all have the same sequence (results not shown). The yields for the A+ form are indicated and lie on the linear curve expected for the cycles determined (Fig. 2.17). Alignment with disagregin from *O. moubata* (Karczewski, Endris and Connolly, 1994) showed, that the cysteines were conserved although the N-terminal sequences show little similarity. A RGD motif in the sequence of savignygrin corresponds to the RED motif in the sequence of disagregin. Significant is that the sequence around the RGD motif is homologous to that of disagregin with the only difference being an aspartic acid residue at position 17 instead of a glutamic acid. This suggests that the sequence around the RGD motif is important for function, with negatively charged residues being prominent.

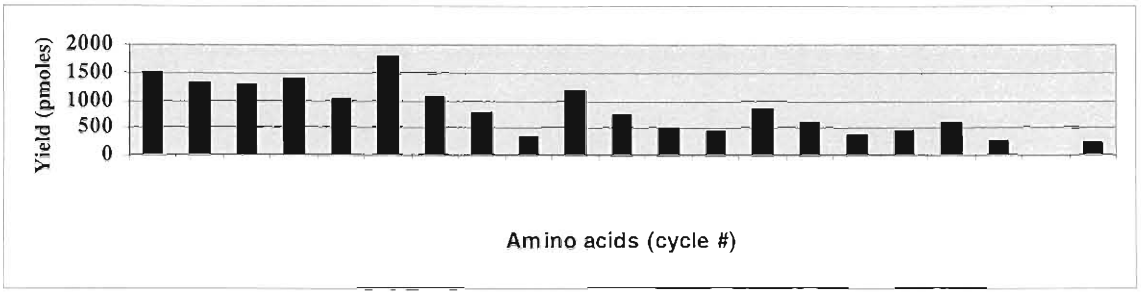

Fig. 2.17: N-terminal sequence analysis of savignygrin. Sequencing yields for different cycles of A+ are indicated. Similar results were obtained for the A-, B+ and B- isoforms.

2.3.13 Isolation of total RNA

Mouse lung total RNA showed the characteristic 28S, 18S and 5.8S rRNA bands. Total RNA from tick salivary glands and nymphs only showed the 18S rRNA band and a second band with a much lower mobility (Fig. 2.18). This is unusual as the 28S rRNA intensity is normally double that of the 18S rRNA (Farrell, 1993). There was however, a fragment with a much lower mobility that may represent unprocessed 28S-5.8S rRNA. Similar results have been obtained when *Xenopus* oocytes are depleted of U8 sno RNA, which is essential for 5.8S and 28S rRNA maturation (Peculis, 1997).

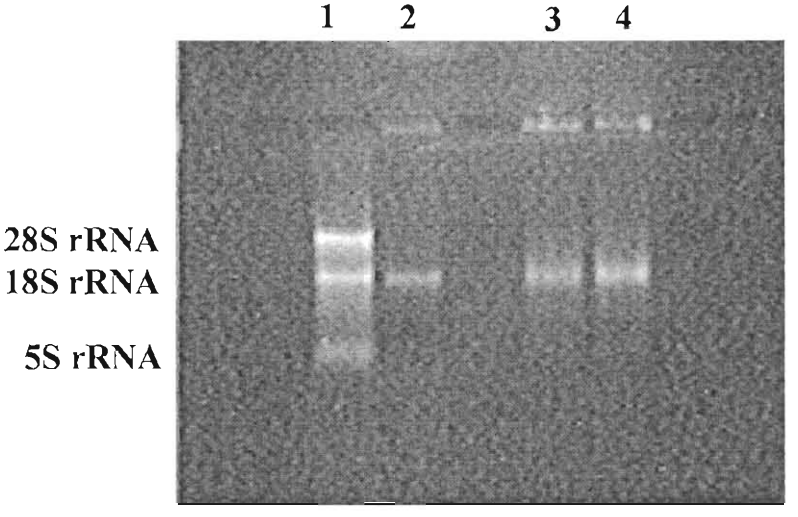

Fig. 2.18: Electrophoretic analysis of total RNA. Lane 1 indicates control RNA isolated from mouse lung. Lane 2 indicates isolations of total RNA from nymphae, and lanes 3 and 4 from tick salivary gland extracts.

2.3.14 Cloning and sequencing of savignygrin

PCR under optimized conditions using the degenerate primer designed from the N-terminal sequence of savignygrin showed a product of 300 bp while 5' RACE of the 5' UTR indicated a slightly smaller product (Fig. 2.19). Using the GrinAB primer a product of 170 bp was amplified for the 3'RACE, while a product of 400 bp was amplified for the 5'RACE using the GrinLMM primer. Sequencing showed that the 3' RACE (291 bp) and 5' RACE (324 bp) fragments corresponded well with the results obtained with PCR for the (+) form (Fig 2.20).

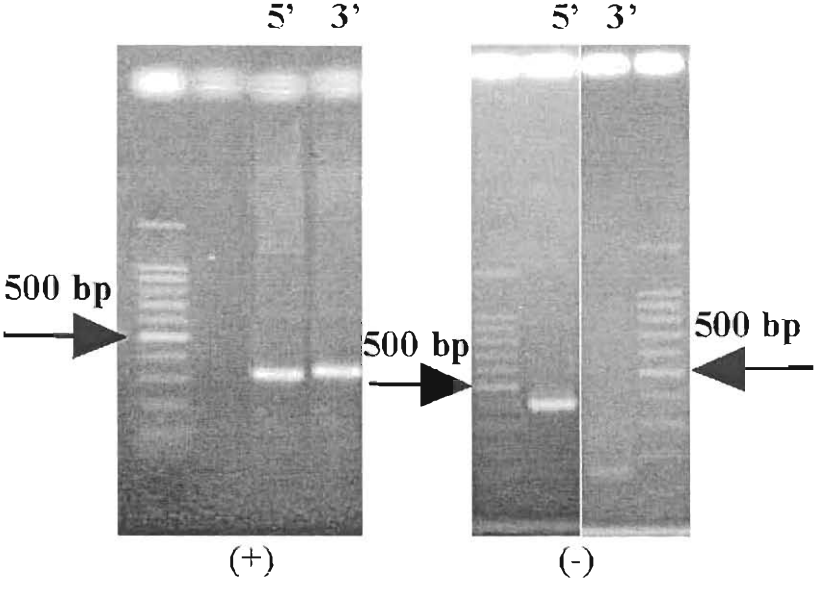

Fig. 2.19: RACE of the high (+) and low (-) mass forms of savignygrin. The 500 bp marker is indicated with an arrow. 5'RACE and 3'RACE products are indicated for the (+) and (-) forms, respectively.

2.3.15 Analysis of the recombinant amino acid sequence of savignygrin

The cDNA sequences obtained for both (+) and (-) forms showed all primers used during PCR and the poly-A tail used during cDNA synthesis. The cDNAs also contained the stop codon (TGA) and the poly-adenylation signal AATAAA. The translated amino acid sequences correlated with an immature protein of 80 amino acids, while the mature chain consisted of 61 amino acids, with the first 21 amino acids corresponding to that obtained with Edman degradation (Fig. 2.20). It is well known that threonine residues give low yields during Edman degradation, which explains the threonine at position 20 that corresponds with the gap in the Edman derived sequence. Analysis of the immature protein using SignalP (Nielsen *et al.* 1997), predicted the presence of a signal peptide (19

amino acids) and the correct cleavage site. There are relatively few differences between the (+/-) forms at sequence level. The only gap present is in the 5'UTR of the (-) form and most of the differences occur at isolated positions in the 3'UTR. Two non-synonymous substitutions occur at positions R52G (R73G immature protein) and N60G (N81G immature protein) for the (+/-) forms, respectively and one synonymous substitution at position K56 (K77 immature protein).

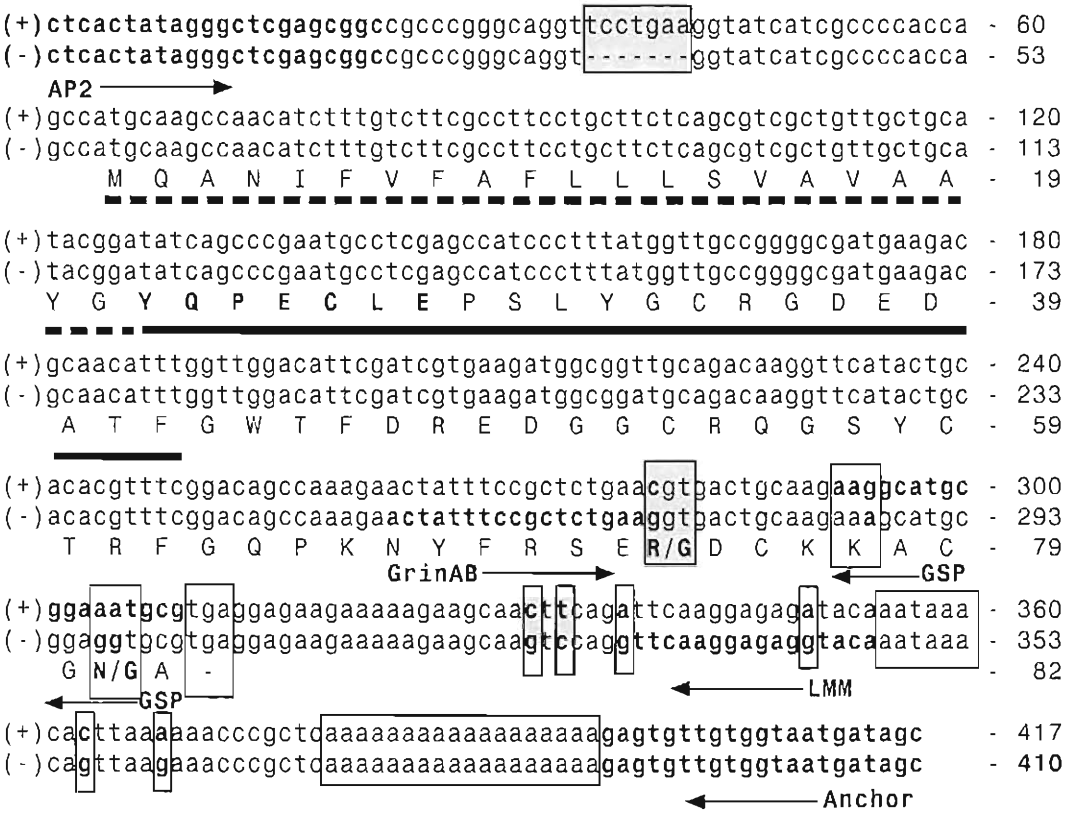

Fig. 2.20: Full-length cDNA sequence for savignygrin. The 5' adapter, 3' gene specific and 3' anchor primer are shown in bold. The stop codon (TGA), the poly-adenylation signal (AATAAA) and the poly-A tail are boxed. The N-terminal sequence obtained with Edman degradation are underlined while the N-terminal sequence used for degenerate primer design is shown in bold. The signal peptide is underlined with a broken line.

2.3.16 Comparison of data obtained from the deduced amino acid sequence and data from native savignygrin

The theoretical peptide masses obtained for a tryptic digest of the deduced amino acid sequence correlate well with the empirical data obtained for the native inhibitors and show that the peptides obtained were distributed across the whole sequence. The calculated masses of the deduced amino acid sequences also correspond with the masses of the (+)/(-) forms obtained with ESMS. Amino acid compositions obtained for the native inhibitors and the composition calculated from the deduced amino acid sequence obtained after cloning correlate closely (Fig. 2.21). Taken together, these data suggest that the correct sequences for the savignygrins were obtained.

a)

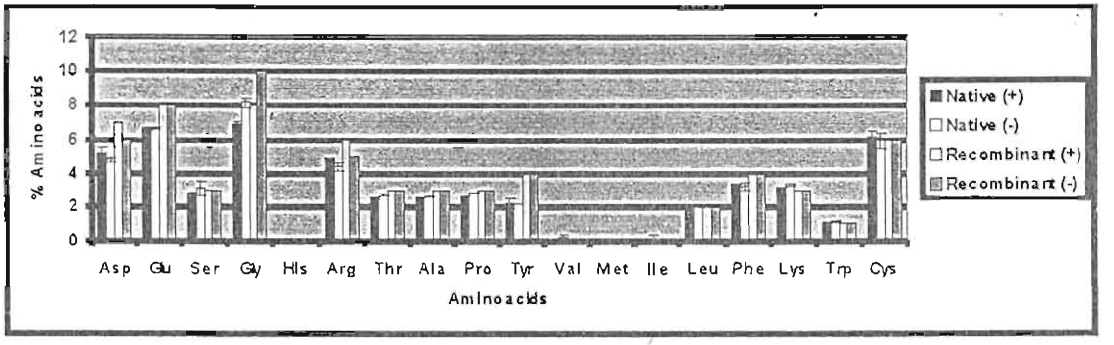

b)

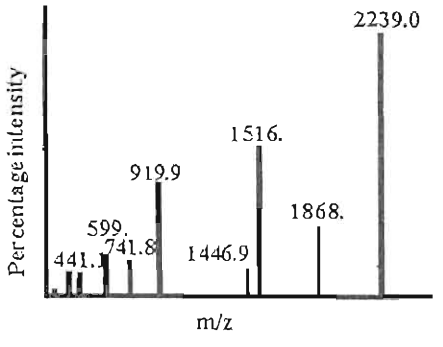

c)

Cleavage product		Molecular mass (Da) Experimental	Deduced
YQPECLEPSLYGCR (1-14)		1868.1	1866.1
GDEDATFGWTFDR (15-27)		1516.6	1516.5
EDGGCR (28-33)		741.6	738.9
QGSYCTR (34-40)		919.6	918.0
NYFR (46-49)		599.6	598.7
GDEDATFGWTFDRED GGCR (15-33)		2238.4	2238.3
Molecular mass of protein	(+)	6966.1	6965.6
	(-)	6808.8	6809.4

Fig. 2.21: Comparison of native savignygrin and the deduced amino acid sequence. (a) A comparison of the amino acid composition obtained for the native (+)/(-) forms and the composition calculated from the deduced amino acid sequences obtained after cloning and sequencing. (b) A representative peptide mass fingerprint of all four iso-forms, obtained for the savignygrins. (c) A comparison of the peptide masses obtained experimentally for the native savignygrins and those calculated for the deduced amino acid sequence. Total protein molecular mass obtained for the (+)/(-) forms by ESMS and a calculated molecular mass are also indicated.

2.3.17 Comparison of savignygrin with disagregin

BLAST analysis of the protein sequences of savignygrin indicated significant homology (E-value: $4x10^{-13}$) to the platelet aggregation inhibitor disagregin, from the related soft tick, *O. moubata*. Alignment using the Dayhoff PAM250 matrix gave an identity of 44% and similarity of 72% (Fig. 2.22).

```
Savignygrin (+): 1-YQPECLEPSLYGCRGDEDATFGWTFDREDGGCRQGSYCTRFGQPKNYFRSERDCKKACGNA - 61
Savignygrin (-): 1-YQPECLEPSLYGCRGDEDATFGWTFDREDGGCRQGSYCTRFGQPKNYFRSEGDCKKACGGA - 61
Disagregin     : 1-SDDKCQGRPMYGCREDDDSVFGWTYDSNHGQCWKGSYCKHRRQPSNYFASQQECRNTCGA- - 60
SSPro prediction:  CCCCCCCCC********CC*EEEEE*CCCCCEEEEEECCCCCCCCCC***HHHHHHH*CC
```

Fig. 2.22: Alignment of savignygrin with disagregin. Identity (66%) is boxed in black, while similar amino acids are boxed in grey. Secondary structure prediction using the SSPro server is indicated with C: random coil, E: extended β-sheet, H: α-helix and *: no consensus secondary structure. GenBank accession codes are for savignygrin (+) (AF452885), savignygrin (-) (AF452886) and disagregin (A54369).

2.3.18 Origins of (+)/(-) forms: alleles or gene duplication?

The origins of protein isoforms are important when the evolutionary history of a protein is considered. Isoforms could be a conformational artefact inherent in the primary structure of the protein itself, as was observed for the A/B forms. Proteins can also be post-translationally modified to various extents, which can confer different chemical and physical properties to isoforms. The (+)/(-) forms have been shown to differ on the gene level. As such, these isoforms might be either different alleles or might be gene duplications. To investigate these different possibilities, savignygrins from twenty individuals were prepared by RPHPLC and analyzed with tricine SDS-PAGE. The analysis indicated that all four isoforms were present in all twenty individuals (Fig. 2.23). It is known that *O. savignyi* is diploid with the sex chromosomes being XX and XY for females and males, respectively (Howell, 1966a). It could further be assumed that the collected ticks are representative of a population that mated randomly. For a diploid random population, the Castle-Hardy-Weinberg Law states that the gene frequencies can be expressed as: $(p+q)^2 = p^2 + 2pq + q^2$, where p and q are the frequencies of the homozygous alleles (AA, aa) and pq the heterozygous alleles (Aa). The frequencies of the alleles vary between 0 and 1 so that the sum always equals 1. Under these assumptions, the maximum heterozygosity attainable is at the point where p=q so that the

frequency of 2pq can never exceed 0.5 (Spiess, 1989). The probability of picking 40 alleles (20 ticks) at random and finding all heterozygous is ~1 in a trillion (0.5^{40}), seems very unlikely. Another possibility could have been the localization of the savignygrins on the sex chromosomes, so that males would always be heterozygous. This was excluded by analysis of females only. The other possibility is positive overdominance, which is found when the heterozygote has a higher mean fitness than either homozygote (Parsons and Bodmer, 1961). In the present case this implies that both homozygotes are lethal as they are not present at all in the analyzed population. The close similarity in sequence and biological activity between the high and low mass forms would make this scenario extremely unlikely. The savignygrins are most of the time stored away until feeding and probably do not interact at all with important cellular processes within the tick. From these considerations, the possibility that the savignygrins are different alleles is very unlikely. The more likely scenario is that of a recent gene duplication event that would ensure representation of the savignygrins in all ticks tested.

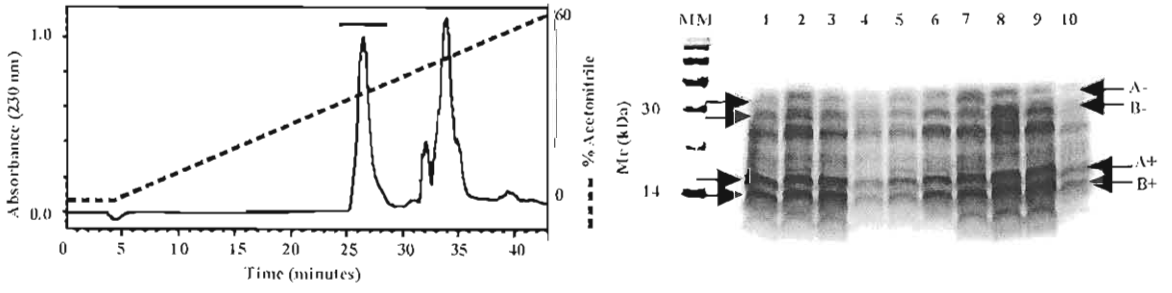

Fig. 2.23: Analysis of savignygrin isoforms in twenty individuals. A representative chromatogram of the SGE from one tick fractionated with RPHPLC is indicated on the left. The horizontal line indicates fractions analyzed. Non-reducing tricine SDS-PAGE analysis of savignygrin preparations from 10 ticks is indicated on the right. Arrows indicate the savignygrin isoforms. Results for the other ten ticks were similar.

2.4 Discussion

2.4.1 Savignygrin (+)/(-) isoforms: conformational and genetic origins

Amino acid composition, peptide mass fingerprinting, ESMS and N-terminal sequence analysis indicate that the 4 isoforms purified for savignygrin, have similar amino acid sequences. The translated amino acid sequences confirmed the near identical sequences of the high (+) and low (-) mass forms and account for the ESMS derived mass difference observed, as well as the separation of these forms during AEHPLC. Careful analysis of the native and recombinant amino acid compositions show that the (-) forms have lower aspartic acid and arginine values, but a higher glycine value, with respect to the (+) forms. This corresponds with the sequence data. It has been shown that the (+)/(-) forms must be gene duplicates. Interestingly, no isoforms were observed for disagregin and no difference could be observed in the electrophoretic mobilities under reduced and non-reduced conditions (Karczewski, Endris and Connolly, 1994). This could indicate that the (+)/(-) gene duplication is a fairly recent event that occurred after the divergence of these two tick species from a common ancestor.

The presence of the A/B conformational isoforms are more problematic, as no sequences were obtained that could explain the differences. It is not surprising to find separation of a single protein into two peaks during RPHPLC and has been observed for a number of proteins. Such two-peak separations are generally observed for proteins that are stable under reversed-phase chromatography conditions (low pH and high concentrations of organic mobile phase), so that native as well as unfolded forms are present (Kunitani and Johnson, 1986). The high stability of the savignygrins correlates well with this data. It is thus proposed that the A/B forms are not sequential isoforms, but rather an artefact of the purification procedure.

2.4.2 Conformational and stability differences observed between the (+)/(-) forms

Electrophoretic analysis and temperature stability studies indicated that the (-) forms are less stable than the (+) forms. The R52G difference between the high and low mass forms occurs in a region predicted to be a α-helix. Destabilization of this α-helix by G52 could lead to the lower stability observed for the low mass form. Glycine has been shown to be

one of the most helix-destabilizing residues (Chakrabartty, Schellman and Baldwin, 1991 and references therein). This destabilizing effect is described as being due to greater flexibility of the glycine peptide backbone, which thermodynamically prefers a random coil stucture instead of the α-helical structure. Glycine also lacks the enthalpic interaction between Cβ and the α-helix backbone that favours the helix. G52 as such probably does not destabilize the helix under native conditions, but under conditions of high temperature and SDS concentration as used during electrophoresis, leads to destabilization of the structure and the observed shift in electrophoretic mobility. The N60G difference between the high and low mass forms occurs outside any secondary stucture elements, right at the end of the protein sequence and would not be expected to have significant effects on the protein structure.

2.4.3 Electrophoretic behaviour of the savignygrins

All isoforms showed a decrease in electrophoretic mobility under non-reducing conditions, suggesting a compact structure that inhibits SDS binding. This is a phenomenon observed for proteins with intra-chain disulphide bonds (Pitt-Rivers and Impiombato, 1968). The same unusual electrophoretic behaviour was observed for echistatin under non-reducing conditions, while an unusual rapid migration was observed for the S-alkylated protein (Gan *et al.* 1988). The low hydrophobicity (13% hydrophobic amino acids) of the savignygrins could also influence electrophoretic behaviour, as it was observed that peptides with a low hydrophobicity behave unusually during electrophoresis, presumably due to reduced SDS binding (Hayashi and Nagai, 1980). A compact structure stabilized by disulphide bonds could explain the high temperature stabilities and why these inhibitors are not fixed by normal methanol:acetic acid fixation procedures after electrophoresis under non-reducing conditions. High temperature stabilities have also been observed for proteins with low hydrophobicity (Russouw *et al.* 1995).

2.4.4 Biological activity of savignygrins

The biological activity of the savignygrins was not affected by sequence or conformation differences, as indicated by similar IC_{50} values (~130 nM) for all four isoforms. This

could be accounted for in part by the RGD motif that is present in all four isoforms. Activation of platelets pre-incubated with savignygrin was indicated by a decrease in transmittance during inhibition of platelet aggregation induced by various agonists. Electron microscopic analysis of platelets incubated with savignygrin before activation with ADP confirmed the discoid to spherical shape change associated with activation. Maintenance of a spherical shape during disaggregation of aggregated platelets by savignygrin indicated that no signal transduction events occur except for a dissociation of fibrinogen from $\alpha_{IIb}\beta_3$. This suggests post-activation inhibition by the savignygrins and implicates the common denominator of platelet aggregation, the integrin $\alpha_{IIb}\beta_3$. Inhibition of the binding of αCD41-FITC in the presence or absence of ADP strongly suggests that savignygrins bind to resting as well as activated $\alpha_{IIb}\beta_3$, corresponding with the above hypothesis. This is furthermore supported by the inhibition of binding of purified $\alpha_{IIb}\beta_3$ to fibrinogen. The discrimination observed for savignygrin between $\alpha_v\beta_3$ and $\alpha_{IIb}\beta_3$ was also found for disagregin (Karczewski, Endris and Connolly, 1994).

2.4.5 The RGD motif of the savignygrins

It has been shown that disagregin inhibits the binding of echistatin (which contains the RGD motif) to platelets, suggesting interaction with the RGD binding site of $\alpha_{IIb}\beta_3$ (Karczewski, Endris and Connolly, 1994). This is strongly supported by the presence of an RGD motif in the sequence of savignygrin. Although disagregin has a RED motif and peptide studies showed that the peptide REDV does not inhibit platelet aggregation, a restricted conformation induced by the three dimensional structure of disagregin could account for inhibitory activity (Chen *et al.* 1991). This is supported by the dependence of savignygrin on intact disulphide bonds for the maintenance of an active but restricted biological conformation. The sequence adjacent to the RGD motif of savignygrin (YGCRGDEDA) is similar to that of disagregin (YGCREDDDS), which suggests that the sequence around the RGD motif could have an important effect on its function. Of particular interest is the fact that the two downstream residues are negatively charged. It is possible that these residues interact with the Ca^{2+} binding site localized inside the $\alpha_{IIb}\beta_3$ ligand-binding locus speculated to interact with the negatively charged aspartic acid of the RGD motif (Calvete, 1994). It was also shown that disagregin can inhibit the

binding of the dodecapeptide sequence of γ-fibrinogen to $\alpha_{IIb}\beta_3$ (Karczewski and Connolly, 1997). There may thus be other binding sites for $\alpha_{IIb}\beta_3$, apart from the RGD motif in the savignygrins.

Secondary structure elements are normally conserved in proteins with the same structural folds. This is exemplified by the conserved areas observed for the predicted β-sheet and α-helix elements in the alignment of disagregin and savignygrin. Of interest is the fact that the region surrounding the RGD/RED motif is the largest conserved stretch between disagregin and savignygrin. However, no consensus secondary structure is predicted in this region. As residues are normally conserved either for structural or functional purposes, this suggests that this region is important for activity.

2.4.6 Secretion of savignygrin during feeding

To have any biological significance during tick feeding, bioactive components have to be secreted (Law, Ribeiro and Wells, 1992). Secretory proteins are targeted to the endoplasmic reticulum via a hydrophobic signal peptide in their N-terminus, from where they are transported to the Golgi-network and finally secreted by either constitutive or regulated secretion in secretory granules. Extracellular proteins in general are disulphide rich and disulphide bonds are absent in intracellular proteins due to the reducing environment inside the cell (Gierasch, 1989; von Heijne, 1990; Fahey, Hunt and Windham, 1977). The presence of a signal peptide in the full-length sequences savignygrin and the fact that all cysteines are involved in disulphide bonds, indicate that the savignygrins are targeted to the secretory pathway. No evidence that suggests secretion has been described for variabilin (Wang *et al.* 1996) or disagregin (Karczewski, Endris and Connolly, 1994).

2.4.7 Independent adaptation of hard and soft ticks to a blood feeding environment

Variabilin, a 40 amino acid platelet aggregation inhibitor from the hard tick, *D. variabilis* contains a RGD motif in the last third of its sequence (Wang *et al.* 1996). There is no amino acid sequence similarity between variabilin and savignygrin and the RGD position is completely different. This suggests that platelet aggregation inhibitors with RGD-like

motifs have evolved after the divergence of hard and soft ticks. This implies that the main tick families have adapted to their blood feeding environments independently.

2.5 Summary

The relationship between the different isoforms of savignygrin is summarized in Fig. 2.24.

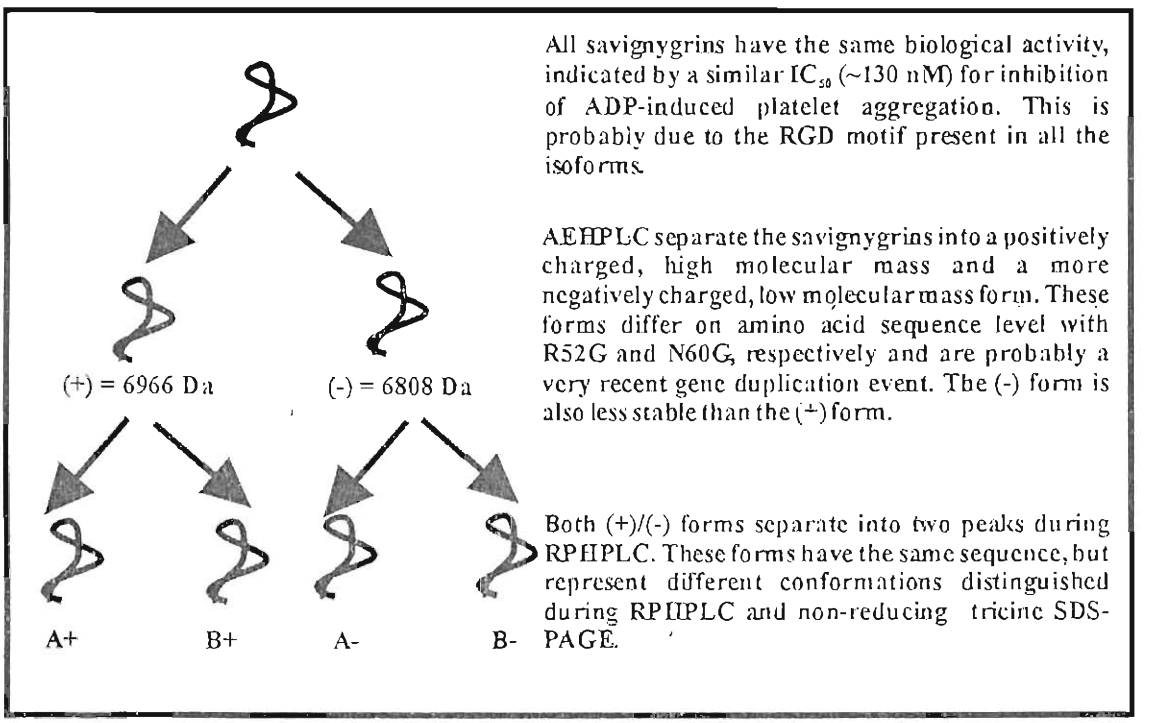

Fig. 2.24: The relationship between the different isoforms of savignygrin.

During the characterization of savignygrin, it became apparent that the platelet agregation inhibitors were related to the BPTI-like coagulation inhibitors of soft ticks. This relationship and its implications for the structure and function of the platelet aggregation inhibitors will be treated in Chapter 4. The amino acid sequences for the fXa inhibitors of *O. savignyi* and *O. moubata* were known, as well as the sequence for ornithodorin, the thrombin inhibitor from the tick, *O. moubata*. The amino acid sequence for savignin, the thrombin inhibitor from the tick *O. savignyi* was not known at this stage and for the sake of a complete phylogenetic analysis, savignin was also cloned and sequenced. Chapter 3 deals with the cloning, sequencing and molecular modeling of savignin and will serve as an introduction to the coagulation cascade inhibitors found in soft ticks.

Chapter 3: Homology modeling of savignin, a thrombin inhibitor from the tick *Ornithodoros savignyi**

*Part of the work presented in this chapter has been accepted for publication in Insect Biochemistry and Molecular Biology (Mans, Louw and Neitz, 2002a)

3.1.1 Introduction: The mechanism of serine protease activity

Serine proteases are a ubiquitous family that has been found in vertebrates, invertebrates, plants and prokaryotes. Serine proteases function as digestive enzymes (trypsin, chymotrypsin and elastase), clotting agents (blood coagulation cascade) or play a role in invertebrate immunity. Phylogenetic studies indicate that most serine proteases are homologous except for subtilisin from *B. substilis* that attained its similar mechanism of action through convergent evolution (Perona and Craik, 1997). The central mechanism of action of serine proteases consists of a nucleophilic attack on the carboxyl group of the scissile peptide bond by a reactive serine (Fig. 3.1).

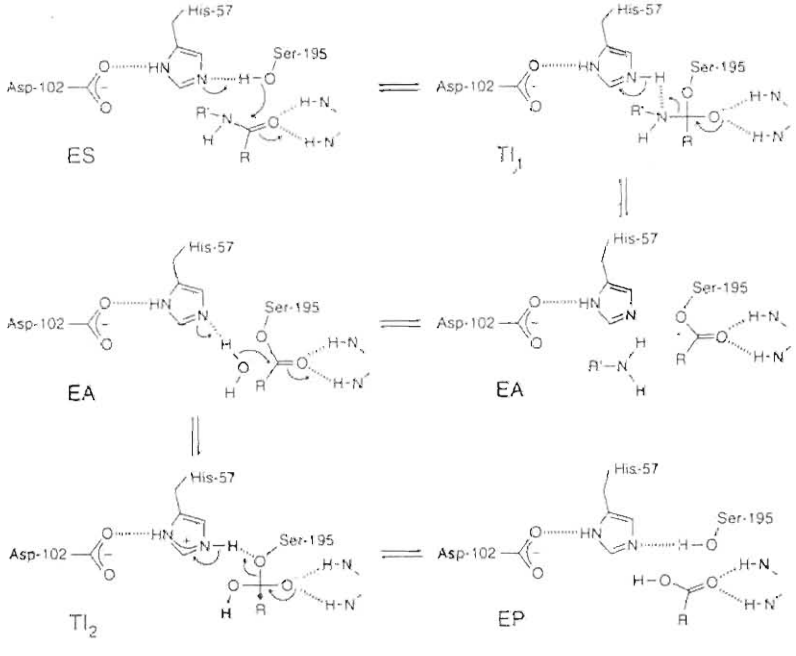

Fig. 3.1: Mechanism of action of serine proteases. The serine proteases form a noncovalent enzyme-substrate complex. Attack by the hydroxyl group of serine gives a tetrahedral intermediate that collapses to give the acylenzyme and the released amine. The acylenzyme hydrolyzes to form the enzyme-product complex via another tetrahedral intermediate followed by release of the carboxyl group. Adapted from Fersht (1999).

The active-site serine is highly reactive due to the specific conformation formed with histidine and aspartic acid (catalytic triad) that facilitates removal of the proton from serine's hydroxyl group, thus increasing the nucleophilic character of the oxygen, making serine more reactive (Fig. 3.2).

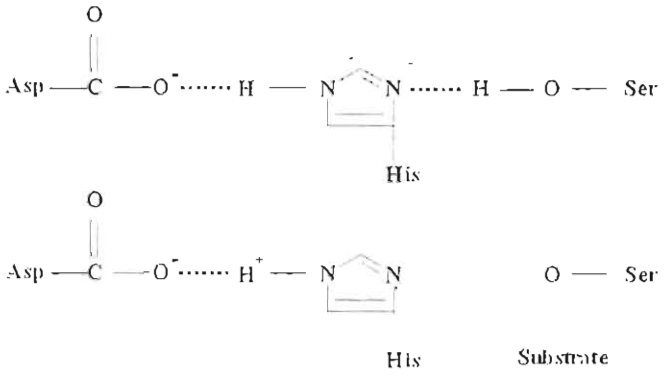

Fig. 3.2: The catalytic triad of the serine proteases. Due to the charge relay system of the catalytic triad, aspartic acid and histidine facilitates the removal of a proton from serine's hydroxyl group, allowing nucleophilic attack by serine. Adapted from Fersht (1999).

3.1.2 Specificity of serine proteases

Serine proteases are specific with regard to the sequences that are hydrolyzed. Trypsin and chymotrypsin for example hydrolyzes at the C-terminal side of basic (R, K) or aromatic residues (F, Y, W), respectively. Specificity is determined by a series of subsites in the binding pocket that recognize the scissile residue as well as the adjacent amino acids (Fig. 3.3). Loops close to the reactive site, can enhance steric control to increase specificity. Protease inhibitors that can bind tightly into these restricted conformations are not hydrolyzed because the leaving amino group is constrained and does not diffuse away from the active site of the enzyme (Fersht, 1999).

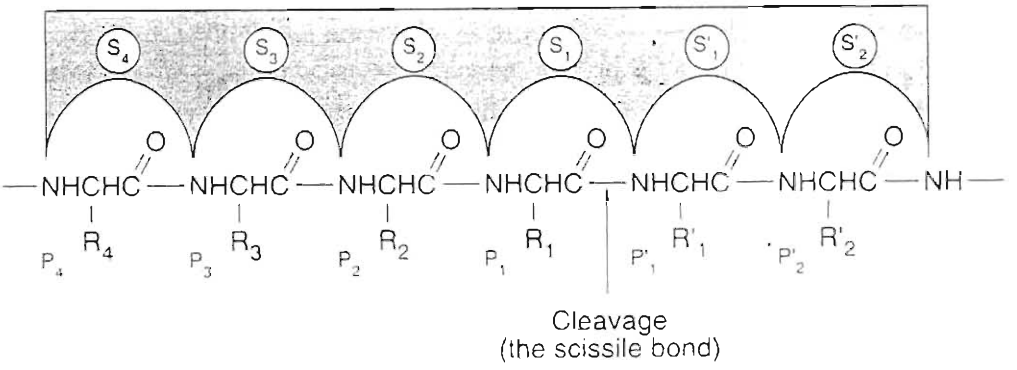

Fig. 3.3: Schechter-Berger notation for binding sites in the binding pocket (Schechter and Berger, 1967). The active site involved in the catalytic active site is named S_1, while the scissile residue is referred to as P_1. Upstream of this residue, the residues are named P'_2-P'_n and downstream to the scissile residue, P_1-P_n. Adapted from Fersht (1999).

3.1.3 Serine protease zymogens and inhibitors

Most serine proteases occur as inactive zymogens that are activated by proteolysis. Activity of the zymogens is very low due to conformational restraints on the binding site. This is an important regulatory mechanism by which levels of active proteases are kept in check, while active serine proteases are regulated by specific inhibitors of which there are at least 16 different families (Bode and Huber, 1992). The PI-1, PI-2, STI-Kunitz, Bowman-Birk and squash seed inhibitors are all from plants. The most extensively characterized inhibitors are the serpins, the Kazal and BPTI (basic/bovine pancreatic trypsin inhibitor) families. The serpins are large glycoproteins (>40kDa) that interact transiently via an exposed binding loop with the active site, until hydrolysis of this loop and release (Bode and Huber, 1992). Most small inhibitors react with their enzymes via an exposed binding loop (reactive site) with a characteristic canonical conformation. Most of these inhibitors have a compact conformation with a hydrophobic core stabilized by disulphide bonds. While the protein folds of these inhibitors might be conserved, the reactive site residue (P_1) is normally hypervariable, so that replacement with another residue normally leads to a change in inhibition specificity. This is in contrast to other proteins, where the active site residues are normally very conserved (Laskowski and Kato, 1980).

3.1.4 The BPTI /Kunitz family of serine protease inhibitors

The BPTI/Kunitz family of serine protease inhibitors is small (50-65 residues), with 6 cysteines arranged in a characteristic disulphide bond pattern (Laskowski and Kato, 1980) (Fig. 3.4A). The basic structure consists of an N-terminal 3_{10}-helix around the first cysteine, a central double stranded anti-parallel β-sheet linked by a hairpin loop and a C-terminal three turn α-helix (Fig. 3.4B). The binding loop exhibits a characteristic conformation from P_3 to P'_3 and is stabilized by a cysteine at P_2 that is disulphide-connected to the hydrophobic core. The binding-site loop associates with the catalytic residues of the cognate enzyme in a similar manner as the productively bound substrate, with the P1 carbonyl carbon fixed in contact with the reactive serine. The scissile peptide bond remains intact, with a slight out-of-plane deformation of the carbonyl oxygen. The P3-P3' sites also interact with their cognate enzymes, while secondary contacts can also occur (Bode and Huber, 1992).

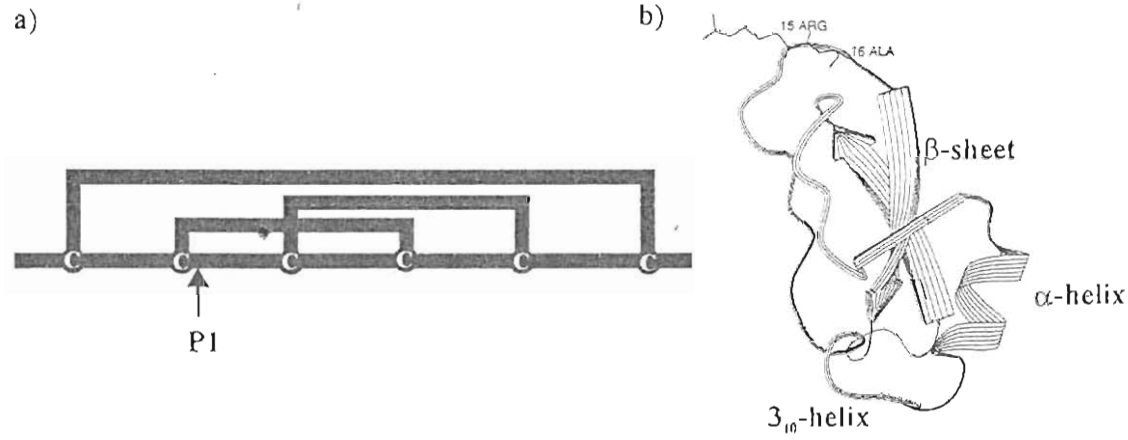

Fig. 3.4: BPTI -Kunitz inhibitor structure. (a) The characteristic disulphide bond pattern of BPTI-Kunitz inhibitors. Cysteines are indicated with dots and the P1 site with an arrow. (b) The structure of BPTI with its reactive arginine indicated. Note the N-terminal 3_{10}-helix, central β-sheet and C-terminal α-helix. Adapted from Bode and Huber (1992).

3.1.5 Tick-derived serine protease inhibitors of fXa and thrombin

Factor Xa (TAP and fXaI) and thrombin (ornithodorin and savignin) inhibitors from soft ticks are part of the BPTI/Kunitz family. The mechanism of inhibition is distinct from that found for the canonical BPTI inhibitors. Both tick inhibitors insert their N-terminal residues into the active site of their enzymes, in a manner reminiscent to that of hirudin, a

thrombin inhibitor from the leach *Hirudo medicinalis* (van de Locht *et al.* 1996; Wei *et al.* 1998). Hirudin inserts its first three N-terminal amino acids into the active-cleft of thrombin, forming a parallel β- sheet structure with thrombin segment Ser214-Gly219. This is in contrast to the anti-parallel binding of the canonical BPTI inhibitors. The catalytic Ser195 of thrombin is not blocked. The extended carboxy-terminal tail of hirudin (I48-I65) runs along a groove extending from the active-site cleft of thrombin to the positively charged fibrinogen secondary recognition exosite, where it interacts electrostatically (Grütter *et al.* 1990, Rydel *et al.* 1990).

3.1.6 The TAP-fXa complex

TAP is the first inhibitor of fXa purified from soft ticks. It consists of 60 amino acids, with a molecular mass of 6850 Da (Waxman *et al.* 1990). It was recombinantly expressed in yeast and rTAP exhibited all the characteristics of the wild type inhibitor (Neeper *et al.* 1990). TAP has limited homology to the Kunitz-type inhibitors, but determination of its disulphide bond pattern showed that it shared the characteristic disulphide bond pattern of the prototype BPTI-fold (Sardana *et al.* 1991). Determination of the solution NMR structure of TAP also indicated that the β-sheet and α-helical secondary structure elements were similar to that of the BPTI-fold. Due to insertions and deletions in the primary structure of TAP the loops before and after the β-sheets differ extensively in conformation from the prototype BPTI-fold (Antuch *et al.* 1994). It was shown that TAP is a tight-binding competitive inhibitor of fXa that binds to fXa via a two-step mechanism that involves a secondary binding-site (Jordan *et al.* 1990; Jordan *et al.* 1992). Site-directed mutagenesis indicated two areas of the primary structure involved in fXa interaction, the primary recognition site being the first four N-terminal amino acid residues as well as a secondary site between residues 40-54 (Dunwiddie *et al.* 1992). The mechanism of TAP interaction is thus completely different from that of canonical BPTI-inhibitors. Determination of the crystal structure of the TAP-fXa complex (Fig. 3.5) confirmed these biochemical studies and showed that the three N-terminal residues bind inside the P1, P2 and aryl binding pocket of the active-site while Asp47-Tyr49 and Asp55-Ile60 interact with a secondary binding site close to the active-site (Wei *et al.* 1998). To account for the two-step kinetic mechanism observed for TAP, it has been

suggested that an initial slow-binding step occurs at the secondary binding site, which induces a conformation change in the N-terminal residues with concomitant binding into the active site. This could in part explain the slow-tight binding kinetics observed for these inhibitors. Recently, the structure for a TAP-BPTI complex has been determined and it was shown that the conformation of the N-terminal residues probably differ quite extensively for the free and fXa bound TAP, which supports the hypothesis that the N-terminal undergoes a conformational change upon binding (St Charles *et al.* 2000).

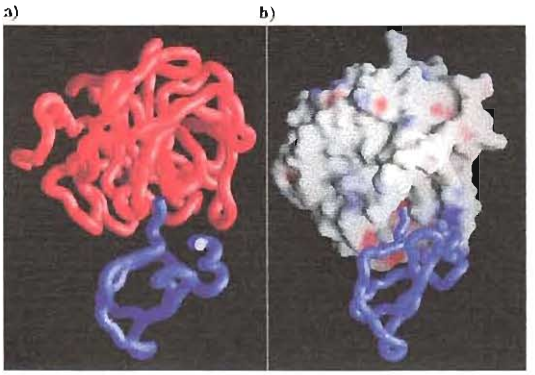

Fig. 3.5: The fXa-TAP complex. (a) Factor Xa is indicated in red and TAP in blue. (b) TAP is indicated in blue and fXa as a surface model. Blue and red surfaces correspond to positive and negative electrostatic potentials, respectively. The coordinates were obtained from the protein databank (PDB: 1KIG).

FXaI is orthologous to TAP and has been purified from *O. savignyi*. It is a slow-tight binding inhibitor (Ki~0.83 nM) with a molecular mass of 7183 Da, consisting of 60 amino acids and it shows 46% identity and 87% similarity to TAP (Fig. 3.6) (Gaspar *et al.* 1996; Joubert *et al.* 1998).

```
fXaI : YNRLCVKPQDFTKQCSDDEDAVKVFFPHDKKSCEPFWICPEEDNGVDYYSTKEDCLSACF : 60
TAP  : YNRLCIKPRDWIDECDSNEGGERAYFRNGKGGCDSFWICPEDHTEADYYSSYRDCFNACI : 60
```

Fig. 3.6: Alignment of fXaI and TAP. Shown is the conserved BPTI-fold disulphide bond pattern and similarity according to the PAM250 matrix (boxed in black).

3.1.7 The ornithodorin-thrombin complex

Thrombin is characterized by its high specificity. This is in part due to insertion loops (loop 60 and 149) present around the active site, which restrict access to the active site, so that typical BPTI-like inhibitors cannot bind (Stubbs and Bode, 1993). Thrombin also

contains a basic fibrinogen recognition exosite, which is important for substrate recognition. Ornithodorin, a thrombin inhibitor from the tick *O. moubata* has been co-crystallized with thrombin (van de Locht, 1996). It consist of a N-terminal BPTI-like domain (1'-53') and a C-terminal BPTI-like domain (60'-119') connected by 7 amino acid residues. The N-terminal domain is involved in interaction with the thrombin active site, via its N-terminal residues as well as secondary interaction with the insertion 60 loop. It's C-terminal domain interacts with the basic fibrinogen recognition site via the C-terminal α-helix and possibly the overall negative electrostatic potential of this domain (Fig. 3.7). No mechanism of conformational rearrangement has as yet been proposed for ornithodorin.

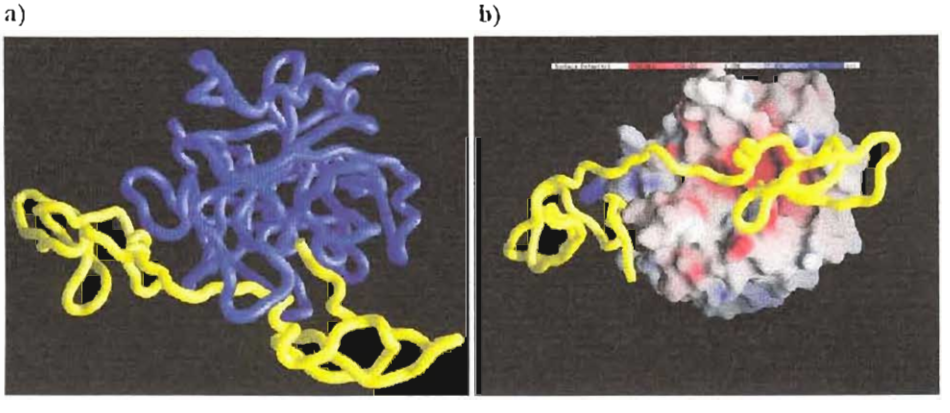

Fig. 3.7: The ornithodorin-thrombin complex. (a) Insertion of the N-terminal residues of ornithodorin (yellow) into the active-site of thrombin (blue) are shown, as well as the proximity of the insertion loops of thrombin to its active-site. (b) Interaction of the C-terminal helix with the basic fibrinogen recognition site is clear. The blue and red surfaces indicate basic and acidic electrostatic potentials, respectively. Coordinates are (PDB:1TOC).

Savignin, an orthologous inhibitor from the tick *O. savignyi* has been kinetically characterized and was shown to be a potent slow-tight binding inhibitor (Ki~5pM), although no specific mechanism could be assigned to it. A much lower affinity (Ki~22 nM) for γ-thrombin, which lacks the fibrinogen recognition exosite, indicated that this site is important for high affinity binding. Changes in the ionic strength had no effect on the Ki of savignin, which indicates that electrostatic interaction is not the main type of interaction (Nienaber, Gaspar and Neitz, 1999). This chapter deals with the further characterization of savignin on the molecular level.

3.2 Materials and methods

3.2.1 Cloning, sequencing and sequence analysis of savignin

The experimental procedures described in Chapter 2 have essentially been followed to clone and sequence savignin. To obtain the coding gene and 3' untranslated region (3' UTR), a degenerate primer (ThrombA: YTN AAY GTI MGI TGY AAY AA) was designed using the first seven amino acids (LNVRCNN) obtained previously (Nienaber, Gaspar and Neitz, 1999). To obtain the 5' UTR and signal peptide sequence a gene specific primer (ThrombC1: CTC GAG TTC CAT TGA AAC GCC ACA) complementary to the coding sequence of the last six amino acids of savignin (CGVSME) was designed. 3'RACE and 5'RACE was performed as described and a 500bp product obtained for 3'RACE and a 450bp product for 5'RACE. These were cloned into the pGEM T-Easy Vector for sequencing.

3.2.2 Molecular modeling of savignin

The deduced protein sequence of savignin, was submitted to the SWISS-MODEL Automated Comparative Protein Modeling Server (Peitsch 1995; Peitsch 1996; Guex and Peitsch, 1997) for modeling. Procheck provided Ramachandran plot parameters (Laskowski *et al.* 1996) and ProFit V1.8 the root mean square deviation (RMSD) (http://www.biochem.ucl.ac.uk/~martin/swreg.html) values for carbon α backbone fits of ornithodorin and savignin. WHATIF (Vriend, 1990) was used to validate the model obtained and LIGPLOT (Wallace, Laskowski and Thornton, 1995) to calculate which residues interact between inhibitors (savignin and ornithodorin) and thrombin. The structure of the ornithodorin-thrombin complex (PDB ID: 1TOC) was obtained from the RCSB Protein Databank (Berman *et al.* 2000; http://www.rcsb.org/pdb/). All worm figures and surface models were constructed with the Graphical Representation and Analysis of Surface Properties (GRASP) program (Nicholls, Sharp and Honig, 1991). Molecular distances were measured using Rasmol v3.7. The nomenclature used was adapted from van de Locht *et al.* (1996) so that savignin and ornithodorin residues are indicated by primes.

3.3 Results

3.3.1 RACE and sequencing of savignin

3'RACE under optimized conditions with the degenerate primer designed from the N-terminal sequence of savignin gave a product of approximately 500 bp which include the ORF and 3'-UTR. 5' RACE resulted in a product of approximately 450 bp, which include the ORF and 5'-UTR (Fig. 3.8). The cDNA sequences obtained revealed all primers used during PCR and the ORF, 5' and 3' UTR's. The cDNA also contains the stop codon (TAG) and an unusual poly-adenylation signal AATACA.

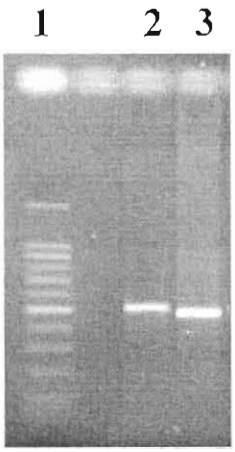

Fig. 3.8: RACE of savignin. The ORF and 3'UTR of savignin were obtained from single-stranded cDNA with 3'RACE using a 5' N-terminal degenerate primer and 3' poly-T anchor primer (lane 2). The 5' UTR and signal peptide sequence were obtained from double-stranded cDNA using 5'RACE with a 3' gene specific primer and a 5' adapter primer (lane 3). Lane 1 is 100 bp ladder with the 500 bp marker showing twice the intensity of the other markers.

3.3.2 Analysis of the recombinant amino acid sequence of savignin

The translated amino acid sequence gave a protein of 134 amino acids, while the mature chain consisted of 118 amino acids. The first 11 amino acids of the ORF corresponded to that obtained with Edman degradation (Fig. 3.9; Table 1). Analysis of the immature protein using SignalP (Nielsen *et al.* 1997), correctly predicted the presence of the signal peptide (16 amino acids) and the correct cleavage site.

```
aactcactatagggctcgagcggccgcccgggcgggtgctttaccagccagaagatgctcttttacgtcgtaataact -75
                                                        M  L  F  Y  V  V  I  T  - 8

ctcgtcgctggaacggtttctggattgaacgttcgatgcaacaacccgcatactgccaactgcgaaaatggtgcaaag -150
 L  V  A  G  T  V  S  G  L  N  V  R  C  N  N  P  H  T  A  N  C  E  N  G  A  K  - 34

cttgagagctattttagggaggggggaaacgtgcgtagggtcaccagcatgtcctggagaaggatacgccactaaggag -225
 L  E  S  Y  F  R  E  G  E  T  C  V  G  S  P  A  C  P  G  E  G  Y  A  T  K  E  - 60

gactgtcagaaggcctgtttccctggcgggggagaccacagcactaatgtcgacagctcatgctttggtcaaccgccc -300
 D  C  Q  K  A  C  F  P  G  G  G  D  H  S  T  N  V  D  S  S  C  F  G  Q  P  P  - 86

acttcctgcgagactggagcggaggtaacctactacgattctggtagcagaacgtgtaaggtactacaacatggctgt -375
 T  S  C  E  T  G  A  E  V  T  Y  Y  D  S  G  S  R  T  C  K  V  L  Q  H  G  C  -112

ccatcgagtgaaaacgcattcgattcagagattgagtgccaagtcgcttgtggcgtttcaatggaatagcagggctgt -450
 P  S  S  E  N  A  F  D  S  E  I  E  C  Q  V  A  C  G  V  S  M  E  -             -134

aggaagacacagcgtgaagtcggcatctgaaccgaacccaatctaatcatgacacagaaaatacagcctgtagtaaaa -525

aagtcaaaaaaaaaaaaaaaaagagtgttgtggtaatgatagc                                    -569
```

Fig. 3.9: cDNA sequence and deduced protein sequence of savignin. A cDNA sequence of 569 base pairs was obtained. The 5' adapter, 3' gene specific and 3' anchor primer are shown in bold. The stop codon (TAG), and unusual poly-adenylation signal (AATACA) and the poly-A tail are boxed. The N-terminal sequence previously obtained with N-terminal Edman degradation is underlined while the N-terminal sequence used for degenerate primer design is shown in bold. The signal sequence is underlined with a dashed-line.

3.3.4 Comparison of the recombinant sequence data with data from native savignin

The predicted amino acid composition of recombinant savignin corresponds well with that obtained for the native inhibitor (Fig. 3.10).

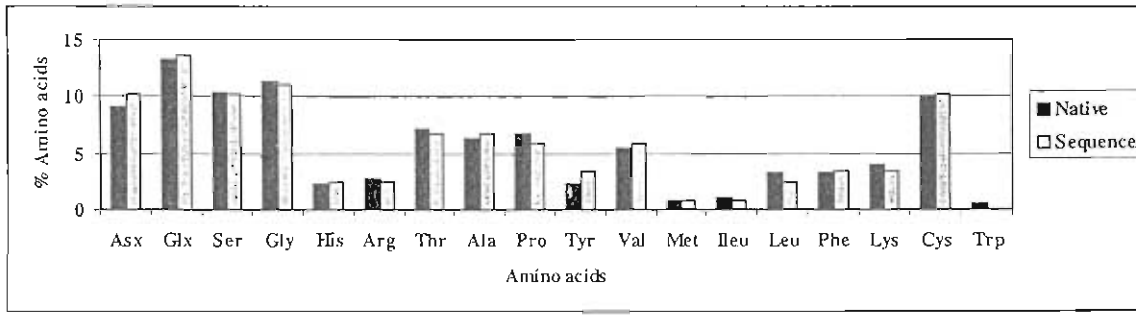

Fig. 3.10: Amino acid composition of native and recombinant savignin. Comparison of the amino acid analysis values obtained for the native protein (adapted from Nienaber, Gaspar and Neitz, 1999) and the deduced amino acid composition obtained for recombinant savignin.

Furthermore, the molecular mass of savignin as determined by electrospray mass spectrometry (Nienaber, Gaspar and Neitz, 1999), correlated with the calculated mass obtained for the recombinant inhibitor (Table 3.1). The number of basically charged residues also corresponded with the number of charged species obtained during ES-MS (results not shown). The predicted iso-electric point is midway between the empirically determined points of the two iso-forms described previously. Taken together these results confirmed the correctness of the cDNA sequence as well as the deduced amino acid sequence of savignin.

Table 3.1: Experimental parameters for native savignin compared with the values calculated from the recombinant sequence. The N-terminal sequence, molecular mass and iso-electric point of native savignin (Nienaber, Gaspar and Neitz, 1999), compared with the deduced amino acid sequence and molecular mass and iso-electric point calculated from the deduced amino acid sequence. Iso-electric points were calculated using compute pI/Mr at the Expasy server (Bellqvist *et al.* 1993)

	Native protein	Recombinant sequence
N-terminal sequence	LNVRXNNPHTA	LNVRCNNPHTA
Molecular mass	12430.4 Da	12435.4 Da
Iso-electric point	4.2, 5.0	4.55

3.3.4 Sequence alignment of savignin with ornithodorin

The DNA sequence of savignin had 83% identity with the DNA fragment (Genbank accession code: A23191) that codes for the thrombin inhibitor ornithodorin (Fig. 3.11), from the related soft tick, *O. moubata* (van de Locht *et al.* 1996).

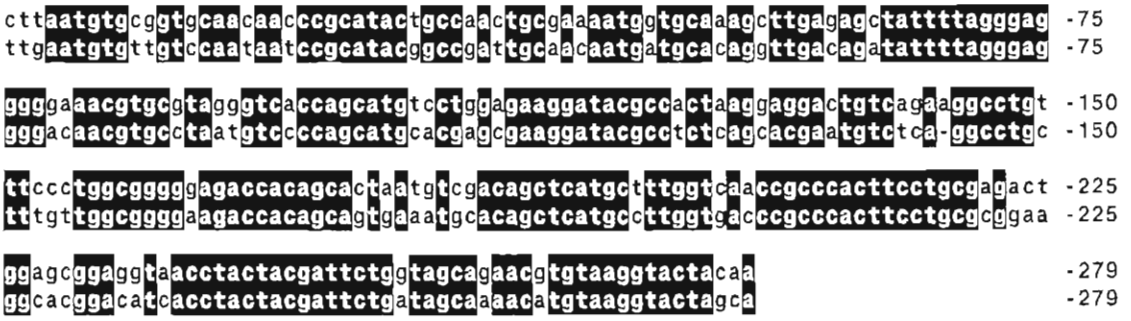

Fig. 3.11: cDNA sequence alignment of savignin (top rows) with ornithodorin (bottom rows). The cDNA fragment of ornithodorin obtained for the cloning gene (which include the first 275 bp) corresponds with residues 103-379 of savignin (Fig. 3.9). Identity (83%) is boxed in black. Genbank accession codes are savignin (AAL37210) and ornithodorin (A23191).

BLAST analysis of the deduced protein sequence of savignin indicated significant similarity (E-value: $1e^{-30}$) to ornithodorin (Genbank accession code: P56409). Alignment using the Dayhoff PAM250 matrix gave an identity of 63% and similarity of 89% (Fig. 3.12).

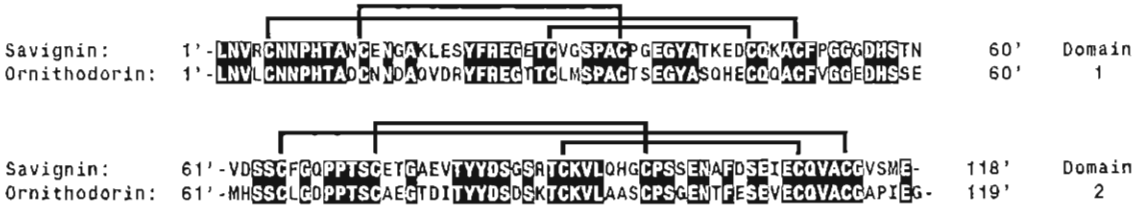

Fig. 3.12: Protein sequence alignment of savignin with ornithodorin. Identity (63%) is boxed in black while similar residues (89%) using the PAM 250 matrix (DENQH, SAT, KR, FY and LIVM) are shaded in gray. The N-terminal BPTI-like domain is from residue 1-53 and the C-terminal BPTI-like domain from residue 61-118. The distinct disulphide bond pattern of the BPTI fold is indicated for each domain. Genbank accession codes are savignin (AAL37210) and ornithodorin (P56409).

3.3.5 Homology modeling of savignin

Superposition of the α-carbon backbone structure of savignin onto that of ornithodorin gave an RMSD value of 0.252 Å for the full-length sequence (Fig. 3.13a). The N- (1'-53') and C-terminal (60'-118') domains gave values of 0.108 Å and 0.103 Å respectively, while the linker region (53'-60') showed the largest deviation (0.177 Å). The modeled surface structure of savignin shows the two separate domains distinctly with the single

chain linker in-between. The C-terminal domain is shown to consist of a predominantly negative electrostatic potential necessary for its proposed association with the basic fibrinogen binding exosite of thrombin (Fig. 3.13b).

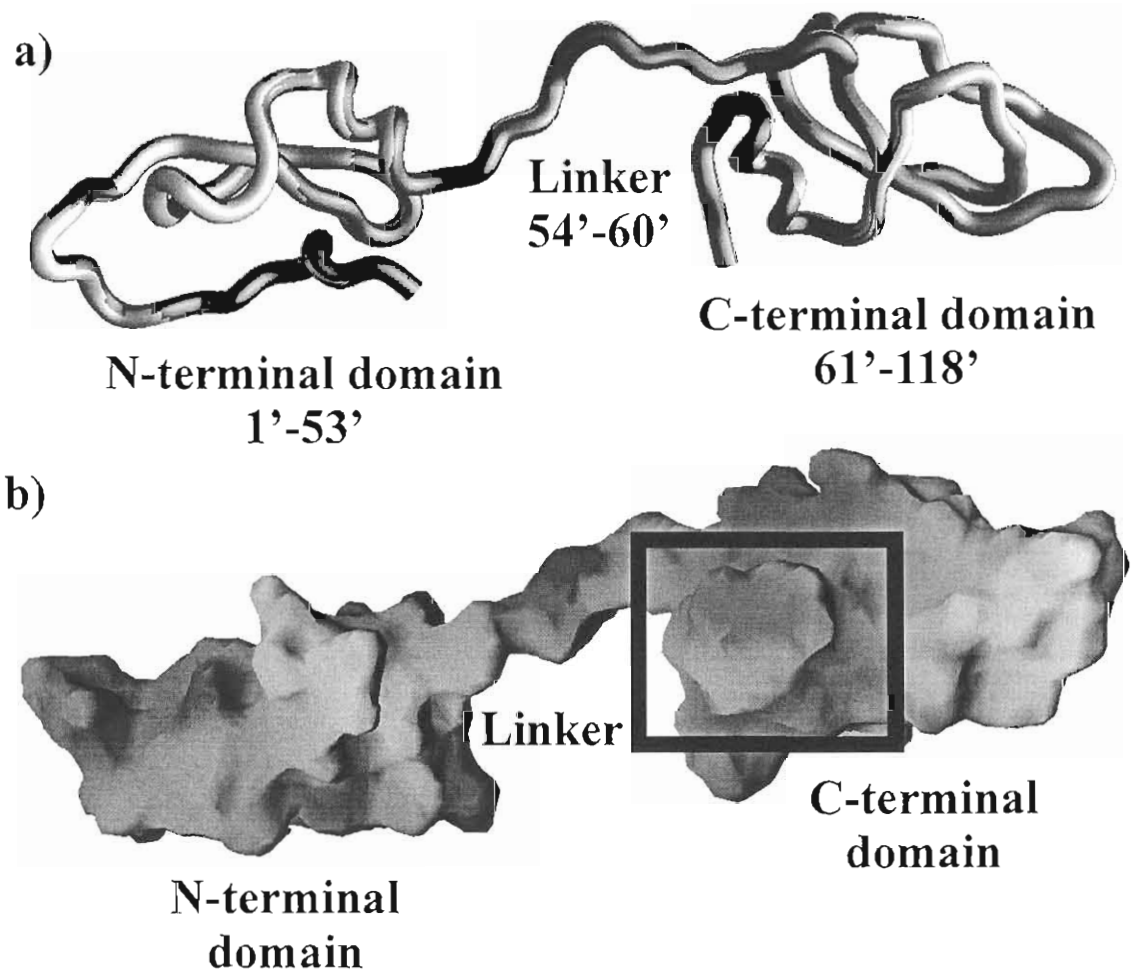

Fig. 3.13: Modeled structure of savignin. (A) Model of the backbone structure of savignin (light gray) superimposed on that of ornithodorin (dark gray). The RMSD value obtained for the two backbone structures is 0.25 Å. (B) A surface model of savignin with the C-terminal surface that interacts with thrombin's basic fibrinogen binding exosite boxed. The darker shadings of gray on the surface indicate acidic surface potential. In the current orientation, no significant basic surface potential is observed.

3.3.6 Interaction of savignin with thrombin

Docking of savignin with thrombin shows that the N-terminal fits inside the active site cleft of thrombin, as is found for ornithodorin (Fig. 3.14a). It also shows the C-terminal domain helix of savignin interacting with the fibrinogen binding exosite of thrombin. A surface model of savignin fitted to thrombin shows insertion of the N-terminal sequence into the active site of thrombin, while interaction with the fibrinogen binding exosite is even more evident (Fig. 3.14b). Prediction of the residues of savignin that interact specifically with thrombin in the modeled structure indicates three main regions (Table 3.2). The first is the N-terminal residues involved in the binding of savignin to the active site cleft of thrombin. The second region is the linker region between the two domains of savignin that is buried inside the structure of thrombin (Fig. 3.14b). The third region is around the C-terminal domain helix that is proposed to bind to the basic fibrinogen-binding site on thrombin. All interactions are mediated via hydrogen bonds or hydrophobic interactions. Residues of savignin involved in interaction with thrombin correlate to those of ornithodorin, suggesting similar mechanisms of action.

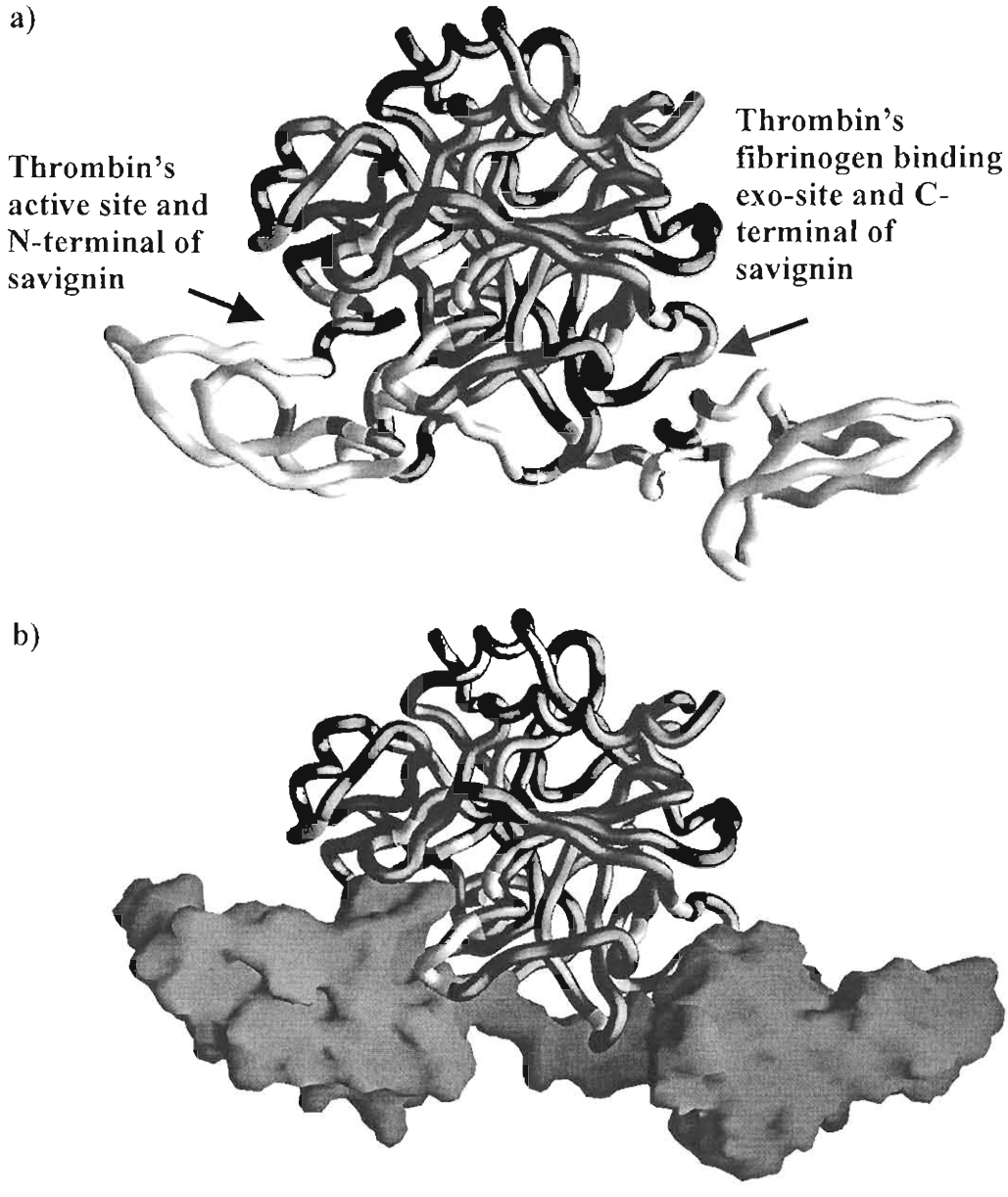

Fig. 3.14: Interaction of savignin with thrombin. (a) Structure of savignin (light gray) fitted into that of thrombin (dark gray). The N-terminal of domain 1 of savignin fits into the active site cleft of thrombin while the C-terminal α-helix of domain 2 of savignin shows close proximity to the fibrinogen-binding exosite of thrombin. Residues that interact between the two structures are indicated as dark and light grey for savignin and thrombin, respectively. (b) Surface model of savignin (gray) shows how the N-terminal residues are accommodated in the active site cleft of thrombin (dark gray), while the Arg4' is excluded from the active site (not shown). The proximity of savignin's C-terminal domain and α-helix region to the basic fibrinogen-binding exosite of thrombin, is evident. Indicated in light gray are the residues of thrombin that interact with savignin.

Table 3.2: Residues of ornithodorin and savignin that interacts with thrombin as predicted by LIGPLOT. Chain parameters are obtained from the PDB file (1TOC) of ornithodorin and thrombin.

Region of savignin	Ornithodorin	Savignin
N-terminal domain		Leu 1'– His 57
	Leu 1'– Leu 99	Leu 1'– Leu 99
	Leu 1'– Tyr 60A	Leu 1'– Tyr 60 A
	Leu 1'– Trp 60D	Leu 1'– Trp 60D
	Leu 1'– Ser 214	Leu 1'– Ser 214
		Leu 1'– Gly 216
	Asn 2'– Gly 219	Asn 2 – Gly 219
		Val 3'– Ile 174
	Val 3'– Gly 216	Val 3'– Gly 216
	Val 3'– Glu 217	Val 3'– Glu 217
	Val 3'– Trp 215	Val 3'– Trp 215
	Leu 4'– Glu 217	Arg 4' – Glu 217
	Leu 4'– Gly 219	Arg 4'– Gly 219
	Leu 4'– Arg 221	Arg 4' – Arg 221
	Cys 5'– Trp 60D	Cys 5'– Trp 60 D
	Asn 6'– Trp 60D	
	Asn 6'– Tyr 60A	
Linker region	Phe 51'– Glu 192	Phe 51'– Glu 192
	Asp 56'– Arg 73	Asp 56'– Arg 73
	Ser 58'– Thr 74	Ser 58'– Thr 74
	Glu 60'– Thr 74	Asn 60'– Thr 74
	His 62'– Arg 77A	
	Ser 64'– Arg 77A	
C-terminal domain	Glu 100'– Arg 77 A	Glu 100'– Arg 77A
	Thr 102'– Arg 77 A	Ala 102'– Arg 77A
	Phe 103'– Arg 77 A	
	Val 107'– Leu 65	Ile 107'– Leu 65
		Ile 107'– Ile 82
		Ile 107'– Met 84
	Glu 108'– Ile 82	Glu 108'– Ile 82
	Gln 110'- Gln 38	Gln 110'– Gln 38
	Val 111'– Gln 38	Val 111'– Gln 38
	Val 111'– Leu 65	Val 111'– Leu 65
	Val 111'– Ile 82	Val 111'– Ile 82
	Ala 112'– Tyr 76	
	Gly 114'– Gln 38	Gly 114'– Gln 38
	Ala 115'– Gln 38	Val 115'– Gln 38
	Ile 117'– Lys 36	
	Ile 117'– Leu 65	
Other	Arg 24'– Trp 60 D	Arg 24'– Trp 60 D
	Glu 25'– Trp 60 D	
	Gly 26'– Pro 60 B	Gly 26 – Pro 60 B
	Tyr 40'– Glu 146	Tyr 40 – Glu 146
	Gln 48'– Trp 148	Lys 48 – Trp 148

3.3.7 Quality assessment of the modeled structure of savignin

Analysis of the model of savignin using Ramachandran plots at a resolution of 2 Å indicates that 75% of the residues are in regions that are most favored, 20.8% are in additional allowed regions, 1% in generously allowed regions and no residues in disallowed regions (Fig. 3.15 and Table 3.3).

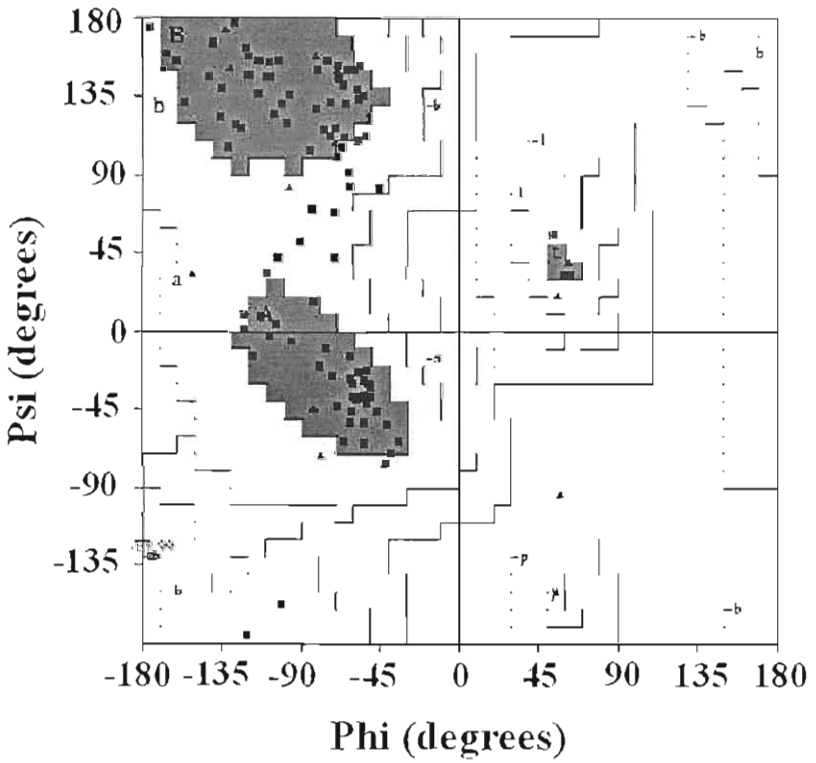

Fig. 3.15: Ramachandran plot of modeled structure of savignin. Position of residues is indicated by squares. Dark gray indicates most favored positions while lighter shades of gray indicate additionally and generally allowed regions respectively.

Compared to the expected values of the main chain parameters (quality assessment, peptide bond planarity, alpha carbon tetrahedral distorsion, hydrogen bond energies and overall G-factor) at 2 Å, the obtained values are within the normal distribution or even better (results not shown). It can be concluded that the model proposed for savignin is of high quality.

Table 3.3: Statistics of Ramachandran plots of savignin and ornithodorin. The number and percentage of residues and their localization on the Ramachandran plot is indicated for both ornithodorin and savignin. Values obtained with Procheck.

Characteristics	Ornithodorin	Savignin
Residues in most favoured regions	75 (75%)	75 (78.1%)
Residues in additional allowed regions	25 (25%)	20 (20.8%)
Residues in generously allowed regions	0	1 (1.0%)
Residues in disallowed regions	0	0
Number of non-glycine and non-proline residues	100	96 (100%)
Number of end-residues (exl. Gly and Pro)	3	2
Number of glycine residues	9	13
Number proline residues	6	7
Total	118	118

3.38 Unusual conformation of savignin and thrombin

The number of thermodynamically unfavorable solute-solvent interactions is minimized, by burying hydrophobic residues inside a protein structure. Generally the reduction of a protein's surface that is exposed to solvent is achieved by adoption of a spherical structure and hence the globular nature of most proteins (Jones and Thornton, 1995). In terms of this general observation, the structure of savignin and ornithodorin seems unusual, in that it is not globular but rather extended, with a single amino acid chain being exposed to the solvent in the linker area. To see whether this is truly a deviation from general trends, the relationship between molecular mass and protein volume of various proteins were investigated. It is clear that a direct relationship exists between the molecular mass and volume of globular proteins (Fig. 3.16). A volume of ~28000 $Å^3$ is calculated for savignin with its mass as 12430 Da. However, the volume measured (using the Rasmol package) from the structure of ornithodorin and the modeled structure of savignin is ~49000 $Å^3$, for which a molecular mass of ~19 kDa is calculated. This is clearly outside normal deviation. Bikunin, which is also a double BPTI-domain protein, falls well into the expected mass volume relationship (Xu *et al.* 1998).

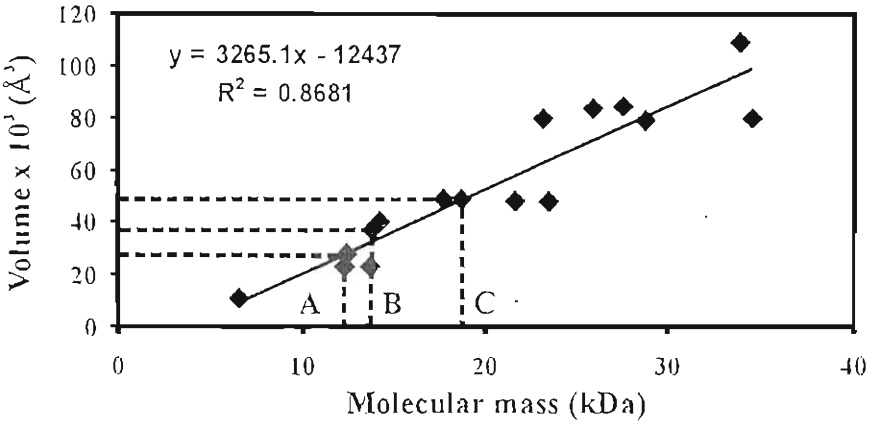

Fig. 3.16: Relationship between molecular mass and volume ($Å^3$) of various proteins. Hydrodynamic data of the various proteins were obtained from Creighton (1992). Dashed lines indicate values for (A) savignin's volume calculated from its molecular mass, (B) mass and volume for bikunin and (C) savignin's mass calculated from its measured volume.

Table 3.4: Proteins used for determination of the relationship between molecular mass and volume. Values were obtained from Creighton (1992). Masses and volumes determined from structures and sequence.

Protein	Mr (Da)	Dimensions (Å)	Volume ($Å^3$)
BPTI	6520	29 X 19 X 19	10469
Cytochrome c	12310	25 X 25 X 37	23125
*Savignin	12430	85 X 23 X 25	48875
Ribonuclease A	13690	38 X 28 X22	23408
*Bikunin	13850	52 X 29 X 24	36192
Lysozyme	14320	45 X 30 X 30	40500
Myoglobin (sperm whale)	17800	44 X 44 X 25	48400
Adenylate kinase	21640	40 X 40 X 30	48000
Bovine trypsin	23200	50 X 40 X 40	80000
Bence Jones REI	23500	40 X 43 X 28	48160
Bovine chymotrypsinogen	23660	50 X 40 X 40	80000
Porcine elastase	25900	55 X 40 X 38	83600
Substilin	27530	48 X 44 X 40	84480
Carbonic anhydrase	28800	47 X 41 X 41	79007
Superoxide dismutase	33900	72 X 40 X 38	109440
Carboxypeptidase A	34500	50 X 42 X 38	79800

3.4 Discussion

Savignin is the first serine protease inhibitor of thrombin from ticks for which a full-length cDNA has been obtained, which includes 5' and 3' UTR's, a signal peptide sequence and the full-length gene coding for the protein (Fig. 3). Noteworthy is the presence of the less common poly-adenylation site, AATACA (Mason *et al.* 1985) of savignin, which differs from the more commonly found AATAAA sequence (Whale 1992). An important characteristic for assignment of biological significance is the secretion of bio-active components during feeding. The presence of a signal peptide indicates targeting to the endoplasmic reticulum and the salivary gland granules, suggesting that savignin is secreted during feeding (von Heijne 1990). This is supported by the presence of a thrombin inhibitory activity identified in salivary gland secretions (Nienaber, personal communication).

Comparison of the sequences of savignin and ornithodorin and their functions indicate that these proteins are orthologs. Significant is the conserved cysteine pattern characteristic of the Kunitz bovine pancreatic trypsin inhibitor (BPTI) family, which is present in both domains (Laskowski and Kato, 1980).

3.4.1 Interaction of savignin with the thrombin active-site

Savignin is classified as a slow, tight binding competitive inhibitor of thrombin. Kinetic studies indicated that savignin competes with Chromozym TH, a chromogenic substrate for the active site of thrombin (Nienaber, Gaspar and Neitz, 1999). This is confirmed in the modeled structure, where the N-terminal residues (Leu1-Cys5) of savignin bind inside the active site cleft and associates extensively with Ser214-Gly219 of thrombin (Fig. 3.14, Table 3.2) by forming a parallel β-sheet arrangement. Secondary interactions of the N-terminal domain are between the β-hairpin loops of ornithodorin and savignin (Arg24-Gly26) and the thrombin 60loop and residues 40 and 48 of the α-helix with the thrombin 148loop (van de Locht *et al.* 1996).

3.4.2 Interaction of savignin with thrombin's fibrinogen recognition site

Interaction of savignin with the fibrinogen recognition exosite of thrombin is crucial for the potent inhibition observed for α-thrombin (Ki~5 pM). γ-thrombin lacks the fibrinogen binding exosite due to excision of Ile68-Arg77 (Stubbs and Bode, 1993). The affinity (Ki~22.3 nM) of savignin for γ-thrombin was found to be three orders of magnitude lower than for α-thrombin (Nienaber, Gaspar and Neitz, 1999). Interaction of the C-terminal helix of savignin with the fibrinogen recognition exosite as predicted for the modeled structure would thus seem to be of major importance in the stabilization of savignin-thrombin interactions. Hirudin interacts with the fibrinogen recognition exosite via ionic interactions (Grütter *et al.* 1990), while an increase in ionic strength did not influence the Ki value of savignin (Nienaber, Gaspar and Neitz, 1999). This indicates that ionic interaction between savignin and the fibrinogen recognition exosite of thrombin is not the major type of interaction (Nienaber, Gaspar and Neitz, 1999). The model of savignin interaction with thrombin confirms this, in that the main residues of savignin (Glu100'-Val115'), which includes the C-terminal α-helix of the second BPTI-like domain, interacts with the fibrinogen binding exosite of thrombin (Lys70'-Glu80') with specific H-bond interaction of Glu100' and Asn102' of savignin with Arg77A of thrombin (Table 3.2). Triabin, a thrombin inhibitor from the triatomine bug, also shows hydrophobic interaction with the fibrinogen-binding exosite, rather than ionic interactions (Fuentes-Prior *et al.* 1997).

3.4.3 Unusual conformation of complexed savignin and thrombin

The crystal structure of ornithodorin in complex with thrombin, and the modeled structure of savignin have an unusual conformation. It consists of two globular domains with a flexible linker area that interacts with thrombin via non-bond interactions (Table 3.2). The question is whether it is the normal conformation in which the uncomplexed inhibitors exist, and the conclusion is that it is very unlikely, since a stretch of 9 amino acids (in the linker) face the solvent. A solution to this dilemma would be if the two globular domains fold back upon them self, with a turn in the linker area. Such a structure has been observed for the uncomplexed form of bikunin (a plasma serine protease inhibitor that also has two BPTI-like domains) (Xu *et al.* 1998).

Association of the globular domains with each other could explain some of the phenomena observed for native savignin. Multiple associations of the globular domains with each other could give rise to conformational isoforms that were observed previously for savignin under both iso-electric focusing conditions as well as non-reducing SDS-PAGE (Nienaber, Gaspar and Neitz, 1999). Under non-reducing conditions savignin also migrated at a much lower mass due to stabilizing disulphide bonds and/or domain association. To resolve this, the structure of the thrombin inhibitors in an uncomplexed form has to be determined.

3.4.4 Kinetic mechanism of thrombin inhibition

Several mechanisms of inhibition by slow binding inhibitors have been proposed (Sculley, Morrsion and Cleland, 1996). In mechanism A, interaction is slow due to structural barriers encountered by the inhibitor, while in mechanism B the inhibitor reacts rapidly with the enzyme to form an intermediate, which slowly undergoes a conformational change to form the stable-enzyme-inhibitor complex. Analysis of the ornithodorin-thrombin complex indicates no major conformational changes in thrombin's structure upon binding of ornithodorin (van de Locht *et al.* 1996). This suggests that any major structure rearrangements would have to take place in the structures of savignin and ornithodorin upon binding to thrombin. The time it takes for this conformational change to take place could explain the slow binding kinetics observed for savignin and ornithodorin. TAP has been shown to bind to fXa in a two-step fashion, with initial slow-binding to the secondary site and subsequent rearrangement of the N-terminus leading to tight binding into the active site cleft of fXa (Jordan *et al.* 1992; Wei *et al.* 1998).

3.5 Summary

A schematic summary of savignin's proposed mechanism is shown in Fig. 3.17.

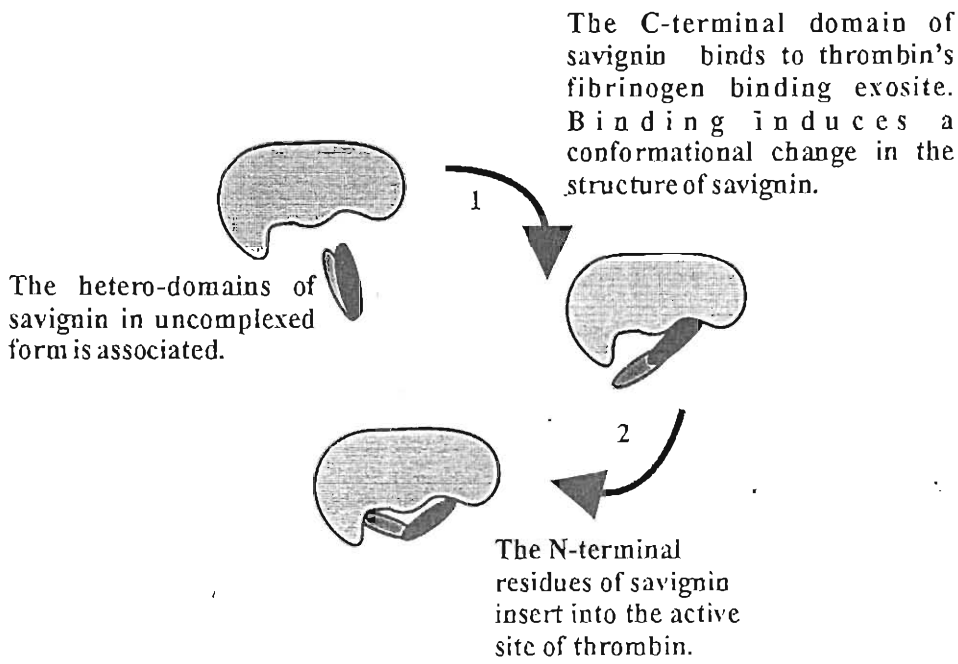

Fig. 3.17: A two-step mechanism for savignin binding to thrombin.

Chapter 4: Evolution of soft tick Kunitz/BPTI anti-hemostatic components*

*Part of the work presented in this chapter has been accepted for publication in the The Journal of Biological Chemistry (Mans, Louw and Neitz, 2002b) and Molecular Biology and Evolution (Mans, Louw and Neitz, 2002c).

4.1.1 The Kunitz/BPTI protein family

The fact that BPTI-proteins are ubiquitous in plants, vertebrates and invertebrates, suggests that they originated at least 500 MYA and diversified through a series of gene duplications, very early in their evolution (Ikeo, Takahashi and Gojobori, 1992). Phylogenetic analysis of these proteins has been problematic, due to evolutionary convergence and gene duplication. Pritchard and Dufton (1999) recently conducted a phylogenetic analysis of 74 Kunitz/BPTI sequences (Fig. 4.1). Rather than grouping into an organismal hierarchy, these inhibitors are grouped into functional classes that indicate their paralogous nature (Dufton, 1985; Ikeo, Takahashi and Gojobori, 1992; Pritchard and Dufton, 1999).

4.1.2 β-bungarotoxins

β-bungarotoxins are the outlier of the whole BPTI family and occur as a fusion protein with phospholipase A_2. This is probably an ancient gene duplication in the ancestor of both mammals and reptiles (Dufton, 1985).

4.1.3 Inter-alpha trypsin inhibitor

Inter-alpha trypsin inhibitors (bikunin) are synthesized as a double Kunitz domain fusion protein with the lipocalin, α1-microglobulin, from which it is cleaved during secretion. Bikunin can inhibit trypsin, elastase and plasmin. It is intracellularly modified by attachment of a chondroitin sulphate chain to Ser_{10} and before secretion is covalently bound to the C-terminal amino acid residue of other larger chains (HC1-3), via a protein-glycosaminoglycan-protein linkage (Åkerström *et al.* 2000). This fusion protein probably plays a role in extracellular matrix binding and stabilization (Bost, Diarra-Mehrpour and Martin, 1998).

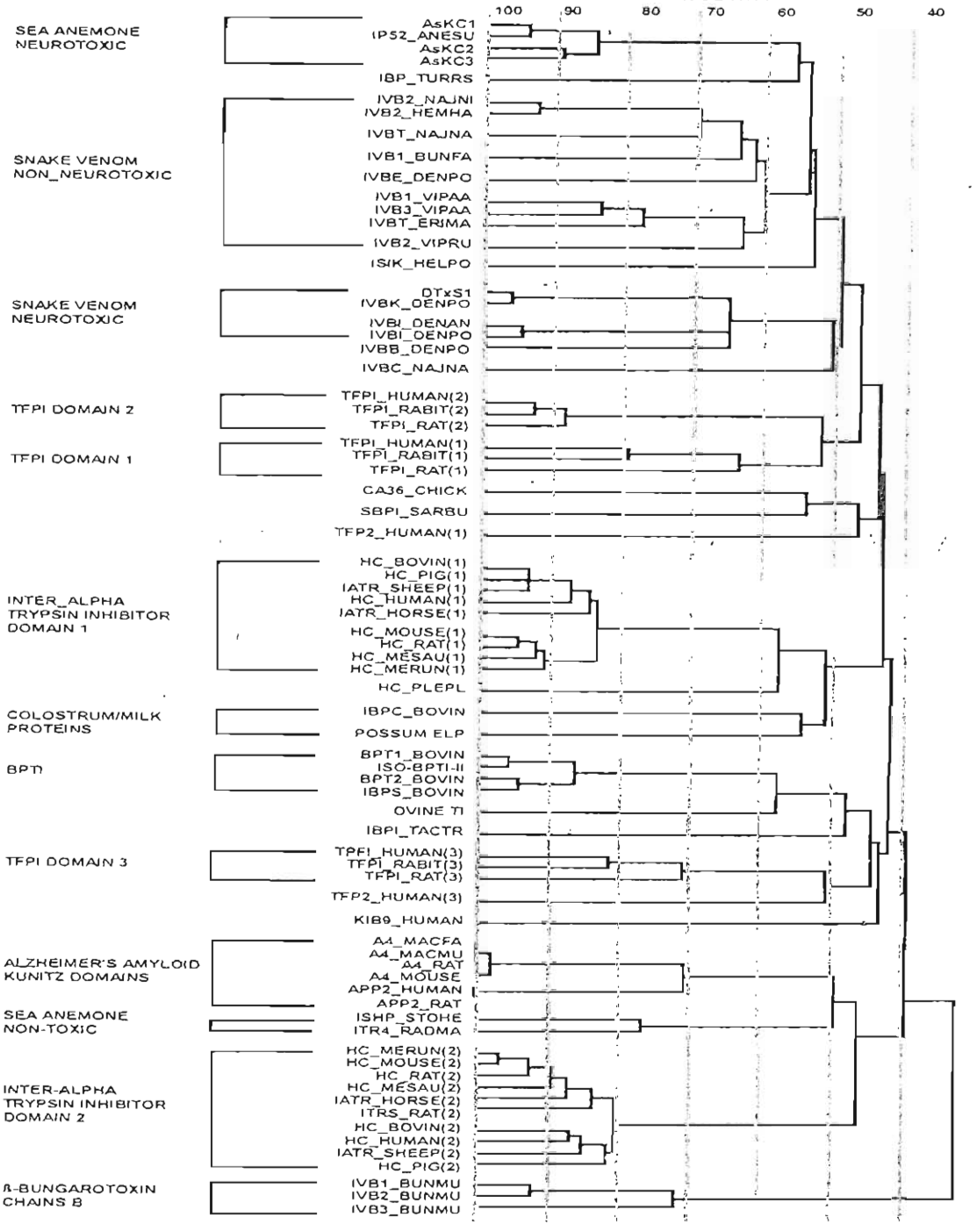

Fig. 4.1: UPGMA dendrogram from 74 Kunitz/BPTI-homologous sequences. The clustering of sequences reflects functionality and class of target rather than species ancestry, with a high degree of paralogy (Pritchard and Dufton, 1999).

4.1.4 Sea anemone Kunitz inhibitors

Kunitz inhibitors from sea anemones show either protease inhibitory activity with a narrow specificity (serine proteases) or a broad protease specificity that include serine, cysteine and aspartic proteases (Minagawa *et al.* 1997; Delfin *et al.* 1996). Some also display neurotoxic as well as trypsin inhibitory activity (Schweitz *et al.* 1995).

4.1.5 Alzheimer's amyloid Kunitz domain

The Alzheimer's amyloid Kunitz domain is part of the β-amyloid precursor protein for which no function has yet been elucidated (Ikeo, Takahashi and Gojobori, 1992).

4.1.6 Tissue factor pathway inhibitor (TFPI)

TFPI exists as three tandemly linked Kunitz domains of which the second domain inhibits fXa and regulates hemostasis by inhibition of the tissue factor-fXa complex (Burgering *et al.* 1997).

4.1.7 BPTI

The BPTI-family functions as basic proteinase inhibitors in serum, although a specific function is not known (Birk, 1987).

4.1.8 Colostrum BPTI inhibitors

Colostrum BPTI inhibitors are found in milk and probably function in allowing intestinal transmission of undegraded macromolecules, such as immunoglobins in young animals (Telemo *et al.* 1987).

4.1.9 Snake venom Kunitz inhibitors

The snake venom Kunitz inhibitors can be divided into those that inhibit proteases and those that show neurotoxicity and it is fairly certain that the gene duplication events giving rise to this family took place within the evolutionary history of the snake family (Dufton, 1985).

4.1.10 Arthropod derived Kunitz inhibitors

Various serine proteases have been identified in insect hemolymph (Sasaki, 1984; Sasaki, 1988; Papayannopoulos and Biemann, 1992). It is thought that these inhibitors function in the immune system of insects, by inhibiting fungal and bacterial serine proteases. Other functions might involve the regulation of endogenous proteases involved in hemolymph coagulation, pro-phenol activation or cytokine activation (Sasaki, 1988; Kanost, 1999).

4.1.11 Tick derived Kunitz inhibitors

Kunitz inhibitors from ticks involved in the regulation of blood coagulation have been described (Chapter 3). Of interest are the recently described double-domain Kunitz inhibitors from larvae of the hard tick *Boophilus microplus* that inhibits trypsin, elastase and kallikrein (Tanaka *et al.* 1999). There is also another BPTI-like sequence from *B. microplus* deposited in the Genbank named carrapatin (P81162), for which a BLAST search indicates very high similarity with the second domain of TFPI. The present chapter investigates the relationship between the platelet aggregation and blood coagulation inhibitors from soft ticks and the functional mechanism of platelet aggregation inhibition.

4.2 Materials and Methods

4.2.1 Protein fold prediction of platelet aggregation inhibitors

Amino acid sequences of disagregin and savignygrin were analyzed using the EMBL's advanced WU-BLAST 2.08 server (BLASTP2) with the non-redundant database (nrdb95) using the default settings (Yuan *et al.* 1998.) Protein fold prediction was performed by submission to the 3D-PSSM Server (Kelley *et al.* 2000). Protein family classification was performed with the Family Pairwise Search v2.0 (Grundy and Bailey, 1999).

4.2.2 Retrieval of BPTI sequences

Tick BPTI-sequences as well as those for the tick platelet aggregation inhibitors were obtained from the literature or generated in our own laboratories (Waxman *et al.* 1990;

Karczewski, Endris and Connolly, 1994; van de Locht *et al.* 1996; Joubert *et al.* 1998; Tanaka *et al.* 1999; Mans *et al.* 2002a). Other Kunitz inhibitor sequences were retrieved from the National Center for Biotechnology Information (NCBI) Genbank database, using the search term Kunitz. A representative subset of 62 sequences was used for multiple sequence alignment (Prichard and Dufton, 1999). Except for some tick-derived BPTI-inhibitors, all sequences were SWISS-PROT database entries. SWISS-PROT entries are followed by the common description and SWISS-PROT accession numbers. For proteins with no SWISS-PROT entry the descriptive names used in the literature are employed while the Genbank accession codes are provided below:

TAP_ORNMO: Tick anticoagulant peptide (P17726), fXaI: fXa inhibitor (AAD09876), ORNT_ORNM1: Ornithodorin domain 1 (P56409), Savignin1: Savignin domain 1 (AAL37210), DISG_ORNMO: Disagregin (g544163), Savignygrin (AF452885), ORNT_ORNM2: ornithodorin domain 2 (P56409), Savignin2: Savignin second domain (AAL37210), A4_RAT: Alzheimer's disease amyloid 4 (P08592), A4_MACFA: Alzheimer's disease amyloid 4 (P53601), A4_SAISC: Alzheimer's disease amyloid 4 (Q95241), A4_MOUSE: Alzheimer's disease amyloid 4 (P12023), APP2_RAT: Amyloid-like protein 2 (P15943), APP2_HUMAN: Amyloid-like protein 2 (Q06481), AMBP_BOV2: bovine alpha-1-microglobulin domain 2 (P00978), IATR_SHEEP2: sheep alpha-1-microglobulin domain 2 (P13371), AMBP_PIG2: pig alpha-1-microglobulin domain 2 (P04366), AMBP_HUMAN2: human alpha-1-microglobulin domain 2 (P02760), AMBP_RAT2: rat alpha-1-microglobulin domain 2 (Q64240), ITR4_RADMA: trypsin inhibitor *Radiantus macrodactylus* (P16344), ISH1_STOHE: serine protease inhibitor from *Stichodactyla helianthus* (P31713), BPTI1_BOVIN: bovine pancreatic trypsin inhibitor (P00974), BPTI2_BOVIN: spleen trypsin inhibitor (P04815), IBPS_BOVIN: serum basic protein (P00975), TFPI_HUMAN3: human tissue factor pathway inhibitor domain 3 (P10646), TFPI_RABIT3: rabbit tissue factor pathway inhibitor domain 3 (P19761), TFPI_RAT3: rat tissue factor pathway inhibitor domain 3 (Q02445), ISC1_BOMMO: silkworm chymotrypsin inhibitor (P10831), ISC2_BOMMO: silkworm chymotrypsin inhibitor (P10832), TIMTC3: silkworm chymotrypsin inhibitor (TIMTC3), SBPI_SARBU: grey flesh fly protease inhibitor (P26228), TIFHBP: flesh fly proteinase inhibitor (TIFHBP), CRPT_BOOMI: carrapatin *Boophilus microplus* (P81162), BMTI-2: *B. microplus* trypsin inhibitor second domain (Tanaka *et al.* 1999), TFPI_HUMAN1: human tissue factor pathway inhibitor domain 3 (P10646), TFPI_RABIT1: rabbit tissue factor pathway inhibitor domain 3 (P19761), TFPI_RAT1: rat tissue factor pathway inhibitor domain 3 (Q02445), AMBP_BOV1: bovine alpha-1-microglobulin domain 1 (P00978), IATR_SHEEP1: sheep alpha-1-microglobulin domain 1 (P13371), AMBP_PIG1: pig alpha-1-microglobulin domain 1 (P04366), AMBP_HUMAN1: human alpha-1-microglobulin domain 1 (P02760), AMBP_RAT1: rat alpha-1-microglobulin domain 1 (Q64240), TIBOC: bovine colostrum inhibitor

(TIBOC), TFPI_HUMAN2: human tissue factor pathway inhibitor domain 3 (P10646), TFPI_RABIT2: rabbit tissue factor pathway inhibitor domain 3 (P19761), TFPI_RAT2: rat tissue factor pathway inhibitor domain 3 (Q02445), AsKC1: kalicludine sea anemone toxin (AAB35413), AsKC2: kalicludine sea anemone toxin (AAB35414), IP52_ANESU: sea anemone protease inhibitor SA5 II (P10280), ISIK_HELPO: roman snail isoinhibitor K (P00994), IVBK_DENPO: dendrotoxin K (P00981), IVBI_DENAN: alpha dendrotoxin (P00980), IVBE_DENPO: dendrotoxin E (P00984), IVB1_VIPAA: venom trypsin inhibitor I (P00991), IVB3_VIPAA: venom basic protease inhibitor 3 (P00992), IVBT_ERIMA: venom trypsin inhibitor (P24541), IVB1_BUNFA: venom basic protease inhibitors IX AND VIIIB (P25660), IVBT_NAJNA: venom trypsin inhibitor (P20229), IVB2_NAJNI: venom basic protease inhibitor II (P00986), IVB2_HEMHA: venom basic protease inhibitor II (P00985), IVB1_BUNMU: beta-1 bungarotoxin chain B (P00987), IVB3_BUNMU: beta-2 bungarotoxin chain B (P00989).

4.2.3 Multiple Sequence Alignment

Sequences were processed to give only a single BPTI core-domain, by truncation of amino acid sequences one amino acid before and after the first and last cysteine of the BPTI-fold, respectively (Pritchard and Dufton, 1999). For BPTI-proteins that exist as multiple-domains, each domain was treated as a single BPTI-fold. Multiple sequence alignment was performed with ClustalX, using the PAM250 matrix and default gap penalty options (Jeanmougin *et al.* 1998). Alignments were manually adjusted based on conserved cysteine positions and secondary structure considerations (Antuch *et al.* 1994).

4.2.4 Neighbor joining Analysis of the BPTI-Family

Phylogenetic analysis on the total BPTI-family was conducted using MEGA version 2.0 (Kumar, Tamura and Nei, 1994). Neighbor joining (NJ) was performed using the number of amino acid differences per site to construct a distance matrix between sequences. Positions that contain gaps were completely deleted so that 39 informative sites were used for analysis. The confidence of the consensus tree obtained was estimated using 10 000 bootstraps. Branches were collapsed below 60% confidence.

4.2.5 Maximum Parsimony Analysis of Tick derived BPTI-Inhibitors

NJ did not completely resolve the relationships within the soft tick BPTI-inhibitor clade. To obtain a more accurate description of the underlying relationships between tick BPTI-

inhibitors, maximum parsimony (MP) using the PHYLIP package, Version 3.2 were performed employing the PROTPARS method using 1000 bootstraps, with or without gapped positions (Felsenstein, 1989). For comparative purposes BPTI-inhibitors from hard ticks as well as insect hemolymph were included, while β-bungarotoxin chain B, proposed to be an outlier of the whole BPTI-family was used as outgroup (Ikeo, Takahashi and Gojobori, 1992; Dufton, 1985).

4.2.6 Phylogeny of Soft Tick Inhibitors based on Protein Structure

Three-dimensional protein structure is generally more conserved in evolution than sequence, so that homologous structures resemble each other closer than more distantly related ones. It has been indicated that structure comparison could indeed resolve phylogenetic relationships (Johnson, Sutcliffe and Blundell, 1990). Construction of a pairwise distance tree based on root mean square deviation (RMSD) of the α-carbon backbone structure could assist in the estimation of distant homologies. As the X-ray diffraction structure of ornithodorin (PDB code: 1TOC; van de Locht *et al.* 1996) and NMR structure of TAP (PDB code: 1TAP: Antuch *et al.* 1994) are known, modeling of their orthologs (savignin and fXaI, respectively) were conducted using the SWISS-MODEL Automated Comparative Protein Modeling Server (Guex *et al.* 1999) and MODELLER (Sali *et al.* 1995). The low percentage identity observed between the platelet aggregation inhibitors (PAI), ornithodorin and TAP complicate their modeling using automated servers. Model structures using the MODELLER package could however, be obtained. The structure of BPTI (PDB code: 1BPI) considered to be the prototype BPTI-fold, was used as outgroup. RMSD values between structure pairs were determined by fitting of the backbone structures using the McLachlan algorithm (McLachlan, 1982), as implemented in the protein least squares fitting program, ProFit V1.8 (http://www.biochem.ucl.ac.uk/~martin/#profit). The phylogenetic tree was constructed by using a pairwise distance matrix of RMSD values and the program NEIGHBOR of the PHYLIP package. The quality of the modeled structures was assessed by construction of Ramachandran plots using Procheck (Laskowski *et al.* 1996). Protein structures were obtained from the RCSB Protein Databank (Berman *et al.* 2000; http://www.rcsb.org/pdb/).

4.2.7 Assay for serine protease inhibitory activity

Serine protease inhibitory activity was assayed as described (Nienaber, Gaspar and Neitz, 1999). Concentrations used were, 0.5 nM fXa, 10 nM plasmin, 50 nM trypsin, and 5 nM thrombin. Enzymes were obtained from Enzyme Research Laboratories, Inc. (South Bend, OR, USA). Enzyme and inhibitor (2.6 μM savignygrin, final concentration) were incubated for 15 min at 37°C before substrate was added and the reaction monitored at 405 nm for 5 minutes. All experiments were performed in triplicate. Thrombin (5 nM) was incubated with savignygrin in 200μl buffer (50mM Tris-HCl, pH 8.3, 227 mM NaCl, 0.1% BSA) before addition of 20μl Chromozym TH (final concentration: 250μM, Roche Molecular Biochemicals). fXa (0.5 nM) was incubated with savignygrin in 200μl buffer (50 mM Tris-HCl, pH 7.4, 0.15M NaCl, 0.1% BSA) before addition of 20μl Chromozym X (final concentration: 1000 μM, Roche Molecular Biochemicals). Bovine trypsin (50nM) was incubated with savignygrin in 200μl buffer (50 mM Tris-HCl, pH 7.4, 20 mM $CaCl_2$) before addition of 20μl BAPNA (N-α-benzoyl-L-arginine-4-nitranilide, final concentration, 500 μM, Roche Molecular Biochemicals). Plasmin (10 nM) diluted in buffer containing PEG6000 and 50mM glycine, pH 2.5, was incubated with savignygrin in 220μl buffer (50 mM Tris-HCl, pH 8.2, 0.1M NaCl) before addition of Chromozym PL (final concentration: 500 μM, Roche Molecular Biochemicals). Chromozym PL was prepared in 100 mM glycine, 0.2% Tween. Enzyme concentrations were determined by active-site titration using 4-NPGB (p-nitrophenyl-p'-guanidinobenzoate in 2.25% dimethyl formamide in acetonitrile) (Chase and Shaw, 1967). 4-NPGB (50 μM) was used in the case of thrombin, trypsin and plasmin and 33.2μM for fXa. Enzymes (100 μl) were added to 400μl veronal buffer (0.1M sodium barbiturate, pH 8.3, 20 mM $CaCl_2$) and incubated for a minute before addition of 5μl of 4-NPGB. Reactions were mixed by inversion before measuring the burst at 410 nm (Hitachi U2000) until a plateau was reached. Enzyme concentrations were calculated from the released p-nitrophenol observed during the burst.

4.3 Results

4.3.1 Protein fold prediction for the platelet aggregation inhibitors

BLASTP2 analysis of disagregin and savignygrin indicated similarity to proteins from the BPTI-family with P(N)-values ranging from 0.011-0.74 for the first fifty hits. The highest scoring protein folds obtained for disagregin and savignygrin with the 3D-PSSM

Server are part of the BPTI-like superfamily (E-values: 0.178-0.855 for the first ten proteins), and contains the functionally diverse proteins BPTI, dendrotoxin, bungarotoxin and knottins. Assignment to a protein family in the structural classification of proteins (SCOP) database (Murzin *et al.* 1995) using the Family Pairwise Search indicated identity to the SCOP BPTI-like superfamily with E-values of 1.6e-15 and 7.97e-16, for disagregin and savignygrin, respectively. The second highest hits gave E-values ranging from 0.09-1.42, indicating the high similarity to the BPTI protein fold relative to other protein folds. This strongly suggested that the platelet aggregation inhibitors exhibit a BPTI-fold. As both fXa and thrombin inhibitors with BPTI-folds have been identified in this tick genus, the hypothesis that all share a common ancestor was advanced.

4.3.2 Multiple alignment of savignygrin with BPTI inhibitors

Alignment with various members of the BPTI family indicated that savignygrin and disagregin exhibit the conserved cysteine pattern characteristic of the BPTI-fold (Fig. 4.2). Significant differences of the soft tick BPTI-inhibitors compared to the rest of the BPTI-family include amino acid insertions that lengthen the loops before the first β-sheet and the C-terminal α-helix. Significant deletions are a single deletion before C14 (BPTI notation) and a deletion of G37 (BPTI notation), a residue conserved throughout the BPTI family. G37 precedes C38 (BPTI notation) that disulphide bonds with C14. This leads to displacement of the disulphide bridges and major distortion of the binding loop conformation (Antuch *et al.* 1994; van de Locht *et al.* 1996). Of interest is the occurrence of the RGD and RED motif in savignygrin and disagregin at the P_1, P'_1, P'_2 positions respectively, normally associated with the substrate binding loop of canonical BPTI-like inhibitors (Laskowski and Kato, 1980). The high and low mass forms of savignygrin have been shown to differ at position R52G that occurs in the α-helix (Chapter 2). Of interest is that no glycine residues occur in the indicated α-helix for the other BPTI-like sequences used in the alignment. Also note the preponderance of serine and threonine at the start of the α-helix, which is in accord with the N-terminal capping preferences of α-helixes (Aurora and Rose, 1998).

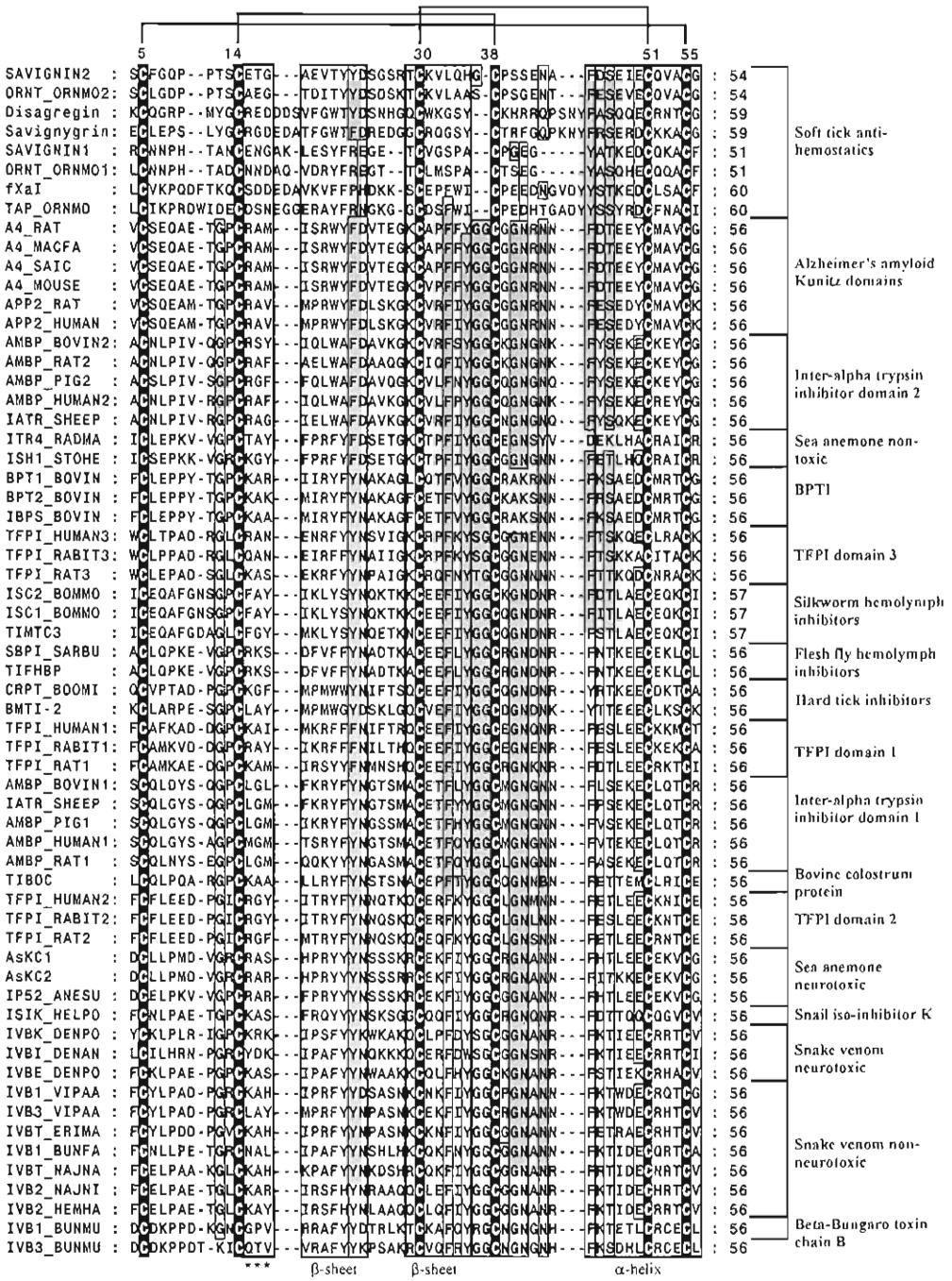

Fig. 4.2. Multiple sequence alignment of BPTI inhibitors with the sequences of disagregin and savignygrin included. Identity (100%) is boxed in black, while 80% similarity using the PAM 250 matrix (DENQH, SAT, KR, FY and LIVM) are boxed in dark gray. The conserved disulphide bond pattern observed for BPTI proteins are indicated by connecting lines. Secondary structure was assigned according to known crystallography structures (Antuch *et al.* 1994). Proteins are grouped according to phylogenetic analysis and the different functional properties are indicated. Sequence names correspond to SWISS-PROT entries. In the case of tick BPTI inhibitors names are indicated as used in the literature. Residue numbering is according to BPTI notation. The *** indicate the P_1, P'_1 and P'_2 (Schechter Berger notation) of the substrate binding loop of canonical BPTI-inhibitors.

4.3.3 Identity and similarity within ortholog groups of the BPTI-family

Comparison of the percent identity/similarity between different ortholog groups indicates that the orthologs of the BPTI-family generally have a constant rate of evolution within ortholog groups with an average percent identity and similarity of 81% and 89%, respectively (Fig. 4.3). The percent identity/similarity of two domains of the thrombin inhibitors (NTI for the N-terminal domains and CTI for the C-terminal domains) is slightly lower than average although this is probably insignificant. In contrast, the percent identity/similarity of the fXa and platelet aggregation inhibitor orthologs fall well below average. While the percent identity and similarity of the family in general is similar, the percent similarity for the tick inhibitors is almost twice that of the identity. These results indicate that soft tick inhibitors show a higher evolutionary rate compared to other BPTI-inhibitors and a higher rate of non-synonymous versus synonymous substitution. This suggests positive Darwinian selection, which could indicate selective pressure on ticks to adapt to a blood-feeding environment (Graur and Li, 2000). It has been shown that the structure of TAP has an increased internal mobility relative to BPTI (Antuch *et al.* 1994). This could indicate a less constrained structure for the fXaI and PAI that might be able to accommodate higher evolution rates. Higher evolutionary rates might also imply a relaxation of structural/functional constraints that is reflected in the fact that both fXaI and PAI are phylogenetically the most divergent of the tick BPTI-like proteins.

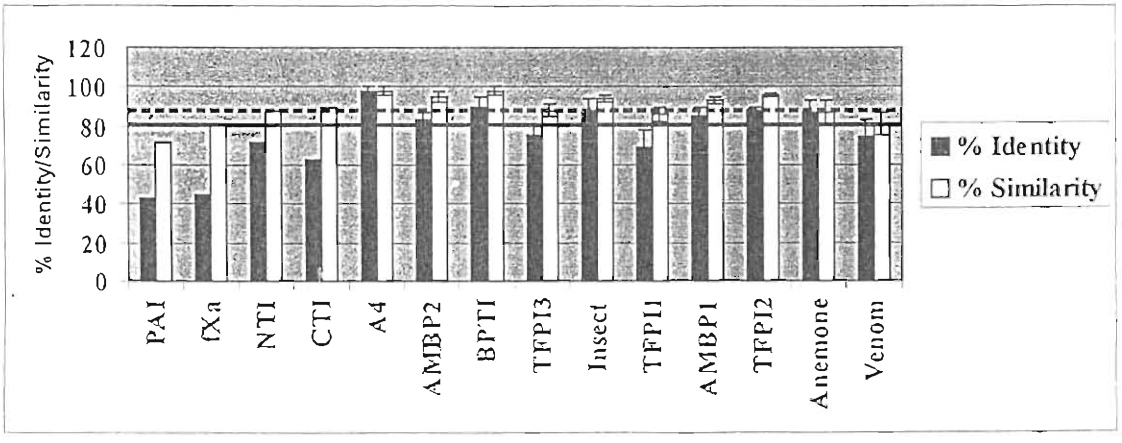

Fig. 4.3. Percent identity and similarity observed between orthologs of the different functional classes from the BPTI-family. Indicated are average values with standard mean deviation for orthologs within a specific functional class. The average values for the whole family are indicated with a solid line for percent identity and dashed line for percent similarity. Percent similarity was obtained using the Dayhoff PAM 250 matrix.

4.3.4 Neighbor joining analysis of the BPTI-family

NJ grouped the BPTI-inhibitors into functional classes previously observed (Dufton, 1985; Ikeo, Takahishi and Gojobori, 1992; Pritchard and Dufton, 1999). These include the β-bungarotoxins which form an outlier group to the whole family, Alzheimer amyloid domains, the two inter-alpha-trypsin inhibitor domains that group into separate clades, the sea anemone BPTI inhibitors that group into non-toxic and neuro-toxic clades, insect hemolymph derived inhibitors, which include inhibitors from the hard tick *B. microplus*, the TFPI domains that group into three separate clades and the snake venom BPTI-like inhibitors that group into neurotoxic and non-neurotoxic clades (Fig. 4.4). It was previously observed that no information on the organismal hierarchy could be obtained from UPGMA constructed trees of the BPTI-like family (Dufton, 1985; Pritchard and Dufton, 1999). This was also observed during the present study. Reasons proposed previously for this problem include the limitation on divergent change by protease inhibitory function and small size that probably led to evolutionary convergence of character states, that does not reflect the total number of changes that have taken place in the past (Dufton, 1985). Numerous gene duplication events further complicate the issue. However, the soft tick blood coagulation and platelet aggregation inhibitors grouped into a monophyletic clade that indicates a common ancestor for these functionally distinct inhibitors and that these paralogous gene duplication events took place within the soft tick family. Disagregin, savignygrin, fXaI, savignin and ornithodorin have all been isolated from salivary gland extracts. The possibility of a common origin for the platelet aggregation and blood coagulation inhibitors due to gene duplication is thus highly probable if it is considered that these inhibitors are all expressed in the tick salivary glands. In contrast, the BPTI-inhibitors from the hard tick *B. microplus* group closer to BPTI inhibitors derived from insect hemolymph that inhibit trypsin and chymotrypsin. BMTI inhibits trypsin, elastase and kallikrein further supporting functional similarity with insect hemolymph derived proteins (Tanaka *et al.* 1999).

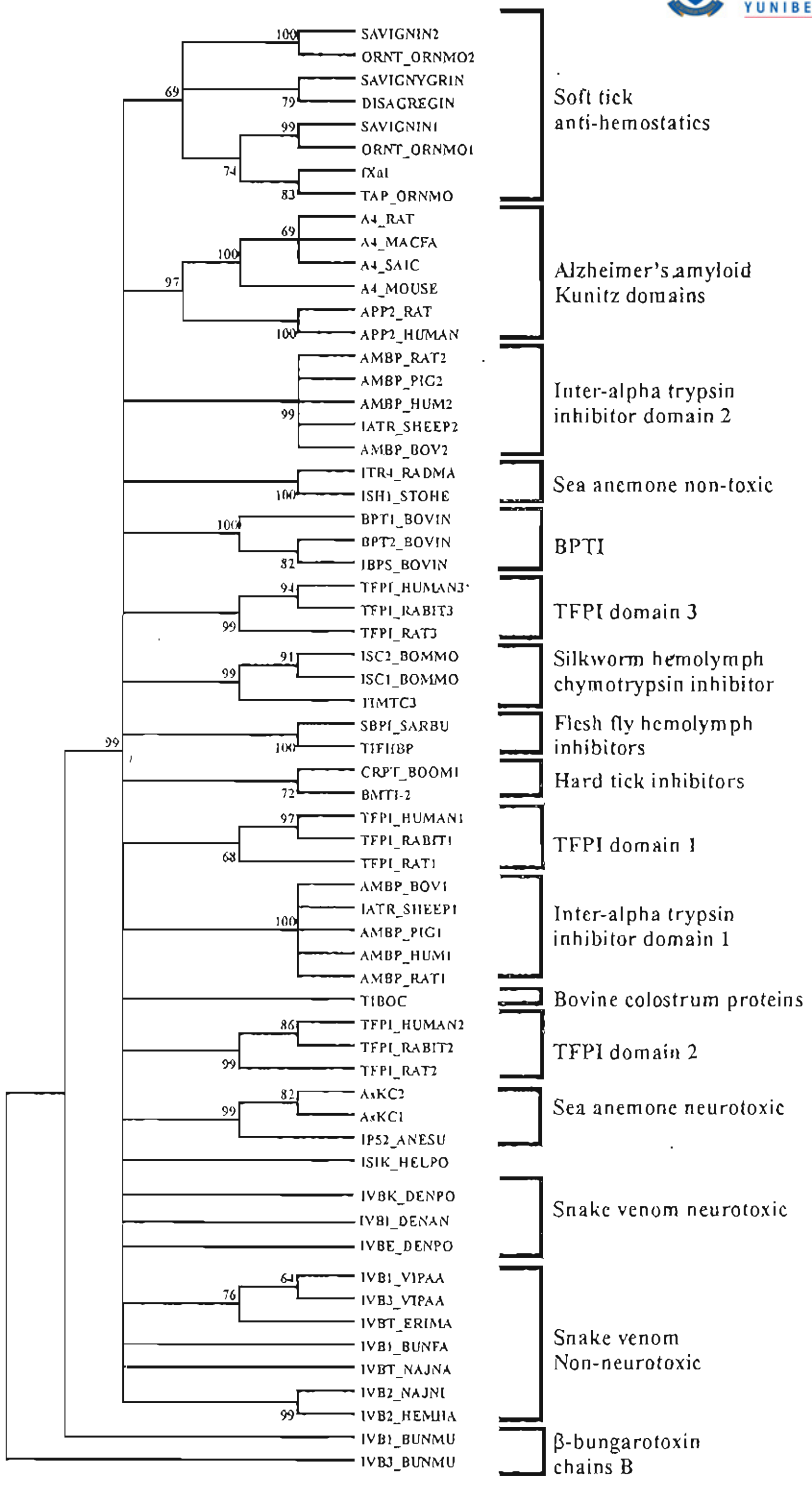

Fig. 4.4: A Neighbor joining dendrogram of 62 BPTI sequences. The tree was constructed based on amino acid differences per site. Indicated is the percent confidence level from 10 000 bootstraps. Branches with confidence levels lower than 60% were collapsed.

4.3.5 Maximum parsimony analysis of the tick-derived BPTI-inhibitors

Maximum parsimony using the alignment where gapped positions were removed, grouped BPTI-inhibitors derived from insect hemolymph and hard ticks into a monophyletic clade, while the soft tick anti-hemostatic inhibitors were grouped into their own monophyletic clade (Fig. 4.5a). The same unresolved relationship between the soft tick-derived inhibitors as for NJ was observed. In this case, fXaI and NTI are grouped together, while CTI is closer to PAI. However, the gapped positions observed in the alignment, especially the insertions before the first β-sheet and C-terminal α-helix could be information rich in terms of structure and functional constraints of these inhibitors. Maximum parsimony analysis using this information gave a more clear relationship between the tick-derived inhibitors (Fig. 4.5b). CTI is basal to this clade, followed by NTI. The fXaI and PAI then group as the terminal clade. This indicates that at least three separate paralogous gene duplication events had occurred, with the evolution of platelet aggregation inhibitory activity being one of the last events.

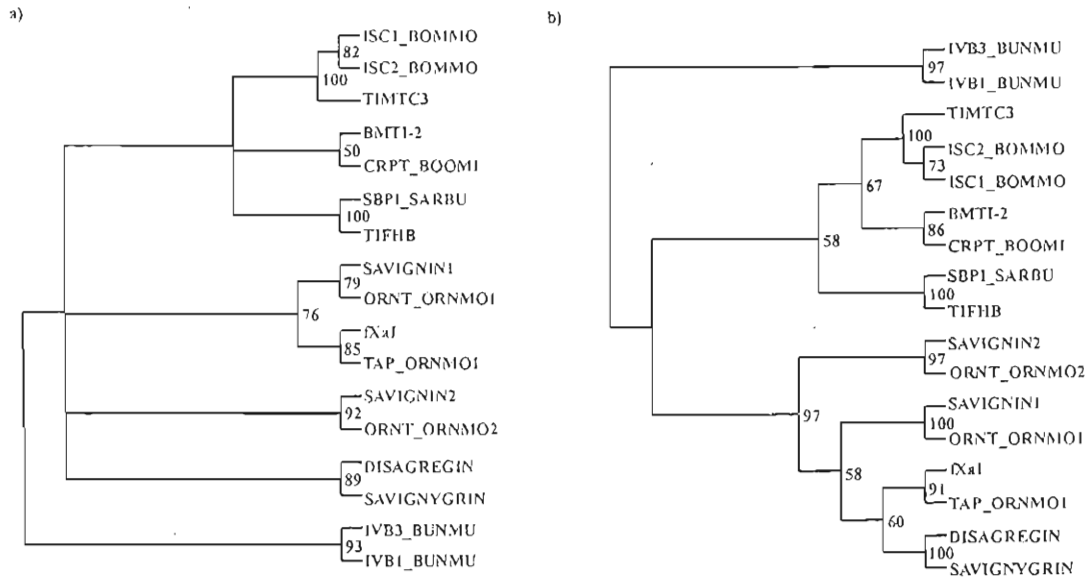

Fig. 4.5: Maximum parsimony analysis of tick BPTI inhibitors. (a) Maximum parsimony analysis of BPTI inhibitors derived from insect hemolymph and hard ticks, as well as soft tick inhibitors. Percent confidence is indicated for 1000 bootstraps. As outgroups the β-bungarotoxins were used. All gapped positions in the alignment used were ignored. (b) Maximum parsimony analysis of the same dataset using the same conditions, with inclusion of the gapped positions. Branches with confidence levels below 50% were collapsed.

4.3.6 Structural comparison of the soft tick-derived BPTI-like inhibitors

To differentiate between the different phylogenies obtained with maximum parsimony, an independent tree based on structural similarities was constructed. The general topology of the structure tree is the same as that obtained with maximum parsimony, using the gapped alignment (Fig. 4.6). The CTI domains show closest structural similarity to BPTI (RMSD: 2.83±0.31Å), followed by the NTI domains (RMSD: 3.4±0.39Å) and lastly the fXa inhibitors (RMSD: 4.3±0.1Å). Because the platelet aggregation inhibitors are paralogs to all three inhibitor folds they were modeled on all three inhibitor folds to test the hypothesis of being closer related to the fXa inhibitors. Models based on the CTI fold (RMSD: 1.8±0.24Å) and NTI fold (RMSD: 3.24±0.52Å) gave higher RMSD values than models obtained based on the fXaI fold (RMSD: 1.13±0.29Å). RMSD values between model pairs for disagregin and savignygrin also indicated lowest RMSD values for the TAP derived models (RMSD: 0.748Å) compared to the models obtained from the thrombin inhibitor folds (RMSD: 2.035 and 1.82 for the N- and C-terminal domain derived models, respectively). These results suggest that the closest structural, as well as ancestral relative to the platelet aggregation inhibitors are the fXa inhibitors.

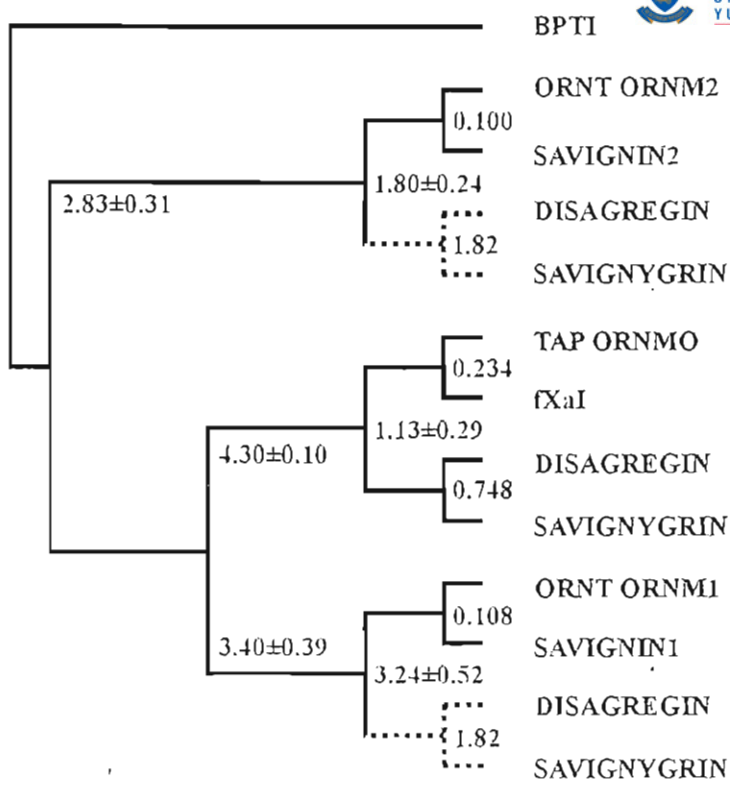

Fig. 4.6: A phylogenetic tree based on pairwise distances of root mean square deviation values (RMSD) obtained from comparison of different structural models. BPTI (PDB code: 1BPI) were used as the prototype BPTI structural outgroup. The structures of TAP (PDB code: 1TAP) and ornithodorin (PDB code: 1TOC) were used to model the structures of fXaI, savignin, disagregin and savignygrin. Values at terminal nodes indicate the pairwise RMSD values between orthologs. Values at internal nodes indicate the average RMSD ± standard deviation for the grouped paralog pairs. Values indicated at horizontal branches designate the respective average RMSD ± standard deviation for the internal branch values in relation to that of BPTI. Branches for platelet aggregation inhibitors shown as dashed lines indicate models with the largest RMSD values and lowest confidence.

4.3.7 Homology modeling of savignygrin

Because the TAP derived model of savignygrin gave the lowest RMSD values, this model was used for structural and functional analysis. Fitting the structures of savignygrin and disagregin onto that of TAP gave RMSD values of 1.0 Å and 1.5 Å respectively (Fig. 4.7). Considering that RMSD values of 1.0-1.5Å are normally obtained for structures of ~40% sequence identity, this model is useful to predict functional parameters (Chothia and Lesk, 1986), especially considering that these proteins show 16-26% identity, in contrast to the assumed ~30% sequence identity needed for building a

structure with molecular modeling (Sali *et al.* 1995). This is probably due to the rather conserved size of these proteins as well as the disulphide bond pattern.

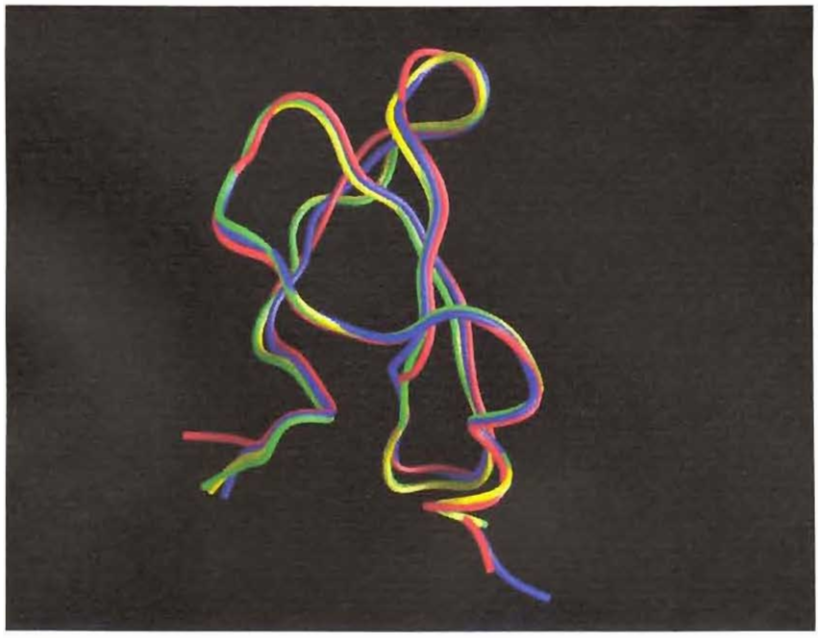

Fig. 4.7: Comparison of the PAI structural models with the fXa inhibitors. Structures of modeled fXai (green), savignygrin (blue) and disagregin (red), superimposed onto the structure of TAP (yellow). RMSD values are 0.2 Å, 1.0 Å and 1.5 Å for fXai, savignygrin and disagregin, respectively.

4.3.8 Analysis of modeled structure

Ramachandran plots showed that 6.2% of the amino acids of savignygrin were in disallowed regions. (Fig.4.8; Table 4.1). Reasons for this high number, is probably due to the low sequence identity/similarity (26/44%) observed between TAP and savignygrin, which complicate modeling procedures. However, at least one disallowed residue (C39) in the structure of TAP is also in the disallowed region for savignygrin (C38). This is probably the reason for the second disallowed residue (C13), which is the corresponding disulphide-bonding partner. The other reason for this distortion in conformation is the presence of an indel (2 residue deletion) in the sequence of savignygrin just before C13, which probably puts a torsion stress on the formation of the loop and disulphide bond leading to the distortion of D16 which also resides on this loop.

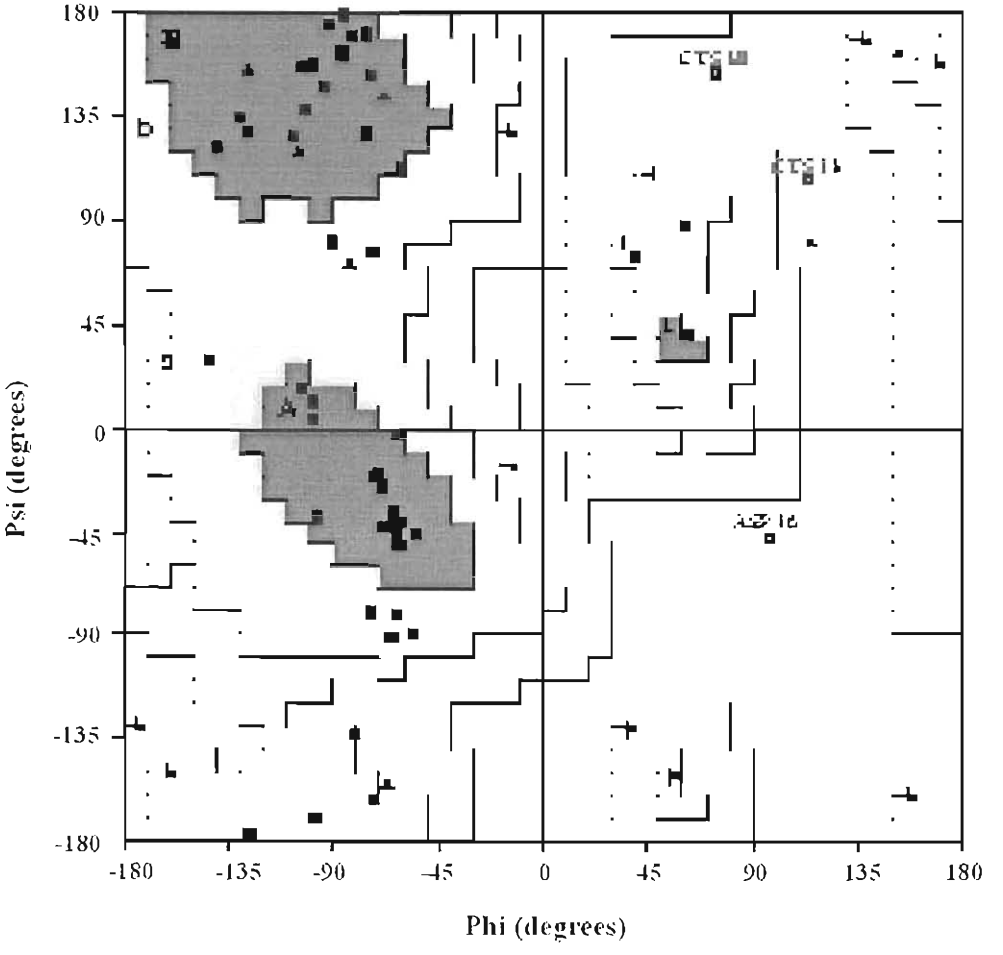

Fig. 4.8: Ramachandran plot of the modeled structure of savignygrin. Position of residues is indicated by squares. Dark gray indicates most favored positions while lighter shades of gray indicate additionally and generally allowed regions respectively.

Table 4.1: Statistics of Ramachandran plots of fXaI and savignygrin. The number and percentage of residues and their localization on the Ramachandran plot is indicated for both ornithodorin and savignin. Values obtained with Procheck.

Characteristics	fXaI	Savignygrin
Residues in most favoured regions	23 (60.5%)	30 (62.5%)
Residues in additional allowed regions	14 (36.8%)	15 (31.2%)
Residues in generously allowed regions	0	0
Residues in disallowed regions	1 (2.6%)	3 (6.2%)
Number of non-glycine and non-proline residues	**38**	**48**
Number of end-residues (exl. Gly and Pro)	14	2
Number of glycine residues	6	8
Number of proline residues	2	3
Total	**60**	**61**

4.3.9 Structural implications for savignygrin

The modeled structures indicate that the RGD and RED motifs of savignygrin and disagregin respectively, are located after the second cysteine on the substrate-binding loop associated with canonical Kunitz inhibitors (Fig. 4.9A). The modeled structure also indicates the formation of three disulphide bonds (C5-C58, C13-C38, C32-C54) that corresponds with that of the general Kunitz BPTI-fold. This is important, as disulphide bond partners were not specifically designated during the modeling procedure and as such are completely dependent on the generally allowed stereochemistry of disulphide bridges (Sali and Blundell, 1993). These stereochemical requirements consist of distances between the respective cysteine, α–carbon (4.6-7.4Å) and sulphur (2-3Å) atoms. Dihedral angle (Cβ-S-S-Cβ) constraints are bimodal with peaks at –87.1°C and 93.9°C with a standard deviation of 10°C (Thornton, 1981; Sali and Blundell, 1993). This in itself is a further confirmation of the BPTI-fold of the PAI, but also that the modeled structures are probably very close to the native structure. A surface model of savignygrin, indicates that the RGD motif extends into the surrounding solvent. Of interest though, is the observation that the downstream acidic residues form with the RGD motif a binding epitope (Fig. 4.9B). This suggested that the RGD motif as well as surrounding residues might indeed be involved in the inhibitory activities of these platelet aggregation inhibitors.

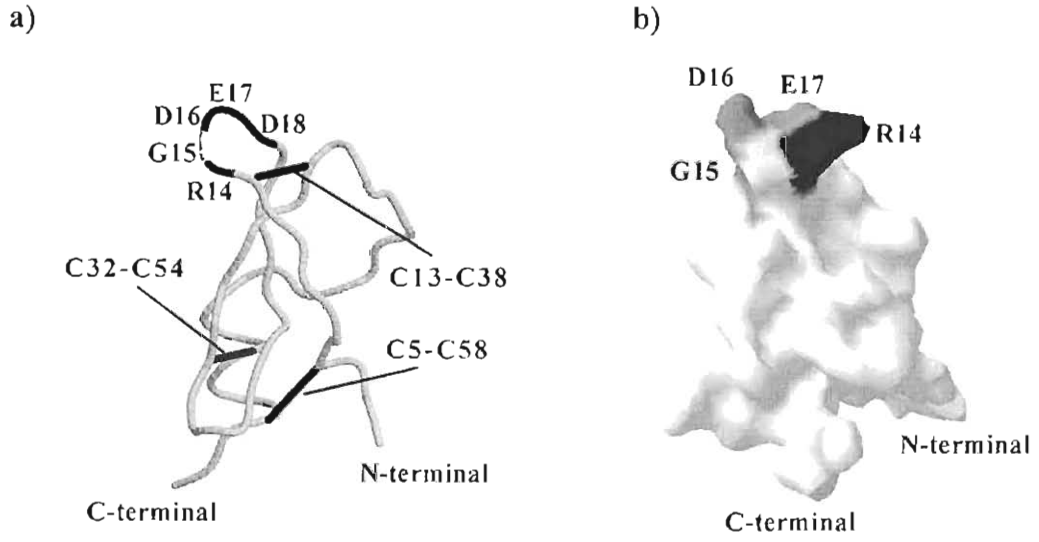

Fig. 4.9: The structure of savignygrin. (a) Intact disulphide bonds (black) predicted by the model and the position of the RGD motif, with R14, G15, D16, E17, D18 indicated. (b) A surface model of savignygrin showing acidic (gray) and basic (black) electrostatic potentials. Indicated is the RGDED binding epitope, projecting upwards from the page.

4.3.10 Serine protease inhibitory activity

The savignygrins have an arginine residue at the P1 position of the canonical BPTI-like inhibitors. As inhibitors with an arginine or lysine at the P1 position inhibit trypsin-like enzymes (Laskowski and Kato, 1980), inhibitory activity against trypsin, thrombin, fXa and plasmin (all recognize arginine at position P1) was investigated. No significant inhibitory activity was observed for any of the proteases tested (Table 4.2).

Table 4.2: Inhibition of serine protease activity. Activity is expressed relative to control values. SD± is indicated for triplicate values. Values in parenthesis indicate the molar ratio of savignygrin to protease.

Serine protease	Activity compared to control
Thrombin (480:1)	114 ± 5%
FXa (436:1)	107 ± 13%
Trypsin (48:1)	95 ± 12%
Plasmin (240:1)	105 ± 11%

4.4 Discussion

4.4.1 A novel BPTI-platelet aggregation inhibitor

Savignygrin is the first platelet aggregation inhibitor described that is part of the Kunitz/BPTI inhibitor family. Presentation of the RGD motif on the canonical substrate-binding loop is a novel way in which this motif is used to antagonize $\alpha_{IIb}\beta_3$. This could open the way for the design of a new class of platelet aggregation inhibitors based on the BPTI-fold. Furthermore, homology with inhibitors of fXa and thrombin in the same tick genus, indicates definite gene duplication events that explains the evolutionary mechanisms of soft tick adaptation to a blood-feeding environment.

4.4.2 Implications of the BPTI-fold for the structure of savignygrin

Assignment of savignygrin to the BPTI family allows the assignment of disulphide bond partners for the previously described disulphide nature of this inhibitor. It also sheds light on some of its properties previously elucidated. Savignygrin was previously shown to be extremely stable in non-reduced form under conditions of high temperature and in the presence of SDS and only unfolded under conditions of high temperature, SDS and urea. The high stability previously observed for the savignygrins are concurrent with a BPTI-like fold, as native BPTI has a melting point of ~95°C (Moses and Hinz, 1983). The high stability of BPTI has been attributed to the stabilizing effect of the disulphide cross-links. BPTI has also been shown to occur as a very disordered polymer in its reduced form, even in the absence of denaturants (Creighton, 1978). This could also be the case for the reduced forms of savignygrin that did not show any activity.

4.4.3 Savignin is a highly conserved protein: implications for structure

It has been shown that a positive Darwinian selection existed for fXaI and PAI. This implied a specific evolutionary pressure applied to the tick during adaptation to a blood-feeding environment. A much lower level of such selection seemed to have operated on the thrombin inhibitors. This would seem strange, as the thrombin inhibitors according to the phylogenetic analysis was a first defense against the host's hemostatic system. However, there could be several reasons for this. The thrombin inhibitors possess a double BPTI domain, which show multiple interactions with thrombin (van de Locht *et*

al. 1996). A higher degree of conservation could be expected due to functional constraints, although this alone could not explain the high degree of conservation (non-selection). Interactions with thrombin are after all still predominantly localized to the N-terminal sequences of the first domain and the C-terminal α-helix of the second domain (van de Locht *et al.* 1996). Structural conservation to maintain the BPTI fold of the two domains could have been a reason for the high degree of conservation, but it has been shown that the structure of the thrombin inhibitors already deviate to some extent from that of the canonical inhibitors (van de Locht *et al.* 1996). It was shown in Chapter 3 that the complexed structure of savignin with that of thrombin is highly unusual and that the two domains might rather associate in their native uncomplexed form as observed for bikunin. This would add another "protein-protein interaction functionality" to this protein, thus placing more selective pressure on it, thereby reducing the rate of divergence.

4.4.4 Soft tick BPTI proteins: a functional paradox

The Kunitz family is a diverse group of proteins that were initially identified as protease inhibitors sharing the common characteristics of a conserved cysteine pattern and canonical inhibition mechanism (Laskowski and Kato, 1980). The soft tick inhibitors are the only serine protease inhibitors of the BPTI-family that do not inhibit their respective enzymes by the canonical mechanism (van de Locht *et al.* 1996; Wei *et al.* 1998). Their similar mechanisms are in fact totally unrelated to the canonical mechanism. The question raised is how could proteins with a very restricted protein fold have evolved a totally different mechanism to perform a similar function (i.e. why did the tick BPTI inhibitors, switch mechanisms)?

4.4.5 Evolution of tick BPTI-proteins: a paradox resolved

It has been suggested that the only way new protein functions could evolve from duplicated genes, is by way of gene sharing for a single domain protein or as an existing bi-functional multi-domain protein, where duplication of each domain leads to acquisition of individual functions (Hughes, 1994). In the light of this a probable evolutionary scenario can be proposed based on considerations of thrombin's structure and function (Fig. 4.10).

(A) Thrombin exerts conformational restrictions on BPTI inhibitors due to the insertion loops (loop 60 and 149) present around its active site that prevents inhibition by the canonical mechanism (Stubbs and Bode, 1993). This probably influenced the ancestral CTI domain, to evolve a new functional mechanism: inhibition of fibrinogen binding to thrombin via its basic fibrinogen binding exo-site (Fig. 4.10). This is reminiscent of the inhibition mechanism of triabin, a lipocalin that inhibits thrombin via its fibrinogen binding exo-site (Fuentes-Prior *et al.* 1997). This newly acquired functional mechanism probably relaxed the functional restrictions on the substrate-binding loop so that CTI lost its original protease inhibitory activity exerted via the canonical mechanism through the acquisition of mutations and indels. Targeting of the fibrinogen-binding exosite of thrombin would have allowed the tick to inhibit both clotting as well as platelet aggregation induced by thrombin (Stubbs and Bode, 1995). It is arguable whether this mechanism of inhibition would have been efficient on its own, as it would not have inhibited catalytic activity completely.

(B) A tandem gene duplication and N-terminal fusion event led to the formation of a homodimeric BPTI protein. Conformational restrictions that the CTI domain placed on the NTI domain probably led to evolution of a new mechanism of thrombin inhibition: insertion of its N-terminal residues into the active site of thrombin. This double-mechanism allows a much more specific mode of inhibition, where both enzyme active site as well as additional substrate binding sites are targeted.

(C) It is highly probable that the next gene duplication occurred from the N-terminal domain and led to an inhibitor that retained and modified the existing mechanism of NTI to target fXa. While this would seem to be a redundant strategy, the inhibition of fXa ensures that even lower concentrations of thrombin would be produced. The secondary interaction sites observed for both NTI as well as fXaI is

probably gene -sharing remnants of CTI's interaction with thrombin's fibrinogen binding exosite.

(D) Subsequent duplication of PAI from the fXaI domain led to a utilization of the now defunct and probably highly distorted, but still present substrate binding-loop of the canonical BPTI-inhibitors, to evolve a new specificity for the platelet aggregation receptor $\alpha_{IIb}\beta_3$. An alternative scenario supported by Neighbor joining and maximum parsimony (where gapped positions were ignored), suggest that the PAI might have duplicated directly from the CTI domain, probably after the tandem fusion event. In both scenarios the fibrinogen-mimicking site of CTI probably played an important role in the initial targeting to the platelet fibrinogen receptor. This could explain observations that disagregin targets more than one site on $\alpha_{IIb}\beta_3$ (Karczewski *et al.* 1997) and suggests that the C-terminal α-helix of the PAI might also be involved in integrin interactions. The fact that no inhibition of serine proteases are observed for savignygrin fits with a scenario, where PAI evolved after NTI, CTI and fXaI lost the canonical mechanism of serine protease inhibition.

4.4.6 The BPTI-Fold as Evolutionary Unit

It is not so surprising that soft ticks have used the BPTI-like fold to evolve new protein functions. The BPTI fold *per se* is not novel to serine protease inhibitors. A rather large group of these proteins are found in snake venoms, where they can act as toxins by blocking ion channels of the cardiac and nervous systems (Prichard and Dufton, 1999). Furthermore, the substrate-presenting loop of the BPTI-like fold is the ideal place for the presentation of recognition motifs, as that found for RGD-containing proteins. What is perhaps surprising is the absence of a RGD motif in the snake venom BPTI-like proteins, where the disintegrin protein family exploits this motif (Huang, 1998). This might imply that in the case of snake venoms, the disintegrins were already present when the BPTI-like proteins acquired their respective functions. In ticks, such a disintegrin-like protein might have been absent, forcing the tick to rely on protein families already present in its repertoire, to generate functional diversity. The loss of a restricted canonical substrate-

binding loop conformation probably further allowed utilization of this loop for a novel presentation mechanism, while the utilization of the fibrinogen-mimicking binding site of CTI could have been important for targeting to the relevant binding site.

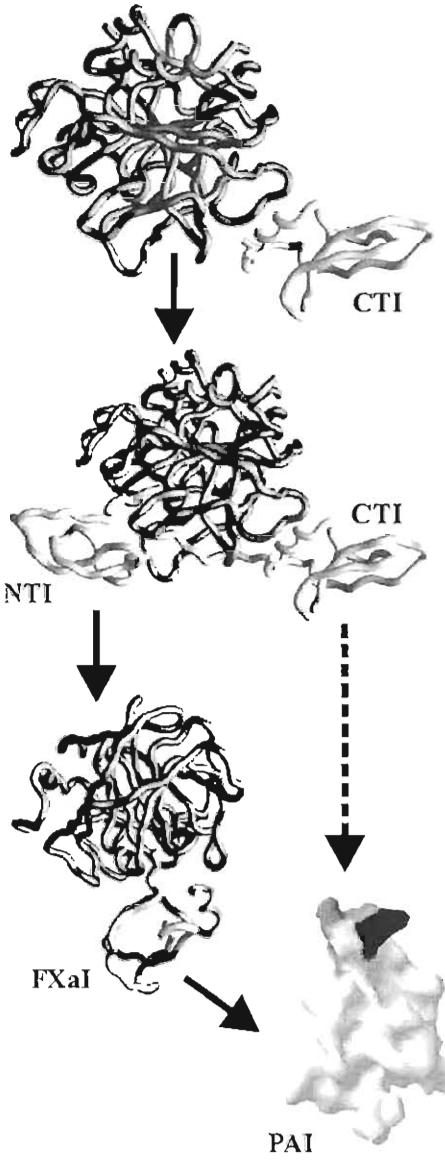

Due to conformational restriction loops around thrombin's active site, canonical BPTI-inhibitors cannot inhibit thrombin. CTI evolved to target the fibrinogen binding exo-site. The canonical BPTI-mechanism is lost due to mutation and indels.

A tandem gene duplication and fusion event to the N-terminal of CTI leads to a homo-dimeric inhibitor. Due to dimeric conformational restrictions a new mechanism of serine protease inhibition evolves: insertion of the N-terminal residues into thrombin's active site, thereby avoiding the restrictive loops.

A gene duplication of NTI leads to utilization of the novel protease inhibitory mechanism, to evolve a new fXa inhibitory capability.

Gene duplication of fXaI leads to utilization of the still existing but redundant BPTI-substrate binding loop to evolve new specificity for the fibrinogen platelet receptor, $\alpha_{IIb}\beta_3$. The alternative evolutionary pathway suggested by Neighbor-Joining and maximum parsimony when gapped positions are ignored, suggest that the platelet aggregation inhibitors might have duplicated directly from CTI.

Fig. 4.10: Evolutionary mechanisms for the acquisition of new anti-hemostatic functions in soft ticks. The solid and broken lines indicate alternative pathways, supported by the different phylogeny approaches. NTI indicates the N-terminal domain of the thrombin inhibitors, while CTI indicates the C-terminal domain of these inhibitors. PAI indicates the platelet aggregation inhibitors and fXaI the fXa inhibitors.

4.4.7 Independent evolution of anti-hemostatic inhibitors in hard and soft ticks

It is interesting that BPTI inhibitors from the hard tick, *B. microplus* is not grouped with the anti-hemostatic factors of soft ticks, but rather with hemolymph derived protease inhibitors, that inhibit their respective enzymes via the classical BPTI mechanism. fXa and thrombin inhibitors from hard ticks have also been described with molecular masses (17-65 kDa) that differ significantly from that of the BPTI fold (Bowman *et al.* 1997). Furthermore, variabilin, a platelet aggregation inhibitor from the hard tick *Dermacentor variabilis* does not resemble the platelet aggregation inhibitors from soft ticks at all (Wang *et al.* 1996). Its cysteine pattern as well as the localization of its RGD-motif differs completely from the observed BPTI-fold and the motif found in savignygrin. This would suggest that soft tick derived BPTI inhibitors only acquired their specific mechanisms of action after the divergence of hard and soft ticks, as well as suggesting independent adaptation to a blood-feeding environment. This is of interest because it would have been expected that ticks, being monophyletic, would have adapted to a blood-feeding environment before divergence. It also raises the question whether anti-hemostatic functions observed in the *Ornithodoros* genus are represented in other soft tick families? However, other signs of probable independent adaptation to a blood-feeding environment include different salivary gland morphologies, feeding behavior and reproductive strategies, that is all intimately linked with blood-feeding (Sonenshine, 1991). However, while this study suggests independent acquisition of novel anti-hemostatic components by the two main tick families, the presence of apyrase in both families have been indicated (Law, Ribeiro and Wells, 1992). Apyrase, (ATP-diphosphohydrolase; EC 3.6.1.5) inhibits platelet aggregation induced by ADP as well as being able to disaggregate platelets aggregated by ADP (Mans *et al.* 1998b; Mans *et al.* 2000). It has been identified in all of the hematophagous arthropod families investigated so far (Ribeiro, 1995), which suggests that this enzyme might have been present in the ancestral non-hematophagous tick. Of interest is the absence of apyrase in the saliva of the tick, *Amblyomma americanum* (Bowman *et al.* 1997).

4.4.8 The driving force behind tick divergence

Independent adaptation to a blood-feeding environment indicates a rapid divergence soon after the origin of the Ixodida (120 MYA), with ticks being adapted to a blood-feeding life by 92 MYA. The question that is raised is what could have triggered such a rapid diversification into different tick families? There is a current controversy around the divergence of early birds and placental mammals, where the fossil records argue for divergence around the Cretaceous-Tertiary (K/T) boundry (~65 MYA), while molecular phylogeny evidence suggest a much earlier divergence in the Early Cretaceous (120-80 MYA) (Benton, 1999; Easteal, 1999; Madsen *et al.* 2001; Murphy *et al.* 2001). A rapid divergence and independent acquisition of hematophagous mechanisms in ticks from ~120-90 MYA fits with the molecular phylogeny hypothesis. Radiation of birds as well as placental mammals would have provided ample opportunity for ticks to find novel niches in which they could excel as blood-feeding arthropods. It could thus be argued that the emergence of hematophagy in ticks was triggered by the divergence of early modern birds and mammals. This provides an interesting counterpoint to suggestions that evolution of ticks was not as much influenced by host specificity as by ecological factors (Klompen *et al.* 1996). While this might be the case for adaptation to the environment, independent evolution of anti-hemostatic strategies would suggest that host diversity could have influenced the adaptation of ticks to the vertebrate hemostatic system. Positive Darwinian selection would indeed suggest that the hemostatic system of the host played a decisive role in the evolution of hematophagy in ticks.

4.4.9 Implications for pharmacological and vaccine development

An intriguing possibility that emerges from this study is the possibility to design a chimeric protein with fXa, thrombin and platelet aggregation inhibitory capacities. Such a protein might be useful as a multi-functional agent to control thrombosis in a regulated manner. Such a multi-epitope protein could also be used as a possible vaccine agent, to generate immune responses that could knock out more than one function necessary for tick feeding.

PART 2

Evolution of the tick lipocalin family

The next three chapters concern the evolution of the tick lipocalin superfamily and their diverse role in host pathogenesis, hemostasis and salivary gland granule biogenesis.

Chapter 5 investigates the localization of savignygrin and apyrase to specific salivary gland granules. While not part of the tick lipocalin family, this chapter serves as a introduction to salivary gland biology and ultrastructure. It shows that anti-hemostatic factors are synthesized in specific cell types where they are localized to granules. These results indicate that there are more than the previously described three cell types of argasid ticks present.

Chapter 6 describes the identification of putative proteins (TSGPs) involved in granule biogenesis based on their abundance in salivary glands and granules. These proteins are characterized in terms of their molecular properties and their possible involvement in granule biogenesis is considered. Two of these proteins are also identified as being toxins that affect the cardiac system of the host rather than being causative agents of tick paralysis. The absence of both toxins in *O. moubata* has interesting implications for the origins of tick toxicoses.

Chapter 7 indicate that the proteins described in the previous chapter are all part of the tick lipocalin family. Their relationship to hard tick lipocalins is investigated and the implications of the lipocalin fold for structure and function is considered. A platelet aggregation inhibitor (savignygen), a homologue of moubatin, a platelet aggregation inhibitor from the soft tick *O. moubata*, was partially characterized. This inhibitor shows close homology to the TSGPs.

Chapter 5: Localization of anti-hemostatic factors to specific salivary gland granules

5.1.1 Introduction: Tick salivary glands

During tick feeding, host fluid is imbibed and saliva is secreted in alternate directions, through a common buccal canal. Saliva originates from paired, alveolar salivary glands lying anterolaterally and extending posteriorly from both sides of the body, resembling bunches of grapes (Fig. 5.1) (Sauer *et al.* 1995). General salivary gland structure and biology have been described in several reviews (Kemp, Stone and Binnington, 1982; Fawcett, Binnington and Voight, 1986; Sauer *et al.* 1986; Sonenshine, 1991; Sauer *et al.* 1995), while salivary gland ultrastructure has been described for the soft ticks *A. arboreus*, *A. persicus* and *O. moubata*, (Roshdy and Coons, 1975; El Shoura, 1985). Several gross differences can be observed between hard and soft tick salivary glands. (1) Soft tick salivary glands are surrounded by a myo-epithelial sheath, that is absent in hard tick salivary glands (L.B. Coons, personal communication). (2) During the extended feeding period observed for hard ticks, the ultrastructure of their granular cells undergoes a great change in structure, size and protein expression levels. The granular cells of soft ticks, which feed more than once for short periods do not undergo such changes.

Fig. 5.1: Salivary glands from the soft tick *O. savignyi*. Note the pair of large (5 mm X 1 mm X 1 mm), white salivary glands lying in an oblique position (Photograph, B.J. Mans, 1996).

5.1.2 Agranular acini

Salivary glands are composed of agranular (type I) and granular acini. Type I acini are found in the anteromesal or anterior portion of the salivary glands of soft and hard ticks, respectively. Type I acini is multi-cellular and include a single large lamellate cell as well as a constrictor cell and a variable number of peripheral lamellate and peritubular cells. The morphology of these acini is similar to that of the salt glands from marine birds and it has been proposed that they function in the regulation of tick water balance. These acini might function by active water sorption from the atmosphere through secretion of hygroscopic substances onto the hypostome and subsequent swallowing of the diluted salt solution (Needham and Teel, 1986).

5.1.3 Granular acini

Morphological studies have revealed significant differences between the granular acini of hard and soft ticks. Argasid salivary glands consists of a single granular acini, with three granular cell types while salivary glands of hard ticks are more complex with at least three granular acini. Type II acini consist of six granular cell types (a, b, c1-c4) and type III acini of three granular cell types (d, e, f). Type IV acini only occur in males (Sauer *et al.* 1995).

5.1.4 Argasid granular acini structure

The classical histological and histochemical studies of the salivary glands of *A. persicus*, provided a detailed view of argasid salivary gland structure. It was shown that at least three distinct granular cell types existed (Roshdy, 1972). This was confirmed during ultrastructural studies of the salivary glands of *A. arboreus* (Roshdy and Coons, 1975). The granules of these cell types differed in electron density and submicroscopic appearance. Cell types a and b contain granules of varying electron density, while cell type c contain granules with an electron dense core (Fig. 5.2). Studies of the ultra-structure of *O. moubata* showed similar granule types (El Shoura, 1985). The "a" cell granules contains an electron dense core similar to "c" cell granules of *A. persicus* and are secreted within 5 minutes of attachment to the host. The "b" cells granules are large and electron dense, while the "c" cells are small (1 μm diameter) with both electron-

lucent and dense zones. For practical purposes, the descriptions of El Shoura (1985) will be used in this discussion as *O. moubata* is the closest to *O. savignyi* and no equivalent for the "c" cell granules have been found in Argas ticks.

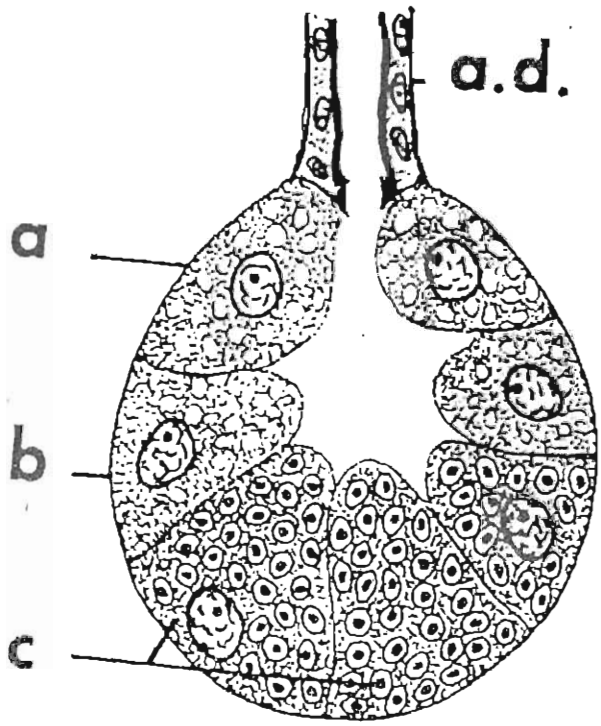

Fig. 5.2: A schematic representation of the granular acini of the argasid tick, *A. persicus*. Adapted from Roshdy (1972). In a toluidine blue stain, "a" and "b" cell type granules appear unstained, while "c" cell type granules show dense core granules. Adlumenal cells (a.d.) line the salivary gland duct. Note the lumen leading into the salivary gland duct, into which granules are secreted during feeding.

5.1.5 Biological significance of salivary gland proteins during feeding

The use of pharmacological stimulants such as pilocarpine (Howell, 1966b) or dopamine (Kaufman, 1977) that induces salivation of ticks, are normally used to infer physiological secretion of a compound by the tick. Proof of secretion is an essential requirement in the characterization of such bio-active compounds, as this is the only way to ascribe possible biological function in tick-host interactions (Law, Ribeiro and Wells, 1992). Whole salivary glands have also been used as a source of bio-active compounds, the rationale being that any bio-active components derived from salivary glands are liable to be

secreted during feeding. This is a rather naïve way to characterize secretory components and require more specific proof that they are indeed secreted. A specific indication of secretion can be targeting to the secretory pathway, as exemplified by the ER-signal peptide or specific localization to secretory granules, which are secreted during feeding.

5.1.6 Evolutionary significance of tick salivary glands

A study into the evolution of secretory components cannot fail to consider the biology of the salivary glands and their possible influence on tick evolution. For example, the number of granular cells differs in hard and soft ticks and can be distinguished based on morphological, histochemical and immunochemical means. These differences must obviously be accounted for by the expression of different proteins or synthesis of other chemical entities, such as carbohydrates by the different cell types. In evolutionary terms the issue is raised whether these different cells all evolved from a single ancestral cell type and if so what effect this had on tick adaptation to a blood-feeding environment. This could be investigated by comparative ultrastructural studies of both hard and soft tick salivary glands and salivary glands from *Nuttalliella namaqua*, as well as glands from their closest sister-group, the holothyrids. If holothyrids have less complex glands this could indicate that tick salivary glands evolved in complexity only after or during their adaptation to a blood-feeding environment. This hypothesis is supported by the fact that hard and soft tick salivary glands differ in complexity and number of granular cells.

In hard ticks, in which extensive changes occur in the glands during feeding, it may be argued that different granular types function at different times during feeding. However, the reason why soft ticks need more than one granular cell type is more problematic. They feed fast, so that granule contents are probably secreted at the same time or very shortly after one another, making more than one granular cell almost redundant. It can so far only be assumed that the different granular cell types perform specific functions.

5.1.7 Salivary glands of other arthropods

The presence of salivary glands and the secretion of salivary gland components is by no means a unique property of ticks, but can be found throughout the arthropoda. As such,

the question of how many processes are shared in salivary gland biology between ticks and other arthropoda and how many processes are unique to ticks are raised. Examples of processes include mechanisms of granule secretion, targeting to the secretory granules and granule biogenesis. Investigations into these properties can indicate whether salivary glands evolved unique ways to accommodate a blood-feeding environment.

5.1.8 Localization of components to granule types

Elucidation of the issues raised is a daunting task at the least and one could expect them to be answered over a number of years of hard and painstaking work. As such, future progress can only be expected with the development of techniques able to distinguish individual granular cell types on an analytical level. Until then, individual localization of different bio-active compounds to one or more granular cell types can contribute to an understanding of how these cells differentiated into such a complex organ as the modern tick salivary gland. It would also allow an initial, although slow step, in the cataloging of granule composition and will give an indication of the similarities and differences that exist between different granule types. This chapter explores the biological significance of savignygrin through specific localization to salivary gland granules.

5.2 Materials and Methods

5.2.1 Assay for apyrase activity

As a marker of secretory activity, the enzyme apyrase was used during this study, as it is known that this enzyme is secreted during pilocarpine stimulation (Mans, 1997). Apyrase activity was assayed as described previously (Mans, 1997; Mans *et al.* 1998a). Fractions tested (10 μl) were added to 90 μl of reaction medium (20mM Tris-HCl, 0.15M NaCl, 5mM $MgCl_2$ and 2mM nucleotide, pH 7.6) per well of a microtitre plate, covered with plastic wrap and incubated at 37 °C for 30 min. The enzyme reaction was stopped by the addition of the molybdic acid mixture (reducing solution) and free phosphate was determined as described below. The amount of phosphate released was determined from a standard orthophosphate standard curve. One enzyme unit (U) is defined as 1 μmole of inorganic phosphate released/min. A mixture (25 ml) of 2.5% molybdate (w/v) and 13.3% concentrated sulphuric acid (v/v) was added to 8 ml of a 1% ascorbic acid solution

and mixed thoroughly. Thirty-three microlitres of this reducing reagent were then added to a standard orthophosphate or sample solution (100 µl) in a microtitre well and shaken for 10 minutes after which the absorbance was read at 620 nm with a SLT 340 ATC scanner (SLT Labinstruments).

5.2.2 Purification of apyrase by HPLC

Apyrase was purified by SEHPLC and AEHPLC (Mans *et al.* 1998b). A size-exclusion column (G3000SWxl, 7.8 mmx30 cm, TosoHaas) and step gradient conditions were employed in the first purification step. SGE was applied in 20mM Tris-HCl, pH 7.6, followed by elution with 20 mM Tris–HCl, 0.15 M NaCl, pH 7.6. A flow speed of 1 ml/min was maintained for 20 min, while the effluent was monitored at 280 nm. Apyrase activity was then eluted with higher ionic strength buffer (20 mM Tris–HCl, 0.5 M NaCl, pH 7.6) from the column. Fractions from the size-exclusion column were dialyzed against 0.1 M NaCl (Slide-A-Lyzer cassettes, Pierce), before application to the AEHPLC as described in Chapter 2.

5.2.3 Preparation of anti-sera

Purified apyrase and savignygrin were prepared for immunization by tricine SDS-PAGE and Coomassie Brilliant Blue staining. Bands (~10 µg) were cut out, homogenized and suspended in 400 µl of 0.1M phosphate buffered saline, pH 7.2 (PBS). The adjuvant was prepared as described (Vulliet, 1996). New Zealand White rabbits were first bled to obtain naïve sera and then immunized with antigen emulsified in Freund's complete adjuvant. After 6 weeks the rabbits were boosted with antigen prepared in Freund's incomplete adjuvant and this schedule repeated until a specific response could be seen at x1000 dilution (~18 weeks) with western blotting. Rabbits were bled ten days after each immunization to gauge the immune response.

5.2.4 Western blot analysis of SGE

SGE (~0.5 glands) was fractionated with tricine SDS-PAGE and blotted onto Hybond-P membranes (Amersham Pharmacia Biotech) using a Trans-Blot SD Semi-Dry Transfer

Cell (Bio-Rad) blotting apparatus (20V, 45 min). Membranes were blocked with 1% non-fat milk powder in PBS for 1 hour before rotary incubation overnight in their respective anti-sera (x500 dilution of sera in 0.1% non-fat milk powder). Blots were washed in PBS (x3) and incubated with peroxidase conjugated goat anti-rabbit IgG antibody (Sigma Co., USA) for 3 hours. After washing in PBS (x3), blots were developed in 20% methanol, 0.06g chloronaphtol (Sigma Co., USA) and 60μl peroxide (SigmaCo., USA) in 100 ml PBS.

5.2.5 Secretion of salivary gland components by various stimulants

To investigate the secretion of salivary gland components, several procedures were investigated. (A) Ticks were allowed to feed to complete engorgement on rabbits, by confining them to the ears. Salivary glands were then dissected at various time intervals for EM analysis. The salivary glands of two ticks were analyzed for each time interval taken. (B) Female ticks were also injected with a 1% pilocarpine hydrocloride or dopamine solution into the genital pore with a 24G syringe (Howell, 1966b). Salivation was allowed to proceed until completion, before glands were dissected for EM analysis. (C) A backless-tick explant (Bell, 1980) was prepared by removing the dorsal cuticle and gut before bathing the glands in a 1% pilocarpine or dopamine solution. Ticks were monitored for saliva secretion and glands were removed for EM analysis. (D) Salivary glands were dissected and bathed in solutions of 1 μM pilocarpine or dopamine dissolved in salivary gland solution (20 mM TrisHCl, 0.15M NaCl, 2 mM KCl, 50 mM D-glucose, pH 7.6). After 5 minutes of incubation, the supernatant was tested for secretion of salivary gland components by assaying for apyrase. (E) Salivary glands from ten female ticks were dissected in 9% saline. Salivary glands were then transferred to 1 ml salivary gland solution. Salivary glands were sheared by repetitive trituration using a 100μl pipette. Acini were allowed to settle by gravitation and were washed 3X with 1 ml TBS. Acini were suspended in 1 ml TBS and 100 μl were added to 900μl TBS with pilocarpine or dopamine to give a final concentration of 1 μM. After incubation for 10 minutes, aliquots (10μl) were taken of the supernatant and tested for apyrase activity. Acini were also processed for SEM and TEM analysis. (F) Twenty unfed female ticks with similar masses were compared to assess the efficiency of salivary gland secretion. Ten unfed

female ticks were allowed to feed to complete engorgement on mice before dissection of their salivary glands. Salivary glands from ten unfed ticks were dissected as controls and apyrase activity as well as protein concentration were determined as described previously.

5.2.6 Preparation of tick salivary glands for immuno-localization

Salivary glands from female ticks that had not fed for at least two months were dissected in PBS and immediately fixed in 1% formaldehyde and 0.1% gluteraldehyde for 3 hours. For SEM analysis, glands were additionally fixed in 0.1% osmium tetra-oxide. Glands were then dehydrated in a sequential series of 30, 50, 70 and 100% ethanol (15 min x3) and critical point dried in CO_2, sputter-coated with gold and analyzed with a JEOL 840 SEM (5 or 30 kV). For immuno-localization and TEM analysis, glands were sequentially incubated in 30, 50, 70 and 100% LR White resin, for 15 minutes each. After 3 hours incubation in 100% LR White resin, the glands were embedded in 100% LR White and polymerized at 60 °C for 48 hours. Sections of 0.5 μm were prepared using an ultramicrotome for light-microscopy studies. Sections were either stained with a solution of 0.1% toluidine blue or were further processed for immuno-cytochemistry at the light microscope level. Sections were blocked with 1% antibody dilution solution (ADS, 1% fish skin gelatin, 10 min) and stained with primary anti-sera or naïve sera (200 X dilution) for 1 hour. Sections were washed 3 X with ADS before incubation with biotinylated goat α-rabbit IgG (1:200) for 1 hour. Sections were washed 3 X with PBS (0.15M phosphate buffer, pH 7.4) before incubation with an avidin-biotinylated horse-radish macromolecular complex (VECTASTAIN Elite ABC Reagent, Vector Laboratories, Inc., CA, USA). Sections were washed 3 X with PBS before incubation with DAB. Color development was observed until an adequate level of marking was reached.

5.2.7 Immuno-cytochemical labeling of thin sections

Thin sections (0.1 μm) were prepared with an ultramicrotome and mounted on nickel grids for immuno-cytochemical labeling. To remove excess aldehyde groups, thin sections were blocked in 50 mM glycine for 5 minutes. Non-specific binding of

antibodies was prevented by blocking in 10% fetal calf serum. Sections were washed in PBS (x3) and then incubated in prepared anti-serum (x500 dilution) for 60 minutes. Anti-sera were changed every 30 minutes. After washing in PBS (x3) the sections were incubated with gold conjugated (10 nm) goat anti-rabbit serum (Sigma) at x500 dilution for 60 minutes and then washed in PBS (x3) before fixation in 0.1% glutaraldehyde for 5 min. The sections were washed in PBS (x5) followed by water (x5) before contrasting with uranyl acetate. It was found that with additional contrasting in lead citrate, no morphological differences could be detected for different granules. Samples were analyzed with a Philips 301 TEM.

5.2.8 Immuno-fluorescent localization of savignygrin, using confocal microscopy

Fixed glands were permeabilized in a graded series of methanol (0-100%) before rehydration in PBS. To minimize auto-fluorescence from glutaraldehyde fixation, glands were incubated overnight at 4 °C in 100 mM $NaBH_4$ with the Eppendorf caps open. Glands were washed 3 X with TBSN buffer (10 mM Tris-HCl, pH 7.4, 155 mM NaCl, 0.1% Triton X-100) for 90 minutes with constant rotation before blocking with 2% BSA in TBSN. Glands were incubated with 50 X dilution of primary anti-sera or naïve sera in PBS and 2% BSA for 8 hours. Glands were washed with TBSN for a further 48 hours with buffer washes every 8-12 hours before incubation with fluorescein-goat-α-rabbit secondary antibody in TBSN (2% BSA) for 8 hours at 4 °C in the dark. Glands were washed in TBSN for 48 hours before dehydration in a graded series of methanol (0-100%) over 90 minutes. Glands were mounted on microscope slides in clearing solution. Glands were viewed with an Olympus BX50 microscope and Bio-Rad MRC-1000 confocal laser scanning imaging system and COMOS imaging software (BioRad, Hercules, CA, USA). For low magnification a series of 2 μm optical sections (Z focus series) spanning 32 μm were merged to form a single image. For high magnification a series of nineteen, 1.34 μm optical sections (Z focus series) were merged to form a single image. Naïve sera were used to assess both specificity as well as auto-fluorescence.

5.2.9 Immuno-fluorescent localization of microtubules using confocal microscopy

Using the same procedures as for savignygrin, α-tubulin was also localized with polyclonal rabbit anti-tubulin antibodies (a kind gift from Prof. Charles Lessman, University of Memphis, Tennessee, USA).

5.2.10 Carbohydrate and membrane staining of salivary glands using the Thièry test

Thin sections (0.1 μm), embedded in LR White resin, were stained with the periodic acid, thiocarbohydrazide (TCH) –silver-proteinate method (Courtoy and Simar, 1974). Specific controls included staining with silver-proteinate alone, periodic acid oxidation and silver proteinate, TCH and silver-proteinate without periodic acid oxidation and oxidation with periodic acid and staining with TCH and silver-proteinate. Periodic acid (3%) incubation was performed for 30 minutes and sections washed three times with ddH_2O. Reactions with TCH (0.2% in 20% acetic acid) were allowed to proceed for 4 hours before washing in 10% acetic acid, 5% acetic acid and 1% acetic acid (x3). Sections were washed in ddH_2O and incubated with silver-proteinate (1%) for 60 minutes and rinsed three times in ddH_2O. Analysis was performed with TEM.

5.2.11 Scanning electron microscopy of the salivary gland membrane system

The presence of the Golgi-apparatus was investigated by SEM using the O-D-O (osmium, DMSO, osmium) method (Tanaka and Fukudome, 1991). This method is useful to observe membrane systems within the cell. Salivary glands were fixed in 0.5% gluteraldehyde, 0.5% formaldehyde (0.075 M phosphate buffer (PB), pH 7.4) before post-fixation with 1% osmium tetroxide for 2 hours. After rinsing with buffer the glands were immersed for 30 minutes in 25% and 50% dimethyl sulfoxide (DMSO), respectively. The glands were frozen on a metal plate prechilled with liquid nitrogen and were split open with a scalpel. The split pieces were immediately thawed in 50% DMSO at room temperature, before rinsing 5 X with PB until all DMSO was removed. A further fixation of 1 hour with 1% osmium tetroxide was followed by an osmium maceration step (0.1% osmium tetroxide in PB, pH 7.4 for 72 hours at 20°C). Glands were washed with buffer (3 X PB) before incubation with 1% osmium tetroxide for 1hour followed by 2% tannic acid solution overnight and again 1% osmium tetroxide for 1 hour. Glands were

dehydrated in a graded series of ethanol (0-100%) before critical point drying. Glands were coated with a ion beam gun using platinum. Samples were observed in the JEOL 840 SEM.

5.2.12 Sub-cellular fractionation of salivary gland granules using collagenase

During the characterization of the salivary gland granules (chapter 5), granules were initially prepared using collagenase treatment of glands. Twenty glands were incubated with 0.5 mg collagenase type VII (Sigma, St. Louis, MO, USA) in digestion buffer (20 mM Tris-HCl, 2 mM $CaCl_2$, 2 mM $MgCl_2$, pH 7.4). Glands were gently resuspended every 20 minutes with a 1 ml thin tip pipette. After 1 hour, fine spherical particles could be observed that sedimented under the influence of gravitation. After 3 hours of incubation the preparation was loaded onto a 0-50% preformed Percoll (Sigma Co., USA) gradient (5% per 2 ml~20 ml in a column of ~1 cm diameter). Granules were allowed to sediment using gravity and fractions were collected after the first visible sediment reached the bottom (~ 30 minutes). All fractions were tested for apyrase activity and labeled as (1) the supernatant after collagenase treatment, (2) the first fraction that sedimented, (3) first ml from the bottom, (4) second ml from the bottom, (5) to (15). Fractions were also prepared for SEM as described for platelets (Chapter 2).

5.3 Results

5.3.1 Purification of apyrase and generation of specific polyclonal anti-sera

The generation of polyclonal anti-sera specific for savignygrin commenced at a stage when the characterization of apyrase was still in progress (Mans, 1997). Localization of another anti-hemostatic component in tick salivary glands for comparative purposes were considered to be a fruitful endeavor. To this end, apyrase was purified by use of non-specific interaction with a silica-based size exclusion matrix (Mans, 1997; Mans *et al.* 1998b), followed by AEHPLC (Fig. 5.3a and Fig. 5.3b). Tricine SDS-PAGE electrophoresis of apyrase and savignygrin was used as an extra purification step for the preparation of anti-sera (Fig. 5.3c). The specificity of the prepared anti-sera was determined using Western blot analysis of crude salivary gland extract. No cross reactivity with salivary gland antigens were observed with naïve sera. Apyrase and savignygrin specific anti-sera showed labeling of a 67 kDa and 7 kDa component, respectively (Fig. 5.3d). No other cross reactivity was observed at this dilution (x1000). This was taken as an indication that the sera were mono specific for their antigens at the dilutions used.

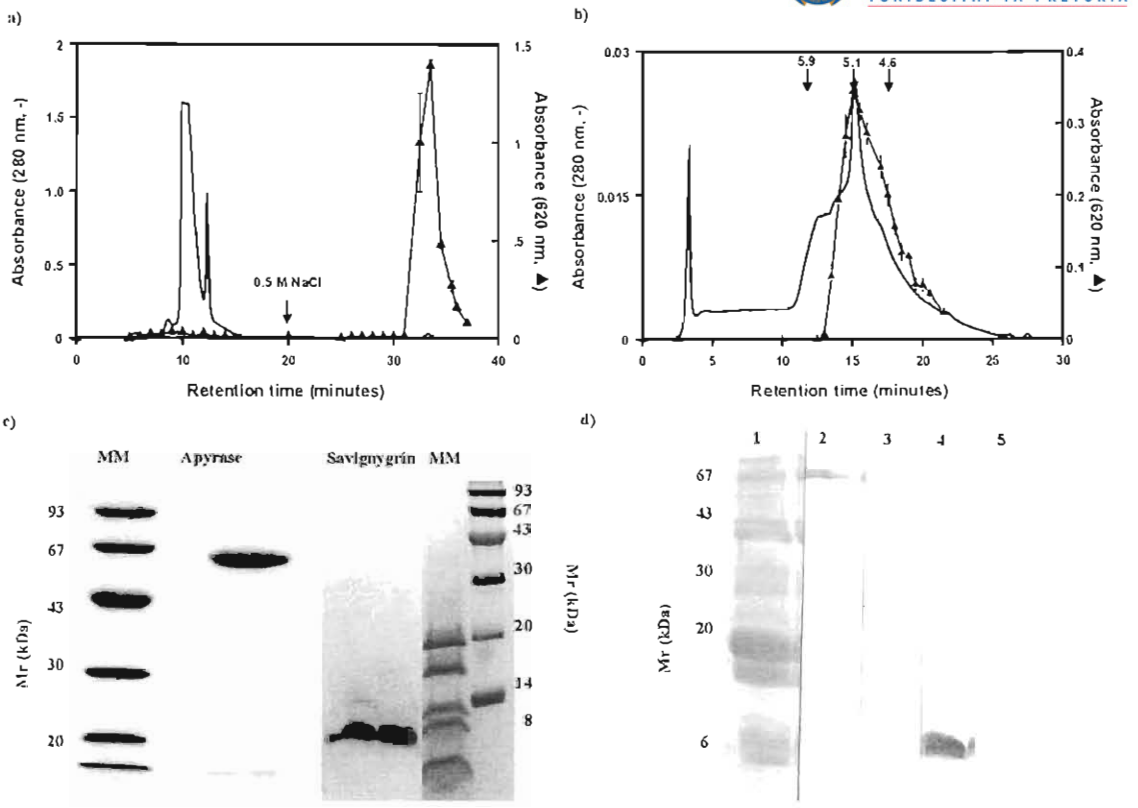

Fig. 5.3: Purification of apyrase and specificity of anti-sera. (a) SEHPLC of SGE. Apyrase was eluted from the SEHPLC matrix using a high ionic strength buffer. (b) AEHPLC of apyrase fractions from SEHPLC. Activity is indicated with triangles. (c) SDS-PAGE purification of apyrase and savignygrin for production of anti-sera. (d) Western blot analysis of α-apyrase and α-savignygrin anti-sera. Lane 1 indicates Coomassie Blue stain of salivary gland extract, lane 2 α-apyrase, lane 3 naïve sera, lane 4 α-savignygrin, lane 5 naïve sera.

5.3.2 Morphological studies on the salivary glands of *O. savignyi*

No descriptive study on the salivary gland morphology of *O. savignyi* could be located in the literature. For comparative purposes as well as for the sake of interest, morphological characterization of the salivary glands was conducted. Intact salivary glands are enclosed by a myo-epithelial sheath (L. Coons, personal communication) (Fig. 5.4a; Fig. 5.4b). Individual acini can be observed, which upon exposure to higher electron voltages show the granules inside the cells (Fig. 5.4c). At least 4 different granular cells forming pyramidal shaped cells can be distinguished. Granules ranged in size from 4-7μm in diameter (Fig. 5.4d).

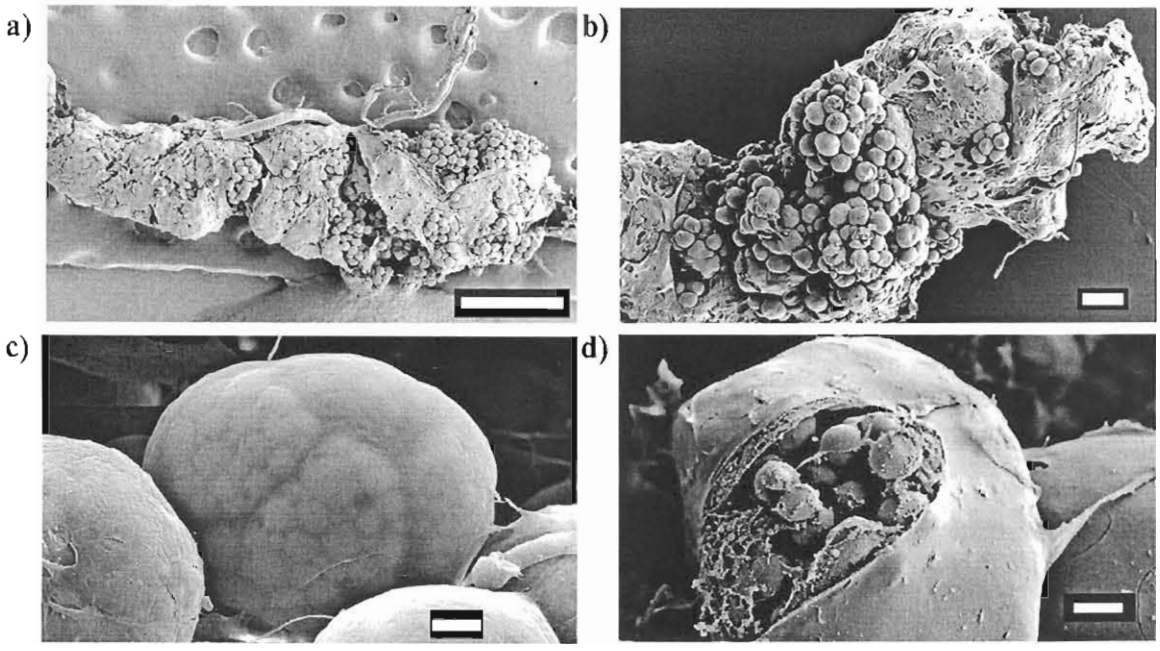

Fig. 5.4: SEM analysis of salivary glands from *O. savignyi*. (a) An intact salivary gland with the myo-epithelial sheath visible, as well as single acini (~40-70 μm diameter). Scale bar = 500 μm. (b) An intact salivary gland showing the myo-epithelial sheath as well as prominent acini, clustered together. Scale bar = 100 μm. (c) An acini at high electron voltage (30 keV) show the packing of the salivary gland granules through the cell membrane. Scale bar = 10 μm. (d) A ripped acini shows granules packaged inside a cell. Scale bar = 10 μm.

5.3.3 Ultrastructural studies of the salivary glands

Cross-sections through the salivary glands show their arrangement in acini and the pyramidal shaped granular cells (Fig. 5.5). At least three different cell types can be distinguished based on light microscopy observations. These include cell type a with dense core granules (diameter of 3-5 μm), cell type b with homogenous granules (diameter of 4-10 μm) that seem to occur more than once in an acini and cell type c with granules (diameter 1-2 μm) with electron lucent cores. No other distinctive organelles inside the granular cells could be distinguished.

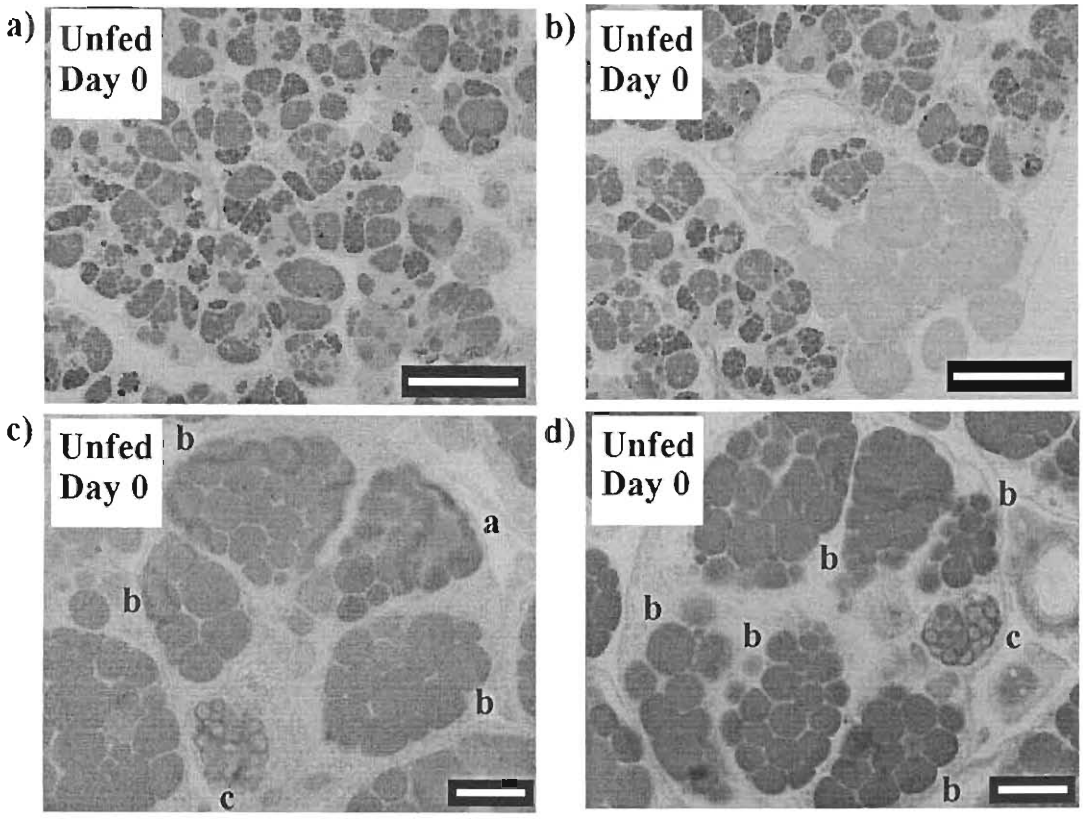

Fig. 5.5: Sections though a salivary gland cell of an unfed tick. (a) The grouping of various granular cells in acini is clear. Cells with dense core granules, as well as cells with homogenous granules can be observed. Scale bar = 100 μm. (b) Agranular acini can be observed in the lower right hand corner. Scale bar = 100 μm. (c) A single acini with at least five different granular cells. A cell with dense core granules (a), three homogenous granular types (b) and a cell with granules with an electron lucent core (c) can be observed. Scale bar = 10 μm. (d) Another acini containing at least seven cells. Scale bar = 10 μm.

5.3.4 Morphology of salivary glands from fed ticks

The hypothesis that bio-active components are stored inside the salivary gland granules, has been advanced. Salivary glands from fed ticks were analyzed to investigate secretion of granules. Salivary glands showed secretion of granules immediately after feeding, although not to the extent expected (total release of salivary gland granule contents across the whole gland). Most cells that showed granule release also retained several granules. Organelles (mitochondria) not previously observed were prominent in those cells that showed secretion (Fig. 5.6).

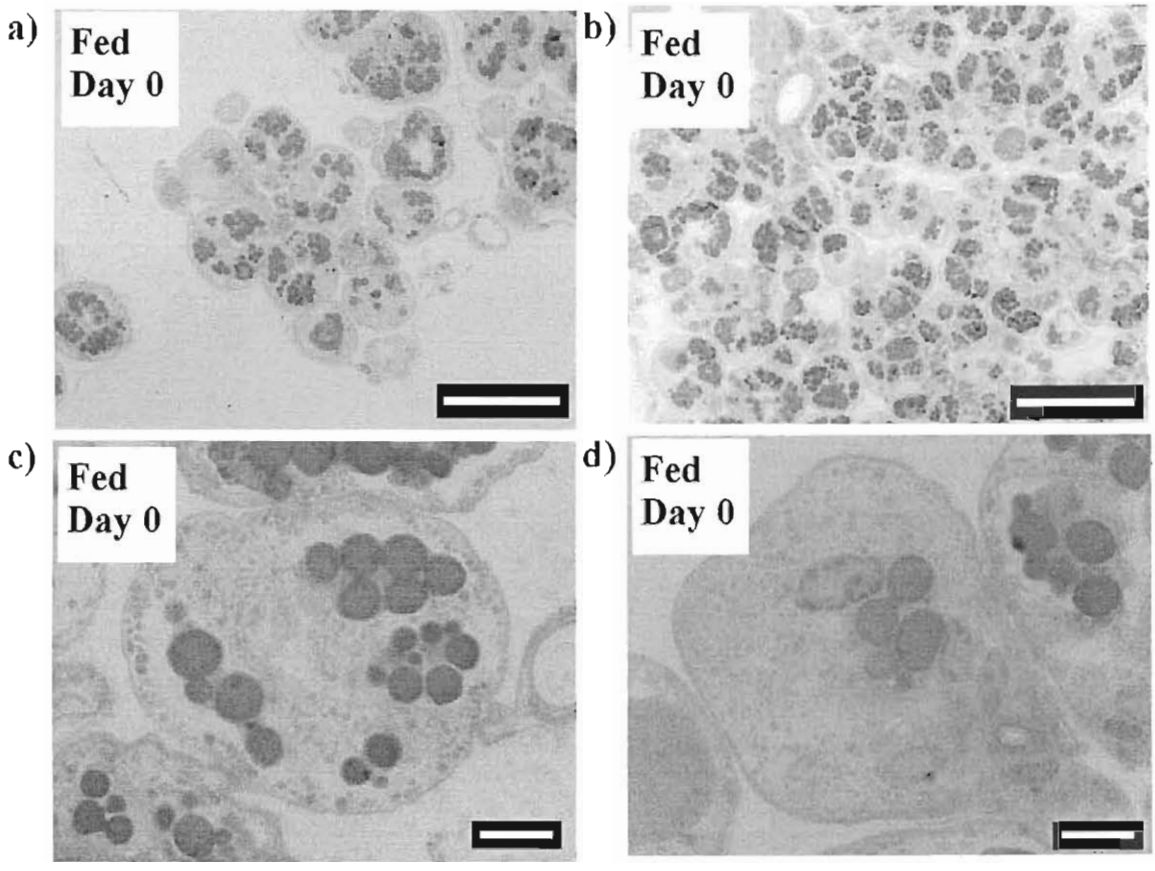

Fig. 5.6: Salivary glands from ticks dissected 10 minutes after feeding to engorgement on a rabbit. (a) Granular cells show signs of granule secretion and a dilated lumen. Scale bar = 100 μm. (b) Many acini do not show any signs of secretion or granule mobilization. Scale bar = 100 μm. (c) An acini with a reduced number of granules. Prominent are the other cellular organelles (mitochondria) visible after secretion, that's not normally observed in the salivary glands from unfed ticks. Scale bar = 10μm. (d) An acini that shows even more signs of granule secretion. Scale bar = 10 μm.

5.3.5 Morphology of salivary glands several days after feeding

Salivary glands quickly recovered and one day after feeding resumed the general morphology observed for salivary glands of unfed ticks. The only differences observed were some acini that still showed a dilated lumen, although their granular cells were still packed with granules (Fig. 5.7a; Fig. 5.7b). After 4-7 days no differences could be observed between unfed and fed tick salivary glands (Fig. 5.7c; Fig. 5.7d).

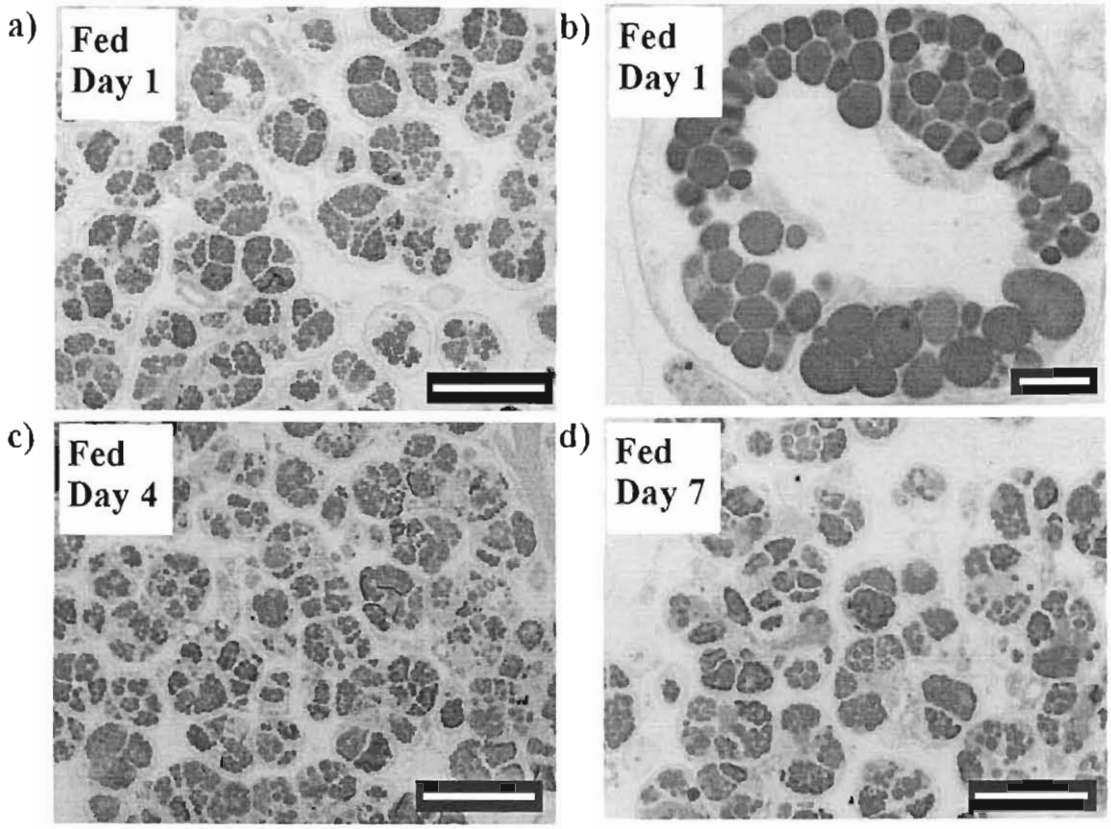

Fig. 5.7: Salivary glands from ticks at different time periods after feeding. (a) Salivary glands one day after feeding appear as those of unfed ticks, although acini with dilated lumen are still visible. Scale bar = 100 μm. (b) An acini with a dilated lumen. Scale bar = 10 μm. (c) Salivary glands four days after feeding appear as those of unfed ticks. Scale bar = 100 μm. (d) Salivary glands seven days after feeding appear as those of unfed ticks. Scale bar = 100 μm.

5.3.6 Secretion of salivary gland components induced by various stimulants

Secretion of salivary gland components was also investigated for the neurostimulants pilocarpine and dopamine. Results show that pilocarpine injected into the tick haemocoel induces salivation (Howell, 1966b). Using the same technique, dopamine failed to elicit a response. EM analysis showed that very little secretion of granules could be observed for pilocarpine-stimulated salivation. This is concurrent with results that showed that apyrase specific activity was much higher in salivary gland extracts than salivary secretion (Mans, 1997). Addition of pilocarpine to a backless tick explant induced salivation while dopamine did not. Neither pilocarpine nor dopamine induced secretion of apyrase in intact dissected salivary glands. These results did not correlate with those obtained for

hard ticks, where dopamine injected into the hemocoel or applied to isolated salivary glands induced fluid secretion (Kaufman, 1976; McSwain, Essenberg and Sauer, 1992). It was considered that the myo-epithelial sheath might hinder access to the acini in the intact salivary glands. For this purpose acini were mechanically sheared (Qian *et al.* 1998) before addition of pilocarpine or dopamine. Surprisingly dopamine induced higher secretion of apyrase than did pilocarpine, which was only slightly more than the background (Fig.5.8). EM analysis of these acini revealed no detectable secretion of granules.

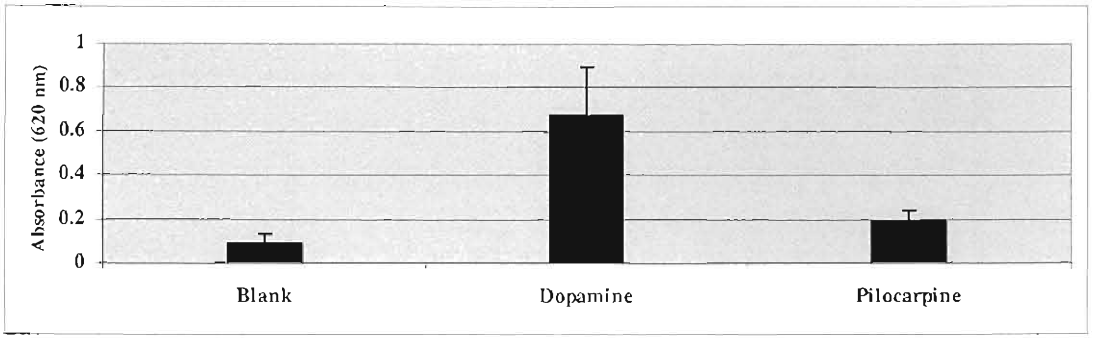

Fig. 5.8: Secretion of apyrase from exposed acini induced by dopamine. Mechanically sheared salivary glands were incubated with either dopamine or pilocarpine (1 μM) before assaying for apyrase activity.

5.3.7 Secretion efficiency of salivary glands during feeding

The low levels of secretion observed using EM analysis and chemical stimulation was further investigated using feeding ticks. Ten unfed ticks with similar masses (~0.169g) were allowed to feed to engorgement (or until they dropped off) before dissection of salivary glands and compared to salivary glands from 10 unfed ticks (Fig. 5.9). Engorged body masses from fed ticks showed a large standard deviation, while standard deviation values for both apyrase and protein concentration of the salivary glands were more comparable with those from unfed ticks. On average only 17% of the total apyrase activity and 37% of the total salivary gland protein were secreted.

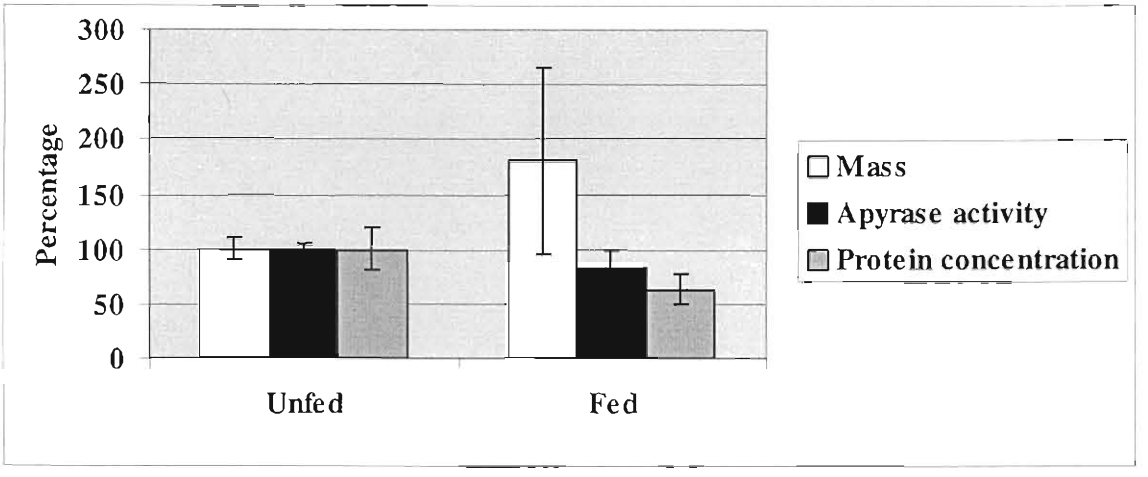

Fig. 5.9: A comparison between salivary glands of unfed and fed ticks. Indicated are body masses for ticks before and after feeding expressed as a percentage of the average unfed mass. Apyrase activity is expressed as percentage activity from the average unfed tick salivary gland extract. Protein concentration is expressed as a percentage of the average unfed tick salivary gland extract concentration.

5.3.8 Immunolocalization of apyrase and savignygrin on light microscope level

Immunolocalization of apyrase and savignygrin on light microscope level showed localization of both to granules of two different granular cell types (Fig. 5.10). Localization of savignygrin was more distinct than that of apyrase, although specific marking was evident if compared to the naïve controls. One of the granule types could be identified as cell type "a" dense core granules and the other as cell type "b" with a homogenous appearance. An additional granular cell type, "d" also had a homogenous appearance but showed no localization (Fig. 5.11). This brings the number of granular cell types observed for argasid ticks to a total of four. Note that this fits well with the results from Fig. 5.5 that indicate that the homogenous granules occur more than once per acini.

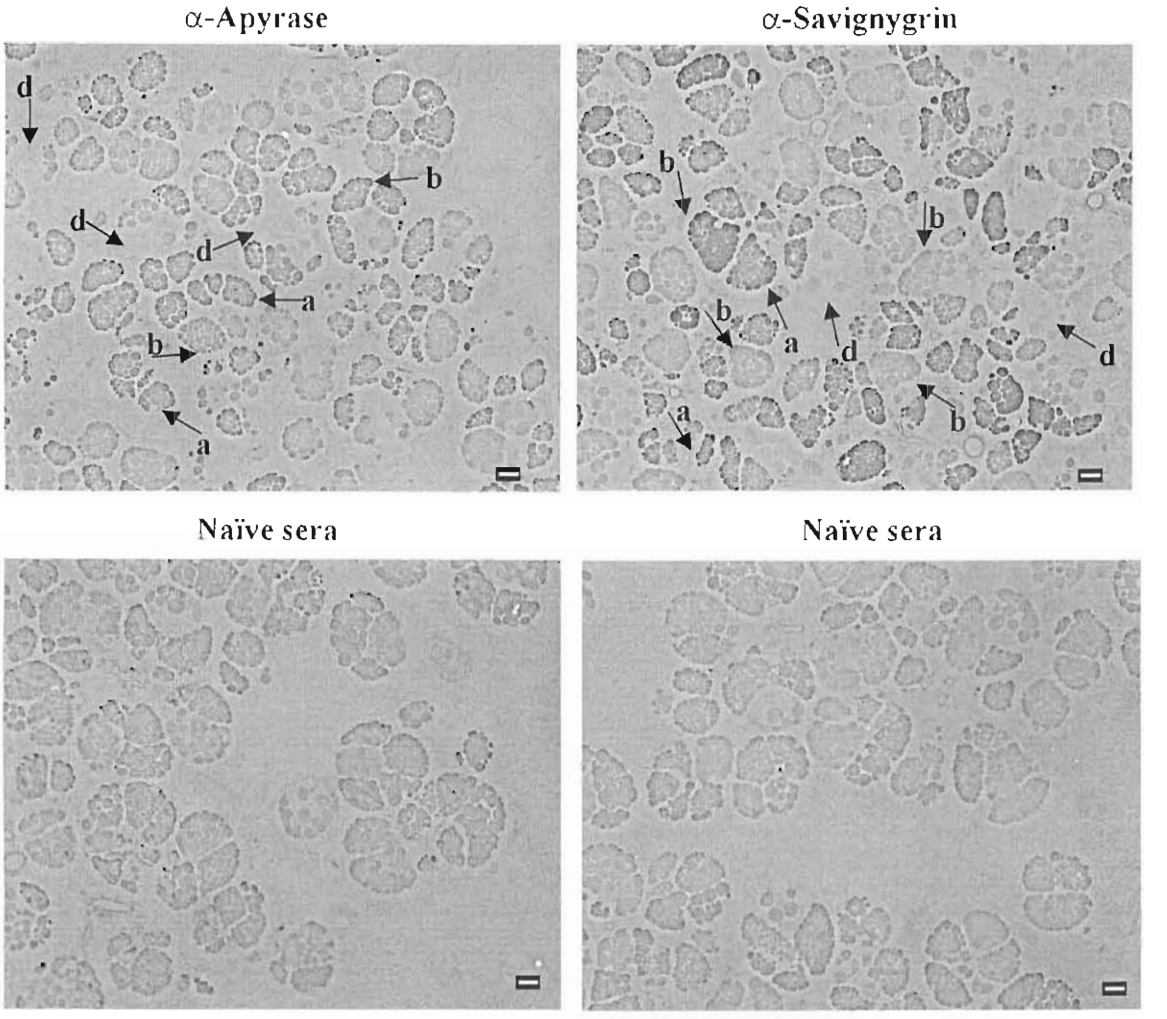

Fig. 5.10: Immunolocalization of apyrase and savignygrin. Light micrographs for sections labeled with anti-apyrase, anti-savignygrin or their respective naïve sera are indicated. Localization to dense core granules (a) and homogenous granules (b), as well as granules considered to be unlabeled (d) are indicated. Scale bar = 10 μm. All micrographs were taken using the same brightness and contrast.

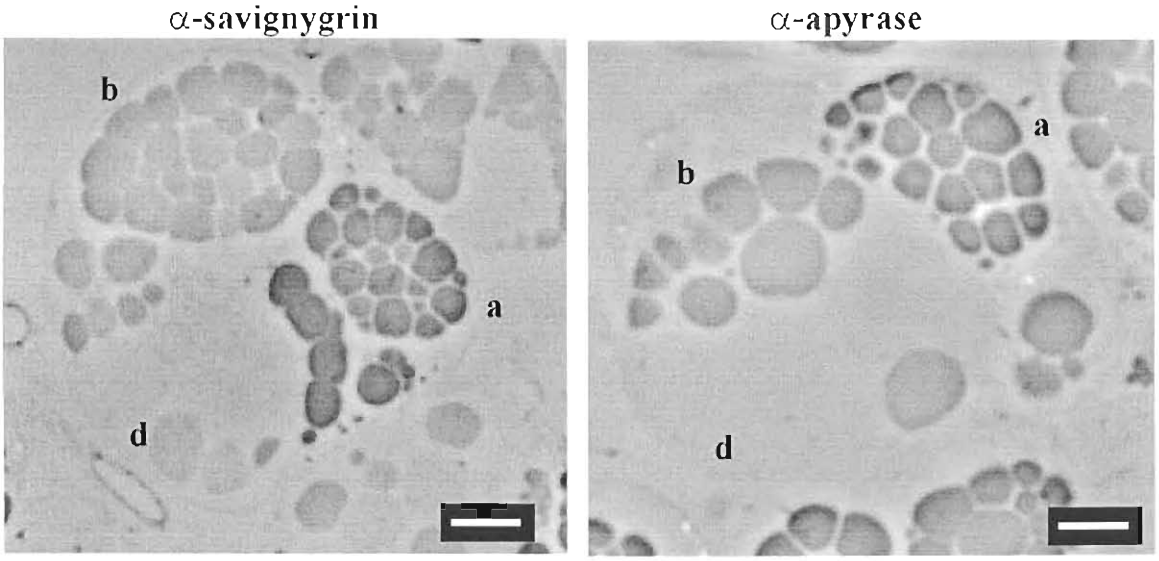

Fig. 5.11: Immunolocalization at a higher magnification. Localization to dense core granules (a) and homogenous granules (b) are indicated. Note the absence of marking in granule type (d). Scale bar = 10 μm.

5.3.9 Co-localization of apyrase and savignygrin at the ultrastructural level

It was observed that both apyrase and savignygrin were localized to the same granule types. The dense core type "a" granules and type "b" granules which have a homogenous appearance showed specific labeling (Fig. 5.12a; Fig. 5.12b). Granule types "c" and "d" that could be distinguished morphologically gave no significant labeling (Fig. 5.13). Negative controls using naïve sera at the same dilutions did not show any specific labeling (results not shown).

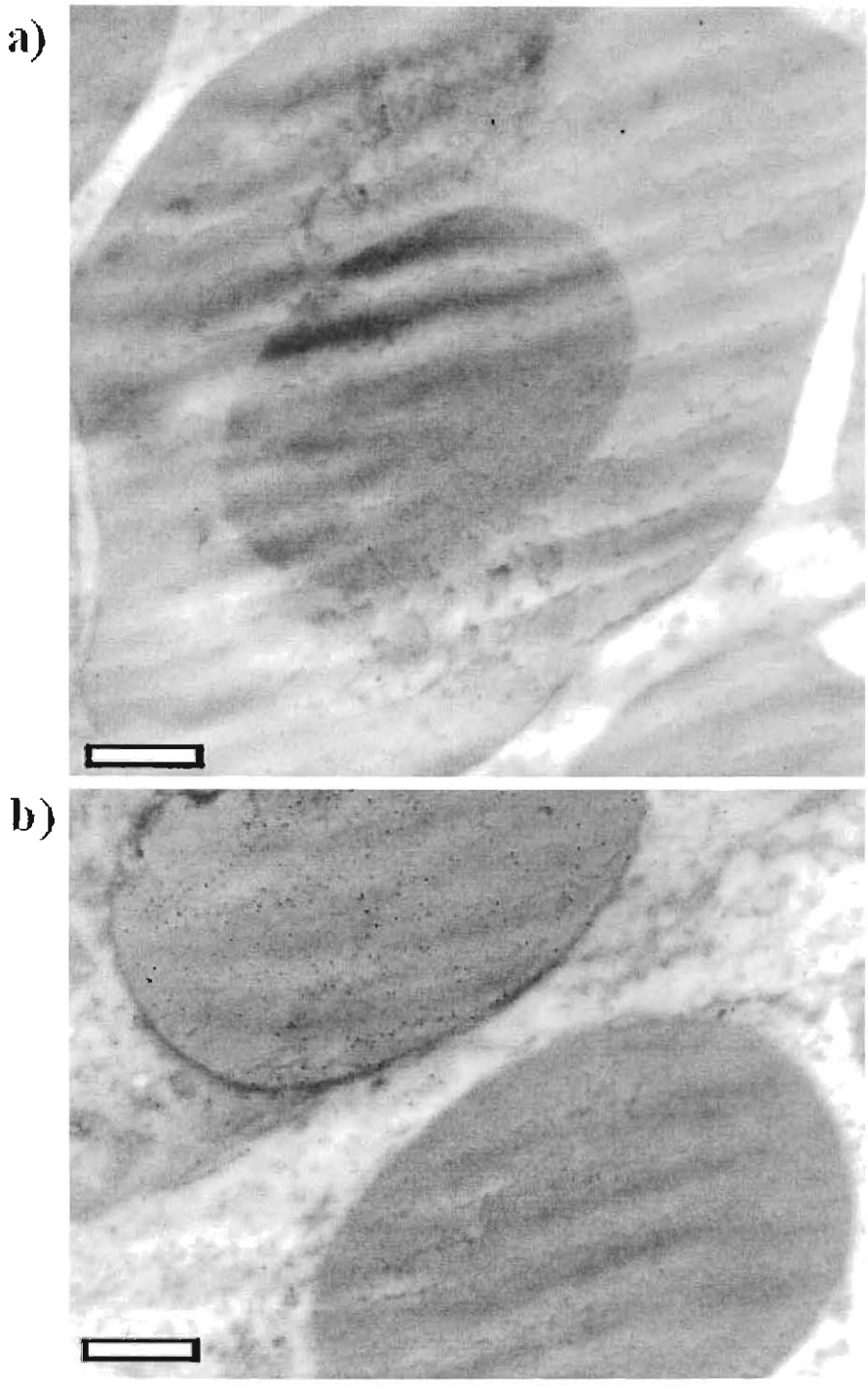

Fig. 5.12: Co-localization of apyrase and savignygrin using immuno-gold labeling. (a) Localization of both apyrase (10 nm gold) and savignygrin (20 nm gold) to the dense core granules (cell type "a"). (b) Localization of apyrase (10 nm gold) and savignygrin (20 nm gold) to homogenous granules (cell type "b"). Also indicated is a type "d" granule from another cell that shows no localization. Scale bar = 500 nm.

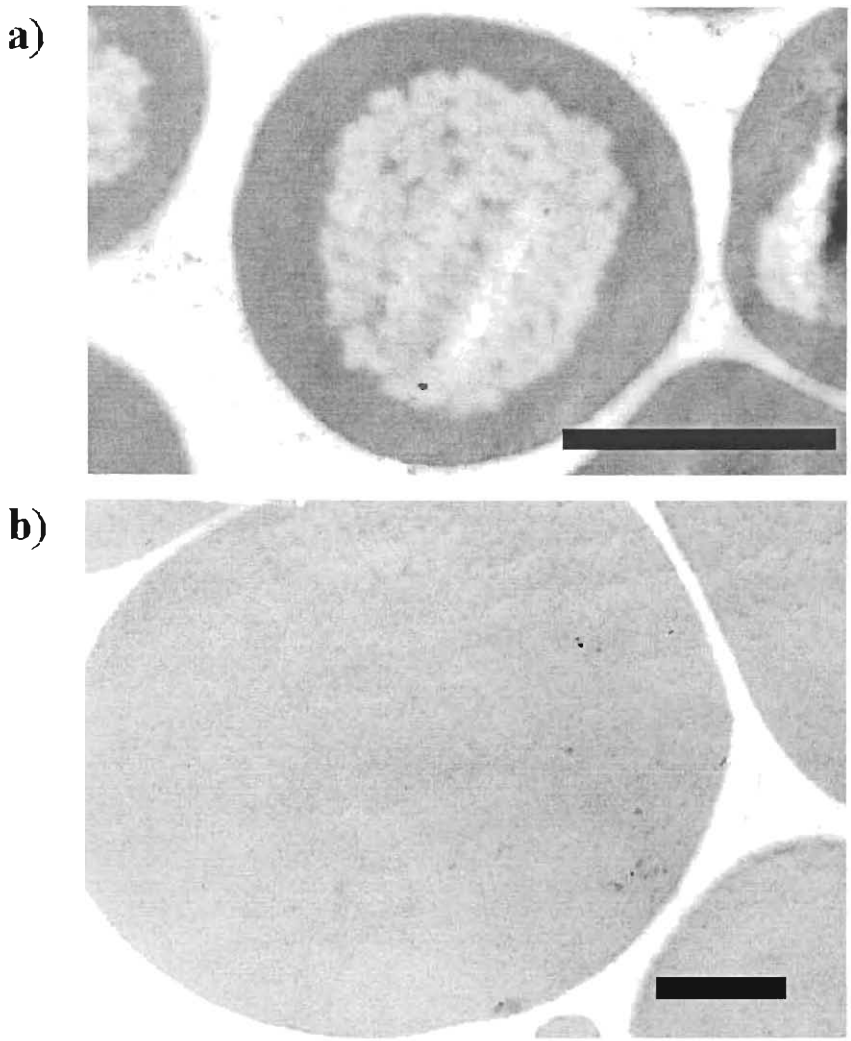

Fig. 5.13: Granular cells that did not show significant labeling. (a) Cell type "c" cells and (b) cell type "d" cells did not show any labeling. Scale bar = 1 μm.

5.3.10 Immuno-fluorescent localization of savignygrin to salivary gland granules

During a visit to the laboratory of Dr. Lewis Coons (May-June 2000, University of Memphis, Tennessee), I had the opportunity to localize savignygrin in the salivary glands using immuno-fluorescent confocal microscopy. In contrast to the light microscopy and TEM results, which showed labeling of two different granule types, consistent labeling of only one granule type per acini was obtained (Fig. 5.14a). Granules also showed higher labeling on their outer edges compared to their cores (Fig. 5.14b). An absence of labeling in some acini also suggests that there may be as yet an unidentified acini and granular cells present in soft tick salivary glands.

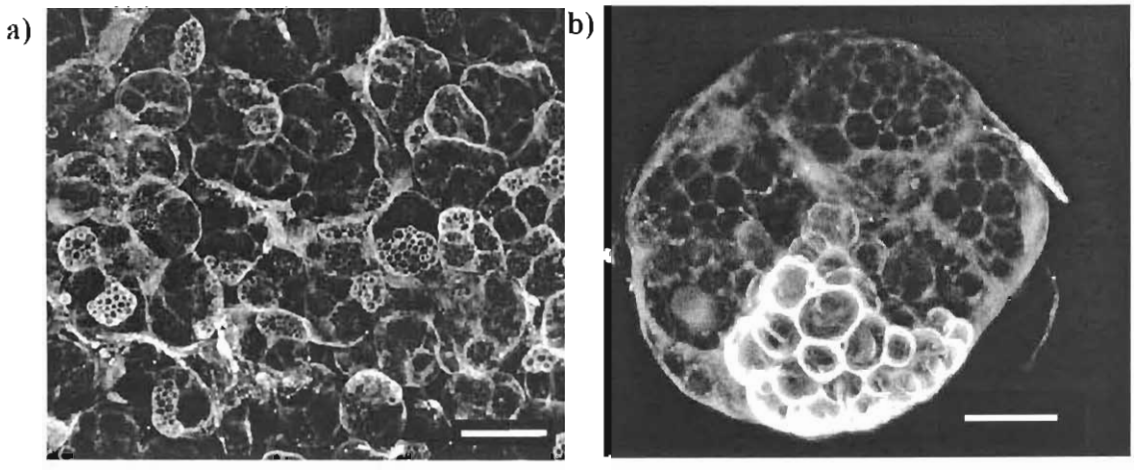

Fig. 5.14: Localization of savignygrin to a specific granule cell type with immuno-fluorescence confocal microscopy. (a) Localization of savignygrin to only one cell type per acini is clear. Note that for some acini no labeling is obtained. Scale bar = 100 μm. (b) Labeling at a higher magnification shows that granules are only labeled at their outer perimeters. Scale bar = 20 μm.

5.3.11 Absence of membrane vesicles involved in granule formation in mature cells

The absence of any membrane systems such as endoplasmic reticulum or Golgi apparatus were noticed in the thin sections prepared. To investigate this, a Thiery stain that gives good contrast for membranes and which also stains carbohydrates were employed. The only specific carbohydrate staining observed was the electron lucent cores of granule type "c" (Fig. 5.15a). In granular cells with mature granules, no ER or Golgi apparatus were observed although extensive membrane systems where found in a cell where immature granules were evident (Fig. 5.15b).

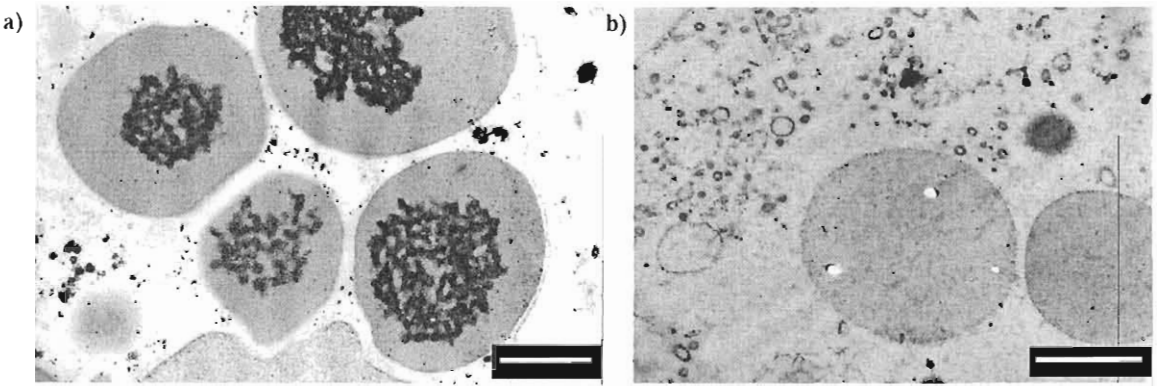

Fig. 5.15: Thiery stain of salivary glands. (a) Only cell type "c" showed positive staining for carbohydrates in its electron lucent core. (b) Membrane systems (ER, Golgi?) were only observed once in the presence of small immature granules. Scale bar = 1 μm.

5.3.12 SEM investigation into membrane systems of salivary glands

A technique that allows the selective removal of cytoplasmic components while membrane systems are retained was employed to investigate the presence of Golgi apparatus (Tanaka and Fukudome, 1991). This technique has been successfully used to investigate the three dimensional structure of various cell organelles such as ER, Golgi complex and mitochondria. In the salivary glands the only membrane systems left after osmium maceration, seem to be associated with the cytoskeleton (Fig. 5.16). All the granules seemed to have been removed completely. No structures that resemble the classic Golgi complex could be recognized.

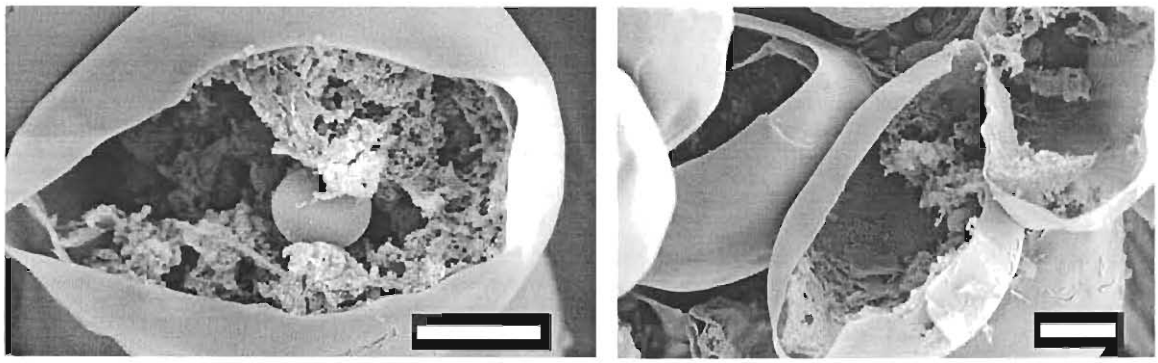

Fig. 5.16: SEM analysis of membrane systems of the salivary glands after osmium maceration. Most of the salivary gland granules were completely removed by this process and the only membrane systems present seem to be associated with the cytoskeletal network.

5.3.13 Sub-cellular fractionation of salivary gland granules after collagenase treatment

Results obtained from initial fractionation attempts of the salivary gland granules (see Chapter 6 for reason) could suggest reasons for the results obtained for the osmium maceration steps. Digestion with collagenase resulted in intact granule preparation as observed by the absence of apyrase in the supernatant fraction (fraction 15) with which the preparation was washed before loading onto the Percoll gradient. Fractionation showed that apyrase could be detected in a range of fractions, notably fraction 1, that represents the sedimented fraction, that consist of partially digested intact gland preparation and fractions (4-10) that represent granules in various degrees of association (Fig. 5.17).

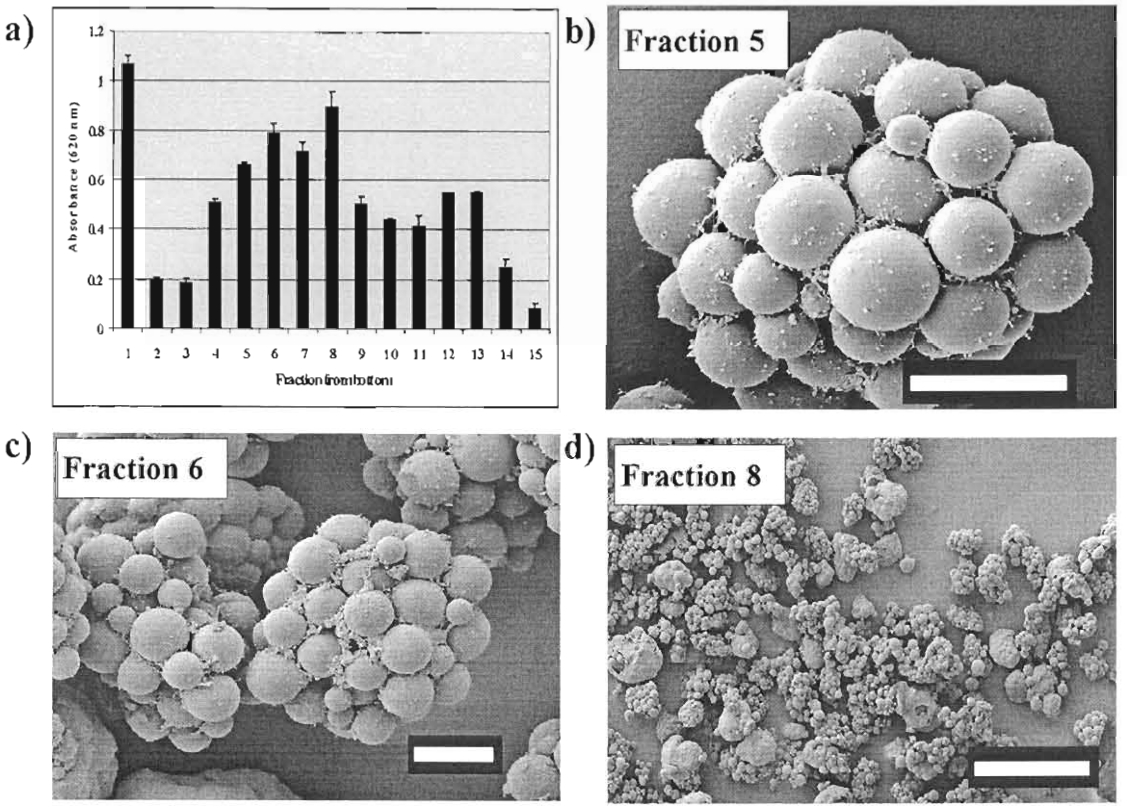

Fig. 5.17: Sub-cellular fractionation of salivary gland granules using density gradient centrifugation collagenase treatment. (a) Apyrase activity tested for different fractions collected. Fraction 1 represents sedimented material, fraction 2-14 represent 1 ml fractions (5% increments of Percoll, 0-50% gradient) collected from the bottom of the gradient and fraction 15 the supernatant of the last wash buffer before granule preparations were loaded onto the gradient. Granules preparations of fractions 5 (b), 6 (c) and 8 (d) are indicated. Scale bar = 10 μm (b, c) or 100 μm (d).

5.3.14 Immuno-localization of α-tubulin to tick salivary glands

Microtubules serve to organize the ER and Golgi complex as well as transporting secretory vesicles. Localization of the microtubules could thus indicate the possible presence of a Golgi complex. Microtubules (as detected by the presence of α-tubulin) could be detected in agranular acini of both hard and soft ticks, cells from the myo-epithelial sheath, but no extensive pattern network could be observed in granular cells. Some localization between granules is evident, although it is clear that these microtubules do not serve an organizing role (Fig. 5.18).

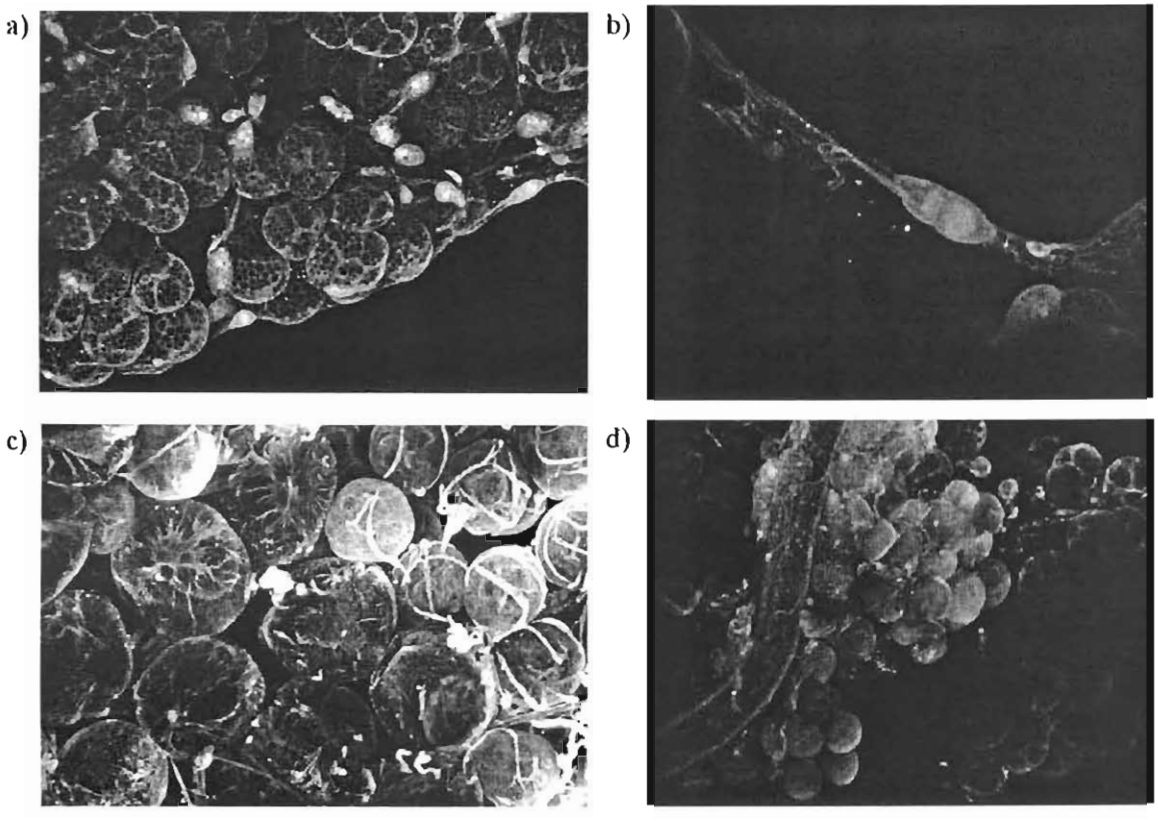

Fig. 5.18: Localization of α-tubulin to salivary gland granules. (a) Granular as well as cells from the myo-epithelial sheath are indicated. (b) A cell from the myo-epithelial sheath. (c) Agranular acini from the hard tick *Dermacentor variabilis*. (d) Agranular acini from the soft tick *O. savignyi*.

5.4 Discussion

5.4.1 Importance of the salivary glands in secretion

Tick salivary glands differentiated into highly sophisticated organs during the adaptation of ticks to a blood-feeding environment. Control of tick homeostatic volume (Sauer *et al.* 1986), secretion of cement by hard ticks (Kemp, Stone and Binnington, 1982) and proteins involved in mating (Feldman-Muhsam, 1986) can be considered as important functions performed by salivary glands. The biosynthesis, storage and secretion of bio-active compounds by feeding ticks can however, be considered as the main salivary gland function (Sauer *et al.* 1995), especially in soft ticks. For ticks to feed successfully an ample supply of feeding facilitating compounds must be available at the time of feeding (Bowman *et al.* 1997). This is especially important in the case of argasid ticks for which feeding times are relatively short (30 –60 min) and not sufficient for the induction of protein synthesis as observed for hard ticks (Fawcett, Doxley and Büscher, 1986). However, secretion of granules by the salivary glands of soft ticks seem to be very inefficient if considered that less than ~10% of a salivary gland acinus showed signs of secretion after feeding on rabbits or stimulation with chemical agonists. Only ~17% of apyrase and ~37% of the total salivary gland protein was secreted. It would seem implausible that the remaining granules are stored for future use during feeding, as the glands had recovered sufficiently a few days after feeding. The large size of the salivary glands is also totally unrelated to the amount of secretory product. In energy conservation terms this is a waste of biological resources. It can only be assumed that the tick pays this high price in order to ensure an adequate supply of anti-hemostatic factors. This again underlines the importance of the tick salivary glands in feeding and tick survival.

5.4.2 Secretory mechanisms of argasid tick salivary glands

This study did not specifically investigate the secretory mechanisms of the salivary glands. Preliminary results obtained do however suggest several possibilities. The data obtained correlate with results from studies that showed that salivary glands are not stimulated directly by cholinergic mimetics such as pilocarpine, but that this stimulation probably occurs via activation of the central nervous system (Kaufman, 1976; Kaufman and Harris, 1983). Secretion of apyrase induced by dopamine also suggests that this

adrenergic stimulant might directly stimulate salivary glands, probably through release of dopamine at the neuroeffector junction of nerves and salivary glands (Sauer, Essenberg and Bowman, 2000). In hard ticks it has been shown that dopamine can activate adenylate cyclase and PLA_2 thereby mediating the synthesis of cAMP and PGE_2 (Sauer, Essenberg and Bowman, 2000). Furtermore, PGE_2 can function as a autocrine or paracrine hormone in salivary glands that can activate the PLC pathway leading to formation of IP_3, mobilization of intra-cellular calcium and exocytosis of anti-clotting factors (Qian *et al.* 1997; Qian *et al.* 1998). It would be interesting to know whether the secretory mechanisms of hard and soft ticks differ at all. From an evolutionary viewpoint it can be predicted that these mechanisms would not differ too much, as the ancestral mite probably also secreted proteins during feeding.

5.4.3 Localization of apyrase and savignygrin

The co-localization of anti-platelet factors into specific granules suggests that other anti-hemostatic factors might be localized in the same granules. Western blot results and the high degree of localization suggest that immunolocalization was specific even though no adsorption controls were performed. Significant is the localization to dense core granules (cell type "a"). Dense core granules in other organisms are specifically involved in regulated secretion (Chidgey, 1993). It was also shown that these granules were released five minutes after the tick *O. moubata* commenced with feeding (El Shoura, 1985) implicating it in the feeding process. It has been previously shown that apyrase is secreted in tick salivary secretion after stimulation by pilocarpine (Mans *et al.* 1998a) and taken together with the results that indicate secretion of dense core granules it can be assumed that savignygrin is also secreted. The presence of a signal peptide in the sequence of savignygrin correlates with these results (Chapter 2).

The anti-hemostatic components are also localized to another granule type (cell type "b") apart from the dense core granules. The possibility that these granules may be immature forms of the dense core granules cannot be excluded. This would however, suggest a high degree of synchronization in the maturation of these granules and given the large size of these granules would seem to be unlikely. Differences in the labeling of the different

granules might be due to a higher degree of condensation inside the dense core granules that could mask the antigenic epitopes. Apyrase was labeled to a lesser extent than savignygrin that could be due to either, a lower antibody titer or a lower concentration of apyrase sequestered in the granules. Apyrase is also present at a lower concentration in the salivary gland extract (~0.7 μg per salivary gland; Mans *et al.* 1998b) compared to savignygrin (~5.0 μg per gland) and has a 9 times lower molar ratio (67 kDa: 7 kDa) compared to savignygrin. Comparisons of Western blots also show that the anti-sera directed against apyrase gave a much lower signal than that observed for savignygrin.

5.4.4 Paradoxes between light, TEM and confocal microscopy

Discrepancies were observed for the localization of savignygrin when normal immunocytochemical techniques that employ thin sections is compared to confocal microscopy that uses whole tissue. It is known that antibodies only penetrate tissue up to ~10μm during confocal microscopy. Most secretory granules are also very dense due to "condensation" of secretory proteins. Inadequate penetration of granules could thus account for labeling of only the outer surfaces of granules. Granules with dense cores can be assumed to have higher densities than homogenous granules. This could also account for labeling of only one type of granule, because penetration of the dense core granule by antibody is hindered due to high density or masked binding epitopes of the antigen. This correlates with the fact that less labeling is observed for dense core granules compared to homogenous granules as observed during TEM.

5.4.5 Thiery staining of salivary glands

Carbohydrate staining using the Thiery test showed a positive reaction with the electron lucent cores of type "c" granules. No other granule type showed any specific carbohydrate staining, but rather showed staining with the silver control. This could indicate that proteins sequestered inside these granules are not glycosylated. In contrast, the type "b" and "c" granules and the periphery of the dense core granules (type "a") in the salivary glands of *O. moubata* stained positive with the PA-TCH stain (El Shoura, 1985). Alternatively it is also possible that all the controls necessary to ensure specific carbohydrate staining were not completed in the latter study.

5.4.6 ER and Golgi apparatus in the salivary glands

The Golgi apparatus was observed in the mature granular cells of *O. moubata* (El Shoura, 1985), which indicates active biosynthesis of granule proteins. This study showed that cells with mature granules had less vesicular membrane system in contrast to cells where biogenesis of granules is still taking place. Of interest are the salivary glands of the hard tick *R. appendiculatus* where no Golgi apparatus could be observed in the "d" and "e" cells of acinus III. It was speculated that granule formation occurs directly from the endoplasmic reticulum and it was taken as confirmation that no Golgi specific glycosylation events takes place and hence the absence of positive carbohydrate staining in these granule types (Fawcett, Binnington and Voight, 1986). This observation is quite astonishing, as these are the only cells known to display this property.

5.4.7 Relationship between ER, Golgi apparatus and secretory granules

An inverse correlation between the extent of ER and the number of secretory granules was observed in secretory cells from the parotid, salivary glands and pancreas (Ghadially, 1988). It was speculated that this might either be due to the plane of sectioning or that as the granules accumulate the ER regresses. Studies on the trans-Golgi network (TGN) have shown that extensive multilayered TGN occur in cells that do not form large secretory granules, such as Sertoli cells, nonciliated cells of ductuli efferentes and spinal ganglion cells. In cells (mucous cells of Brunner's gland, pancreatic acinar cells, plasma cells, enterocytes, cardiocytes) that produce small to medium-sized secretory granules, the TGN is small. The TGN is absent in cells (secretory cells of seminal vesicles, lactating mammary glands) that form large secretory granules (Clermont, Rambourg and Hermo, 1995). Recent evidence into the nature of the Golgi complex has indeed indicated that this is a dynamic organelle not restricted to a specific morphological structure (Glick, 2000). The cisternal maturation hypothesis propose that the Golgi is a dynamic outgrowth of the ER, with ER-derived membranes coalescing into new cis-cisterna that progresses (maturates) through the different Golgi compartments until it disintegrates into transport vesicles. Experiments that inhibited ER-to-Golgi traffic caused the Golgi to collapse into the ER. Other experiments where ER exit was blocked showed that Golgi elements

disappeared in the order cis, medial, trans and when the block was released the Golgi elements reappeared in the same order (Glick, 2000). SEM, TEM and confocal microscopy in this study all showed that granular cells are filled with granules in what can be almost described as "bursting point". From this it should be clear that these cells are basically filled to capacity and as such would need some mechanism to stop granule biogenesis. It would seem logical that a removal of ER and Golgi would halt granule biogenesis. The mechanism of this process can only be speculated on. It is envisaged that the sequestration of all Golgi-network membranes into formation of granules might be part of a regulatory event in the synthesis of secretory proteins. Specific feedback mechanisms must exist that would down regulate protein synthesis and granule biogenesis when granule formation has been saturated.

5.5 Conclusions derived from this study

Apyrase and savignygrin were localized to two types of granules (type "a" and type "b"). Type "b" cannot be distinguished on a morphological or histochemical basis from another cell type (type "d") that did not show any labeling. Localization of savignygrin using immunofluoresent confocal microscopy also suggests that there might be another granular acini not previously recognized. This data imply that the morphological and histochemical classification of salivary gland cell types should be approached with caution, as granules with the same appearance do not necessarily have the same protein expression patterns. New schemes of classification should rather consider the specific composition of the granules in terms of the proteins expressed in specific cell types. This urges for a more thorough investigation of granule composition, a task that might be accomplished by the new field of proteomic analysis (Wilkins *et al.* 1997).

5.6 Salivary glands, toxins and granule formation

The large size of the granules and their dense packing in the salivary glands stimulated our interest into the processes by which these granules might form. The next chapter deals with this phenomenon and identifies possible candidates that might be involved in the process of granule biogenesis. It also looks into the nature of toxicity described for this tick species. *O. savignyi* has been implicated in pathogenesis of domestic animals,

initially thought to be due to exsanguination of the host. However, it was shown that death could be due to toxic components present in tick salivary gland secretions and a toxic protein and a non-toxic homologue has been purified (Howell, 1966b; Neitz, Howell and Potgieter, Howell, Neitz and Potgieter, 1975). Conflicting reports indicated molecular masses of 15400 Da or 6346 Da, determined by sedimentation equilibrium centrifugation or based on amino acid composition, respectively (Neitz, Howell and Potgieter, 1969; Neitz *et al.* 1983). The toxin also eluted at a position similar to that of the savignygrins during AEHPLC (Neitz, 1976). The low molecular mass reported as well as the behaviour during ion exchange suggested that the savignygrins might be the toxin previously described. It made sense that the savignygrins might have been toxic as some members of the BPTI-family are neurotoxic (Dufton, 1985). The possible toxicity of savignygrin was thus investigated. While it was eventually shown that the savignygrins are not the toxins, a firm belief was established that although specific toxic activities are present in the salivary glands, toxicity was of secondary function and that the toxins might have other more benign functions, such as a role in granule biogenesis.

Chapter 6: Major salivary gland proteins from the tick *O. savignyi* function as toxic and granule biogenic proteins*

*Part of this chapter has been published in Electrophoresis (Mans *et al.* 2001) and Toxicon (Mans *et al.* 2002)

6.1 PART 1: THE SECRETORY PATHWAY

6.1.1 Targeting of secretory proteins to the secretory pathway

All tick secretory proteins have to enter the secretory pathway. The conventional pathway of protein secretion starts with targeting to the endoplasmic reticulum (ER), vesicular transport to the Golgi-apparatus and shuttling through the Golgi compartments to the trans-Golgi network (TGN), where sorting of proteins to their various destinations takes place (Arvan and Castle, 1998). Secretory and plasma membrane proteins are sorted to vesicles that are continuously secreted (constitutive pathway). This anterograde movement up the secretory pathway is considered to occur by default for all proteins that do not contain any other targeting signals to other cellular compartments. Secretory proteins with the correct sorting signals may also be packaged into regulated secretory granules or sorted to endosomal organelles such as lysosomes (Kelly, 1985; Chidgey, 1993; Blazquez and Shennan, 2000).

6.1.2 Targeting to the ER and Golgi-apparatus

All proteins destined for secretion, sub-cellular organelles or the plasma membrane have an N-terminal signal peptide that targets it to the ER during protein translation (Nielsen *et al.* 1997). The common structure of signal peptides from eukaryotic proteins includes a positively charged n-region (only slightly arginine rich), followed by a hydrophobic h-region (short, very hydrophobic) and a neutral but polar c-region. The (-3, -1)-rule states that the residues at positions –3 and -1 (relative to the cleavage site) must be small and neutral for cleavage to occur correctly (von Heijne, 1990). The signal peptide ensures translocation across the ER-membrane and after translocation is cleaved off by a signal peptidase. In the ER, chaperone assisted folding occurs as well as the formation of disulphide bonds. While disulphide bonds are absent in cytoplasmic proteins, most of the

cysteines present in secretory proteins are disulphide bonded and function as a stabilizing force in the protein's structure (Fahey, Hunt and Windham, 1977). N-glycosylation occurs in the ER and is involved in correct protein conformation folding. A C-terminal retention signal (KDEL) is present in resident ER proteins and ensures retention in the ER and retrieval from the cis-Golgi, if ER-proteins escape the ER (Nilsson and Warren, 1994). Non-resident proteins are transported via COPII coated vesicles to the Golgi apparatus (Chidgey, 1993; Blasquez and Shennan, 2000). In the Golgi apparatus O-linked glycosylation can occur, while sorting of proteins to their different cellular destinations takes place in the TGN. There are three pathways by which proteins are targeted: constitutive, regulatory and lysosomal (Kelly, 1985).

6.1.3 The constitutive and regulated secretion pathway

Constitutive secretion is ubiquitous in all cells and considered to be the bulk-flow pathway of secretion, which secretes proteins without distinction. The secretory vesicles are normally small, electron lucent and characterized by uninterrupted secretion. Proteins secreted are normally plasma-membrane proteins or proteins secreted at a constant level. The regulatory pathway is limited to endocrine, exocrine and some neuronal cells. The vesicles that the proteins are packaged into are large, electron dense and are referred to as secretory granules. Secretion only takes place upon stimulation by a pharmacological agent (Chidgey, 1993: Urbé, Tooze and Barr, 1997; Arvan and Castle, 1998; Tooze, 1998; Glombik and Gerdes, 2000). As such, tick salivary glands can be described as exocrine glands that undergo regulated secretion during feeding. There is a selective sorting of regulated secretory proteins to granules and exclusion of those not involved, in contrast to the indiscriminate bulk-flow of the constitutive pathway (Urbé, Tooze and Barr, 1997). No specific signal sequence for regulatory secretion has been identified to date, due to the lack of sequence homology between secretory proteins. It has been suggested that targeting signals may be comprised of surface epitopes rather than being sequence specific (Chidgey, 1993). Currently two possible targeting mechanisms are considered.

6.1.4 "Sorting for entry" or "sorting by retention"

During "sorting for entry", proteins are selected in the TGN prior to immature secretory granule (ISG) formation, while "sorting by retention" indicate selective retention of granule specific proteins in the ISG and removal of mis-sorted proteins from the ISG (Arvan and Castle, 1998).

6.1.5 Aggregation as a means of sorting

The most characteristic feature of the regulated secretory pathway is the high concentration of secretory proteins and their aggregation into dense core granules. This process has been referred to as concentration, multimerization, polymerization and condensation. This part of the formation of granules (condensation of soluble secretory proteins into large aggregates) will henceforth be described as granule biogenesis. These interactions seem to reflect progressive protein insolubility that limits the ability of proteins to escape from the maturing granule (Arvan and Castle, 1998). A high local concentration of secretory proteins in the TGN is necessary for efficient aggregation, so that soluble secretory proteins are generally very abundant in cells with a regulated secretory pathway (Urbé, Tooze and Barr, 1997). Specific proteins are involved in granule biogenesis by sorting of other secretory proteins to the regulated secretory granules by co-aggregation (Arvan and Castle, 1998). These proteins have been identified in most endocrine and exocrine cells. They are present in high abundance, have acidic iso-electric points and can aggregate under conditions of mild acidity (pH5-6) and high calcium concentrations (50-100 mM), the conditions thought to be present in the TGN (Huttner, Gerdes and Rosa, 1991; Urbé, Tooze and Barr, 1997; Blasquez and Shennan, 2000).

6.1.6 Granule biogenesis in tick salivary glands

In the soft tick *Ornithodoros moubata*, dense core granules were shown to be secreted within five minutes after attachment (El Shoura, 1985) suggesting that these granules are intracellular stores of bioactive components. Such dense core granules are known to be universal among regulated secretory cell types (Arvan and Castle, 1998). One specific characteristic of granule biogenic proteins is their unusual abundance. In this study,

proteins from tick salivary glands were identified as potential proteins involved in granule biogenesis based on their high abundance and are referred to as tick salivary gland proteins (TSGPs). A study of granule contents could provide important information on proteins involved in granule biogenesis and could aid the understanding of the observed diversity in the number of different granular cell types observed for tick salivary glands. Disruption of granule formation and subsequent secretion of granule contents could be an efficient strategy to control tick feeding.

6.1.7 Granule biogenesis and tick toxicoses

During the investigation into the toxicity of savignygrin and the characterization of the TSGPs, the surprising discovery was made that some of the TSGPs are the toxins previously described for the tick *Ornithodoros savignyi*. Therefore, a brief review of tick toxicoses is imperative.

6.2 PART 2: TICK TOXINS

6.2.1 Tick toxicoses

Certain tick species can cause pathological changes in their host by inoculation of non-infectious components during feeding. Tick toxins have been identified in whole tick extracts, salivary gland secretions (SGS), SGE and tick eggs. Toxins can be a natural tick product that is either in itself toxic or is transformed into a toxic component in the host, or toxins are derived from breakdown of host tissue or are a product of a symbiotic organism in the tick (Gregson, 1973). Various other possibilities have also been reviewed (Neitz *et al.* 1983). While, arthropods such as spiders and scorpions are notoriously venomous organisms that utilize their toxins for protection as well as predation, the advantages of ticks being toxic is unclear. It has been suggested that tick paralysis may be a vestigial function conserved in ticks, when ticks evolved a parasitic lifestyle (Stone *et al.* 1989). Paralysis toxins have been attributed with functional significance during feeding of the tick, in that host mobility and grooming is impaired. Paralysis would also affect the respiratory system leading to heightened breathing rates and an increase in carbon dioxide expiration. This together with pheromone secretion could attract ticks to

the paralyzed animal, which accelerates the finding and feeding of ticks. It has been argued that this might be true for most ticks, even though no clinical symptoms can be observed in the majority of feeding events (Gothe, 1983). Toxins might also exert local anaesthesia, prevent blood coagulation or act as a general feeding stimulant (Stone *et al.* 1989). A role as a regulator of protein synthesis has also been suggested for the paralysis toxin from *R. evertsi evertsi*, based on localization to chromatin in the nuclei (Crause *et al.* 1993).

6.2.2 Toxicoses from an evolutionary perspective

Another consideration is whether tick toxins have a common ancestor shared with toxins from other toxic arthropods, as this would assign biological significance or function to tick toxins. Toxins might also have specific functions related to their toxicity that was specifically acquired during adaptation to a blood-feeding environment. Toxicity could also be a byproduct of proteins being in a novel environment and recognition of host targets, a chance event. To investigate these possibilities, it is important to clearly delineate various forms of toxicoses and find their shared properties or differences (mechanism of pathogenesis, homology), as this will give valuable information as to their origins. Such comparative studies are the one way in which a holistic view of tick toxicoses will be attained.

6.2.3 Tick paralysis

The most important tick toxicoses for veterinary and human medicine are tick paralysis (Gothe and Neitz, 1991). Of the approximately 869 tick species, paralysis has been described for 55 hard ticks and 14 soft ticks (Gothe, 1999). However, for many of these species only a few, often inadequate or dubious records regarding the actual toxicity exist in the literature. The most important include the hard ticks *Ixodes holocyclus* (Australia), *Dermacentor andersoni*, *D. variabilis* (North America), *I. rubicundus* and *Rhipicephalus evertsi evertsi* (South Africa). Soft ticks for which paralysis has been described, demonstrated or suspected include *Argas walkerae*, *O. capensis*, *O. savignyi*, *Otobius megnini* (South Africa) and *O. lahorensis* (Eurasia). In all ticks that induce paralysis the secretion of neurotoxin coincide with a definite repletion phase. For *R. evertsi evertsi*

paralysis, toxicity is associated with a short period between day 4 and 5 of feeding and a specific body mass of 15-21 mg (Gothe and Lämmler, 1982; Neitz and Gothe, 1986). Paralysis induced by the tick *I. holocyclus* only set in after 4-5 days of feeding, while paralysis for *D. variabilis* is only detected after approximately 6-8 days after attachment (Gregson, 1973; Masina and Broady, 1999). In the soft tick *A. walkerae*, it is only larvae that cause paralysis, which occurs after 5-6 days of feeding (Gothe, 1983; Gothe and Neitz, 1991). In all instances, paralysis coincides with the rapid engorgement phase that is marked by the production and secretion of numerous protein products by the salivary glands.

6.2.4 Pathogenic mechanisms of tick paralysis toxins

Paralysis is normally exhibited as an ascending flaccid tetraplegia, due to an impaired nervous system (Gothe and Neitz, 1991). While these are general observed symptoms, most neurotoxins have specific characteristics not necessarily shared with toxins from other tick species.

6.2.5 *Dermacentor andersoni*

D. andersoni affects motor neurons of the efferent pathway and not the afferent. The neuromuscular junction of peripheral nerves is targeted through inhibition of acetylcholine release from the synapse, suggesting a pre-synaptic target (Gothe and Neitz, 1991). Feeding ticks affect dogs, sheep, cattle, guinea-pigs, hamsters and man, but not cats, rabbits, rats and mice. In those animals affected the symptoms could be fairly rapidly reversed on removal of ticks, except for marmots that frequently do not recover (Emmons and McLennan, 1980). Gross symptoms of paralysis in marmots include the loss of the animals normal piercing cry (paralysis of the vocal cords) followed by an ataxia and weakness of the hind limbs. The condition progressess until the fore limbs are paralyzed and the animal is unable to move and lie on its side. There is retention of urine and faeces (Emmons and McLennan, 1980). No paralysis could be observed when SGE from fast feeding ticks were injected subcutaneously into mice and lambs and intraspinally into puppies (Gregson, 1943). Fractionated extracts also failed to produce any symptoms. However, paralysis was observed when saliva from fed females was

continuously injected subcutaneously into marmots and hamsters (Gregson, 1973). Variation in the ability of individual ticks to cause paralysis was also observed. This highlights the problems associated with paralysis from *D. andersoni*. It also points out why progress on this specific toxicoses has been so slow in recent years. No development of immunity has yet been reported for *D. andersoni*, while immunity to the holotoxin from *I. holocyclus* is well established. Hyper-immune serum against holotoxin also fails to relieve *D. andersoni* paralysis (Gregson, 1973).

6.2.6 *Ixodes holocyclus*

I. holocyclus can paralyze dogs, cats, cattle, horses and humans. Only adult ticks have been associated with paralysis, while larvae only causes local irritation. SGE affects dogs and mice, although only suckling mice (4-5g) are generally affected, while adult mice (20-25g) do not show paralysis symptoms (Stone and Binnington, 1986). An increase in blood pressure occurs during paralysis, in contrast to paralysis caused by *D. andersoni* where blood pressure stays normal. Purification attempts of the neurotoxin from *I. holocyclus* showed that the paralysis toxin was associated with high molecular mass complexes (40-80 kDa) (Masina and Broady, 1999). A toxic lethal fraction (Mr<20 kDa) without paralyzing activity was also identified in *I. holocyclus* and it was suggested that this might be the agent of cardiovascular failure previously attributed to holotoxin (Stone, Doube and Binnington, 1979). Recently this toxin was purified and cloned and was shown to have a molecular mass of ~5 kDa which binds to rat synaptosomes in a temperature dependent manner (Thurn, Gooley and Broady, 1992). This temperature dependence coincides with earlier observations that there is a temperature-dependent inhibition of evoked acetylcholine release during paralysis (Cooper and Spence, 1976).

6.2.7 *Rhipicephalus evertsi evertsi*

R. evertsi evertsi affects the peripheral nervous system by inducing a motor polyneuropathy in sheep and is appropriately known as spring lamb paralysis (Gothe and Kunze, 1982). Ticks fed on laboratory animals affected mice, rats, hamsters, guinea pigs and rabbits only slightly or not at all (Gothe and Lämmler, 1982). Injection of SGE into sheep, mice and chickens, failed to elicit a paralysis response (Viljoen *et al.* 1986). A

very sensitive *in vitro* assay using a sciatic nerve -gastrocnemius muscle preparation was developed to characterize this toxin (Viljoen *et al.* 1986). In this assay the dissected nerve was bathed with SGE or purified neurotoxin in a specially constructed nerve bath with a volume of 60 µl. In contrast to the *in vivo* tests, both SGE and neurotoxin preparations effectively paralyzed muscle contraction (Viljoen *et al.* 1986;. Crause *et al.* 1994). It could thus be argued that the neurotoxin affects the nerve and not the neuromuscular junction. Large quantities of SGE (400-900 mg protein) were however used to elicit a response and it could be argued whether this was a truly specific response. However, total inhibition of nerve impulse propagation was observed with purified preparations (74µg/ml), which is probably much closer to physiological conditions (Viljoen *et al.* 1986). The toxin from *R. evertsi evertsi* that purified as a ~68 kDa protein (Viljoen *et al.* 1986), was later shown to be the trimeric form of a ~20 kDa protein (Crause *et al.* 1994). A monoclonal antibody directed against this toxin showed cross-reactivity with both non-paralysis (*R. appendiculatus*, *Hyalomma marginatum rufipes*, *Boophilus decoloratus* and a non-paralysing strain from *R. evertsi evertsi*) as well as paralysis-inducing ticks (*I. rubicundus*, *A. walkerae* and a paralysis-inducing strain of R. *evertsi evertsi*). Significant was the fact that only paralysis-inducing ticks seem to posses a ~68 kDa reactive antigen (Crause *et al.* 1994).

6.2.8 *Argas walkerae*

Electromyographical studies indicated that the fast conducting nerve fibers of the peripheral nervous system were affected and the paralysis was classified as a motor polyneuropathy that does not affect the afferent paths (Gothe *et al.* 1971; Gothe and Kunze, 1971; Kunze and Gothe, 1971; Gothe and Neitz, 1991). The toxin seems to affect the liberation of acetylcholine as well as its receptor's sensitivity at the myoneural synapse (Gothe and Neitz, 1991). The monoclonal antibody directed against the toxin from *R. evertsi evertsi* also recognized protein complexes of molecular mass 60-70 kDa from crude *A. walkerae* extracts and prevented paresis of day old chicks (Crause *et al.* 1994). The toxic fraction was purified using a bioassay based on injection of day old chicks. The purified fraction showed two bands, with molecular masses of 32 and 60 kDa, using reducing SDS-PAGE, while one band (pI~4.5) was obtained with iso-electric

focusing. Macromolecular complexes (80-100 kDa) were observed using size exclusion chromatography (Viljoen *et al.* 1990). Recently, a monoclonal antibody directed against the toxin from *R. evertsi evertsi*, was used in an attempt to purify the neurotoxin from *A. walkerae* extracts and whilst a 68 kDa toxin was detected using western blot analysis, a 11 kDa protein was purified that showed cross-reactivity with the mAb using enzyme linked immunosorbent assay (ELISA), although not being detected during western blot analysis (Maritz *et al.* 2000). Crude *A. walkerae* larval extracts inhibited potassium stimulated and veratridine evoked release of [^{3}H] glycine from rat brain synaptosomes, suggesting that the toxin might be targeting ion channels involved in depolarization (Maritz *et al.* 2001). These conflicting results between purification by bio-assay and detection with a monoclonal antibody have not been resolved yet.

6.2.9 Common ancestors for paralysis toxins

There is no consensus yet whether the paralysis toxins from different species are homologs. Based on sequence similarity of holotoxin with scorpion toxins (data not yet published) it was speculated that other paralysis toxins from ticks might also be related (Masina and Broady, 1999). On the other hand, insect neurotoxins from predatory mites, *Pyemotes tritici* (Superorder: Acariformes) have been shown to be unique with molecular masses of ~30 kDa (Tomalski and Miller, 1991; Tomalski *et al.* 1993). Toxins from different arachnid subclasses (spiders and scorpions) also do not all fall into the same protein families (Mênez, 1998; Escoubas, Diochot and Corzo, 2000; Rash and Hodgson, 2002). Ticks are also more closely related to the ricinulei (tick-like spiders) and spiders, than scorpions (Lindquist, 1984; Schultz, 1990). The conclusion derived from this is that evolutionary relationships between toxins from the different arthropod classes cannot yet be inferred with certainty.

6.2.10 Other forms of toxicoses considered as non-paralytic

The fact that some forms of tick toxicoses are considered to be non-paralytic indicates that a study into the toxic mechanisms of ticks should take this into account. If toxicoses can be shown to clearly differ in their mechanisms of action, it would provide a specific reference point in cataloging the different toxicoses forms.

6.2.11 Toxins from tick eggs

It has been shown that tick egg extracts from 17 ixodid species are toxic, while extracts from 5 argasids species were not (Riek, 1957). Egg toxins are interesting due to their possible relationship with tick paralysis and other tick toxicoses. They have been studied in various species (*A. hebraeum, R. eversti evertsi, H. truncatum, B. microplus, B. decloratus*) (Neitz *et al.* 1981; Viljoen *et al.* 1985). The toxin from *A. hebraeum* exhibits protease inhibitory activity. After injection with crude extracts, guinea-pigs showed several symptoms: hyperaestasia, serous nasal and eye discharge accompanied by conjunctivitis and rhinitis, ascending paresis and a loss of voice over a 15-36 hour period. Pathology included necrosis of the liver and oedema of the urinary bladder, lungs and skin (at the site of injection). Lesions were probably all of vascular origin. The toxin had a molecular mass of ~10 kDa and a pI ~7.5-8.5 (Neitz *et al.* 1981). Egg extracts and purified fractions from *R. evertsi evertsi*, *H. truncatum*, *B. microplus* and *B. decloratus* all induced anorexia and severe hyperaestasia, hyperaemia of the skin, muco-purulent occulo-nasal discharge, mucoid diarrhea which prior to death become haemorrhagic. Only partial paresis was observed. The egg toxins differed in molecular mass: 27-40 kDa for *H. truncatum*, *B. microplus* and *B. decloratus* and ~5-6 kDa for *R. evertsi evertsi*. The *R. evertsi evertsi* toxin also had a lower pI (~6) compared to the other toxins (8.3-9.3) (Viljoen *et al.* 1985). This indicates that the toxic entities in *R. evertsi evertsi* salivary gland and egg extracts are different molecular entities.

6.2.12 Sweating sickness caused by *Hyalomma truncatum*

Sweating sickness affects especially young calves and this disease is widely distributed in central, eastern and southern Africa. Lethal, as well as two milder forms, Mhlosinga and Magudu occur and are associated with sweating sickness-inducing (SS+) strains of *H. truncatum*, while non-inducing strains (SS-) also exist (Neitz, 1962). Symptoms include fever, eczema and anorexia. Removal of ticks results in immediate recovery and salivary gland secretions have been implicated in the disease, suggesting the presence of a toxin (Neitz, 1959). Analysis of anti-sera raised against SS+ and SS- forms shows the presence of at least four novel antigens in SS+ salivary gland extracts, which might be associated with toxicity (Burger *et al.* 1991).

6.2.13 Sand tampan toxicoses

O. savignyi causes death of domestic animals, especially young calves and lambs. While death has been attributed to exsanguination (Howell, Neitz and Potgieter, 1975), the presence of a proteinaceous toxin in SGS, SGE and larval extracts of *O. savignyi* has been described. Toxic activity has not been found in coxal secretions or tick eggs, in contrast to eggs from hard ticks (Neitz, Howell and Potgieter, 1969; Neitz *et al.* 1983; Howell, Neitz and Potgieter, 1975). An acidic toxin has been purified and characterized in terms of molecular mass (15400 Da) and N-terminal sequence (Neitz, Howell and Potgieter, 1969; Neitz *et al.* 1983).

6.2.14 Pathogenesis of sand tampan toxicoses

A summary of the only report compiled yet on the symptoms produced by sand tampan toxicoses (C.J. Howell, unpublished research report, Onderstepoort Veterinary Research Institute, South Africa, 1969) follows:

(1) "A Fries bull of 14 months (300 kg) was confined to a tampan infested camp where it was tethered to a tree for two hours daily. The animal remained in a standing position while in the camp and died shortly after removal on day four (8 hours exposure). All bites were confined to the legs of the animal. No clinical signs of ill-health were observed during this period and only on day four, immediately after leaving the infested camp, did the animal appear in a state of shock prior to sudden collapse and death. Pathology showed edema in the myocardium, integument, intestinal tract, lungs, regional lymph glands and kidney. Eosinophilic granules were observed in the capillaries of the brain, myocardium, kidneys and adrenal glands. Degeneration of the myocardium and extensive necrosis, hemorrhage, congestion and edema of the epidermis and petechial hemorrhages in the lungs were also observed. The animal possibly died of heart failure, although the basic lesions are probably due to an increased vascular permeability.

(2) An adult merino wether (40 kg) was injected subcutaneous (2.5ml ~58 mg per subcutaneous site) with 12.5 ml of SGS over a period of 4 hours. Two and a half hours after the final injection the animal lied down, whereupon it died

immediately. No clinical symptoms were observed up to this time, although pathological and histological changes were extensive. Congestion and edema were observed in myocardium, spleen, kidney, lungs and lymph glands. An increased vascular permeability that possibly resulted in a severe degeneration and necrosis of the capillary vessel walls was observed in the integument and subcutaneous region."

(3) "Subcutaneous injection of SGS (100 µl~2.3 mg), into albino rats, caused facial irritation exhibited by rubbing of the face. A clear mucoid substance was discharged nasally after some hours, which soon became hemorrhagic. By this time there were signals of impaired breathing and the rats assumed an upright stance before becoming comatose, after which they never recover. Increasing the dosage rate leads to less symptoms and a more rapid mortality. Pathological changes include congestion, edema and emphysema of the lungs.

(4) The feeding of three ticks on a guinea pig were enough to cause mortality with no symptoms being observed before death (Howell, Neitz and Potgieter, 1975). Pathological changes are confined to the lungs and vascular system and include congestion, edema and hemorrhages.

(5) Subcutaneous injection of mice with SGS resulted in rapid death with few symptoms. Some animals appear completely normal until death, which proceeds swiftly. Some mice may jump in the air and immediately die with a few convulsive movements. Other mice appear slightly ruffled soon after injection, with accelerated breathing, which soon becomes labored, followed by animals reeling drunkenly about for a few seconds before dying after a few convulsive movements. Symptoms for the latter mice suggest respiratory failure, as the heart is still active after all respiratory movement has ceased. No pathological symptoms could be observed." Feeding of one tick on a 20-24g mouse is sufficient to cause death within 30 minutes (personal observation).

The present study characterizes these toxic activities in terms of cardio-toxicity and shows that tick paralysis is not associated with the pathology induced by *O. savignyi*.

Successful neutralization of toxic activities could relieve the burden that these ticks place on their domestic hosts.

6.3 Materials and methods

6.3.1 Two-dimensional polyacrylamide gel electrophoresis

SGE (~120 µg/ 10 µl) were prepared in water and diluted into 100 µl sample buffer (8M urea, 2% CHAPS, 2% IPG-buffer pH 3-10NL, 0.3% DTT) and applied to IPG strips, 3-10NL (non-linear) using the Immobiline® DryStrip Reswelling Tray (Sanchez *et al.* 1997). The Multiphor II system (500V for 10 min, 1500V for 4 hours at 10W) was used for iso-electric focusing (first dimension), under conditions recommended by the manufacturers (Amersham Pharmacia Biotech, Uppsala, Sweden). The second dimension was performed using a vertical 16% tricine SDS-PAGE system (Schägger and von Jagow, 1987). SDS-PAGE analysis without prior iso-electric focusing was performed with 16% tricine SDS-PAGE or 12% glycine SDS-PAGE (Laemmli, 1970). Gels were stained with Coomassie Brilliant Blue G250.

6.3.2 Isolation of salivary gland granules after dispase treatment

Due to the fact that no homogenous preparation of salivary gland granules could be obtained with collagenase digestion (Chapter 5), a new fractionation process was developed using dispase digestion. Salivary glands were dissected and a granule fraction was prepared by digestion with dispase (20 mM Tris-HCl, 0.15 M NaCl, 5 mM $CaCl_2$, 5 mM $MgCl_2$, pH 7.2, Roche Diagnostics) for 3 hours at 37 °C. After centrifugation (100xg, 10 min, room temperature), the pellet was layered onto a preformed Percoll density gradient (70% initial concentration). After density gradient centrifugation (180xg, 15 min, room temperature), visible bands (density ~ 1.14 g/ml) were processed for electron microscopy analysis.

6.3.3 Electron microscopy and X-ray microanalysis of granules

Granules were prepared for electron microscopy as described for platelets (chapter 2). For X-ray microanalysis, whole salivary glands were frozen in propanol, cooled with liquid nitrogen and lyophilized. Analysis was performed under low vacuum on uncoated

glands with a JEOL 5800LV SEM (0.3 Torr, 25 kV) by focusing (3 μm window) on visible granules beneath the cell membrane. Data were collected on a Noran Voyager ED System from four randomly selected granules with 7 μm diameters.

6.3.4 Reconstituting the conditions present in the *trans*-Golgi network (TGN)

Conditions thought to exist in the TGN include a mildly acidic pH and the presence of Ca^{2+} (Arvan and Castle, 1998). It has been shown that proteins targeted to secretory granules can aggregate under these conditions (Colomer, Kickska and Rindler, 1996). Salivary gland extracts (1SG/10μl or ~6mg/ml protein), prepared in water, centrifuged (14000xg, 25 min) and filtered through 0.22 μm filters, were diluted in a high Ca^{2+} buffer (20mM MES, 50 mM $CaCl_2$) and titrated to different pH values with HCl before incubation at 4 °C for 30 minutes. Extracts were centrifuged at 14000xg in a microcentrifuge for 25 minutes at room temperature. The supernatants were removed and precipitated protein washed twice in 1 ml of dilution buffer and recentrifuged before SDS-PAGE analysis.

6.3.5 Purification of the TSGPs

Tick salivary gland extract (60 glands, ~3600 μg) was prepared in 1 ml buffer A (20 mM Tris-HCl, pH 7.4) and were heat treated (60 °C, 5 minutes), as this is known to remove most proteins with molecular masses greater than 20 kDa (Fig. 6.4). Denatured protein was removed by centrifugation (10 min, microcentrifuge) and the supernatant was filtered through a 0.22 μm filter (Millipore Corporation, Bedford, Massachusetts) before application to AEHPLC as described in Chapter 2. Alternatively, supernatant was applied to a cation exchange column (CEHPLC) (SP-5PW, 7.5 mm x 7.5 cm, TosoHaas) using the same conditions as for AEHPLC. Fractions from AEHPLC were adjusted to 1.7 M ammonium chloride and applied to a hydrophobic interaction column (HIHPLC) (TSK-Phenyl-5PW, 7.5 mm x 7.5 cm, Bio-Rad, Richmond, California). Fractions were eluted with a gradient of buffer A (20 mM Tris-HCl, 1.7M NH_4Cl, pH 7.4) and buffer B (20 mM Tris-HCl, pH 7.4) from 0-100% over 15 minutes. Fractions from CEHPLC and HIHPLC were desalted using RPHPLC as described (Chapter 2). Elution was achieved with a gradient of buffer A (0.1% TFA, 0.1% acetonitrile) and buffer B (0.1% TFA, 60%

acetonitrile) from 0-100% over 5 minutes. SEHPLC was performed using isocratic conditions (SEHPLC buffer) with a flow speed of 0.5 ml/min (Mans *et al.* 1998b). In all cases 1ml fractions were collected and 200μl were injected subcutaneous to monitor toxic activity. Adult Balb/c mice (8-11 weeks old, ~20-24g) were used and survival was monitored over a period of 48 hours (Neitz, Howell and Potgieter, 1969). Injections were performed in duplicate.

6.3.6 Characterization of TSGPs

Proteins were quantitated with amino acid analysis, alkylated, N-terminally sequenced, molecular masses determined using tricine SDS-PAGE, MALDI-TOF-MS and ESMS as described in Chapter 2. Peptide mass fingerprinting was performed as described previously.

6.3.7 The effect of SGE on an isolated rat heart perfusion system

An adult Sprague-Dawley rat was anaesthetized with sodium pentobarbitone. The heart was dissected on ice using Tyrode buffer (5.4 mM KCl, 137.6 mM NaCl, 1.8 mM $CaCl_2$, 1.0 mM $MgCl_2$, 5.0 mM Glucose, 11.6 mM HEPES, pH 7.4). The dissected heart was coupled to a reverse Langendorf perfusion system and was perfused at 37°C with Tyrode for 30 minutes until a stable heartbeat was obtained. SGE (10 glands diluted into 10 ml Tyrode buffer: 60 μg protein /ml) was then injected into the flow stream. Experiments were performed in duplicate with different salivary gland preparations.

6.3.8 The effect of toxic fractions on mouse ECG patterns

Female Balb/c mice were anaesthetized with sodium pentobarbitone (6%) solution and electric leads were connected to the left forepaw and right-hindpaw, with the earth lead to the left-hind paw. Mice were monitored until a stable ECG pattern was observed before toxic fractions (200 μl) were injected intra-peritoneal. The ECG pattern was monitored until cardiac seizure was observed.

6.4 Results

6.4.1 Identification of major salivary gland proteins

Putative proteins involved in granule biogenesis were identified by proteome analysis of SGE from *O. savignyi*. Two-dimensional analysis indicated the presence of at least 8 major proteins in salivary gland extracts from *O. savignyi* (Fig. 6.1). Four were identified as major tick salivary gland proteins (TSGPs), based on their high abundance and similar molecular mass (~20 kDa). It was hypothesized, that proteins with similar molecular masses might belong to the same protein family and would thus be suitable candidates for the study of gene duplication in tick salivary gland proteins. Analysis of the TSGPs shows molecular mass differences in decreasing order: TSGP1>TSGP4>TSGP3>TSGP2. This together with tricine SDS-PAGE and MALDI-MS were used to identify the respective purified proteins as TSGPs.

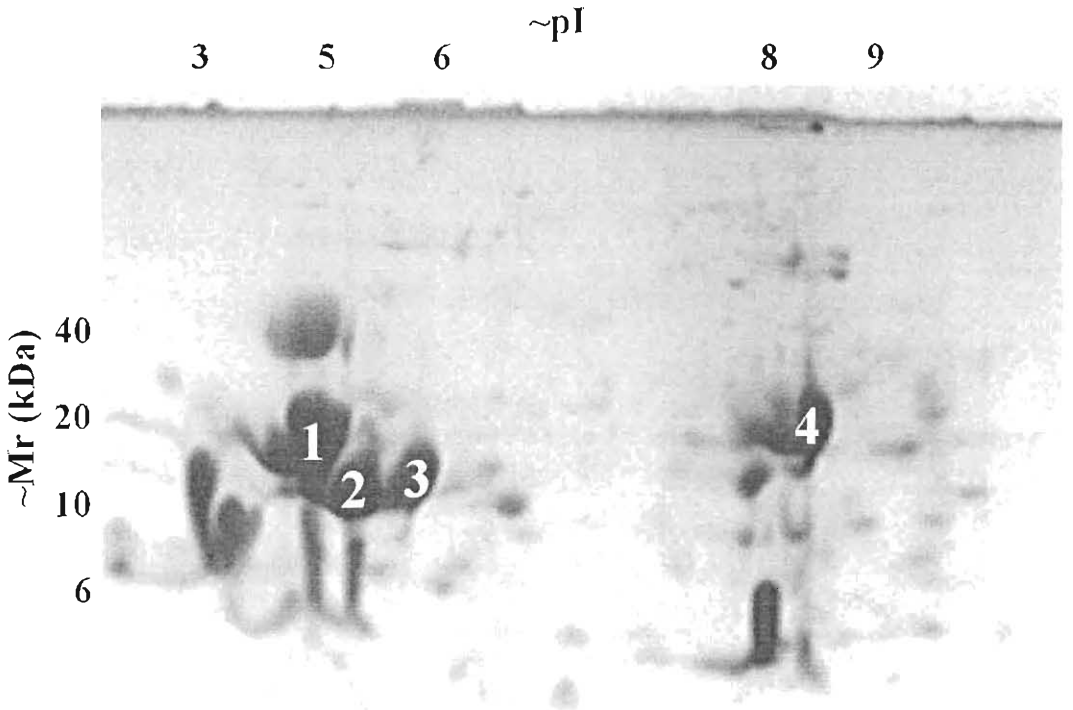

Fig. 6.1: The proteome of tick salivary gland extract. Highly abundant proteins characterized in this study are numbered (TSGP1, TSGP2, TSGP3, TSGP4). Approximate molecular masses and pI's are indicated.

6.4.2 Purification of dense core granules

While SGE can be considered to be representative of the proteins in the salivary glands, confirmation of the abundance of TSGPs in granule preparations was also required. Digestion of salivary glands with dispase and subsequent density centrifugation resulted in a homogenous preparation of dense core granules (Fig. 6.2a-c). Compared to density markers these individual granules had a density of ~1.14g/ml. Analysis of dense core granule showed enrichment of the TSGPs (Fig. 6.2d). The identity of the proteins present in the dense core granules were confirmed by two-dimensional electrophoresis, where they gave a similar electrophoretic pattern as observed in Fig. 6.1 (results not shown).

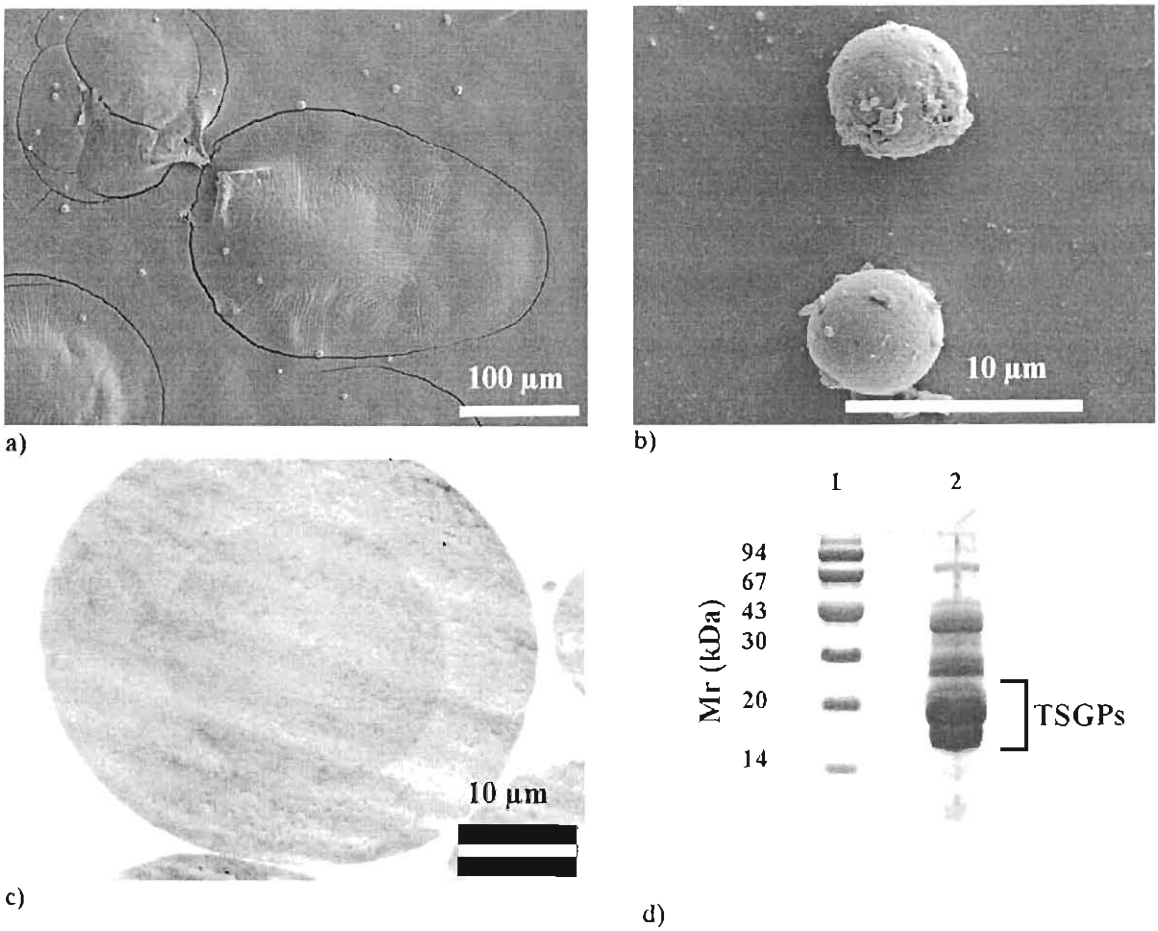

Fig. 6.2: Purification of dense core granules. (a) SEM of a granule preparation after dispase treatment and density gradient centrifugation. (b) An enlarged view of the granule preparation. (c) TEM of the dispase granule preparation, indicating a dense core granule. (d) Tricine SDS-PAGE analysis of a granule preparation.

6.4.3 Aggregation of proteins in acidic medium with high calcium concentration

High calcium concentrations (10-100mM) have been identified as a feature of secretory granules (Huttner, Gerdes and Rosa, 1991; Urbé, Tooze and Barr, 1997; Blasquez and Shennan, 2000). To confirm this in tick salivary glands, calcium was determined by X-ray microanalysis. Granules have calcium concentrations (0.3%-0.8%), which are similar to those of sodium (0.4-0.7%) and chloride (0.5-0.7%). The absence of potassium was notable (Fig. 6.3a). The granules thus have higher calcium concentrations than normally found in the cytoplasm (sodium-10 mM, chloride-8 mM, calcium-0.001 mM, potassium-155 mM), and are closer to what is predicted for the TGN (calcium-10 mM). With a granule density of 1.14g/ml and the elements expressed as a percentage weight basis, then calcium, sodium and chloride concentrations might be as high as 85-227 mM, 199-348 mM and 161-225 mM, respectively.

Secretory proteins aggregate under acidic conditions and high calcium concentrations normally associated with the TGN (Arvan and Castle, 1998). Under these conditions enrichment of specific proteins is evident in precipitated aggregates. Proteins that have equal densities are only found in the supernatant (Fig. 6.3b). The relatively low amounts of protein that precipitated during high calcium and acidic pH could be due to inadequate conditions that do not truly resemble that of the tick TGN or granule. The low concentration of the salivary gland extract (6mg/ml) could also be too dilute for adequate aggregation. Higher concentrations, on the other hand, could lead to non-specific association. Specific aggregation under these conditions was however, observed and it was decided to further investigate the most highly abundant proteins present in the SGE, by HPLC purification.

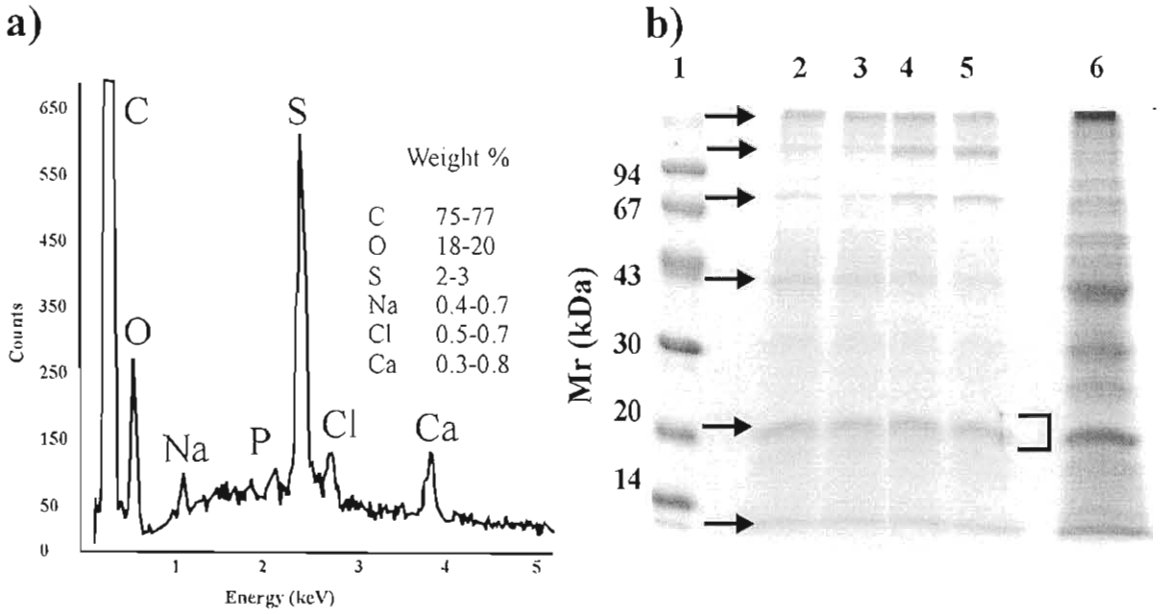

Fig. 6.3: Reconstitution of *in vitro* conditions present in the TGN. (a) X-ray microanalysis of salivary gland granules. Inserted are the % ranges obtained for 4 separate granules. (b) Aggregation of proteins under conditions of high calcium (50 mM) and different acidic pH. Lane 1 molecular mass markers, lane 2, 3, 4,5 at pH 4, 5, 6 and 7 respectively, while lane 6 indicates supernatant. Precipitated protein is indicated with arrows, while the TSGPs are bracketed.

6.4.4 A comparison of the toxicity of SGS and SGE

Some of the TSGPs were shown to be toxic during preliminary studies into the toxicity of the savignygrins (results not shown). For comparative purposes with results obtained for SGS, toxic activity in the SGE was investigated (Howell, Neitz and Potgieter, 1975). It should be noted that three-week old (10g) mice were used for the SGS study, while adult mice (20g) were used for the SGE study. With both SGE and SGS a concentration effect was noted, with survival of mice at gland equivalents of ~0.15 for both (Table 6.1). It was also found that 1 feeding tick caused mortality within 20 minutes after feeding. Previously, 200 μl of SGS was injected into a mouse, which died within 6 minutes (Howell, Neitz and Potgieter, 1975). Considering that a maximum of 10μl of SGS can be collected from a tick, then SGS from 20 ticks were injected (Howell, 1966b). Mice injected with SGE (2 glands) died within 20-30 minutes (Table 6.1). While this is 5X longer than that found for the SGS it is also shorter than the expected 10X. This could be due to the fact that more secretory products are sequestered inside the salivary gland granules than are secreted during stimulation with pilocarpine (Chapter 5).

Table 6.1: The effect of dilution on toxicity of SGE and SGS. Salivary gland or salivary gland secretion equivalents of a gland are indicated against the survival time. Values in parenthesis indicate the dilution factor, while the asterisk indicates times not recorded. SGS values have been reported previously (Howell, Neitz and Potgieter, 1975).

SGE equivalents	Survival time	SGS equivalents	Survival time
1 gland	30-60 minutes	5 glands (1/1)	20 minutes
0.5 glands	8-9 hours	0.6 glands (1/8)	Within 24 hours*
0.25 glands	Within 48 hours*	0.3 glands (1/16)	Within 24 hours*
0.125 glands	Survived	0.15 glands (1/32)	Survived

6.4.5 Investigation into the possible neurotoxicity of SGE

Since it has been shown that toxic activity in SGS is stable to temperatures of ~80°C (Howell, Neitz and Potgieter, 1975), heat precipitation as a purification procedure was investigated. It was found that toxic activity was retained after treatment at 60°C (Table 6.1). Analysis of this preparation by tricine SDS-PAGE shows that the majority of proteins with Mr>20kDa were precipitated (fig. 6.4a). Proteins with Mr 6-20 kDa were fractionated using RPHPLC (Fig. 6.4a and 6.4b). Toxicity tests indicated a possible toxic activity eluting in fraction 3 (Fig. 6.4b). Paralysis like symptoms were however, only observed after ~48 hours. The equivalent of 4 salivary glands was injected, which contrasts with the toxicity observed for one gland and less after heat treatment (Table 6.1). Due to unpublished reports (C.J. Howell, 1969) of possible cardiac failure induced by the toxin, the effect of SGE on a Langendorf isolated rat heart perfusion system was tested.

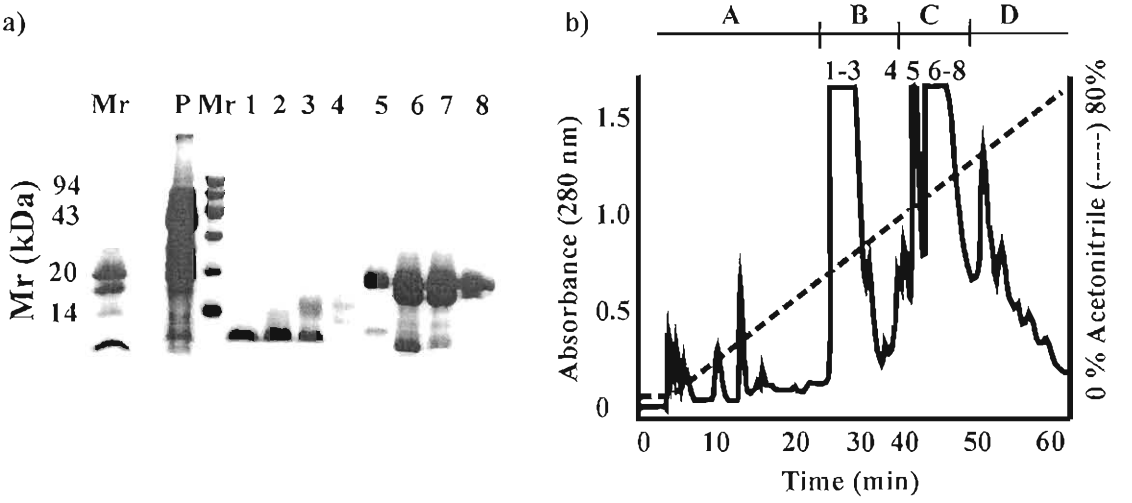

Fig. 6.4: Analysis of temperature inactivated SGE. (a) Tricine SDS-PAGE of heat precipitated fraction (P) and different fractions obtained after RPHPLC fractionation of the supernatant. (b) Preparative RPHPLC of temperature inactivated (60°C, 5 min) SGE (20 glands). Fractions collected, pooled and tested for toxicity is indicated (A-D), as well as those (1-8) analysed by tricine SDS-PAGE (Fig. 6.4a).

6.4.6 The effect of SGE on an isolated rat heart perfusion system

A rhythmic beat was observed that changed shortly after addition of SGE to an arrhythmic beat displaying bradycardia before final heart arrest (Fig. 6.5). This initial experiment was taken as evidence that the cardiac system rather than the nervous system is affected by the SGE from *O. savignyi* and toxic activities were purified before further analysis.

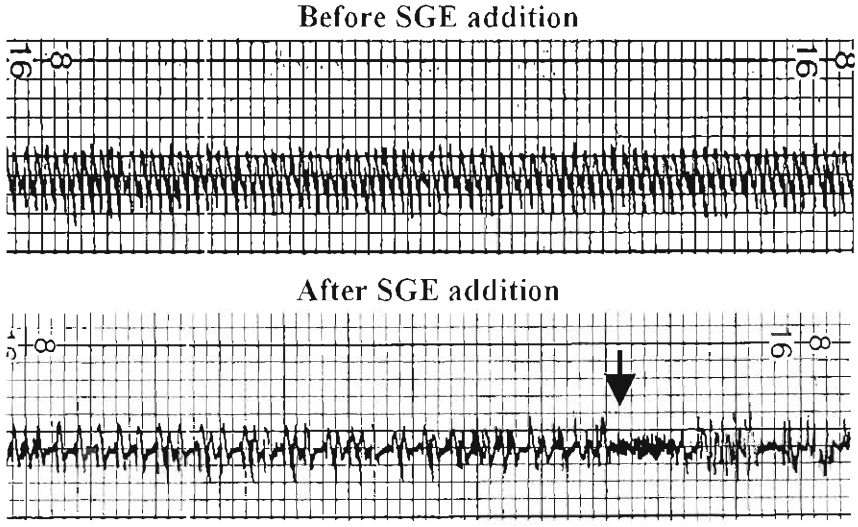

Fig. 6.5: The effect of SGE on a perfused rat heart system. The rhythm of the heartbeat is indicated before and after addition of SGE. The arrow indicates the onset of heart arrest.

6.4.7 Purification of TSGPs and toxins

HPLC purification of salivary gland extracts confirmed that the TSGPs are the main proteins present in tick salivary gland extracts (Fig. 6.6, Fig. 6.7 and Fig. 6.8). Yields of individual purified TSGPs were between 4% and 5% of the total initial salivary gland extract proteins (results not shown), giving the four proteins a cumulative concentration of 20% of the total protein in salivary gland extract. Assuming normal losses (20-50%) incurred after HPLC purification, the true concentration of the TSGP's would even be higher and closer to 40% of the total protein content, based on their densities after two-dimensional electrophoresis and their enrichment in the granule preparation. This is quite extraordinary considering normal expected values of proteins in tissues (0.01-0.1%). The abundant nature of these proteins was confirmed by the similar profiles obtained by two-dimensional electrophoresis and HPLC purification. This is quite important as it confirms the high abundance of specific proteins in the general proteome of the tick salivary gland by two different techniques.

6.4.8 Fractionation of toxic activities

Fractionation with AEHPLC showed that a basic (TSGP4) and acidic (TSGP2) toxic activity is present in SGE (Fig. 6.6a). While both fractions were lethal (survival times of 15-20 min) on the AEHPLC, only TSGP2 showed similar toxicity after CEHPLC. TSGP4 induced inactivity, shivering and muscle twitching that endured for two hours after which the mice recovered (Fig. 6.6b).

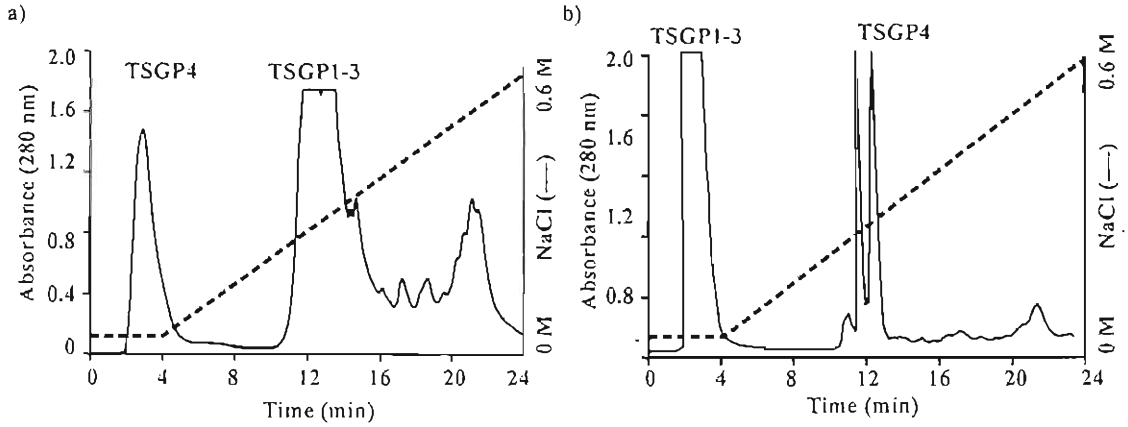

Fig. 6.6: Ion exchange HPLC of tick salivary gland extract. (a) AEHPLC with elution of TSGPs indicated. (b) CEHPLC with elution of TSGPs indicated.

TSGP4 fractionation of the AEHPLC fraction using SEHPLC, showed that toxic activity was associated with a ~17 kDa protein that corresponds with the toxic activity identified for CEHPLC (Fig. 6.7a). A non-toxic low molecular mass protein (LM: ~6 kDa) separated from TSGP4 during SEHPLC. The SEHPLC preparation of TSGP4 was lethal at 34μg within 30 minutes, although toxic activity was rapidly lost if stored. The lability of TSGP4 observed during this study probably accounts for its absence during previous studies into the toxic nature of *O. savignyi* (Neitz, Howell and Potgieter, 1969; Neitz *et al.* 1983; Howell, Neitz and Potgieter, 1975). Using the same SEHPLC conditions it was shown that the toxic activity of TSGP2 also eluted at a Mr~17kDa (results not shown). Rechromatography of the TSGP2 fraction from AEHPLC gave a protein with Mr~15kDa of which 24μg was lethal within 15-30 minutes (Fig. 6.7b). Dilution of this activity to 6 μg was still lethal over the course of one day, but 2μg failed to elicit any response.

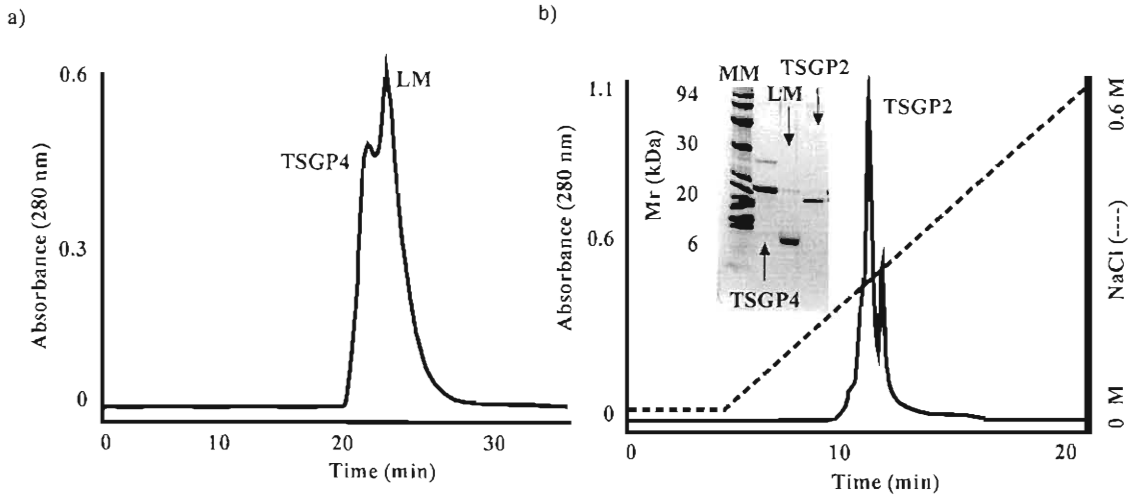

Fig. 6.7: Fractionation of toxic fractions from AEHPLCC. (a) SEHPLC of TSGP4 after AEHPLC. (b) Rechromatography of TSGP2 on AEHPLC. Inserted is a tricine SDS-PAGE gel that shows the TSGP4, LM and TSGP2 after their respective chromatography steps. LM is a low molecular highly abundant non-toxic protein with a similar pI as TSGP4.

Fractionation of TSGP2 from AEHPLC using HIHPLC resolved 3 main peaks of which two components were non-toxic, one a homolog (TSGP3) and the other a highly abundant protein (TSGP1) (Fig. 6.8a). After rechromatography on AEHPLC the toxic preparation (24μg) was also lethal within 30 minutes, supporting the observations of previous results (Fig. 6.8b). The toxicity of TSGP2 as observed during this study contrast sharply with the 400μg of toxin that was necessary to kill a mouse within 90 minutes (Neitz, Howell and Potgieter, 1969).

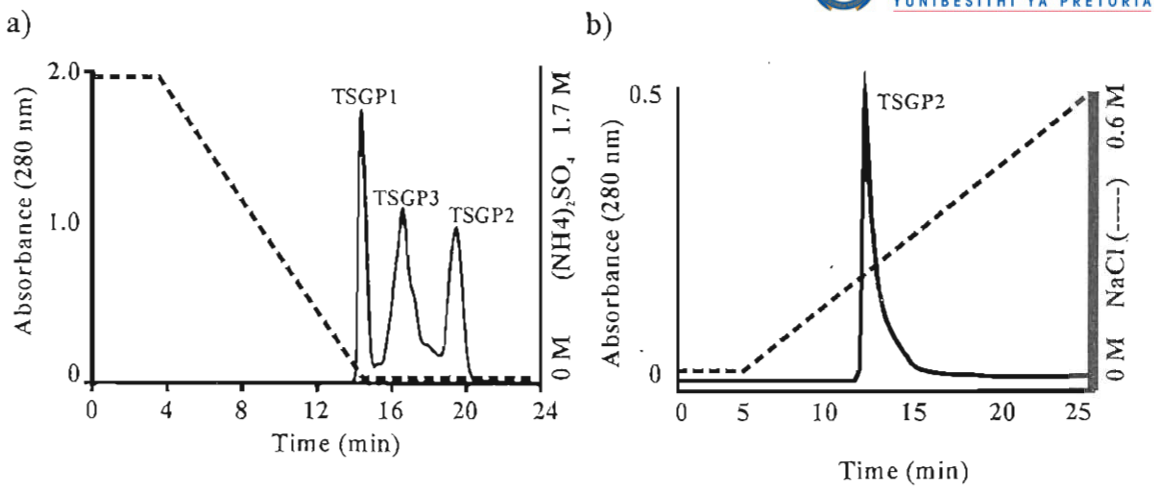

Fig. 6.8. Fractionation of the acidic TSGPs. (a) HIHPLC of the TSGP1-3 fraction after AEHPLC. (b) AEHPLC of TSGP2 after HIHPLC.

6.4.9 The effect of different toxins on the cardiovascular system

The effect of TSGP4 and TSGP2 on the cardiovascular system was investigated by recording ECG patterns of mice injected with purified toxic fractions. Preparations of TSGP4 after SEHPLC (Fig. 6.7) induced development of a hyperacute T-wave (A-I), with first tachycardia (B-C) followed by bradycardia (E-I) with a gradual increase in the P-R interval (F-I) (Fig. 6.9). This eventually manifested as Mobitz type 1 second degree AV block (H), followed by a Mobitz type 2 second degree AV block (I) (Goldberger and Goldberger, 1981).

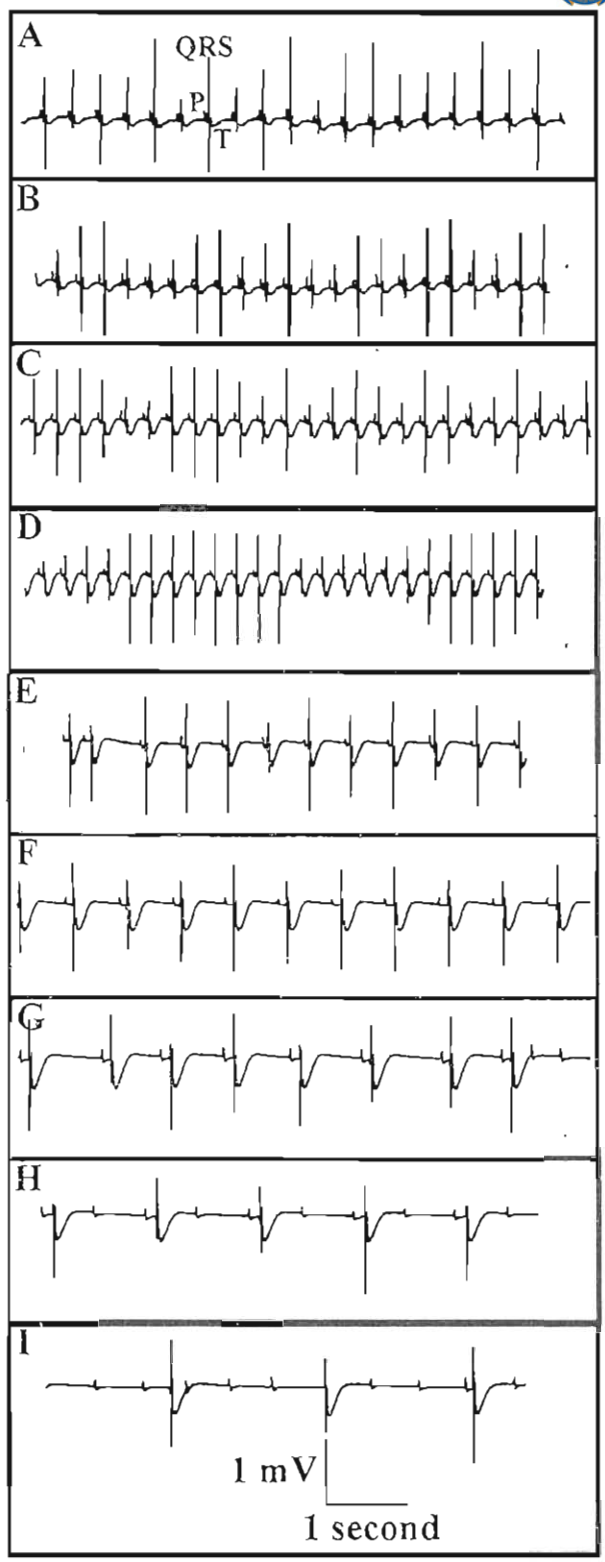

Fig. 6.9: The effect of TSGP4 on the mouse ECG patterns. The top panel indicates the ECG pattern before injection and the lower panels indicate different time periods after injection.

TSGP2 obtained from AEHPLC-HIHPLC-AEHPLC (Fig. 6.8) induced hyperacute T-waves (C) that diminished in amplitute (D), which was accompanied by a prolongation of the QT-interval (B-D) (Fig. 6.10). This was followed by a T-wave inversion and a complete heart block after which a normal pattern was regained (E). Severe ventricular tachycardia ensued with a QT prolongation, reminiscent of "torsades de pointes" (F) (Echardt *et al.* 1998).

Of interest is that non- anaesthetized control mice injected subcutaneous with TSGP2 died within 30 minutes, while mice injected with TSGP2 intra-peritoneal only succumbed after an hour and TSGP4 injected mice survived even longer. Only freshly prepared TSGP4 fractions showed toxicity and lost activity if left overnight at 4 °C. The delayed time of toxic activity could probably in both cases be assigned to the fact that intra-peritoneal injected material is effectively removed due to slow clearance from the intra-peritoneal cavity or sequestration in macrophages and organs. The results obtained together with that from the rat heart perfusion system and the nerve-muscle preparations, suggest that the pathology of these toxins are by targeting of the cardio-vascular system via disruption of electrical conductivity.

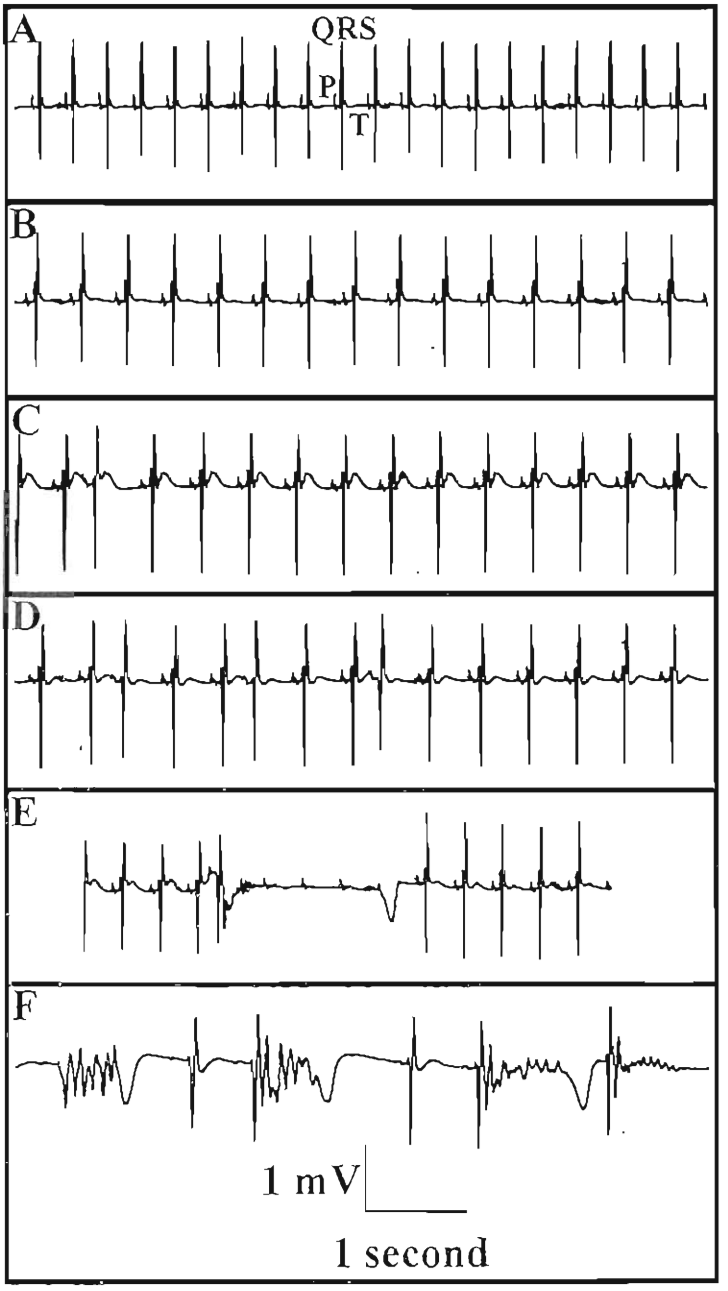

Fig. 6.10: The effect of TSGP2 on the mouse ECG patterns. The top panel indicates the ECG pattern before injection and the lower panels indicate different time periods after injection.

6.4.10 Desalting of TSGPs

Proteins were desalted for sequencing, ESMS and MALDI-TOF-MS purposes using RPHPLC (Fig. 6.11). All gave single peaks, although TSGP1 gave a broad tailing peak.

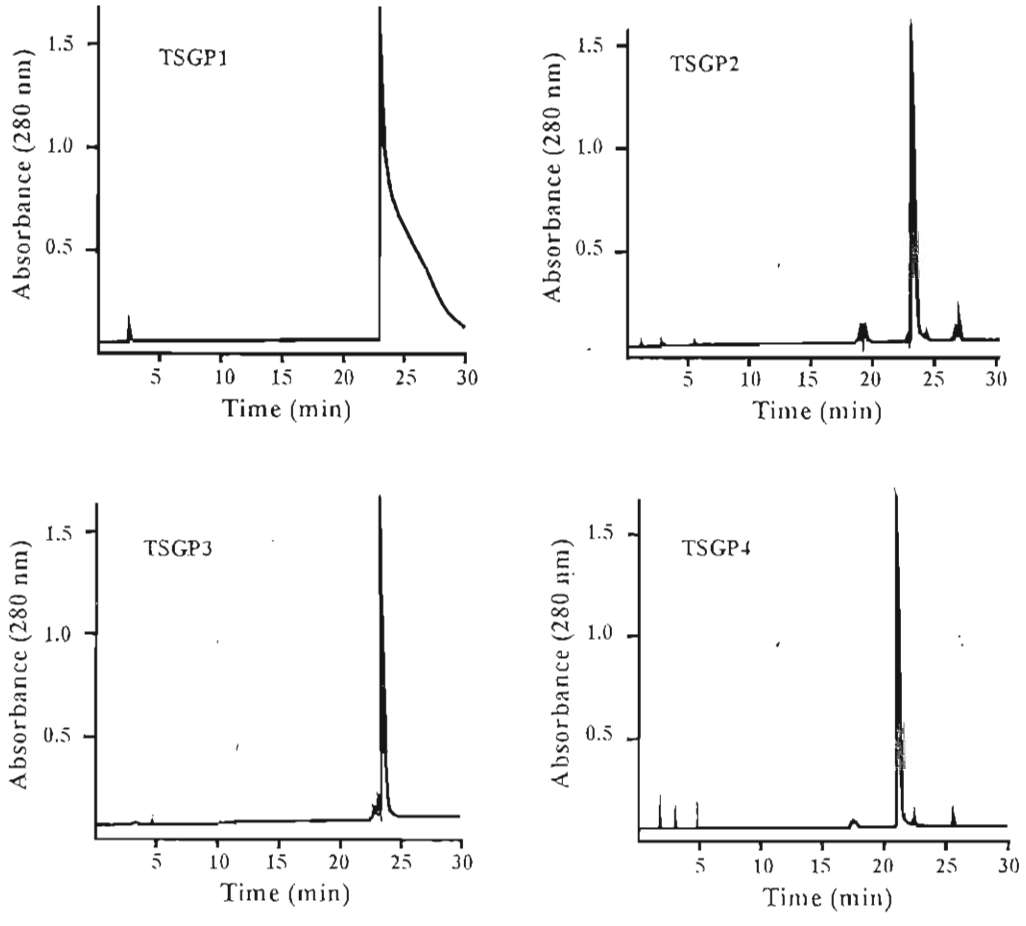

Fig. 6.11: RPHPLC of TSGPs. Fractions obtained of the acidic TSGPs after HIHPLC and fractions obtained of TSGP4 CECHPLC were desalted using RPHPLC.

6.4.11 Molecular mass analysis of TSGPs

Due to previously reported discrepancies on molecular mass of the acidic toxin (Neitz, Howell and Potgieter, 1969; Neitz *et al.* 1983), several different methods were used to determine the molecular masses of the toxins and TSGPs. Tricine SDS-PAGE analysis (Fig. 6.12) correlated well with masses obtained from MALDI-TOF-MS (Fig. 6.13) indicating that the molecular mass of the TSGPs ranged from 15800-18400 Da. MALDI-TOF-MS analysis of pyridylethylated TSGPs also indicated that these proteins have six cysteines.

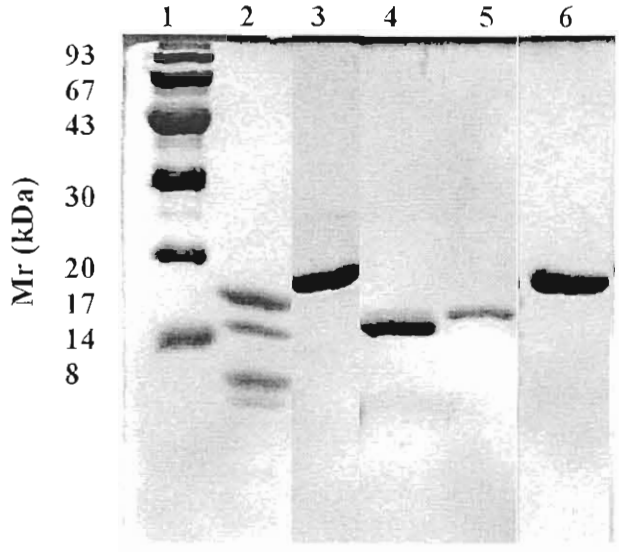

Fig. 6.12. Reducing tricine SDS-PAGE analysis of purified TSGPs. Lane 1 and 2 indicate low molecular mass markers and peptide mass markers respectively. Lane 3, 4, 5 and 6 indicate TSGP1-4, respectively.

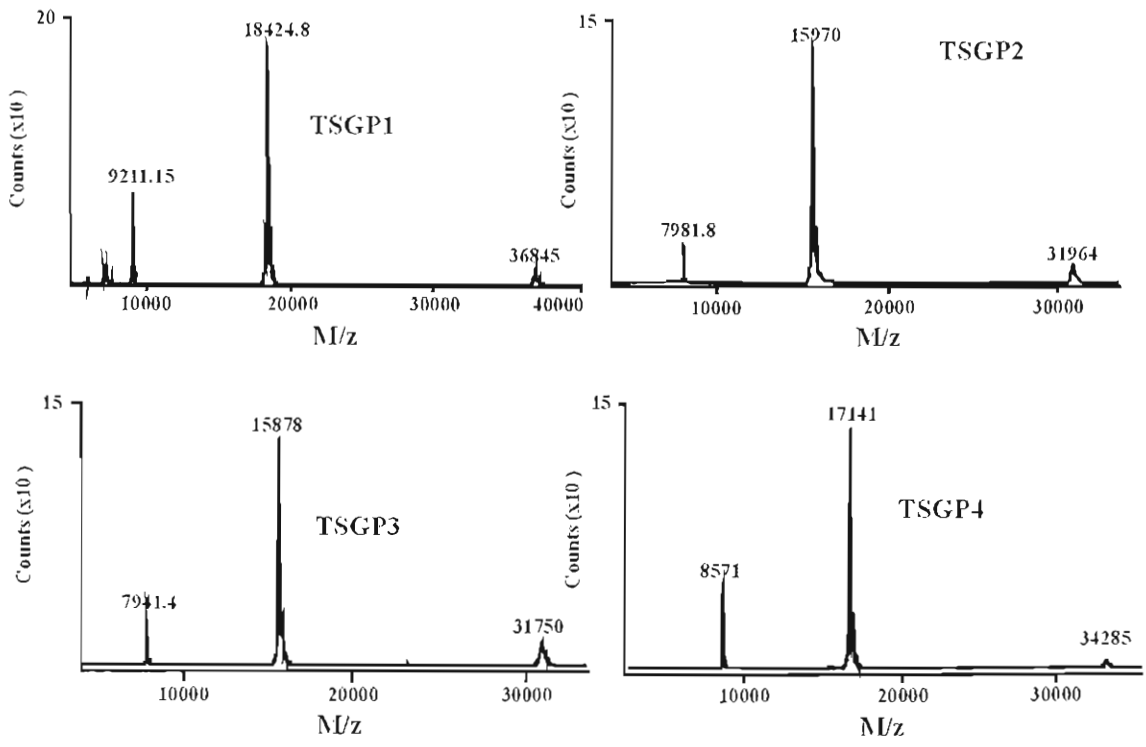

Fig. 6.13. MALDI-TOF-MS of TSGPs. Molecular masses are indicated for the respective proteins, as well as the $M+2H^+$ and $2M+H^+$ ion species.

ESMS analysis indicated masses comparable with those obtained from MALDI-MS and reducing tricine SDS-PAGE. TSGP1 gave multiple ions ranging from +10H to +17H, while TSGP2 and TSGP3 gave ions ranging from +10H to +15H and for TSGP4 multiple ions were obtained ranging from +10H to +19H (Fig. 6.14).

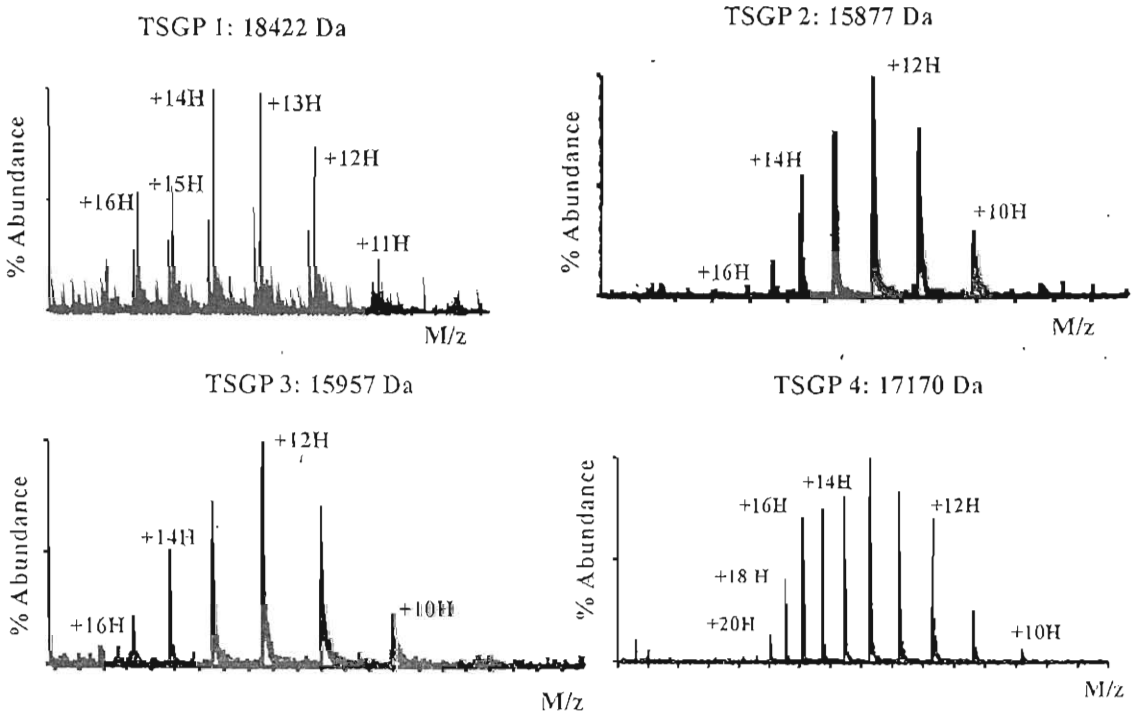

Fig. 6.14: ESMS spectra obtained for the TSGPs. Masses obtained after deconvolution are indicated, as well as multiple ion species.

6.4.12 Peptide mass fingerprinting of TSGPs

Peptide mass fingerprints obtained for the TSGPs indicated that TSGP1 and TSGP4 are unique proteins, while TSGP2 and TSGP3 share at least two peptide fragments and could thus be related (Fig. 6.15).

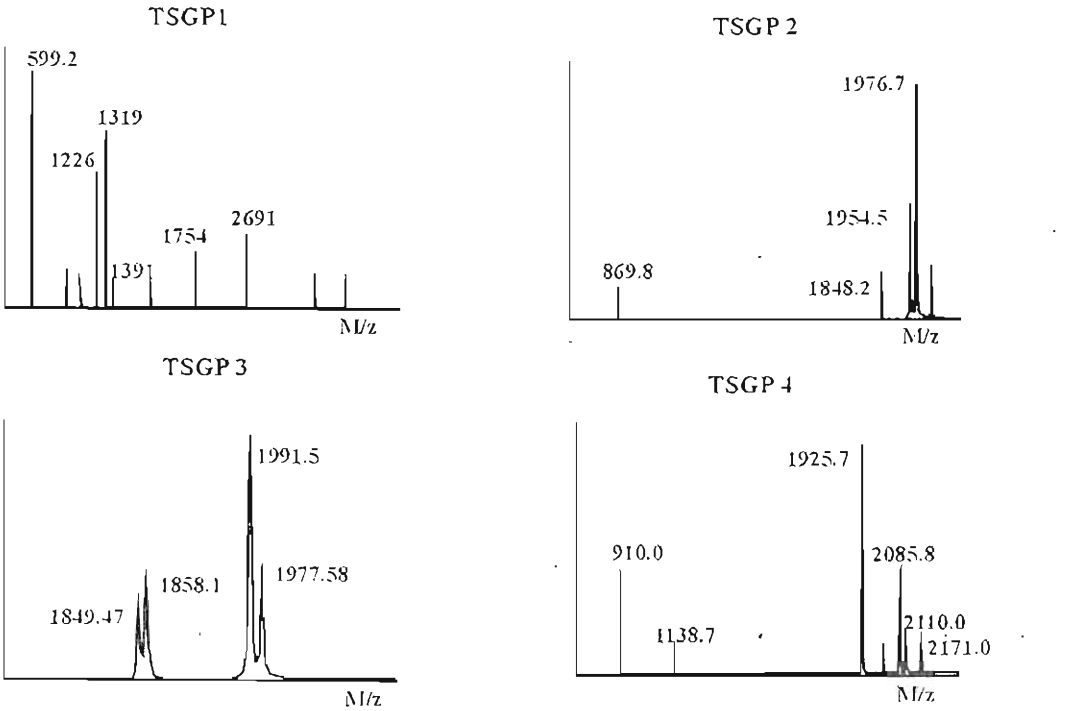

Fig. 6.15: Peptide mass fingerprints of TSGPs. Molecular masses are indicated for respective fragments.

6.4.13 Amino acid analysis of TSGPs

Amino acid analysis of the purified TSGPs indicated that the TSGPs have similar amino acid compositions (Fig. 6.16). Significant differences are the lower Asx and Glx and higher Arg in TSGP4, compared to TSGP1-3. This can explain differences in their iso-electric points. The higher arginine in TSGP4 explains the larger ion species observed for this protein with the ESMS results compared to the other TSGPs. TSGP4 also have significantly higher serine than TSGP1-3. The fact that TSGP1 gave slightly lower values for arginine and lysine compared to TSGP2 and 3, but still gave a higher number of charged species (+17H) compared to TSGP2/3 (+16H), is probably due to its higher mass compared to that of TSGP2 and TSGP3. Pyridylethylation in the presence or absence of a reducing agent also indicated that all cysteines (six according to MALDI-TOF-MS) are involved in disulphide bonds (results not shown).

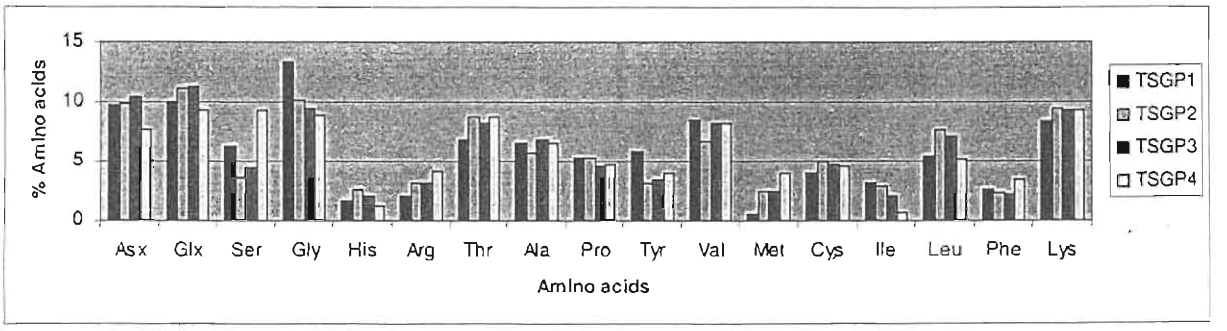

Fig. 6.16: Amino acid analysis of the TSGPs. Indicated is the cysteine content as determined by pyridylethylation.

6.4.14 N-terminal amino acid analysis of the TSGPs

N-terminal amino acid analysis indicated that TSGP1 and TSGP4 have novel sequences, while TSGP2 and TSGP3 were 95% identical and showed identity to previously described toxic and non-toxic homologs (Neitz, Howell and Potgieter, 1969, Neitz *et al.* 1983). No hits could be found using non-redundant BLAST analysis (Altschul *et al.* 1990), indicating that all sequences are unique. When using the Protein Prospector package (http://prospector.ucsf.edu/), which incorporates molecular mass, peptide mass fingerprint and N-terminal sequence data, no hits were found either.

```
TSGP1  :                    G-P-D-G-C-V-G-S-T-E-A-K-V-A-V      -15
20A1*  :          E-E-N-Q-R-G-K-G-M-L-G-S-T-A-A-S-V-A-V      -19

Toxin*:           G-C-P-P-G-V-P-T-R-A-Y-V-A-F-V-E-G-X-G-A    -20
TSGP2  :          D-C-P-T-G-K-P-T-D-A-Y-V-A-F-N-X-G-Q-G-A    -20
TSGP3  :          D-C-P-T-G-K-P-T-E-A-Y-V-A-F-N-X-G-K        -18
Non-toxin*:       D-C-P-P-T-K-P-T-R-A-Y-V-A-F-X-E-G-E        -18

TSGP4:            A-N-D-V-W-N-V-L-K-G-S-D-S-K-F              -15
```

Fig. 6.17: N-terminal sequence analysis of the TSGPs. N-terminal sequences obtained for the TSGPs are indicated. Cysteine residues were identified as their perethylated derivatives. The X in the sequences of TSGP2 and TSGP3 represent unidentified, modified amino acids. Identity between different sequences is indicated by black boxes. *The N-terminal sequences of toxin (Neitz *et al.* 1983), non-toxin (Neitz, 1976) and 20A1 (Baranda *et al.* 2000) were obtained from literature.

6.4.15 Specificity of polyclonal anti-sera for TSGPs

Polyclonal anti-sera were generated against the different TSGPs. Western blot analysis shows that all sera are specific for components in the ~20 kDa range in crude SGE (Fig. 6.18a). Anti-sera raised against TSGP1 and TSGP4 did not cross-react with other purified TSGPs. Anti-sera raised against TSGP2 did however cross-react with TSGP3, but not with TSGP1 or TSGP4 (Fig. 6.18c). This together with the shared peptide fingerprints and N-terminal sequences of TSGP2 and TSGP3 indicate sequence similarity and probably homology.

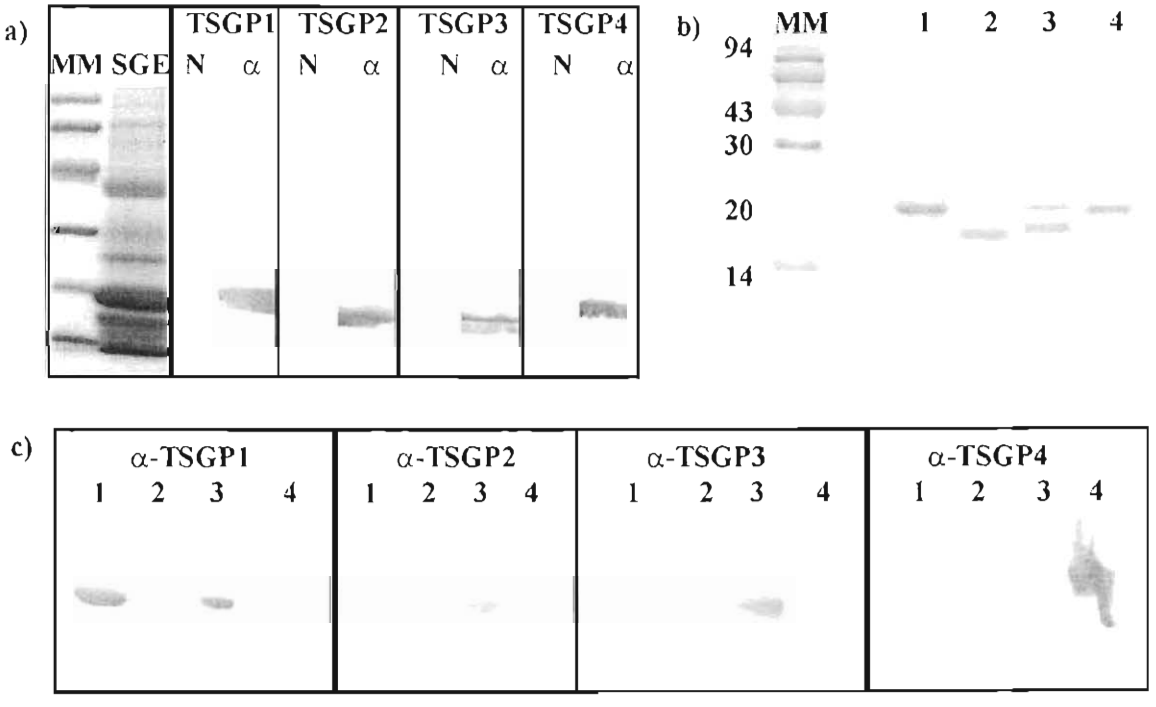

Fig. 6.18: Specificity of polyclonal anti-sera raised against different TSGPs. (a) Western blots of crude SGE with anti-sera against TSGP1-4, respectively. Also indicated is naïve serum (N) before immunization. (b) Purified fractions used for cross-reactivity studies between the various TSGPs. Indicated is TSGP1 (1), TSGP2 (2), TSGP3 (3) and TSGP4 (4). (c) Cross-reactivity of anti-TSGP1, anti-TSGP2, anti-TSGP3 and anti-TSGP4 with purified TSGP1 (1), TSGP2 (2), TSGP3 (3) and TSGP4 (4), respectively.

6.4.16 Localization of TSGPs to salivary gland granules

If the TSGPs are involved in granule biogenesis then this should be mirrored in their localization to different granule types. Localization of the TSGPs to all the granule types

identified in the salivary glands (Chapter 5) first came as a surprise (Fig. 6.19). It is however, logical that proteins involved in granule biogenesis should be present in all granule types if they assist in their formation.

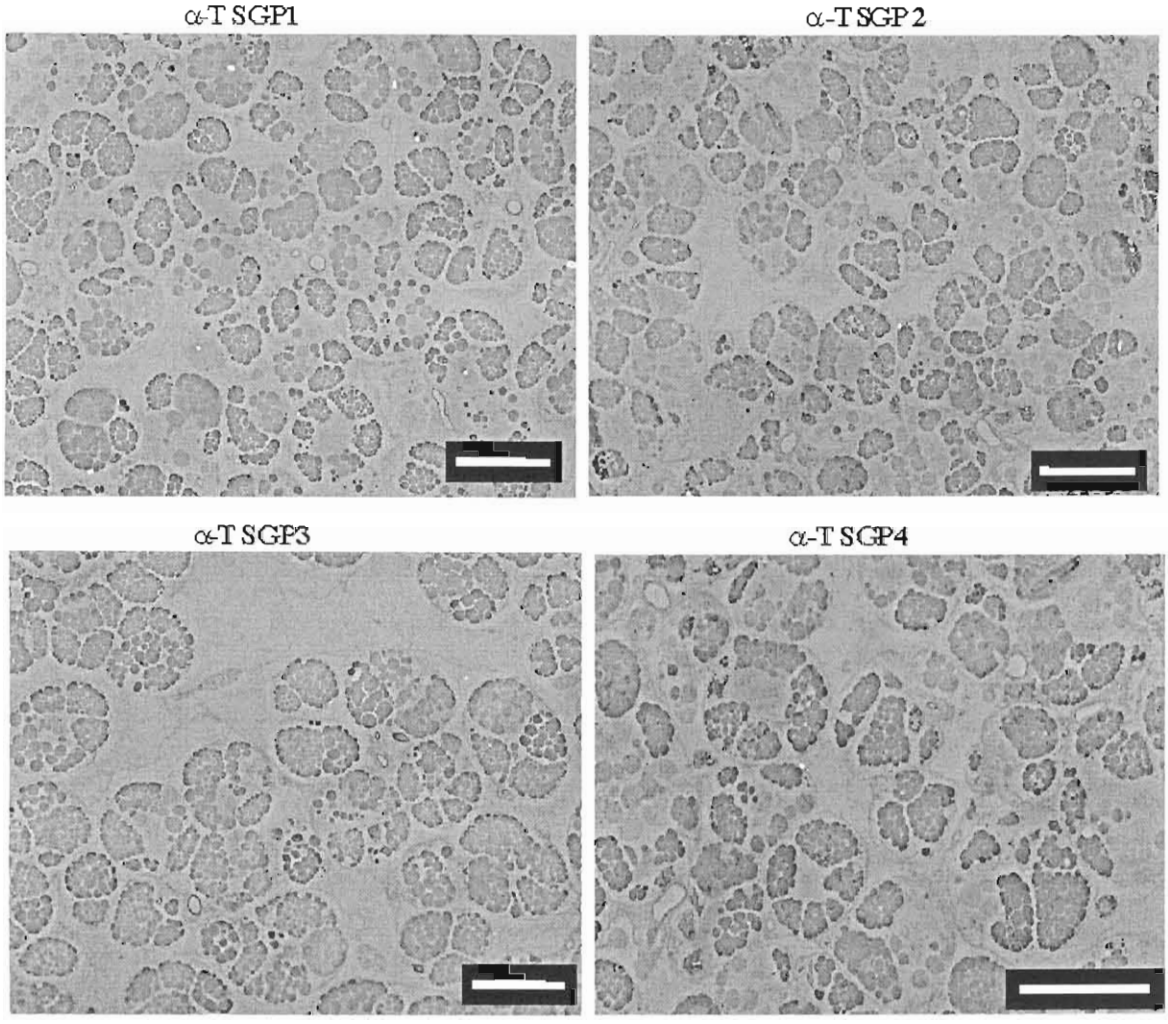

Fig. 6.19: Localization of the TSGPs to different salivary gland granules. Scale bar = 100 μm.

6.4.17 Protein concentration and its influence on granule biogenesis

Granule formation takes place at high protein concentrations in the TGN, resulting in high intra-granular protein concentrations (~0.1g/ml) (Urbé, Tooze and Barr, 1997; Arvan and Castle, 1998). The density of the isolated tick salivary gland granules (1.14 g/ml) is approximately 10X the reported intra-granular concentration. Expressed in terms of percentage protein concentration this amounts to 114%. If it is considered that the TSGPs represent between 20-40% of the total soluble SGE proteins, then their density in the granules is 0.228-0.57 g/ml. This is still higher than intra-granular concentrations of 0.1g/ml (Urbé, Tooze and Barr, 1997; Arvan and Castle, 1998).

Our first manuscript on the TSGPs commented on the relatively low amounts of protein that precipitated during conditions of high calcium concentration and acidic pH (Mans *et al.* 2001). It was speculated that the conditions used (Fig. 6.3) do not truly resemble that of the tick TGN or granule and that the concentration of the salivary gland extract (6mg/ml protein) used could also be too dilute for adequate aggregation. Using higher concentrations, could however, lead to non-specific association. However, after a consideration of the implications of the density of the salivary gland granules and further reading into the field of molecular crowding, we were forced to consider the effect that protein concentration might have on granule formation.

6.4.18 Molecular crowding in the cell

Molecular crowding is a phenomenon that would seem obvious, but for most part is ignored by the general biochemistry community when considering physiological cellular conditions. Cellular interiors have high total concentrations of macromolecules (20-30% of the total volume: compare this with the estimated 114% of the dense core granules!). Due to steric exclusion the volume occupied by these molecules are unavailable to other macromolecules: the excluded volume effect (Ralston, 1990; Zimmerman, 1993; Minton, 1997; Minton, 2000; Minton, 2001; Ellis, 2001a; Ellis, 2001b). The effect is adequately described by consideration of a macromolecule that occupies 30% of the available space. While the remaining 70% of volume is accessible to smaller molecules, it is inaccessible to any molecules as large or larger than the described macromolecule (Fig. 6.20).

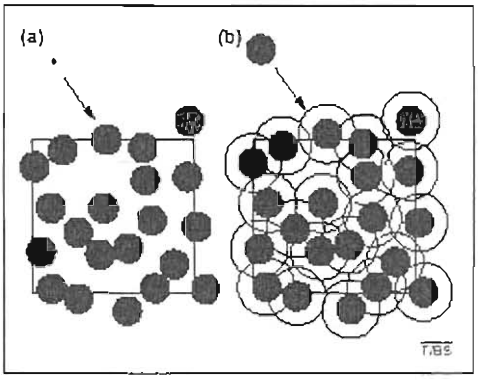

Fig. 6.20: The principle of volume exclusion. (a) The square indicates the volume of which 30% is occupied by a macromolecule. A small molecule has access to all of the remaining 70% volume. (b) A molecule similar in size is excluded from the remaining 70% as it cannot approach the molecules closer than the distance of indicated by the open circles. This is described as the excluded volume of a macromolecule. Figure adapted from Minton (2001).

The phenomenon of molecular crowding has several consequences. By excluding volume to one another, macromolecules reduce configurational entropy and as such increase the free energy of a solution. Volume exclusion in crowded media leads to destabilization of test species, so that the most favored state excludes the least volume. Compact structures exclude less volume than extended structures, while oligomeric or polymeric aggregates also exclude less volume than individual subunits. Macromolecular crowding thus provides a nonspecific force for macromolecular compaction and association in crowded solutions. Such macromolecular compaction or association can probably be equated with the concentration, multimerization, polymerization and condensation previously used to describe granule formation (Arvan and Castle, 1998). Molecular crowding effects could thus lead to condensation of secretory proteins into granules. A simple calculation of the volume that TSGPs encompass in a granule, indicate that they are optimally packed. This further support the possibility that molecular crowding leads to condensation of the TSGPs.

6.4.19 TSGPs as densely packed spheres

To demonstrate this, consider a granule with a diameter of 5 μm.

(A) The volume of a granule with a 5μm diameter is:

$$V = 4/3\Pi(r)^3$$

$$V = 4/3\Pi(2.5X10^{-6}\ m^3)$$

$$V = 6.545X10^{-17}\ m^3$$

(b) Subcellular fractionation and density centrifugation showed that the granule has a density of 1.14 g/ml.

i.e. 1.14g per $1X10^{-6}\ m^3$

From the above it follows that the mass of a granule with diameter of 5μm is:

$7.46X10^{-11}$ g.

(c) It has been shown that the TSGPs can take up to 20-40% of the total SGE protein.

For the granule this means that the TSGPs are:

$1.49X10^{-11}$ g – $2.98X10^{-11}$ g

of the total protein in granule.

(d) Assuming an average molecular mass of 17000 g/mol for the TSGPs, using the above masses we can calculate the amount of moles for the TSGPs in the granules.

This gives: $8.76X10^{-16}$ moles – $1.75X10^{-15}$ moles.

Using Avogadro's number ($6.022X10^{+23}$ molecules/mole) we can calculate the number of TSGP molecules in the granule:

$5.2X10^{+8}$ molecules – $1.05X10^{+9}$ molecules.

(e) Assuming a globular protein structure (this approximation is supported by the results presented in Chapter 7, that indicate that the TSGPs are part of the lipocalin family) and using the linear relationship between molecular mass and volume derived in Chapter 3 (Fig. 3.20), a volume of ~43Å^3 is obtained. As 1Å = $1X10^{-10}$ m, the dimensions can be converted to volume, which gives:

$7.95X10^{-26}\ m^3$.

The total volume for the TSGPs can be calculated:

$4.1X10^{-17}$ m^3 – $8.3X10^{-17}$ m^3.

(f) Using the volume determined for the granule, we find that this works out to 62%-126% of the total volume of the granule.

It would be impossible for the TSGPs to encompass 126% of the total volume of the granules. The estimation of 20%-40% is thus erroneous and the total TSGP concentrations are probably close to the determined 20%. Studies on the close packing of spheres have indicated that the maximum density that a large, random collection of spheres can attain is 63%-74% (Torquato, Truskett and Debenedetti, 2000). At 20% of the total protein concentration of the granule and 62% of the volume, the TSGPs approach the limits of their maximum density. This would have a profound influence on the packing of other macromolecules and the volume exclusion effect should play a significant role during granule formation.

To test whether volume exclusion might play a role during granule formation, SGE was incubated at pH 5.5 in the presence of 100 mM $CaCl_2$ at various concentrations of dextran. Dextran is a useful polymer for the investigation of volume exclusion effects (Ellis, 2001a). With increasing concentrations of dextran, specifically above 10%, more TSGPs and other salivary gland proteins are precipitated (Fig. 6.21). This suggests that volume exclusion (probably due to increasing concentrations of TSGPs in the TGN) could play a significant role during granule biogenesis.

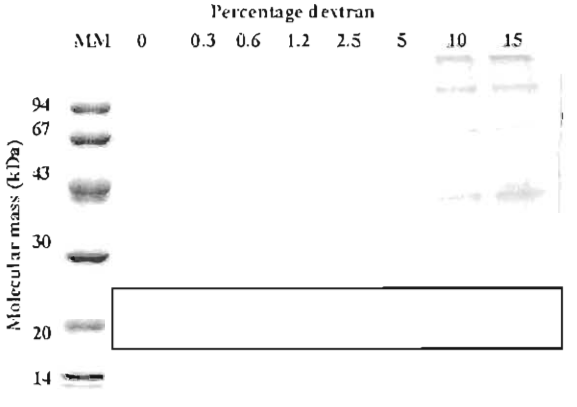

Fig. 6.21: Precipitation of TSGPs in the presence of increasing concentrations of dextran. TSGPs are boxed.

6.5 Discussion

6.5.1 Granule biogenesis in tick salivary glands

Ticks secrete bioactive compounds during feeding that are stored in salivary gland granules until released by a stimulus (Sauer *et al.* 1995). Granule formation plays an important part in this process as a mechanism by which secretory proteins are packaged. An adequate understanding of granule biogenesis can therefore aid in the elucidation of tick secretory mechanisms and defining a potential target for the development of tick control methods.

6.5.2 Evidence of TSGPs being granule biogenic protein's

Several different facts support a possible role for the TSGPs in granule biogenesis:

1. All proteins involved in granule biogenesis occur at very high concentrations in secretory cell types (Urbé, Tooze and Barr, 1997; Arvan and Castle, 1998). The TSGPs are the most abundant proteins in the SGE and granules as determined by two-dimensional electrophoresis, density gradient centrifugation and HPLC.
2. Proteins involved in granule biogenesis tend to aggregate under conditions of acidic pH and high calcium concentration (Huttner, Gerdes and Rosa, 1991; Urbé, Tooze and Barr, 1997; Blasquez and Shennan, 2000). The TSGPs showed aggregation under such conditions.
3. If the TSGPs are involved in the formation of all the different salivary gland granule types, then they should be present in all granules. The TSGPs were immuno-localized to all the different granular types in contrast to apyrase and savignygrin (Chapter 5).
4. The TSGPs aggregated in direct relation to the degree of molecular crowding. It was also indicated that the TSGPs are packed close to the optimum packing that can be attained by spherical particles. These two observations suggest that the TSGPs at high concentrations as observed in the granules would experience molecular crowding effects, i.e. aggregation (Ellis, 2001a). As was explained in the introduction, aggregation is synonymous with granule biogenesis (Huttner,

Gerdes and Rosa, 1991; Urbé, Tooze and Barr, 1997; Blasquez and Shennan, 2000).

5. If the TSGPs all exhibit the same function, then it could be expected that they should belong to the same protein family. Chapter 7 presents results that indicate that the TSGPs are indeed part of the same lipocalin protein family.

Secretory granules have to be formed in some way. Literature has presented several criteria for proteins involved in this process. So far, it would seem as if the TSGPs fit these criteria and are at this stage the best possible candidates for being granule biogenic proteins. The difficulties involved in finding an *in vitro* system that will simulate granule formation makes it difficult at present to give a more conclusive explanation.

6.5.3 Toxins from *O. savignyi*

Results obtained in this study confirmed the presence of at least two highly abundant and similar proteins. N-terminal sequence data, peptide mass profiles and western-blot analysis using polyclonal anti-sera indicate that TSGP2 and TSGP3 have similar amino acid sequences. At least one of these proteins (TSGP2) has been previously identified as a toxin (Neitz *et al.* 1983). A non-toxic homologue (TSGP3) that co-purified with the toxic component has also been identified (Neitz, Howell and Potgieter, 1969). This study reconfirmed the toxicity of TSGP2 and non-toxicity of TSGP3. The molecular masses obtained for TSGP2 (15877 Da) and TSGP3 (15957 Da) compare favorably with the masses obtained for the toxin (15400 Da) and non-toxin (16000 Da), respectively (Neitz, Howell and Potgieter, 1969). The iso-electric point of TSGP2 is more acidic than that of TSGP3 and compares favorably with the lower pI of the toxin (5.01) versus that of the non-toxin (5.1) previously described (Neitz, Howell and Potgieter, 1969). In addition it has been shown that a novel toxic activity is associated with TSGP4 that has a unique N-terminal sequence. TSGP1, showed 56% identity with the N-terminal amino acid sequence of the main antigen (20A1) present in the salivary gland extracts of *O. moubata* (Baranda *et al.* 2000).

6.5.4 Non-paralytic nature of sand tampan toxicoses

O. savignyi has been implicated in causing paralysis (Hoogstraal 1985; Gothe and Neitz 1991; Gothe 1999). All publications ultimately refer back to Kone (1948), Rousselot (1956), Howell (1966b) and Howell, Neitz and Potgieter (1975). Perusal of these publications show however, no direct reference to paralysis associated with *O. savignyi*. Kone (1948) describes severe symptoms and death that ensues after exposure of cattle to tick bites, but interprets this as possible anaphylactic shock. Rousselot (1956) states that several hundreds of cattle on the border of Lake Chad were affected and that after three weeks, high mortality from asphyxiation had resulted, presumably from the bite of *O. savignyi*. Howell (1966b) discussed paralysis in general in the introductory section, but only indicated that bovines died overnight as a result of exposure to *O. savignyi* (Howell, 1966). Perusal of the original literature dealing with toxicoses caused by the sand tampan and unpublished results on the clinical symptoms and pathology of various animals exposed to the tick secretions, gave no indication of characteristic paralysis symptoms (flaccid tetraplegia). Although the toxins could have an effect on the central nervous system, symptoms suggest that the hemostatic, respiratory or cardiac system of the various host's are affected. These findings are concurrent with the data of this present study. This report emphasizes the need for more stringent studies into tick toxicoses. As yet, it is not known how many reports of toxicoses are accurate, which hinders comparative studies that can shed light on the origins of tick toxicoses. Whether tick toxins have a similar origin is of crucial importance, as this would give answers to questions such as whether toxins from different ticks have similar protein structures and toxic mechanisms. A consideration of literature of paralysis toxins argue that the molecular properties differ from that of the sand tampan toxins:

(A) Paralysis toxins tend to form non-specific macro-molecular complexes so that molecular mass determination is complicated. Masses between 5-74 kDa have been reported for paralysis toxins from *I. holocyclus*, *R. evertsi evertsi* and *A. walkerae* (Viljoen *et al.* 1986; Crause *et al.* 1993; Maritz *et al.* 2000; Masina and Broady, 1999). In contrast, molecular mass determination of toxins from the present study, gave similar masses (~15-18kDa) using a variety of techniques,

which include sedimentation equilibrium ultra-centrifugation, MALDI-TOF-MS, ESMS, tricine SDS-PAGE and size exclusion HPLC (Neitz, Howell and Potgieter, 1969; Mans *et al.* 2001). These masses do not compare with any previously described for the paralysis toxins.

(B) A slow feeding period is necessary for toxin production in hard ticks, while subcutaneous injection of SGE of *R. evertsi evertsi* failed to produce paralysis in mice (2.5 mg) and ovines (3.5 mg), although ovines became paralyzed upon challenge with ticks, while *A. walkerae* only paralyze 1 day old chicks (Viljoen *et al.* 1986; Crause *et al.* 1993). In contrast the toxins from *O. savignyi* are present in all tick stages, SGS and SGE and are able to kill a variety of mammals when injected subcutaneously.

(C) A monoclonal antibody directed against the paralysis toxin from *R. evertsi evertsi* was shown to cross-react with epitopes from *A. walkerae* larvae and to protect day old chicks from paralysis (Crause *et al.* 1994). The same monoclonal was used as an assay method to isolate the toxin from *A. walkerae* (Maritz *et al.* 2000). No cross-reactivity was however, observed for salivary gland extracts of *O. savignyi* (Maritz, 1999).

(D) It was also shown that *A. walkerae* larval homogenates inhibit the release of [^{3}H] glycine from potassium-stimulated rat brain synaptosomes (Maritz *et al.* 2001). SGE from *O. savignyi* gave a lower percentage inhibition of this process than did SGE from adult *A. walkerae*, known to be non-paralytic (Maritz, 1999).

(E) Sinus arrhythmia has been shown to occur in marmots exposed to *D. andersoni*, but these effects on the cardiac system were only observed after complete paralysis of all four limbs (Emmons and McLennan, 1980). While paralysis toxins might thus also affect the cardiac system, paralysis symptoms would probably be observed first. In contrast, cardio-pathogenesis caused by *O. savignyi* is unaccompanied by paralysis.

6.5.5 Cardio-pathogenic properties of sand tampan toxin

The toxic effects during rat heart perfusion indicate that SGE can have a direct effect on the cardiac system. Animal toxins induce their specific pharmacological effects through

toxin-receptor interactions, while many interact specifically on different ion channels (Kordiš and Gubensek, 2000). Electrophysiological results suggest that cardiac ion currents are affected by the tick toxins, probably by blocking of specific ion channels. Potassium channel block is normally revealed as a prolongation of the cardiac action potential and its electrocardiac manifestation as a prolongation of the Q-T interval as observed for TSGP2 (Colatsky *et al.* 1994). AV-block as observed for TSGP4 is generally due to impaired ventricular depolarization and conduction through the AV-junction. The main ion channels involved in conduction through the AV-junction are calcium and sodium channels and could as such be the target of TSGP4 (Goldberger and Goldberger, 1981).

6.5.6 Toxicity of TSGP2 *versus* the non-toxicity of TSGP3

N-terminal sequences of TSGP2 and TSGP3 indicate 95% identity while amino acid analysis indicates similar compositions. TSGP2 and TSGP3 have identical elution times during RPHPLC that indicate similar global hydrophobicity. In contrast, TSGP2 and TSGP3 separate on HIHPLC, indicating differences in their surface hydrophobicity and hence surface conformation. This could account for the absence of apparent toxicity in TSGP3 and suggest that toxicity of TSGP2 is due to a local surface conformation difference. A mobile local surface conformation of TSGP4 and TSGP2 can also account for their lability observed during purification.

6.5.7 Biological functionality of toxins

The toxic nature of these proteins is probably of secondary importance, as is exemplified by the non-toxicity of TSGP1 and TSGP3. The environment also has a large effect on the stability of the purified toxins, which could indicate that the toxic nature of these proteins could be a secondary peripheral function. It could be that the toxins perform a very different function in the blood-feeding environment or even in the salivary glands themselves. *O. moubata* has been shown to be non-toxic in a study where 5 female, 10 male adults and 100 nymphs were fed on a mouse to induce an immune response (Astigarraga *et al.* 1997). This is in stark contrast to results obtained for one feeding tick in this study. *O. moubata* is a nidicolous tick that is probably in contact with only a few

individuals in its lifetime, so that any adverse effects could have serious implications for tick survival. *O. savignyi* on the other hand, is free-living and not restricted by the limited set of hosts encountered in a burrow and could thus afford to be more aggressive towards its host (Hoogstraal, 1956). The absence of toxic proteins in the SGE of *O. moubata* is concurrent with this view. While the killing of its host might not affect the survival of the tick population, to argue that toxicity might confer any evolutionary advantage to *O. savignyi* is a premature statement. It has been suggested that the toxins are part of a larger family involved in granule biogenesis of tick salivary gland granules. Possible functions in the regulation of the host's immune and hemostatic systems cannot be excluded either.

This study indicates unique cardio-toxic mechanisms of toxicoses induced by *O. savignyi* and conclude that reports of paralysis caused by this tick species are erroneous. It emphasizes the need for a more thorough investigation into all forms of tick-induced toxicoses, both to catalogue tick toxin variety but also to gain an understanding of toxin origins and possible biological relevance. The next chapter deals with the cloning and molecular characterization of the TSGPs and show that they are all part of the same lipocalin protein family.

Chapter 7: The major tick salivary gland proteins are part of the tick lipocalin family*

7.1.1 Introduction: The lipocalin protein superfamily

A protein family can be described as proteins of which the amino acid sequence similarity is high enough (>35% identity), to ascribe homology based on sequence alone. In contrast, a protein superfamily consists of proteins with sequence similarity so low (<20% identity) that common origins can only be inferred from structural similarity (Skerra, 2000). Lipocalins form such a superfamily of small (150-183 amino acids residues), extracellular secretory proteins with highly divergent sequences (<20% sequence indentity), but with a highly conserved structural fold (Flower, 1996; Åkerstrom *et al.* 2000; Flower, North and Sansom, 2000). Lipocalins are characterized by their ability to bind small hydrophobic molecules. The name lipocalin was derived from this property: lipo (lipophilic) for their ligands and calyx (ligand enclosed by the protein as is the flower by its calyx) to describe their binding mode (Pervaiz and Brew, 1987).

7.1.2 Lipocalin function

Lipocalins have a diversity of functions that include transport of small molecules, arthropod coloration, pheromone transport, prostaglandin synthesis, smell reception, regulation of cell growth, tissue development and metabolism, regulation of the immune response, allergens and has been implicated in various disease states. Ligands bound by the lipocalins include steroids, retinoids, odorants, pheromones, histamine, haem, nitric oxide and ADP. Lipocalins can also bind to cell surface receptors and can form macromolecular complexes (Flower 1996; Akerstrom *et al.* 2000; Flower, North and Sansom, 2000).

7.1.3 Lipocalin three-dimensional structure

The lipocalins share a similar protein fold consisting of a eight (A-H) stranded, continuous hydrogen-bonded anti-parallel β-barrel with a +1 topology (Fig. 7.1). Sheets are linked by short β-hairpin loops, except loop one that is a large Ω loop that link strands A and B. The structure has a flattened elliptical shape as if composed of two different

orthogonal β-sheets stacked together, with one end closed off by a N-terminal 3_{10} helix. Close packing of the barrel, loops (L2, L4, L6) and helix residues in this area forms a hydrophobic core. The other end is open to solvent and a ligand-binding pocket is formed here via the binding cavity and the exposed loops (L1, L3, L5, L7). A C-terminal α-helix packs against one side of the barrel and is followed by a short β-sheet (I). This topology of a barrel with a central cavity closed at one end and open at the other end combined with the flanking α-helix give the lipocalins the resemblance of a cup. The β-barrel structure is highly conserved for most lipocalins and contributes to the structural stability of the protein fold. In contrast, the loops at the open end are highly variable and contribute to the diversity of ligand and receptor recognition displayed by the lipocalins (Fig. 7.1).

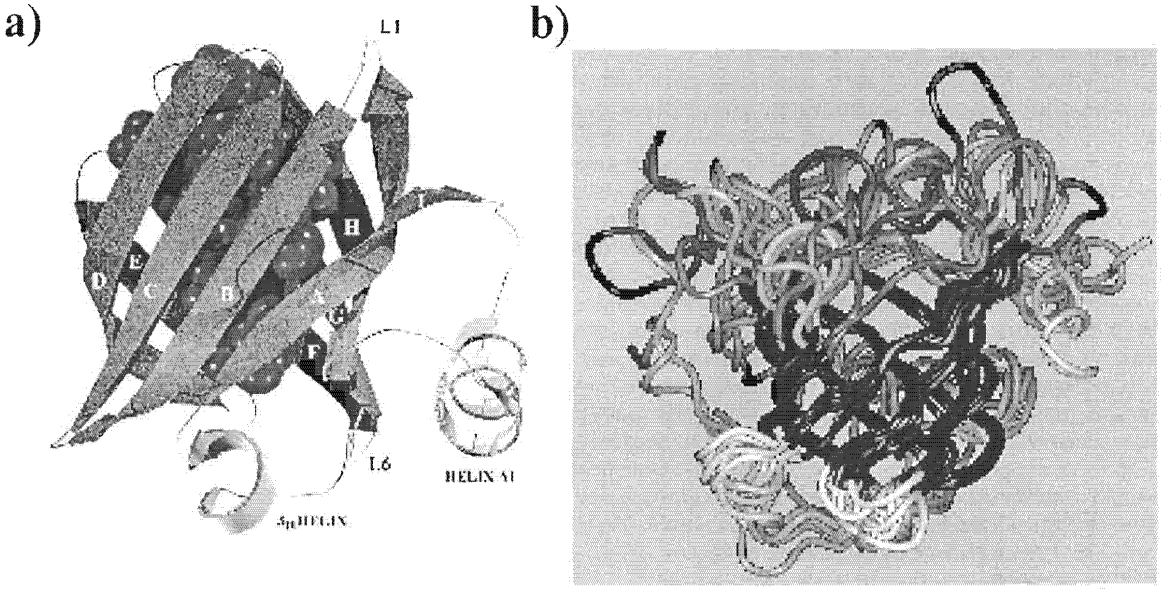

Fig. 7.1: The structure of the lipocalin fold. (a) A schematic drawing of the lipocalin fold with the ligand-binding pocket indicated by space filled spheres. Indicated is the N-terminal 3_{10} helix, the β-sheets (A-H) that form the barrel, the C-terminal α-helix and the single β-strand (I). Adapted from Flower, North and Sansom, (2000). (b) Superposition of six lipocalins that indicates the conserved nature of the β-barrel (black) and closed end (white) and the diversity observed for the variable loops at the open end of the barrel (grey shadings). Adapted from Skerra (2000).

7.1.4 Conserved motifs of the lipocalins

Although highly divergent in sequence, a number of sequence motifs specific for the lipocalins have been described. These structural conserved regions (SCRs) have been used to classify lipocalins into kernel (those that possess all three SCRs) and outlier (those that possess only one or two SCRs). SCR1 is found in the N-terminal 3_{10}-helix and is part of β-strand A. SCR2 comprises regions from both the F and G β-strands, as well as loop L6. SCR3 comprises part of the β-strand H and the C-terminal α-helix, although it corresponds closer to sequence conserved regions than structural topology (Fig. 7.2).

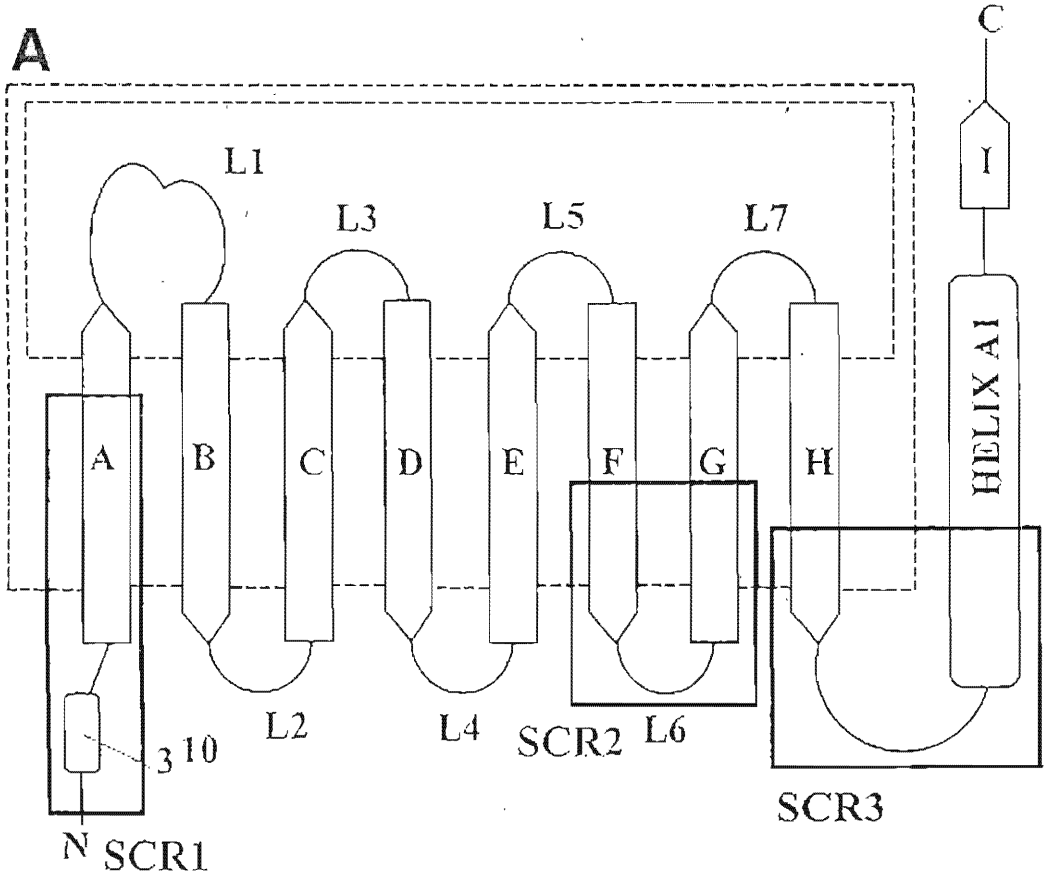

Fig. 7.2: An unwound view of the lipocalin structure. Indicated are the SCRs and their localization, the N-terminal 3_{10}-helix, the +1 topology of the 8 stranded (A-H) β-barrel linked by the short β-hairpin loops (L1-L7), with L2, L4 and L6 at the closed end and L1, L3, L5 and L7 at the open end of the barrel. Adjacent strands are H-bonded indicated by the dotted lines. The C-terminal α-helix and the short β-strand (I) complete the structure. Adapted from Flower, North and Sansom, (2000).

7.1.5 Evolution of the lipocalins

Lipocalins have been identified in prokaryotes, plants and animals (arthropoda and chordata). Prokaryotic and plant lipocalins so far identified are all outlier lipocalins, while both outlier and kernel lipocalins have been identified in animals. This suggests that an outlier lipocalin has been the earliest ancestor and that the conserved motifs of the kernel lipocalins have only appeared at a step in animal evolution that preceded arthopod/chordata divergence. All kernel lipocalins were probably derived from a single ancestor and could probably be traced more easily using phylogenetic methods than the outlier lipocalins that are much more diverged (Salier, 2000).

Evolution of lipocalins has been described using sequence distance, maximum parsimony and maximum likelihood methods. All methods group the lipocalins into various groups according to conserved function, although distance and parsimony methods failed to make any specific conclusions about the relationship between the functional groups (Ganfornina *et al.* 2000; Gutierrez, Ganfornina and Sanchez, 2000). Maximum likelihood was useful to describe relationships between functional groups so that a lineage could be traced from prokaryotic, through arthopoda up to the more recent mammalian lipocalins (Fig. 7.3). The mammalian lipocalins can be divided into ancient and modern lipocalins based on taxonomic representation. The lipocalins from clade II are considered to be ancient metazoan lipocalins based on their presence in arthropods and chordates. Clades III, V and VI are considered to be ancient vertebrate lipocalins and those from IV, VII-XIV to be modern lipocalins. General trends deduced from this analysis included a higher rate of sequence divergence and gene duplication, a reduction in binding surface area and an increase in ligand-binding contacts for modern lipocalins (Ganfornina *et al.* 2000; Gutierrez, Ganfornina and Sanchez, 2000). This analysis was biased however, in that only sequences that show more than 20% sequence identity to its closest relatives and sequences that contained at least two SCR motifs were used for this study. This means that many of the outlier lipocalins were left out from the study, which in evolutionary terms probably show the highest divergence of all lipocalins. It was stated that the outlier lipocalins were not included in the phylogenetic analysis due to problems with sequence alignment.

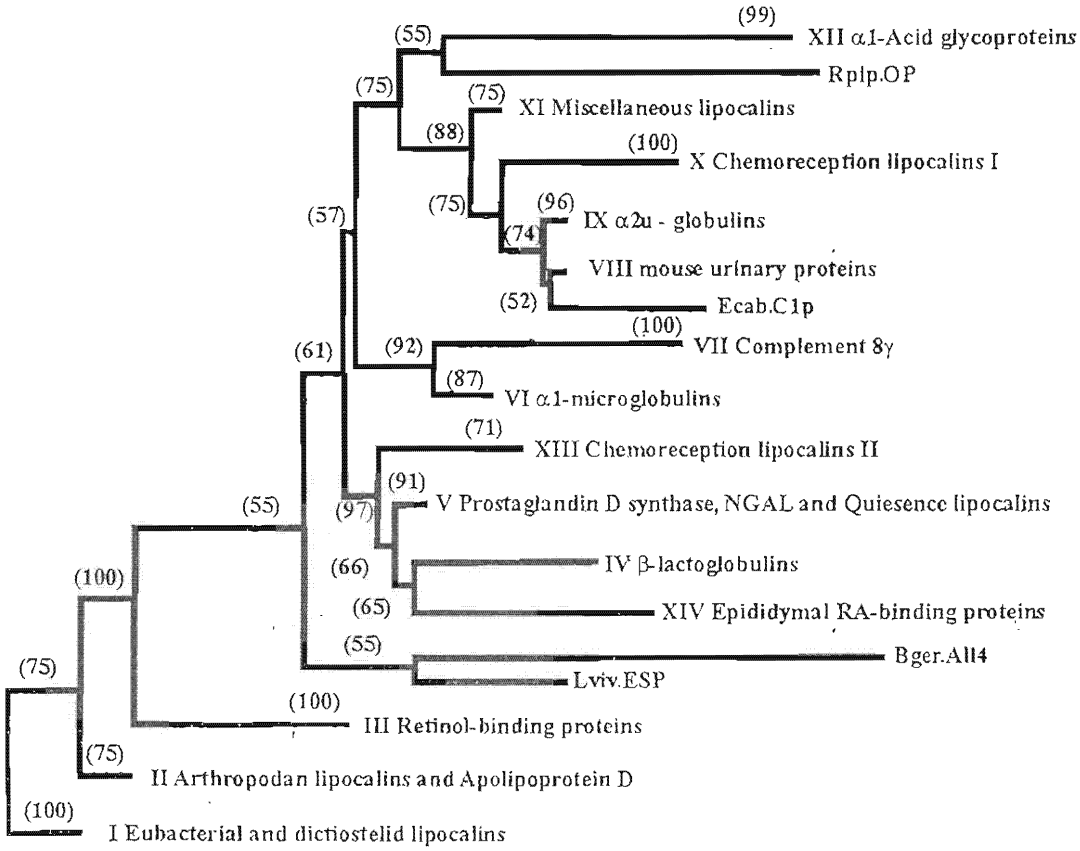

Fig. 7.3: A phylogenetic tree of the lipocalins. Eubacterial and dictyostelid lipocalins were used as outgroup (Clade I), followed by arthopod and mammalian apolipoprotein D lipocalins (clade II), found in metazoans. This is followed by the retinal binding proteins (clade III), β-lactoglobulins (clade IV) and prostaglandin D synthases (clade V) found only in vertebrates. Lipocalins found only in mammals give a more complex relationship, in that some group with lipocalins found only in vertebrates (the chemoreception lipocalins, clade XIII and epididymal RA-binding proteins, clade XIV) and other groups in in higher clades (VI-VIII, IX-XII). Adapted from Gutierrez, Ganfornina and Sanchez (2000).

7.1.6 Lipocalins from hematophagous organisms

Lipocalins have been found in the salivary gland secretions from various hematophagous organisms. Lipocalins identified include seven from *Rhodnius prolixus*, two from *Triatoma pallidipennis*, one from the hard tick *R .appendiculatus*, at least two from the soft tick *O. moubata* and at least four from the soft tick *O. savignyi* (Montford, Weichsel and Andersen, 2000; Mans *et al.* 2001). In *R. prolixus* at least four lipocalins carry heme and are called the nitrophorins (NP1-NP4). All four proteins carry nitric oxide, which is released at the feeding site, causing smooth muscle relaxation and vasodilation (Champagne, Nussenzvieg and Ribeiro, 1995). All four proteins can also regulate

inflammation and the host's immune response by binding histamine. NP2 (prolixin-S) can also inhibit the conversion of fX to fXa (Ribeiro, Schneider and Guimares, 1995). Another three lipocalins from *R. prolixus* do not contain heme, but inhibit platelet aggregation by sequestration of the agonist ADP (Francischetti *et al.* 2000). *T. pallidipennis* inhibits specifically collagen-induced platelet aggregation via the lipocalin, pallidipin (Noeske-Jungblut *et al.* 1994). Triabin is another lipocalin that inhibits thrombin's activity by targeting the fibrinogen-binding exosite (Noeske-Jungblut *et al.* 1995). In the case of triabin an interesting deviation in its topology occurred with an exchange of β-strands B and C of the β-barrel (Feuntes-Prior *et al.* 1997).

In hard ticks, the histamine-binding proteins (HBP1-3) have been identified in *R. appendiculatus* (Paesan *et al.* 1999). Two histamine-binding sites have been described in these lipocalins and they presumably function in the regulation of inflammation during the long feeding periods of hard ticks (Paesan *et al.* 2000). The structurally conserved motifs (SCR1-3) used for lipocalin designation are present in the core lipocalins, while one or more are normally absent in the outlier lipocalins (Flower, 1996; Flower *et al.* 2000). All SCRs are absent in the tick lipocalins although the structure of HBP2 shows lipocalin topology (Paesen *et al.* 1999). Moubatin, an inhibitor of collagen-stimulated platelet aggregation has been described for the soft tick, *O. moubata* and is also a lipocalin based on sequence similarity to the HBPs (Waxman and Connolly, 1993; Keller *et al.* 1993; Paesen *et al.* 1999). TAI an inhibitor of collagen specific cell adhesion (Karczewski *et al.* 1995) has also been identified as a lipocalin based on a sequence contained in a patent (European patent application number 92311218.9) (Guido Paesen and Patricia Nuttall, personal communication).

7.2 Materials and methods

7.2.1 Cloning and sequencing of TSGPs

The strategy used to clone and sequence the TSGPs were described in Chapter 2. Degenerate primers were designed from the obtained N-terminal amino acid sequences. For TSGP1 a primer (20kD: GGI CCI GAY GGI TGY GT) was designed using the first 6 amino acids (GPDGCV), for TSGP2 the primer (TOE: TTY CCI ACI GAR GCN TA) was

designed from amino acids 6-11 (FPTEAY) and for TSGP3 the primer (TOC: TTY CCI ACI GAY GCN TA) was also designed from amino acids 6-11 (FPTDAY), while the primer for TSGP4 (Toks1: GCN AAY GAY GTI TGG AAY GT) was designed from the first 7 amino acids (ANDVWNV). Note that amino acid residue 6 of both TSGP2 and TSGP3 are indicated as phenylalanine. Results obtained with 3'RACE indicated that this position in both sequences is a lysine. This was due to an initial misidentification of lysine for phenylalanine during N-terminal sequence analysis. Original primers (TOKSA: GAY TGY CCN ACN GGI TTY C; TOKSB: GAY TGY CCN ACN GGI TTY CCI AC) designed from the first 6 or 8 amino acids (DCPTGF, DCPTGFPT) yielded spurious products due to mispriming of the phenylalanine. TOKSA amplified ferritin (a 600 bp product), while TOKSB amplified actin (800 bp product) (results not shown). 3'RACE and 5'RACE were performed as described using an annealing temperature of 55 °C and performing 27 cycles. 5' RACE primers used were for TSGP1 (20KDC1: GTG TAG GGG ATG GGG CCA), TSGP2 and (C1T2: CTA GCA GTC CTT GTC TT) and TSGP3 (NTC1: GTT CCA ACA TCC ACA TG), TSGP4 (C1T1: CTA CGG AAC TCT GCA GCC TT). 20KDC1 is complementary to a region in the 3' untranslated region of TSGP1. C1T2 are complementary to the last five amino acids and stop codon of TSGP2 (QDKDC-). NTC1 is complementary to an internal sequence (DMWMLE) of TSGP3 that differs from that of TSGP2 (EMWMLE) at the last position in the codon of aspartic acid. C1T1 is complementary to the last five amino acids and stop codon of TSGP4 (EGCRVP-). Sequences were analyzed as described in Chapter 2.

7.2.2 Multiple alignment of lipocalins

Multiple alignment was performed using ClustalX (Jeanmougin *et al.* 1998), using an identity matrix based on the secondary structures of crystallized lipocalins (Ganfornina *et al.* 2000; Gutiérrez, Ganfornina and Sanchez, 2000).

7.2.3 Phylogenetic analysis of lipocalins

Phylogenetic analysis was performed on sequences in which all gapped positions were ignored using Neighbor-Joining analysis with the Mega2 software package (Kumar, Tamura and Nei, 1994).

7.2.4 Molecular modeling of lipocalins

Structures of the TSGPs were modeled on that of Ra-HBP2 (Paesen *et al.* 1999) using MODELLER (Sali *et al.* 1995). Structures were validated using PROCHECK (Laskowski *et al.* 1996) and WHATIF (Vriend, 1990) and backbone deviations obtained using ProFitV1.8 (http://www.biochem.ucl.ac.uk/~martin/#profit). Surface models were generated with GRASP (Nicholls, Sharp and Honig, 1991).

7.2.5 Partial purification of savignygen

During the present study it became clear that TSGP2 and TSGP3 showed high sequence similarity (73%) to moubatin (Keller *et al.* 1993). In order to investigate the possibility that TSGP2 or TSGP3 might be moubatin orthologs, SGE was fractionated and assayed for inhibitory activity towards collagen-induced platelet aggregation. The microplate method described in Chapter 2 was used, but instead of activating platelets with ADP, 2μg collagen (Diagnostica Stago) was used. Before use collagen (100 μl of 2 mg/ml stock solution) was first diluted in 1900 μl 150 mM Tris-HCl, pH 7.8 and incubated at 37 °C for 3 minutes. SGE was fractionated using RPHPLC as described in Chapter 6 and all fractions assayed by drying 100 μl (from each milliliter fraction) and redissolving in 100 μl buffer (0.15M NaCl, 20 mM Tris-HCl, pH 7.4) before using 10 μl for each experiment. All experiments were done in duplicate. Positive fractions were then dried before application to AEHPLC as described in Chapter 2. Fractions collected were again tested before rechromatography using RPHPLC. As sequence similarity between TSGP2 and TSGP3 have been indicated, fractions from the RPHPLC were also probed using western blotting with polyclonal sera directed against TSGP2.

7.3 Results

7.3.1 RACE of the TSGPs

RACE procedures were performed for the TSGPs. 5'-RACE and 3'-RACE under optimized conditions gave products for TSGP1 (~600bp, ~600bp), TSGP2 (~600bp, ~500bp), TSGP3 (~600bp, ~500bp), TSGP4 (~600bp, ~650bp), respectively (Fig. 7.4). The 5'-RACE products include the 5'UTR, the gene coding for the mature as well as immature protein. The 3'-RACE products include the coding gene, 3'-UTR and poly-A tail sequences.

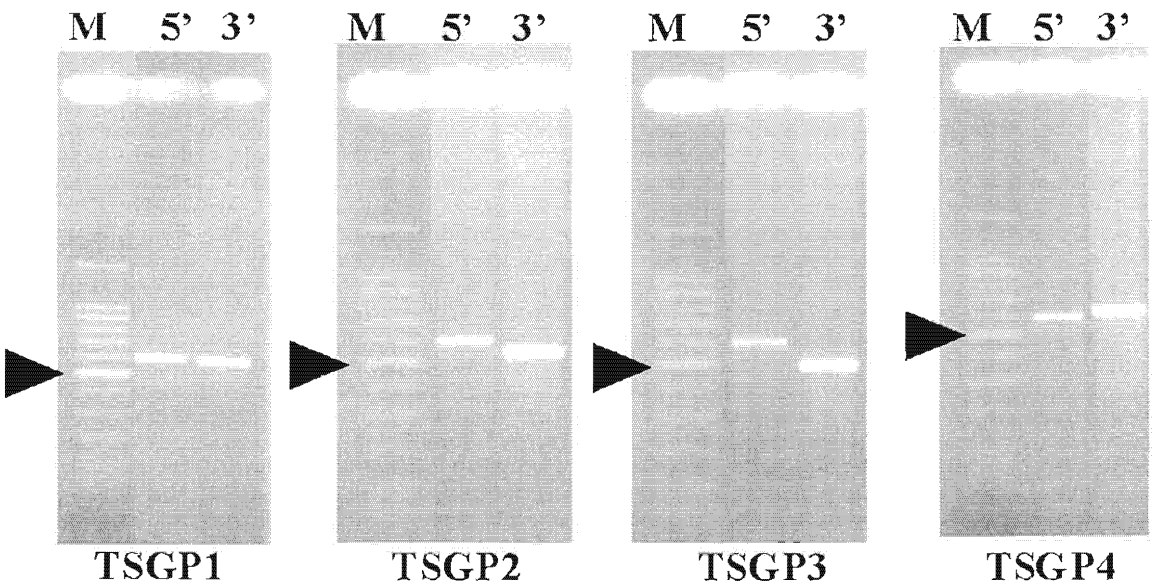

Fig. 7.4: RACE of the TSGPs. Indicated are the results for 5'-RACE and 3'-RACE of TSGP1-4. Arrowheads indicate the 500 bp band.

7.3.2 Amino acid sequences of the TSGPs

Full-length sequences for the TSGP1-4 and savignygen were obtained by overlapping of 5'RACE and 3'RACE product sequences. The sequence lengths corresponded well with the lengths of the RACE products obtained (results not shown). The full-length gene sequences of TSGP1 (673bp), TSGP2 (609bp) and TSGP3 (610bp) and TSGP4 (673bp) all include a stop codon, poly-adenylation site (TSGP1/TSGP4: AATAAA and TSGP2/TSGP3: AGTAAA) and a poly-A tail (Fig. 7.5-7.7). The AGTAAA site was previously also identified in savignin, a thrombin inhibitor from this tick species (Chapter

3). The translated amino acid sequences of the immature proteins contain a signal peptide and consisted of 190 amino acids (TSGP1), 163 amino acids (TSGP2 and TSGP3) and 176 amino acids (TSGP4). Signal P predicted the presence of the signal peptide and the correct cleavage site in all cases (von Heijne, 1990; Nielsen *et al.* 1997). The mature proteins consist of 171 amino acids (TSGP1), 144 amino acids (TSGP2 and TSGP3) and 156 amino acids (TSGP4) that include the previously determined N-terminal sequences (Chapter 6). Of interest is Glu16 in the mature TSGP2/TSGP3 sequences, which showed up as a unidentified amino acid during N-terminal sequencing (Chapter 6). The elution profile of this residue during N-terminal sequencing (personal observation), possibly indicate carboxyl methylation, which could probably be involved in salivary gland granule packaging and exocytotic secretion (Van Waarde, 1987).

```
tcactatagggctcgagcggccccgcccgggcaggtaagatgcaacggc                    M  Q  R  L  L  L  L      7'

ctgattgccctgttctcgctcagctgtgctgaagcagggccggatgggtgcgtgggtagt  -  120
 L  I  A  L  F  S  L  S  C  A  E  A  G  P  D  G  C  V  G  S      27'

acagaggctaaggtggctgtatttggagaaggtggaaatgcaggatctccaactataggg  -  180
 T  E  A  K  V  A  V  F  G  E  G  G  N  A  G  S  P  T  I  G      47'

tactcttaccttgtgaagacaacctatcctgatgaacatgcttgtgtttacattcttcca  -  240
 Y  S  Y  L  V  K  T  T  Y  P  D  E  H  A  C  V  Y  I  L  P      67'

ccctatggcacagcggacgctagtggccgctacccttaccgcatggggtacaaggactca  -  300
 P  Y  G  T  A  D  A  S  G  R  Y  P  Y  R  M  G  Y  K  D  S      87'

aacgatcagtgggtgaagctggatgggaagatcaaaaccgagggcagcaaaatcatcgac  -  360
 N  D  Q  W  V  K  L  D  G  K  I  K  T  E  G  S  K  I  I  D     107'

aacgacccggaatatggcgacactgtgaccacggtgctctacactcaccttgggggtgga  -  420
 N  D  P  E  Y  G  D  T  V  T  T  V  L  Y  T  H  L  G  G  G     127'

tgtgacgttacactcttcgaagggcaaaagggccagagcaaagtacaaggaccattcctg  -  480
 C  D  V  T  L  F  E  G  Q  K  G  Q  S  K  V  Q  G  P  F  L     147'

gaactgtggtaccacagtggagcaagtgaagaatccatgcggtgctgcgaggaagagttt  -  540
 E  L  W  Y  H  S  G  A  S  E  E  S  M  R  C  C  E  E  E  F     167'

aggaagaatcttaaggaagggacggctgttcgaaaggttaacaagaactgtgactatggg  -  600
 R  K  N  L  K  E  G  T  A  V  R  K  V  N  K  N  C  D  Y  G     187'

gacgtcgcctagaagaatgcgtgaactggccccatcccctacacgaacgctcgaaaaaaaa  -  660
 D  V  A  -                                                     190'

aaaaaataaagaaagaaatacaaatcataaaaaaaaaaaaaaaaaaaagagtgttgtggt  -  720

aatgatagc                                                      -  729
```

Fig. 7.5: Full-length sequence of TSGP1. The 5' adapter, 3' gene specific and 3' anchor primers are shown in bold. The stop codon (TAG), poly-adenylation site (AATAAA) and poly-A tail are boxed. The N-terminal amino acid sequence previously obtained with N-terminal Edman degradation is underlined in a solid line and the signal sequence is underlined with a dashed-line. The N-terminal sequence used for degenerate primer design is shown in bold. The Genbank accession code for TSGP1 is AF452888.

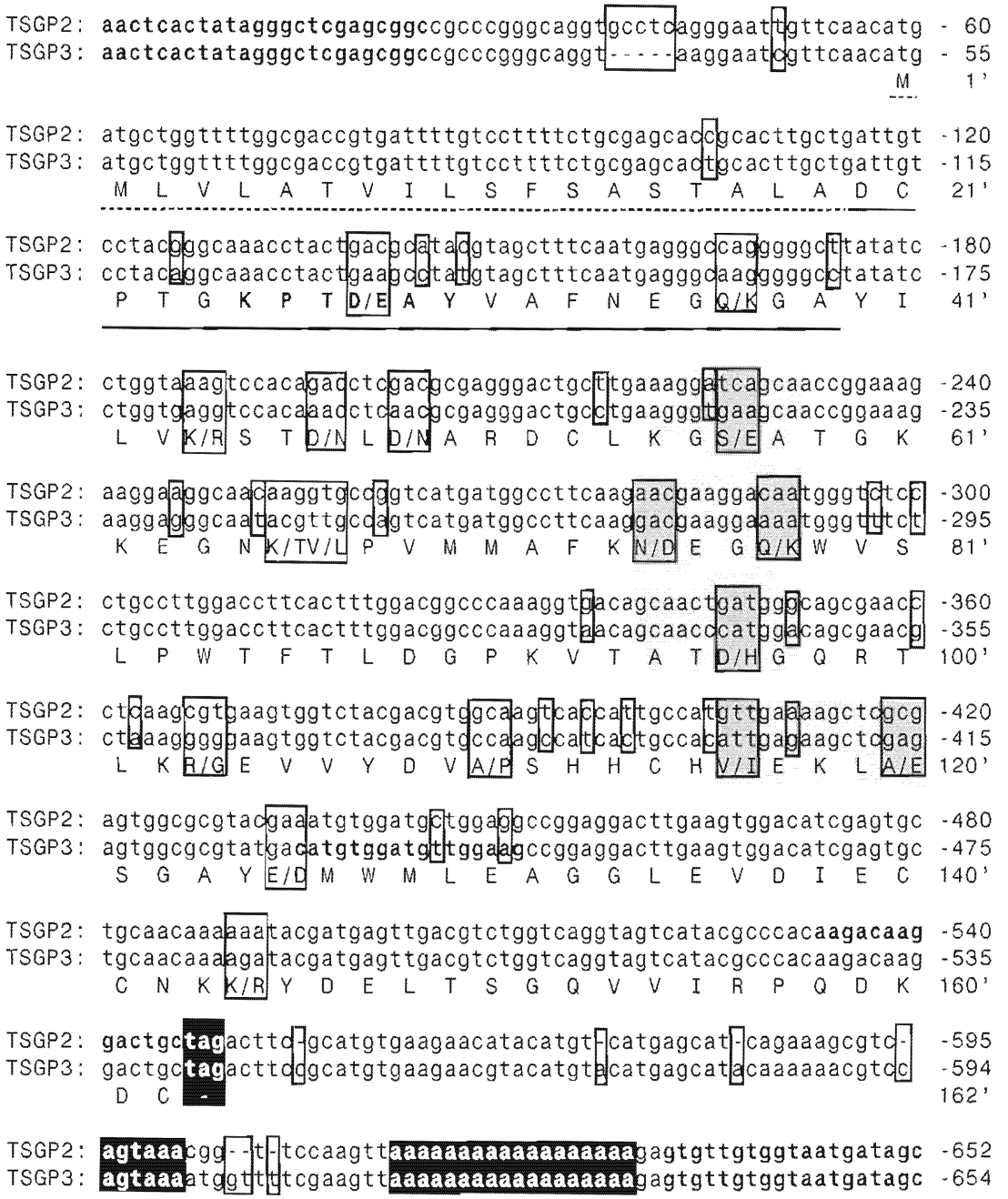

Fig. 7.6: Full-length sequences of TSGP2 and TSGP3. Synonymous nucleotide differences are boxed, while non-synonymous differences are boxed in gray. The 5' adapter, 3' gene specific and 3' anchor primers are shown in bold. The stop codon (TAG), poly-adenylation site (AGTAAA) and poly-A tail are indicated by black boxes. For the deduced amino acid sequences, the differences are indicated by a slash (TSGP2/TSGP3). The N-terminal amino acid sequences previously obtained with N-terminal Edman degradation is underlined in a solid line and the signal sequence is underlined with a dashed-line. The N-terminal sequences used for degenerate primer design is shown in bold. The Genbank accession code for TSGP2 and TSGP3 are AF452889 and AF45890, respectively.

```
aactcactatagggctcgagcggcccgcccgggcaggtcgataaaca

tcgctgcgtaacggaacgaatatggactgcaagcttgtcgccatcgcgctcttcattttc - 120
                          M  D  C  K  L  V  A  I  A  L  F  I  F    13'
tccctagattttgcacatgcggctaacgacgtatggaacgtcctcaaaggcagcgattca - 180
 S  L  D  F  A  H  A  A  N  D  V  W  N  V  L  K  G  S  D  S    33'

aagtttcttatggtcaagagaacatatgaaagaggagcaaacaaatgtgtgtacatgaaa - 240
 K  F  L  M  V  K  R  T  Y  E  R  G  A  N  K  C  V  Y  M  K    53'

cgtacgagcatggacgaaagcagtcatacacttgaagtacttatgggatattcgaaggcg - 300
 R  T  S  M  D  E  S  S  H  T  L  E  V  L  M  G  Y  S  K  A    73'

gggacaacgacggacttcgtagagccatctaagtatactgtgacagcaactagtgagggt - 360
 G  T  T  T  D  F  V  E  P  S  K  Y  T  V  T  A  T  S  E  G    93'

gcaagcacctacaatatgatgactgtgagaaggggacctgcctcgcatggtgtcaaattc - 420
 A  S  T  Y  N  M  M  T  V  R  R  G  P  A  S  H  G  V  K  F   113'

gagctggtgtacagcgatgaccaaggctgcaatattctgcaaatgaagacgagtccattt - 480
 E  L  V  Y  S  D  D  Q  G  C  N  I  L  Q  M  K  T  S  P  F   133'

ccaggaaaatgcgaactgtgggcgccggaaggcaaggcaaagaatgtggaaagcagttgc - 540
 P  G  K  C  E  L  W  A  P  E  G  K  A  K  N  V  E  S  S  C   153'

agcggcaagttcaaggagttatgtggcgacgcagtggaaacgccctacgcagaaggctgc - 600
 S  G  K  F  K  E  L  C  G  D  A  V  E  T  P  Y  A  E  G  C   173'

agagttccgtagttcctggccagattcacagttgtggaactgttttctgaacagactaat - 660
 R  V  P  -                                                    176'

aaagctttaaggcagacagagcaaaaaaaaaaaaaaaaaagagtgttgtggtaatgatag - 720
```

Fig. 7.7: Full-length sequence of TSGP4. The 5' adapter, 3' gene specific and 3' anchor primers are shown in bold. The stop codon (TAG), poly-adenylation site (AATAAA) and poly-A tail are boxed. The N-terminal amino acid sequence previously obtained with N-terminal Edman degradation is underlined in a solid line and the signal sequence is underlined with a dashed-line. The N-terminal sequence used for degenerate primer design is shown in bold. The Genbank accession code for TSGP4 is AF452891.

7.3.3 Comparison of data from native toxins and deduced amino acid sequences

Amino acid compositions of the deduced amino acid sequences compare favorably with data from the native proteins (Table 7.1). The calculated molecular masses also correlate well with those obtained from the ESMS analysis. From these data it is clear that the toxins are not glycosylated, in contrast to previous reports (Neitz *et al.* 1983).

Table. 7.1: Comparison of the amino acid composition from the TSGPs and their deduced amino acid sequences. Indicated are molar ratio's determined using Ile as 1. In the case of TSGP1, TSGP2 and TSGP3 the values were multiplied by a factor that gives six cysteines, as this was determined independently using MALDI-TOF-MS. Also indicated are calculated molecular masses from the amino acid composition and deduced sequences as well as masses obtained from ESMS.

Amino acids	TSGP1		TSGP2		TSGP3		TSGP4	
	AA	Seq	AA	Seq	AA	Seq	AA	Seq
Asx	15	18	15	16	14	15	11	13
Glx	16	17	16	15	16	15	14	14
Ser	10	10	6	6	5	5	14	15
Gly	21	23	13	13	14	14	13	13
His	3	3	3	3	4	4	2	2
Arg	3	5	4	4	4	4	6	6
Thr	11	12	11	11	12	12	13	13
Ala	10	9	10	10	8	8	9	10
Pro	8	8	6	6	7	7	7	7
Tyr	9	12	5	5	5	5	6	7
Val	13	13	12	13	9	11	12	13
Met	1	2	4	4	4	4	6	7
Cys	6	6	6	6	6	6	6	6
Ile	5	5	3	3	4	4	1	1
Leu	9	9	10	10	11	11	8	8
Phe	4	4	3	3	3	4	5	5
Lys	13	13	13	13	13	12	15	14
Total	157	169	140	141	139	141	148	154
Mr	16699	18613	15238	15872	15328	15950	16143	17161
ESMS		18422		15877		15957		17170

Theoretical trypsin peptide mapping corresponds well with peptide mass fingerprints previously obtained (Table 7.2). It also shows correspondence between peptide fragments across the full-length of the TSGP sequences. These results indicate that the correct sequences have been obtained. In the case of TSGP1 there were however, a few peptides that could not be matched to the sequence. RPHPLC did however, indicate that TSGP1 eluted as a broad tailing peak (Chapter 6) that could indicate microheterogeneity on sequence level.

Table 7.2: A comparison of a theoretical tryptic digest of the TSGPs with peptide mass fingerprints previously obtained by MALDI-TOF-MS. Amino acid residues for the different fragments are indicated in parenthesis.

TSGP1		TSGP2		TSGP3		TSGP4	
MS	Sequence	MS	Sequence	MS	Sequence	MS	Sequence
1226	1-12 (1225)			869.8	869 (74-81)	2173.8	2171.4 (16-34)
599.2	59-62 (597.7)	1858.1	1858 (86-100)	1954.5	1954 (85-100)	2085.8	2083.3 (65-83)
2691	143-163 (2697)	1977.5	1977 (126-142)	1976.7	1976 (126-142)	909	908 (84-93)
1319		1849.4	1848 (127-142)	1848.2	1848 (127-142)	2110	2108.4 (93-109)
1391						1138.7	1137.3 (117-125)
1754						1925.7	1923.2 (139-154)

7.3.4 Multiple alignment of tick lipocalins

BLAST analysis of the TSGPs indicated identity to moubatin, a collagen-specific platelet aggregation inhibitor (Fig. 7.8) (Keller *et al.* 1993). Moubatin shows distant similarity to the histamine-binding proteins from the tick *R. appendiculatus* (Paesen *et al.* 1999). Alignment of TSGP1-4 with moubatin and the female HBP2 and male HBP3 shows that there is significant similarity, although identities are very low between sequences. The structural conserved motifs (SCR1-3) used for lipocalin designation are present in the core lipocalins, while one or more are normally absent in the outlier lipocalins (Flower, 1996; Flower *et al.* 2000). All SCRs are absent in the tick lipocalins although the structure of HBP2 show lipocalin topology (Paesen *et al.* 1999). The highest conserved

regions of the tick lipocalins correspond with that of the secondary structure previously obtained for HBP2 and consists of two N-terminal α-helixes, a 8 stranded anti-parallel β-barrel with a $(+1)_7$ topology and a C-terminal α-helix, characteristic of the lipocalin fold (Paesen *et al.* 1999).

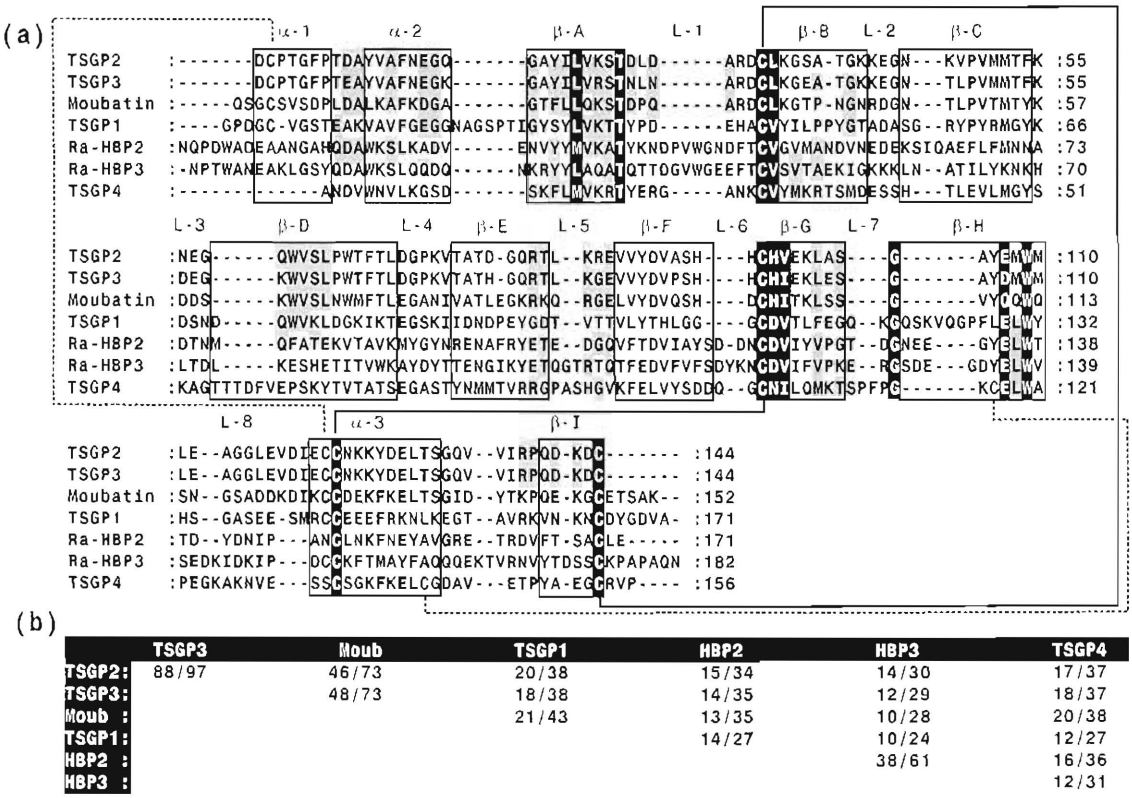

	TSGP3	Moub	TSGP1	HBP2	HBP3	TSGP4
TSGP2:	88/97	46/73	20/38	15/34	14/30	17/37
TSGP3:		48/73	18/38	14/35	12/29	18/37
Moub :			21/43	13/35	10/28	20/38
TSGP1:				14/27	10/24	12/27
HBP2 :					38/61	16/36
HBP3 :						12/31

Fig. 7.8: Multiple sequence alignment of the tick lipocalins. (a) Alignment of TSGPs with the HBPs from the hard tick, *R. appendiculatus* and moubatin, from the soft tick *O. moubata*, the inhibitor specific for collagen-induced platelet aggregation. Secondary structures based on that of Ra-HBP2 are boxed and designated as α-helixes or β-strands. Solid lines indicate conserved cysteines and their corresponding disulphide bonds, as deduced from the structure of Ra-HBP2. Dotted lines indicate hypothetical disulphide bonds of the remaining cysteines for moubatin, TSGP1-3 and TSGP4. (b) Percentage identity/similarity between the different sequences are indicated.

7.3.5 Phylogenetic analysis of tick derived lipocalins in relation to the lipocalin family

Previous phylogenetic analysis of the lipocalins excluded those from blood-feeding organisms, due to the low sequence similarity (<20% identity) with other lipocalins and the absence of SCR motifs (Ganfornina *et al.* 2000; Gutiérrez *et al.* 2000). The extreme

divergence of these lipocalins can introduce serious artefacts in the phylogenetic trees due to long branch attraction. While it would thus be difficult to determine an accurate relationship of tick lipocalins within the larger lipocalin family, phylogenetic analysis could be used to assess their homology and investigate their relationships within a tick lipocalin clade. The alignment of the lipocalin family previously employed to investigate lipocalin evolution (Ganfornina *et al.* 2000; Gutiérrez *et al.* 2000), was used as a profile to align both tick lipocalins as well as lipocalins from triatomine bugs. It is clear that the lipocalin family is highly divergent as exemplified by the low levels of sequence similarity indicated (Fig. 7.9). Only a few residue sites are conserved across the family and correspond to the SCR regions as indicated. From this it is clear that tick lipocalins are outliers even though a few residues in the SCRs are also found in the tick lipocalins.

Figures on following pages

Fig. 7.9: Alignment of the lipocalin family used for phylogenetic analysis. Indicated are the different monophyletic clades into which the lipocalins are grouped as well as the regions corresponding to SCRs of core lipocalins. Indicated are similarities based on the PAM 250 matrix (DNQH, SAT, KR, FY, LIMV) at 80% identity.

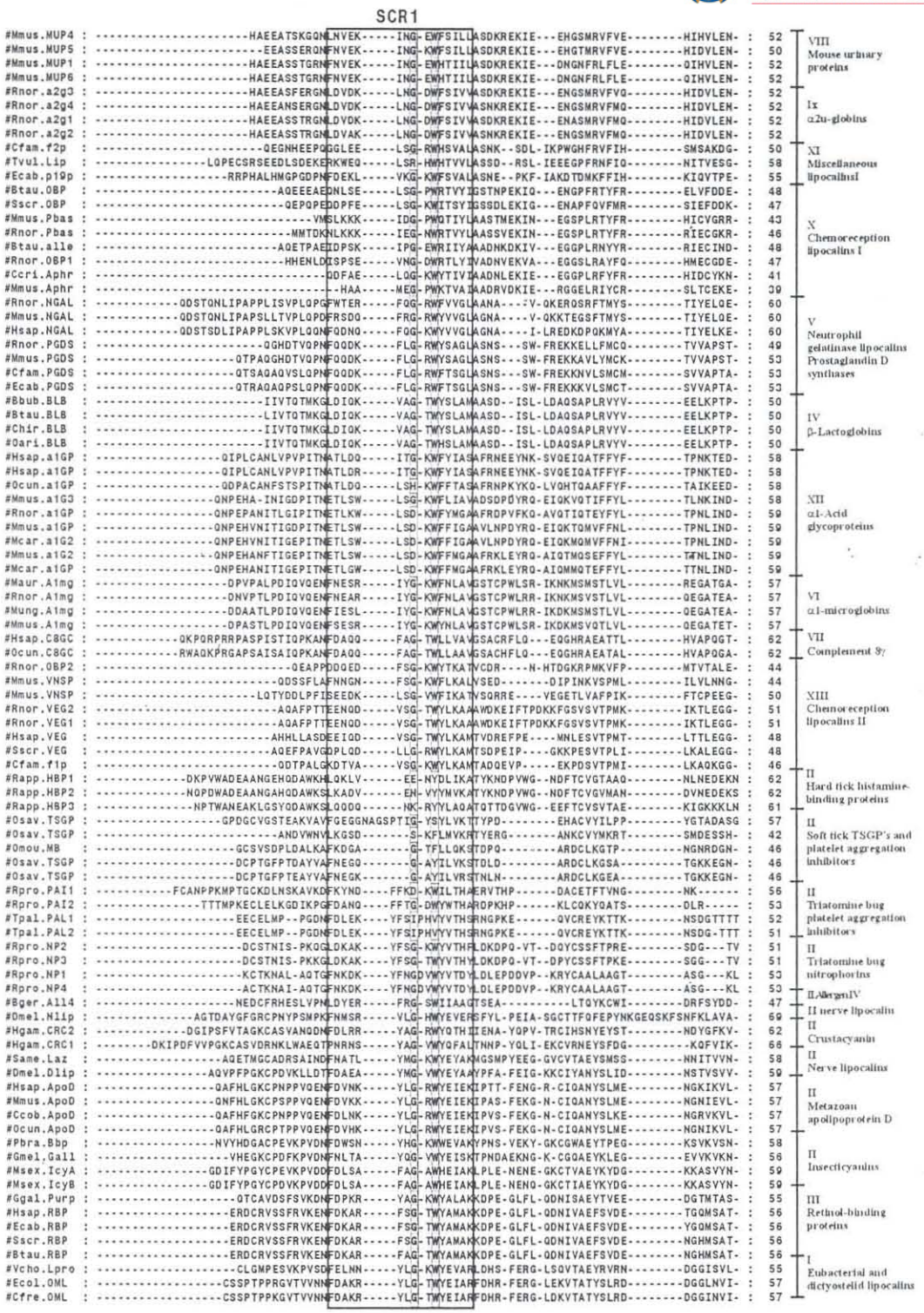
SCR1
VIII
Mouse urinary proteins
IX
α2u-globins
XI
Miscellaneous lipocalins
X
Chemoreception lipocalins I
V
Neutrophil gelatinase lipocalins
Prostaglandin D synthases
XII
α1-Acid glycoproteins
IV
β-Lactoglobins
VII
Complement 8γ
XIII
Chemoreception lipocalins II
VI
α1-microglobins
II
Hard tick histamine-binding proteins
II
Soft tick TSGP's and platelet aggregation inhibitors
II
Triatomine bug platelet aggregation inhibitors
II
Triatomine bug nitrophorins
II
II Allergen IV
II nerve lipocalin
II
Crustacyanin
II
Nerve lipocalins
II
Metazoan apolipoprotein D
II
Insecticyanins
III
Retinol-binding proteins
I
Eubacterial and dictyostelid lipocalins

Fig. 7.9 (Page 1)

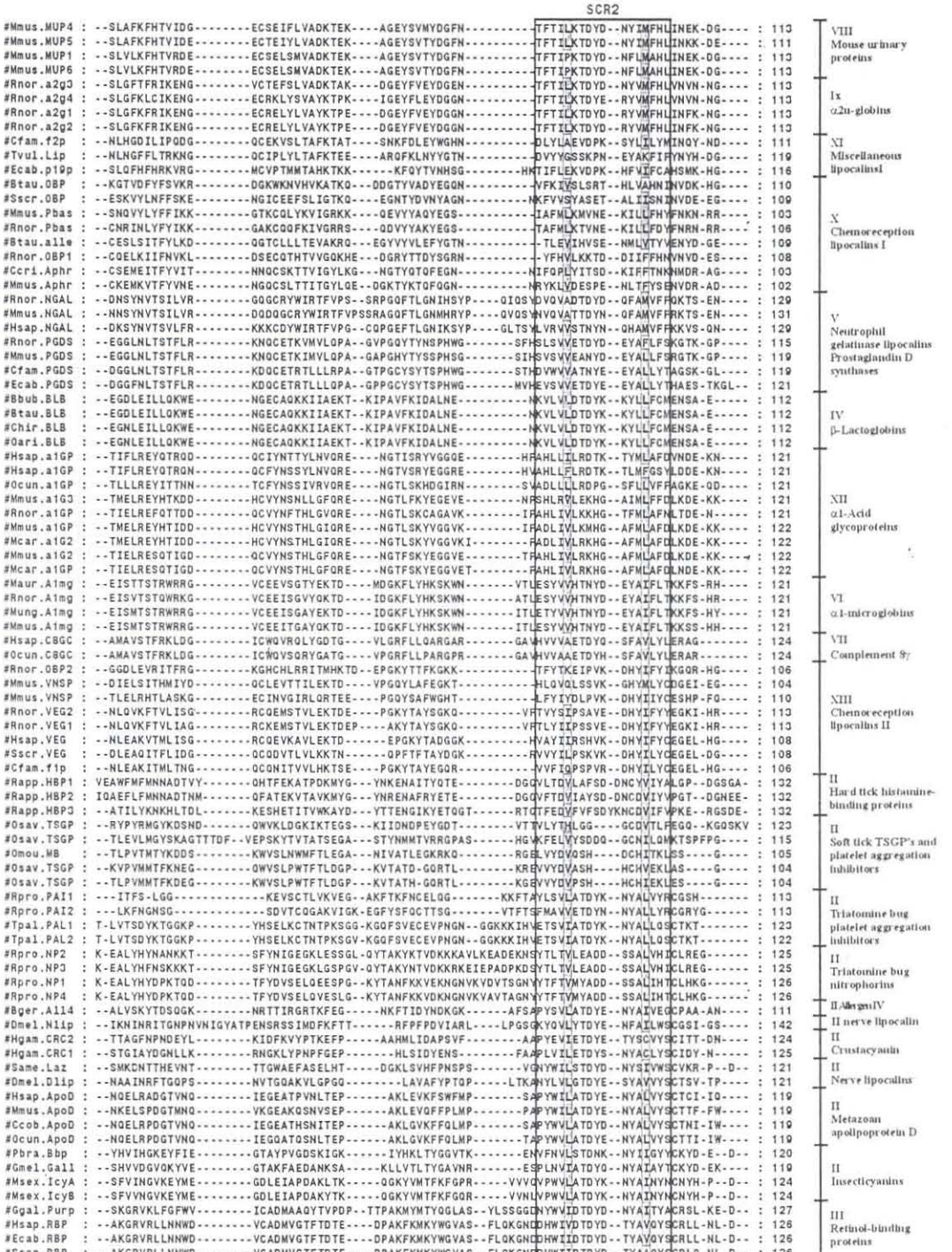
SCR2
VIII Mouse urinary proteins
Ix α2u-globins
XI Miscellaneous lipocalins
X Chemoreception lipocalins I
V Neutrophil gelatinase lipocalins Prostaglandin D synthases
IV β-Lactoglobins
XII α1-Acid glycoproteins
VI α1-microglobins
VII Complement 9γ
XIII Chemoreception lipocalins II
II Hard tick histamine-binding proteins
II Soft tick TSGP's and platelet aggregation inhibitors
II Triatomine bug platelet aggregation inhibitors
II Triatomine bug nitrophorins
II Allergen IV
II nerve lipocalin
II Crustacyanin
II Nerve lipocalins
II Metazoan apolipoprotein D
II Insecticyanins
III Retinol-binding proteins
I Eubacterial and dictyostelid lipocalins

Fig. 7.9 (Page 2)

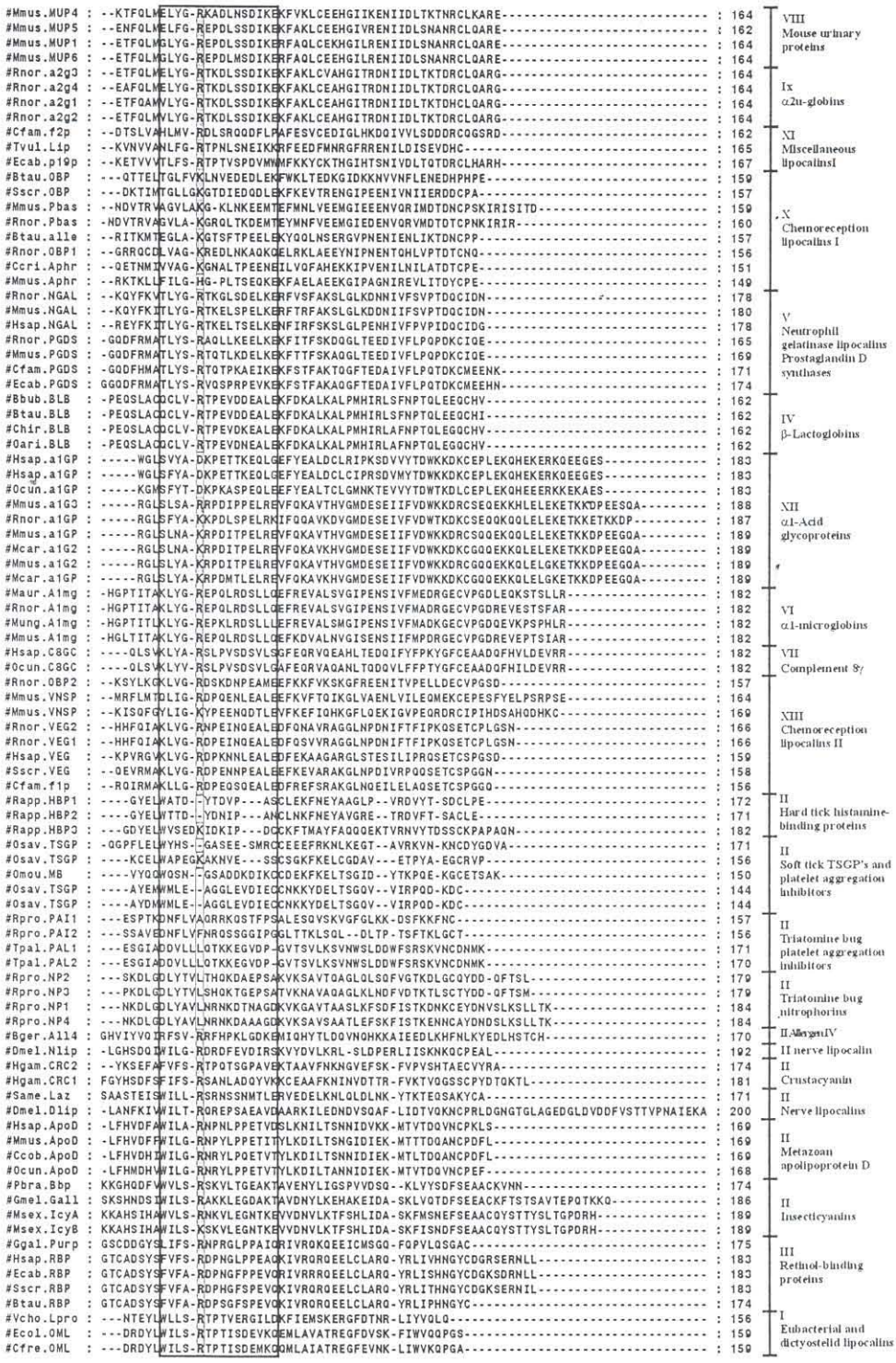
SCR3
VIII Mouse urinary proteins
Ix α2u-globins
XI Miscellaneous lipocalins!
X Chemoreception lipocalins I
V Neutrophil gelatinase lipocalins Prostaglandin D synthases
IV β-Lactoglobins
XII α1-Acid glycoproteins
VI α1-microglobins
VII Complement 8γ
XIII Chemoreception lipocalins II
II Hard tick histamine-binding proteins
II Soft tick TSGP's and platelet aggregation inhibitors
II Triatomine bug platelet aggregation inhibitors
II Triatomine bug nitrophorins
II Nerve lipocalin
II Crustacyanin
II Nerve lipocalins
II Metazoan apolipoprotein D
II Insecticyanins
III Retinol-binding proteins
I Eubacterial and dictyostelid lipocalins

Fig. 7.9 (Page 3)

Although the global tree obtained for the lipocalins using neighbor-joining, differ from that obtained with maximum likelihood, the main monophyletic clades were still present (Fig. 7.10). The groupings within individual monophyletic clades were also essentially the same as found previously (Ganfornina *et al.* 2000; Gutiérrez *et al.* 2000). The lipocalins were still grouped into ancient lipocalins (clades I-III) which still formed a superclade although at cut-off value of 45% confidence, most arthropod groups from clade II were collapsed onto the main branch. This does however, give a better approximation of the true minimum evolutionary tree and shows that the sequences from clade II is problematic. The modern lipocalins (IV-XIII) grouped into a superclade of which the internal relationships differed from previous analysis. Clades VIII-XI, VI-VII and IV-V still grouped as supergroups. The positions of clades XIII (grouping with VI and VII) and XII (grouping with IV) differered from previous analysis where XIII grouped with clades V-IV and XII grouped in a separate clade with IX, X, XI and VIII (Fig. 7. 3). A lipocalin from cockroach (Bger.All4) previously grouped between the ancient and modern superclades, separated from the arthropod clade II (Gutiérrez *et al.* 2000). It was suggested that this is an artefact that reflects the inability of categorizing highly divergent sequences, although it does show sequence similarity to the nitrophorins. Of interrest is that both Bger.All4 and the triatomine bug lipocalins (nitrophorins as well as platelet aggregation inhibitors grouped into a monophyletic clade) as well as the tick lipocalins were placed between the ancient and modern lipocalins. Tick lipocalins grouped as a monophyletic clade, confirming that they are homologous. Internally, the tick lipocalins grouped into two monophyletic sub-clades composed of the hard tick (HBP) and the soft tick (TSGPs and moubatin) lipocalins.

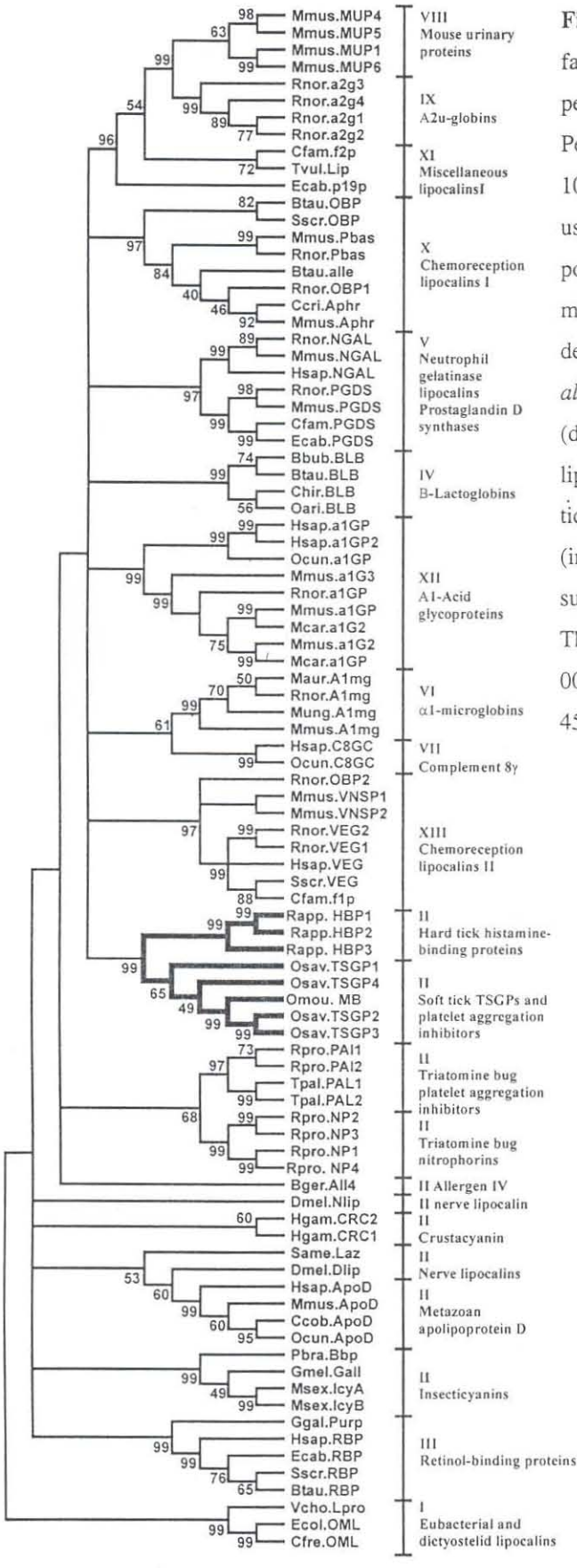

Fig. 7.10: Phylogenetic analysis of the lipocalins family. Neighbor-joining analysis were performed based on amino acid differences. Percentage confidence levels indicated are for 10000 bootstraps. The tree obtained was rooted using the eubacterial lipocalins. All gapped positions were ignored. Indicated is the different monophyletic clades (I-XIII) previously described (Ganfornina *et al.* 2000; Gutiérrez *et al.* 2000). Also present is a new clade (designated part of clade II) into which the lipocalins from the triatomine bugs group. The tick lipocalins group into a monophyletic clade (indicated in bold) that are divided into separate subgroups for the soft and hard tick lipocalins. The percentage confidence is indicated for 10 000 bootstraps and branches were collapsed at 45% confidence value.

7.3.6 Absence of TSGP2-4 in SGE from *O. moubata*

Phylogenetic analysis indicates that TSGP2 and TSGP3 group below moubatin. The high sequence similarity between moubatin and TSGP2-3 suggest that these are fairly recent gene duplication events. The possibility was raised that these events occurred after the divergence *O. moubata* and *O. savignyi*. If so, then it could be expected that TSGP2-3 will be absent from salivary gland extracts (SGE) of *O. moubata*. This possibility was investigated by a comparison of SGE using two-dimensional electrophoresis. There are several differences in protein expression patterns between salivary gland extract from *O. moubata* and *O. savignyi* (Fig. 7.11). Most notably is the different patterns observed for the TSGPs. While the same abundance of acidic TSGPs are observed in the SGE of *O. moubata*, their molecular masses and pI's differ from those of *O. savignyi*. A highly abundant basic protein (TSGP4) which corresponds to the basic toxin is also absent from the *O. moubata* proteome.

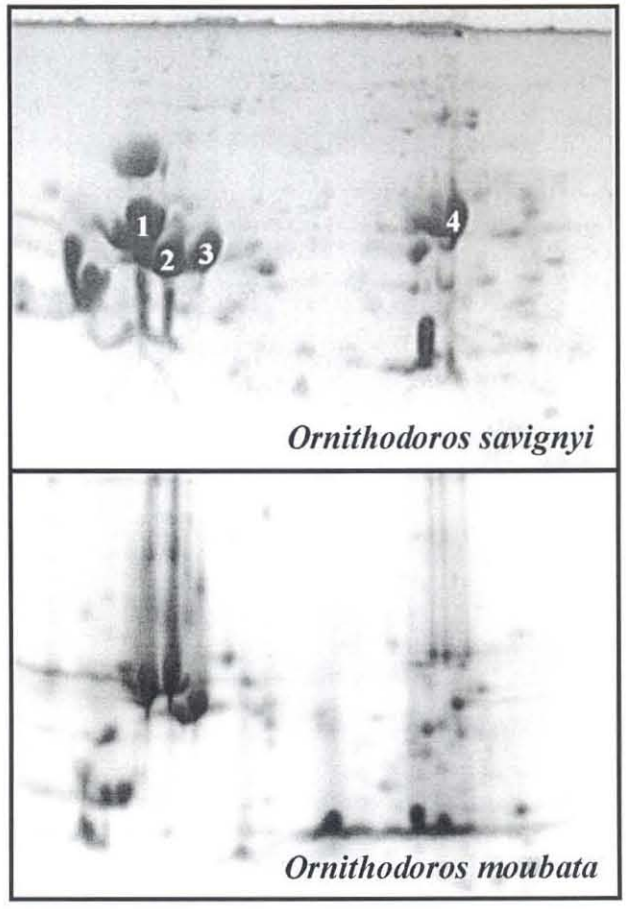

Fig. 7.11: A comparison of the SGE proteomes from *O. moubata* and *O. savignyi*. Acidic pI's are on the left and the anode at the bottom. The TSGPs previously identified are numbered 1-4.

To investigate this further, a comparative western blot analysis of SGE of *O. moubata* and *O. savignyi*, was performed using the polyclonal anti-sera directed against the different TSGPs (Fig. 7.12). Coomassie Brilliant Blue staining of SGE from *O. moubata* and *O. savignyi* shows that the protein concentrations in SGE from *O. moubata* was higher than SGE from *O. savignyi*. A very low dilution factor (500x) was also used with all anti-sera. Under such conditions, the presence of any toxins or proteins with a related sequence should have shown up clearly if present in the SGE from *O. moubata* in equivalent concentrations. Cross-reactivity of a-TSGP1 with a similar antigen in the SGE of *O. moubata* is evident. It is also clear that the signal for the *O. moubata* antigen is higher than that for *O. savignyi*, which fits with the higher protein concentration loaded on the gel. The detected protein is most probably the highly abundant antigen (20A1) previously detected in *O. moubata* (Baranda *et al.* 2000) that also shows N-terminal similarities to TSGP1. In contrast, both anti-sera specific for TSGP2 and TSGP3 gave no cross-reactivity with SGE from *O. moubata*, indicating the absence of both these proteins. There is however, cross-reactivity between TSGP2 and TSGP3 as was shown previously, which results in a broad band within which two distinct bands can be observed. Anti-sera against TSGP4 indicate no cross-reactivity for a strong band present in the SGE from *O. savignyi*, although there seems to be weak cross-reactivity with a lower molecular mass entity. These results do however also suggest that TSGP4 is absent in the SGE of *O. moubata*. Immunodetection is a validated method by which similarities between proteins can be compared. The results obtained clearly indicate the absence of any toxic entities and suggest a reason for the inability of *O. moubata* to produce toxicoses in their hosts.

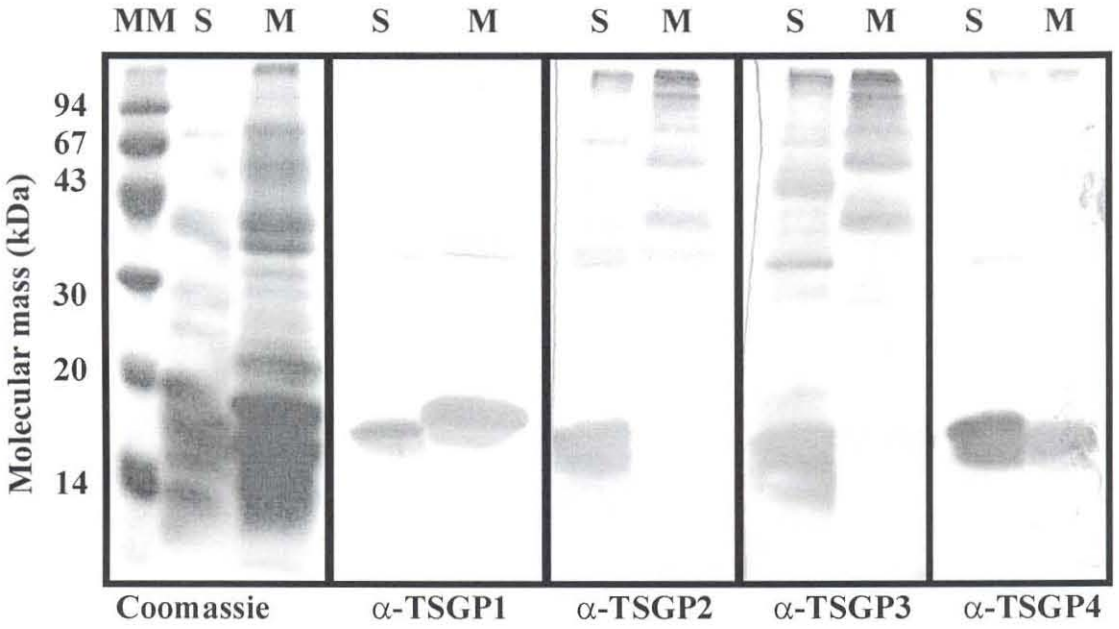

Fig. 7.12: Western blot analysis of TSGPs in SGE of *O. moubata* and *O. savignyi*. Indicated are molecular mass markers (MM), Coomassie Brilliant Blue staining of SGE of *O. savignyi* (S) and *O. moubata* (M). Cross-reactivity between anti-sera raised against TSGP1 can be observed, while there is no cross-reactivity for TSGP2 and TSGP3 anti-sera. A low molecular mass protein cross-reacts with TSGP4 anti-sera, although the main antigen is absent in SGE of *O. moubata*.

7.3.7 Molecular modeling of the TSGPs

The structure of HBP2 has been determined at high resolution of 1.25 Å (Paesen *et al.* 1999). Phylogenetic analysis indicates that the tick lipocalins are homologous, although sequence identity (13-15%) and similarity (27-34%) between the HBPs and TSGPs are quite low. Even with such low identity it might be possible to obtain structural models at low resolution (Fig. 7.13). The models obtained clearly indicate that all TSGPs exhibit the lipocalin fold although the models obtained gave very low RMSD values (4-6Å). Fitting the models obtained onto the structure of HBP2 shows that the main deviations occur in the mobile loop areas, while the β-barrel and α-helix structures are conserved.

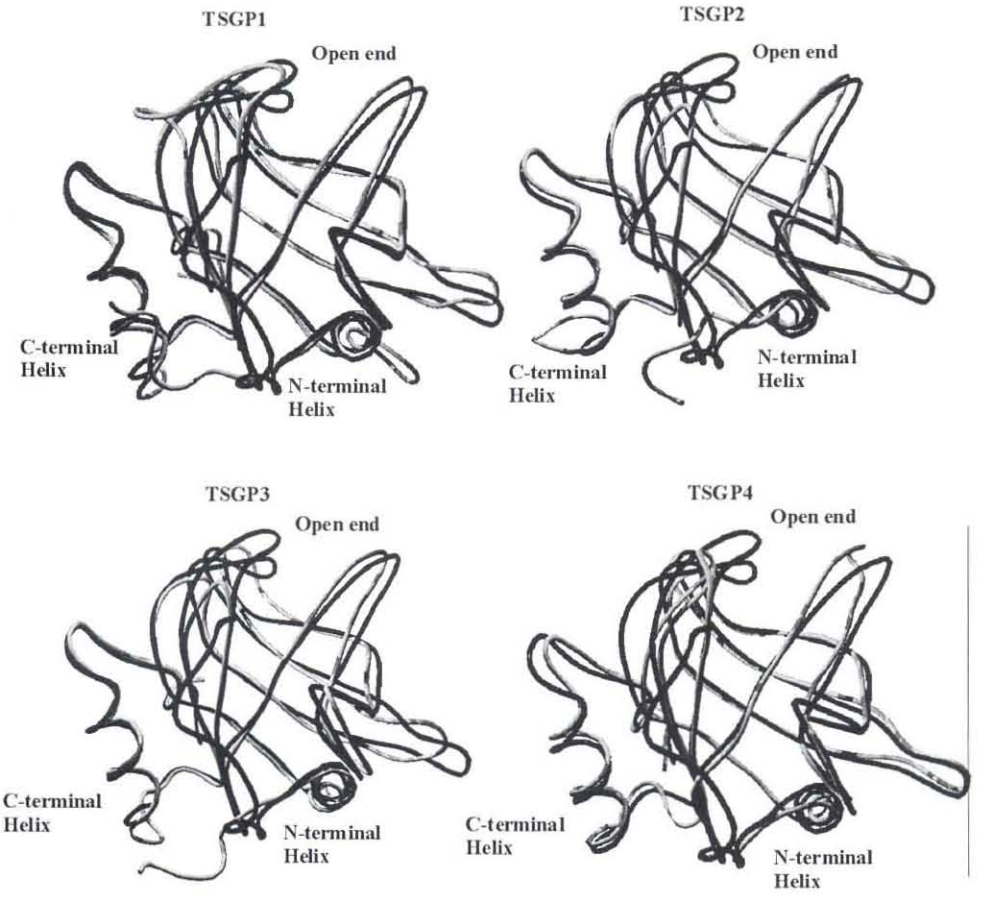

Fig. 7.13: Structural models obtained for the TSGPs fitted onto the structure of HBP2. HBP2 is indicated as the black ribbon tracing and the respective TSGPs as the dark gray ribbon tracing. Also indicated is the open end of the β-barrel and the N-and C-terminal α-helixes.

7.3.8 Analysis of the TSGP structures

Ramachandran plots for the TSGP structural models indicate that most of the psi/phi angles for the majority of the residues are in most favoured positions (Fig. 7.14). This centers around 72-76% for the TSGPs, with TSGP1 (73.4%), TSGP2 (74.8%), TSGP3 (71.1%) and TSGP4 (76.3%). The rest of the residues are predominantly in additionally allowed regions, with TSGP1 (20.9%), TSGP2 (20.3%), TSGP3 (23.1%) and TSGP4 (17.8%). There are 2.2%, 4.9%, 2.5% and 4.4% residues in generously allowed regions for TSGP1-4, respectively.

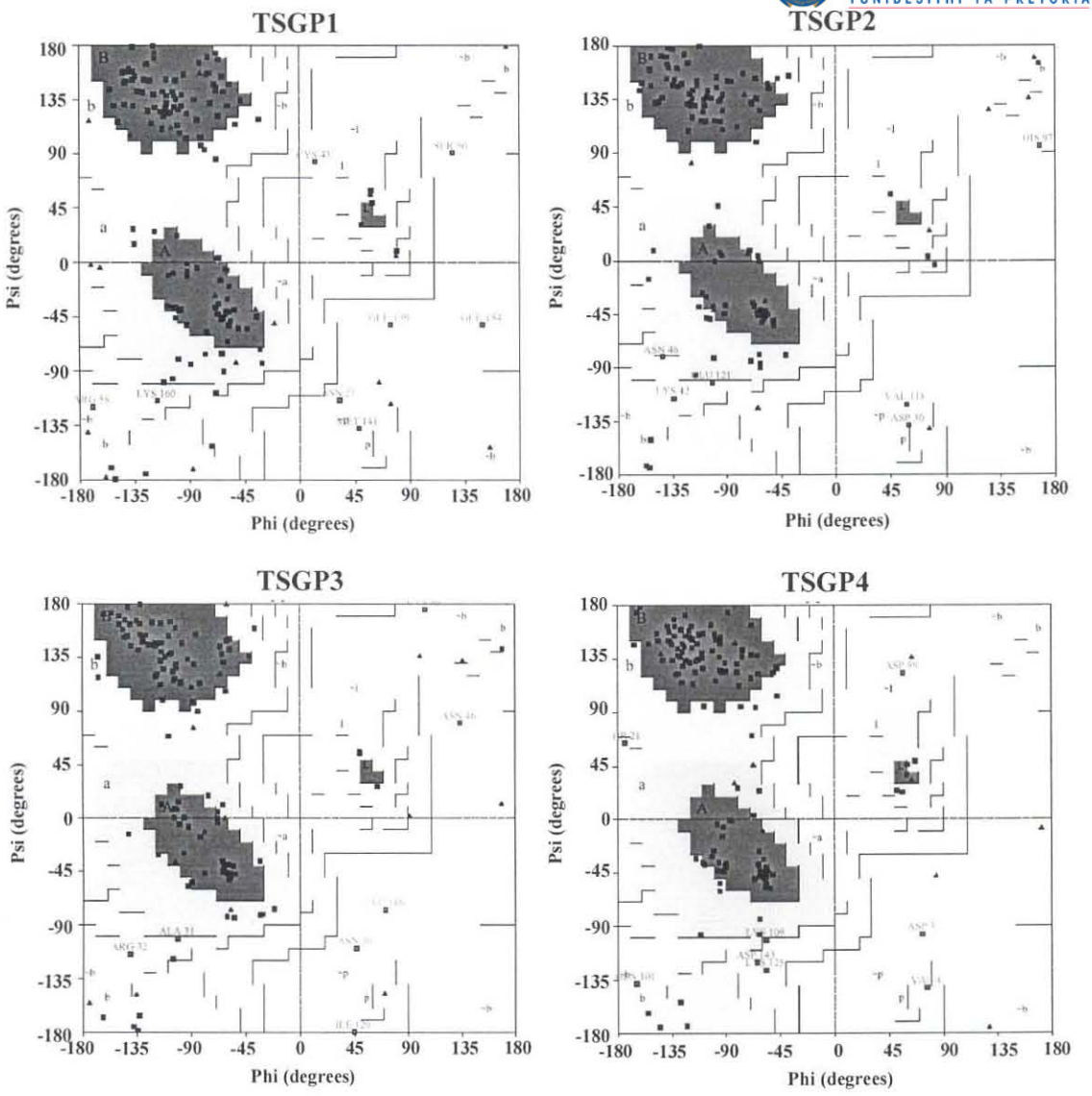

Fig. 7.14: Ramachandran plots for the TSGPs. Residues are indicated by triangles in most favoured (dark gray), additionally allowed (gray), generously allowed (light gray) and disallowed (white) regions.

7.3.9 Implications of the TSGP structures

The TSGP models show the lipocalin β-barrel and in each case three intact disulphide bonds (Fig. 7.15). Of interest is that the disulphide bonds in all the structures are localized to one side of the barrel. This could explain the lability observed for the toxins, as only one side of the barrel on the side of the C-terminal α-helix is stabilized.

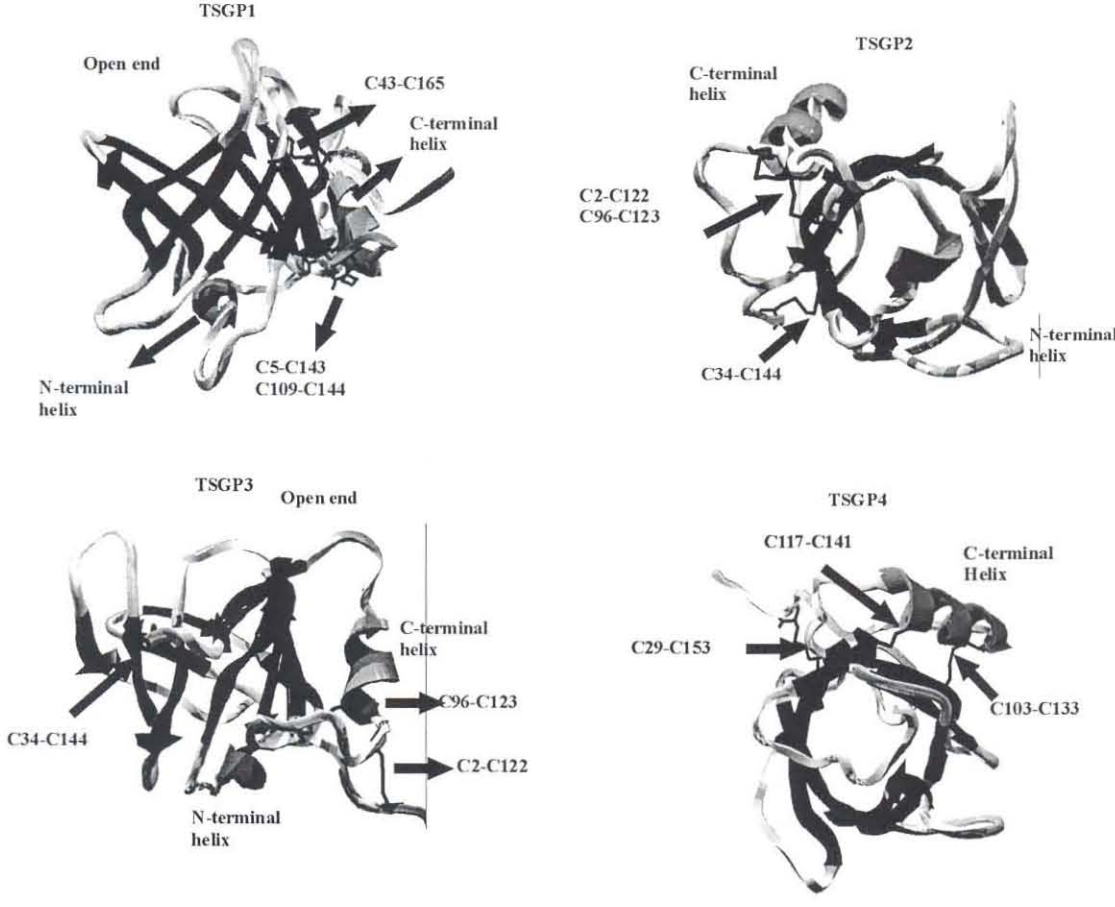

Fig. 7.15: The structures of the TSGPs and their intact disulphide bonds. The β-barrel is shown in black, helixes in dark gray and loops in light gray. The positions of the intact disulphide bonds are indicated. TSGP1 is viewed from the side and looking into the N-terminal 3_{10}-helix that closes the b-barrel. TSGP2 is viewed directly into the barrel from the closed end, so that the N-terminal 3_{10}-helix is at the top. TSGP3 is viewed from the side so that the disulphide bonds can clearly be seen. TSGP4 is viewed directly into the barrel so that the closed end is at the top.

7.3.10 Are toxins platelet aggregation inhibitors?

Sequencing and phylogenetic analysis have shown that TSGP2 and TSGP3 are closely related to moubatin, the inhibitor specific for collagen-induced platelet aggregation. Other lipocalins from the blood sucking bugs *R. prolixus* and *T. pallidipenis* have been shown to be specific inhibitors of the intrinsic Xase complex (nitrophorin-2), ADP-induced platelet aggregation (RPAI), thrombin (triabin) and collagen-induced platelet aggregation (pallidipin). This raised the question whether the TSGPs are involved in the regulation of the hemostatic system. Partial purification of a collagen-specific platelet aggregation inhibitory activity (designated savignygen) using RPHPLC and AEHPLC indicated no ADP- or collagen-induced platelet aggregation inhibitory activity associated with the toxins (Fig. 7.16a). ADP- and collagen-induced platelet aggregatory inhibitory activity was observed after RPHPLC in a distinct peak of which the first part (29-31) corresponded with savignygrin activity (Chapter 2), while the last part of the peak (31-33 minutes) corresponded to a 17 kDa protein that showed cross-reactivity with polyclonal antibodies directed against TSGP2 (Fig. 7.16a and Fig. 7.16b). This fraction was partially purified and showed specific inhibition of collagen-induced platelet aggregation, but not ADP-induced platelet aggregation (Fig. 7.16d). Of interest is that both this protein as well as moubatin elutes at ~20-25% acetonitrile, while the toxins elute at 40-45% acetonitrile (Waxman and Connolly, 1993). The N-terminal amino acid sequence obtained for the 17 kDa protein was: **AQDKCSEVRN** (results not shown).

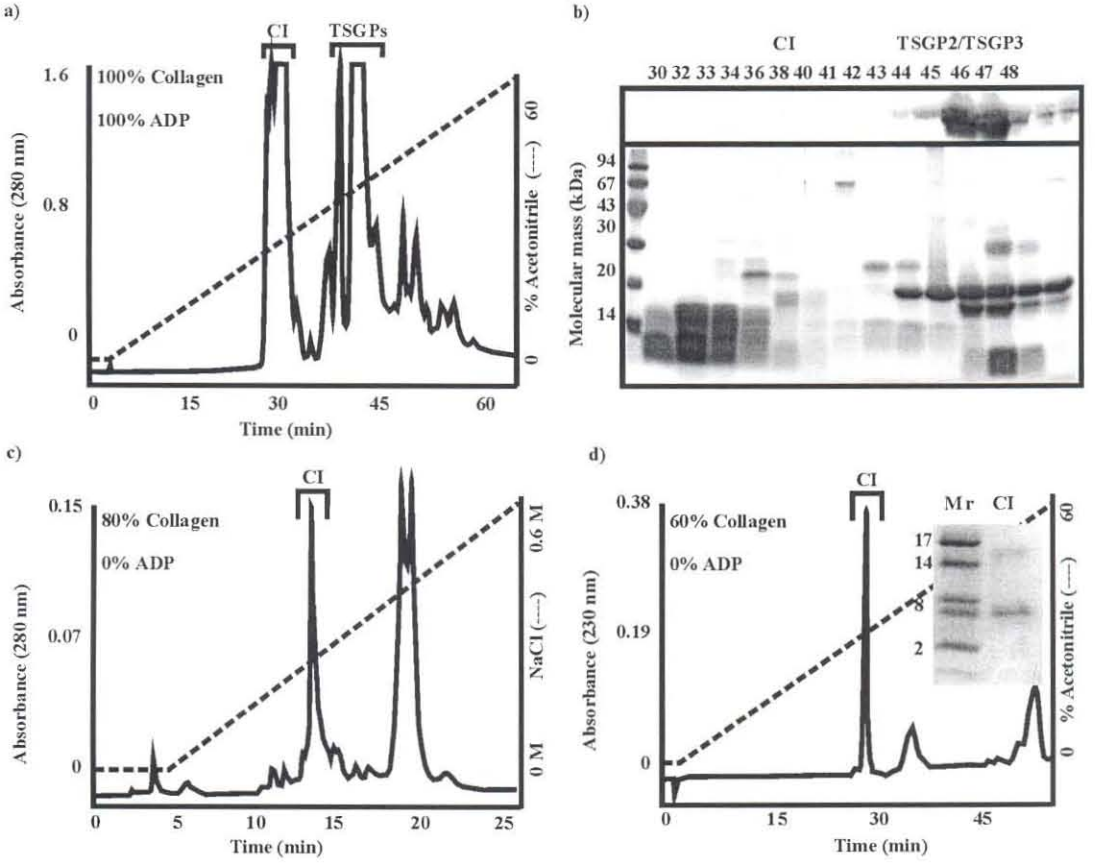

Fig. 7.16: Identification of savignygen, an inhibitor specific for collagen-induced platelet aggregation. (a) RPHPLC of SGE. Indicated are the fractions that inhibited ADP- and collagen-specific platelet aggregation (CI). The TSGPs that did not inhibit platelet aggregation are also indicated. (b) Western-blot analysis of RPHPLC fractions using a polyclonal antibody directed against TSGP2. Included is the corresponding SDS-PAGE electropherogram of the fractions. Numbers corresponds to fractions (in minutes) obtained from the RPHPLC. (c) AEHPLC of the inhibitor fractions (38-40 minutes) after RPHPLC. (d) Rechromatography of the inhibitory fraction obtained after AEHPLC. Indicated is percentage inhibition for ADP- and collagen-specific platelet aggregation inhibition, as well as a tricine SDS-PAGE analysis of the obtained fraction (insert). N-terminal sequence analysis of this fraction gave the sequence: AQDKCSEVNR.

It was also shown previously that no inhibitory activity of thrombin or fXa is associated with the TSGPs (Gaspar *et al.* 1995; Gaspar *et al.* 1996; Nienaber, Gaspar and Neitz, 1999). Using a photodiode array detector to collect wavelength spectra during RPHPLC showed that no prosthetic heme groups are associated with the TSGPs, as is found for the nitrophorins (Montford, Weichsel and Andersen, 2000). Histamine-agarose affinity

chromatography used to purify the HBPs failed to bind any TSGPs (results not shown) (Paesen *et al.* 1999).

Discussion

Evolution of tick lipocalins

The absence of histamine-binding proteins in soft ticks suggests that a lipocalin-like protein was present in the ancestral tick, which after speciation duplicated and evolved new functions. In the case of hard ticks that feed for extensive peroids of time, regulators of inflammation were evolved, while soft ticks that feed rapidly do not need anti-inflammatory mediators. Instead, inhibitors of platelet aggregation as in the case of TAI, moubatin and savignygen evolved to cope with the host's hemostatic system. Recent evidence indicates that ticks originated in the late Cretaceous (~120 MYA) and had already speciated into the main tick families by approximately 94 MYA (Klompen and Grimaldi, 2001). Using this estimate, the divergence of these two lipocalin families can be dated to this period. The selective stress of adaptation to a blood-feeding environment during this period of tick evolution, could account for the high degree of divergence of tick lipocalins relative to those of other arthropod lipocalins.

7.5.2 TSGP1

The placing of TSGP1 basal to the rest of the soft tick inhibitors suggests that it was present before the divergence of *O. savignyi* and *O. moubata*. This fits with the presence of a highly cross-reactive protein in *O. moubata* as well as N-terminal sequence similarity to a highly abundant antigenic protein 20A1 (Chapter 7).

7.5.3 TSGP2 and TSGP3

Phylogenetic analysis indicate that TSGP2 and TSGP3 are grouped below moubatin. The absence of TSGP2/TSGP3 in SGE of *O. moubata*, the high sequence similarity between moubatin and TSGP2-3, as well as between TSGP2 and TSGP3 suggest that these are fairly recent duplication events that occurred after the divergence of *O. moubata* and *O. savignyi*.

7.5.4 Toxicity vs. non-toxicity: TSGP2 and TSGP3

It was previously shown that TSGP2 and TSGP3 have identical elution times during RPHPLC, that indicate similar global hydrophobicity, corroborated by their similar amino acid sequences (Chapter 7). In contrast, TSGP2 and TSGP3 separate on HIHPLC, indicating differences in their surface hydrophobicity and hence surface conformation. This is supported by the differences observed in the surface accessibility of the modeled structures of TSGP2 and TSGP3. The high identity of TSGP2 to TSGP3 and the apparent lack of toxicity for TSGP3 indicate that the toxic activity is probably localized to a very small region of different local surface conformation. A likely candidate is on loop 5, where TSGP2 has an arginine, while both TSGP3 and moubatin have glycines. It seems improbable that two sequences sharing such high sequence identity, would exhibit different biological activities. However, different activities have also been indicated for the nitrophorins. Nitrophorin 2 exhibits anti-coagulant activity, which is absent in nitrophorins 1, 3 and 4 that share a high percentage of amino acid sequence similarity (Zhang *et al.* 1998; Montford, Weichsel and Andersen, 2000). Another example is *Coffea arabica* methyltransferase (CaMXMT) which is an active enzyme in coffee plants, while a set of paralogues CaMTL (*C. arabica* methyltransferase-like) share high identity (80-84%) but show no activity (Ogawa *et al.* 2001).

7.5.5 TSGP4

Western blot analysis has indicated that TSGP2-4 are absent in *O. moubata*, although a degree of cross-reactivity was observed in both *O. savignyi* and *O. moubata* using anti-sera raised against TSGP4. This might indicate a related non-toxic protein present in both species. Phylogenetic analysis places TSGP4 before moubatin, which suggests that

TSGP4 might be present in both tick species. Caution should however, be exercised as these are paralogous genes and no knowledge exists about their last common ancestor. It could even be speculated that TSGP4 duplicated after divergence of the two tick species from a shared ancestral gene, indicated by cross-reactivity by western-blot analysis.

7.5.6 Evolution of tick lipocalins and its implication for tick toxicoses

Gain of toxic function after divergence of *O. moubata* and *O. savignyi* have important implications for the origins of toxicity in ticks. Recent aquisition of genes coding for toxins through gene duplication discounts a common ancient origin for all tick toxins and suggests the probability of multiple unrelated origins for toxins. Protein and sequence data indicate specific differences between the TSGP toxins and paralysis toxins that shows that their molecular nature is different (Chapter 6).

7.5.7 Tick lipocalins as toxins

That lipocalins can be deleterious is not surprising. Many common allergens involved in allergic reactions are lipocalins (Mäntyjärvi, Rautiainen and Virtanen, 2000). Multiple molecular recognition properties and binding to cell surface receptors, are being considered to be general properties of lipocalins (Flower, 2000). It is possible that some exogenous lipocalins, derived from blood feeding organisms can recognize specific receptors and impede their function. In fact, lipocalins that inhibit collagen-induced platelet aggregation, probably interact with the collagen platelet receptor (Waxman and Connolly, 1993).

7.5.8 Structure of TSGPs

The structure of HBP2 has two N-terminal α-helixes that close off the β-barrel in contrast to other lipocalins which posses a N-terminal 3_{10}-helix. Multiple sequence alignment indicate that the other tick lipocalins, probably also diverge from other lipocalins in this respect, although TSGP4 probably lacks the first short α-helix. It was previously shown that all cysteines of the toxins are involved in disulphide bonds (Chapter 6). Four cysteines conserved in al tick lipocalins are involved in disulphide bonds in the HBPs and serve to pin the C-terminal region to the side of the barrel (Paesen *et al.* 1999). Cys119-

Cys148 pins the start of the C-terminal α-helix to the start of the β-G sheet, while Cys48-Cys168 links the C-terminal end with the base of the Ω-loop (Fig. 7.15). Assuming that this disulphide bond pattern are consistent for other tick lipocalins, the remaining disulphide bonds present in the toxins can be inferred from the overall topology of the lipocalin fold of HBP2 (Fig. 7.17). In TSGP4 Cys117-Cys140 also pins the end of the C-terminal α-helix to the start of the β-H sheet. The majority of the TSGP4 structure is thus not stabilized by disulphide bonds and could explain the lability of this toxin. The same is true for TSGP2 and TSGP3, where the extended N-terminal helix is disulphide bonded to the C-terminal helix (Cys2-Cys121). This probably stabilizes the position of the N-and C-terminal helixes relative to one another, but again stabilization of the majority of the structure by disulphide bonds is absent. Of interest is that whereas TSGP2 and TSGP3 have intra-protein disulphide bonds, as exemplified by ESMS and electrophoresis under reducing and non-reducing conditions, HBP3 lacks the N-terminal cysteine and forms a disulphide-linked dimer. It has been shown that the core structure of HBP2 is extremely rigid. In contrast the surface residues were found to be very mobile (Paesen *et al.* 1999). This corresponds to the loop areas, which are also the least conserved in the tick lipocalin family and generally in all lipocalins (Skerra, 2000). Such mobile structures could explain the lability of toxic activity (Chapter 6).

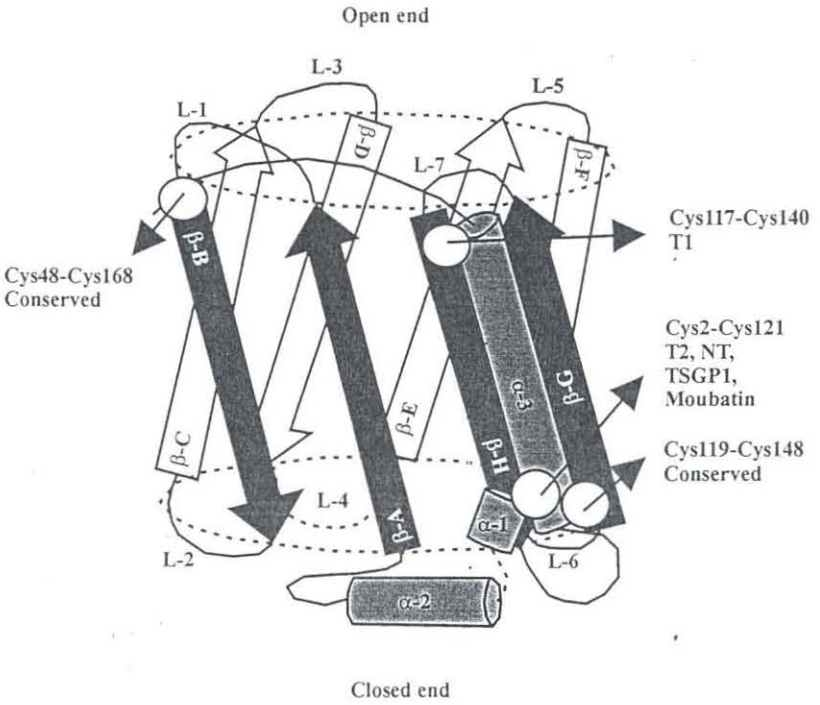

Fig. 7.17: The proposed disulphide bond pattern of the tick toxins. A schematic representation of the topology of HBP2 indicates two N-terminal α-helixes (α-1, α-2) followed by an 8 stranded β-barrel (β-A to β-H), which ends in a C-terminal α-helix α-3) that lies parallel to β-G and β-H. The conserved disulphide bonds of HPB2 is indicated with white circles (Cys48-Cys168; Cys119-Cys148) and shows that the C-terminal end is bound to the start of β-B and the start of the C-terminal helix to the start of β-G. Assuming that this disulphide bond pattern is conserved across the tick family, it follows that for TSGP4 the remaining disulphide bond is between the end of α-3 and the beginning of β-H and for TSGP1, TSGP2, TSGP3, and moubatin at the start of α-1 and the second cysteine at the beginning of α-3. The proposed disulphide bond patterns fits in well with the existing topology known for HBP2 (Paesen *et al.* 1999).

7.5.9 Implications of molecular crowding for the evolution of tick lipocalins

Molecular crowding as mechanism of granule formation has several implications for protein evolution. Molecular crowding as a phenomenon depends on high protein concentrations, while aggregation is also dependent on protein structure. Specific sequence signals possibly do not play such an important role in aggregation. This implies that residues important for the maintenance of the lipocalin fold would be conserved. It has been shown that as little as 8% of all amino acid residues are involved in the maintenance of protein structure (Rost, 1997). For the lipocalins this means that the rest

of the residues are under no selective pressure and can undergo genetic drift under neutrality theory. This could be one of the reasons why lipocalins is such a diverse protein family. It is also the ideal environment for the evolution of new protein function and could account for the fact that even orthologous proteins could be highly diverged. This is counter-intuitive to the general idea of the conservation of orthologous function, but would be the case if protein function is not coupled to specific sequence epitopes, but rather to a general protein fold.

7.5.10 The tick lipocalin family

The TSGPs are part of what is becoming an extended family of tick lipocalins. It is clear that these different paralogs evolved by gene duplication events. It is foreseen that more lipocalins with diverse functions will be found in different tick species. While lipocalins have a conserved fold, there are several significant differences between those of ticks and the rest of the lipocalin family. Vaccines targeted at these specific features, might thus be viable and it is possible that a wide range of cross-protection might be accomplished with these proteins.

CONCLUDING DISCUSSION

"Nothing in biology makes sense except in the light of evolution"

Theodosius Dobzhansky, 1973

The current ideas on tick evolution and their adaptation to a blood-feeding environment were outlined in the introduction to this thesis. Ticks adapted to an efficient host hemostatic system by evolving numerous new protein functions capable of regulating this complex system. While many tick salivary gland proteins have been described, knowledge on the evolution of tick protein families is lacking. Evolution of novel protein function entails gene duplication and subsequent gain or loss of protein function. This implies that proteins with different functions but common ancestors must still share fundamental properties. In this study tick evolution was approached from the perspective of gene duplication and subsequent gain/loss of protein function. This thesis presents the first comprehensive analysis of tick protein families in an evolutionary context.

Two main protein families have been studied, a family of BPTI-like anti-hemostatic factors (Chapter 2-4) and a family of proteins that are part of the lipocalin protein family (Chapter 6-7). Protein family is being defined here as proteins that share a common structural protein fold, although their functions might differ, i.e. paralogous proteins.

The BPTI-like family consists of at least three proteins with different functions. Phylogenetic analysis clearly showed that these proteins are monophyletic, which imply common ancestry. Common ancestry in this sense can only mean that there were multiple gene duplication events and subsequent mutation that led to a gain or loss of protein function.

Several isoforms of the platelet aggregation inhibitor, savignygrin were identified (Chapter 2). As savignygrin was never described before, extensive characterization on protein and functional level was performed. These showed that savignygrin targets the integrin, $\alpha_{IIb}\beta_3$, possesses an RGD motif and is the ortholog of disagregin (Mans, Louw

and Neitz, 2002b). The first evidence of gene duplication in argasid ticks is also presented. It appears to be a very recent gene duplication event, probably after the divergence of *O. moubata* and *O. savignyi*. An interesting question is why this second copy of savignygrin has not yet been inactivated as expected for duplicated genes (Lynch and Conery, 2000). A recent study has shown that duplicate genes might persist in a lineage if they confer an advantage to the organism (Kondrashov *et al.* 2002). Advantage conferred at this early stage of gene duplication is considered to be due to the presence of higher concentrations of the translated protein from a gene. In the case of the savignygrins, this could be a relevant observation as the (+)/(-) forms each constitute ~6% of the total salivary gland proteins. Compared to the yields obtained for disagregin (0.225% of the total SGE) this seems to be exceptionally high (Karczewski, Endris and Connolly, 1994).

O. moubata has a limited number of hosts and predominantly feeds either on man or warthogs, and inhabits the burrow of its host. *O. savignyi* probably has a wider host range and will feed on any animal that shelters in the shade of trees where it resides (Hoogstraal, 1956). This behaviour of *O. savignyi* may explain the higher concentrations of platelet aggregation inhibitor. A wide host range may expose a tick to a diverse repertoire and concentration range of platelet receptors. It should thus be interesting to determine the number of $\alpha_{IIb}\beta_3$ receptors expressed on the platelet surfaces of different hosts. Expression of high concentrations of platelet aggregation inhibitor would obviously be advantageous for the tick to cover as wide a range of platelet receptor concentrations as might be encountered in different hosts. To test the hypothesis that purifying selection could be responsible for the maintenance of two gene copies for the savignygrins, the number of integrin $\alpha_{IIb}\beta_3$ per platelet should be investigated for different domestic and wild animals. It is predicted that animals considered as hosts for *O. savignyi* should have higher numbers of this integrin than *O. moubata* hosts. If this proves to be correct, it can be speculated that the control of platelet aggregation during feeding of *O. savignyi* is still important. While the use of anti-coagulants has been dismissed as a suitable target for vaccine development, targeting of platelet aggregation inhibitors have never been attempted and can still be viable for vaccine development.

An alternative explanation for the two gene copies of the savignygrins, is that this is a very recent gene duplication event, so that one copy still needs to be inactivated, or change function. A date for this gene duplication event can probably be estimated if the divergence of *O. savignyi* and *O. moubata* is considered. If we assume as upper limit that ticks originated 120 MYA (Klompen *et al.* 1996), then a divergence rate for the platelet aggregation inhibitors can be calculated:

$$r = d/2T$$

Where r = rate of mutation expressed as changes per site per million years, d = total number of amino acid substitutions calculated from: -ln (1-p), where p = d/n (d is the number of amino acid differences between two sequences and n is the total number of amino acid residues in sequences of similar length). T = time of divergence in millions of years (Nei and Kumar, 2000).

This gives a substitution rate of 3.32×10^{-9} per site per year for the platelet aggregation inhibitors. Assuming that this rate stays the same for all members of the platelet aggregation family, then the calculated time of divergence for the +/- isoforms of savignygrin is 4.9 MYA. *O. savignyi* and *O. moubata* have most probably diverged after the origination of ticks. If 92 MYA is taken as the time of divergence (Klompen and Grimaldi, 2001), a substitution rate of 4.43×10^{-9} per site per year can be calculated for the platelet aggregation inhibitors. Using this rate gives a divergence time for the +/- isoforms at 3.7 MYA. If very fast rates of substitution are assumed (as exemplified by the positive selection observed for the platelet aggregation inhibitors) then the fastest realistic rate would probably be 1×10^{-8} per site per year (Grauer and Li, 2000). Using this gives a time of divergence between *O. savignyi* and *O. moubata* at ~40 MYA and can probably be taken as the lower limit for time of divergence between these two species. It also gives a time of divergence for the +/- forms at 1.6 MYA.

The lower limit is still close to what is considered as ample time for a duplicated gene to be inactivated (Lynch and Conery, 2000). It could thus be concluded that purifying selection and concerted evolution is probably playing a role in the maintenance of two savignygrin gene copies.

In Chapter 3 the thrombin inhibitor, savignin was characterized on molecular level in order to obtain data for a comprehensive phylogenetic analysis of the tick BPTI-family. Characterization of savignin in terms of its sequence and predicted structure confirmed that it is the ortholog of ornithodorin and that they should have similar mechanisms of inhibition (Mans, Louw and Neitz, 2002a). The results from this study provide a link between the kinetic characterization of savignin (Nienaber, Gaspar and Neitz, 1999) and the structural characterization of ornithodorin, for which no kinetic data were provided (van de Locht *et al.* 1996). The predictions of the intra-domain interactions of savignin provided insights into the evolutionary significance of domain interaction in terms of the conserved nature of the thrombin inhibitors (Chapter 4).

Chapter 4 described the relationship between the platelet aggregation inhibitors, savignygrin and disagregin and other members of the tick BPTI-family. The platelet aggregation inhibitors are identified as novel members of the BPTI-family and it is shown that the RGD motif of savignygrin is presented on what is known as the substrate-binding presenting loop of the canonical inhibitors (Mans, Louw and Neitz, 2002b). Common ancestry between different tick BPTI-like proteins was also investigated. These studies presented the first in-depth analysis of how tick proteins evolved new functions (Mans, Louw and Neitz, 2002c). The conclusions derived in this chapter have far reaching implications for the evolution of ticks and how they adapted to a blood-feeding environment (see below). Investigations into the validity of these conclusions should provide the tick research community with ample study opportunities that will stimulate a new synthesis of tick evolution.

Chapter 5 provides important information on salivary gland morphology, not previously described for the tick, *O. savignyi*. For the first time data is provided that shows the

presence of more than three granular cell types in argasid ticks. This is of cardinal importance for the classification of the granular cell types in tick salivary glands. These results clearly show that morphological and histochemical approaches need to be supplemented by biochemical and immuno-cytochemical techniques in order to describe granular cell types on a more analytical level. The localization of the same anti-hemostatics to different granular types (typed on the basis of morphology), however, complicates the assignment of definite granular types.

Chapter 6 describes proteins that may be involved in granule biogenesis (Mans *et al.* 2001). Tick salivary gland granule biogenesis has not been described to date and this study is the first step in this direction. The nature of sand tampan toxicoses has also been revisited after a number of years since the first descriptions of this form of toxicoses (Neitz, Howell and Potgieter, 1969; Howell, Neitz and Potgieter, 1975). This culminated in the identification and characterization of a novel basic toxin and the confirmation of the properties of the acidic toxin previously described (Mans *et al.* 2001; Mans *et al.* 2002). Pathogenesis of the cardiac system caused by these toxins is a novel form of tick toxicosis and distinguishes sand tampan toxicoses from paralysis toxins (Mans *et al.* 2002).

The identification of the TSGPs led to the discovery of a whole family of argasid tick lipocalins (Mans, Louw and Neitz, 2002d). There are at least 6 different lipocalin proteins in the *Ornithodoros* species (these include toxins and anti-platelet agents) and three more in hard tick species (histamine binding proteins). Except for moubatin, the TSGPs are the first lipocalins described for argasid tick species. It appears as if these proteins have different functions in the host although a common function in granule biogenesis have been proposed. Phylogenetic analysis also showed that these proteins are monophyletic. This again implies gene duplication events and subsequent gain or loss of protein function through mutation. The conclusions derived for the evolution of the tick toxins show that toxins might be recently acquired traits of the sand tampan. This has important implications for the origin and evolution of other tick toxins. The extensive lipocalin

family further supports the concept that gene duplication played an important role during the evolution of novel protein functions in argasid ticks.

A consideration of the results obtained during this study leads us back to the introduction and the questions that were asked concerning the adaptation of ticks to a blood-feeding environment. We can now consider these questions in the light of the findings presented in this study.

Question: How did ticks acquire novel anti-hemostatic strategies?

This study has confirmed evidence of gene duplication of two protein families. A general mechanism for the acquisition of novel protein functions through the use of a few relatively simple protein folds are proposed. Ticks generated functional diversity, by gene duplication and gain or loss of protein function. This allowed the generation of different anti-hemostatic factors by which ticks could regulate the hemostatic system of their host's. Other unknown functions were also generated, which are exemplified by peripheral toxic activities of some of these proteins such as TSGP2 and TSGP4.

The use of a few common protein folds to generate diversity is a simple but elegant way for an organism to become more complex (complexity is here defined as having more potential protein functions and hence being able to adapt to a wide variety of possible environments). It can be foreseen that new functions could still be generated in time from these same protein folds in response to a changing environment. This same principle probably also holds for other, as yet undiscovered proteins present in the salivary glands.

Question: What was the nature of the ancestral tick before adaptation to a blood-feeding environment?

The question can be posed why a few common protein folds are used over and over again, while ticks should at least have the potential of having many more protein folds in its repertoire. It can be predicted that the tick genome should be between 100-200 Mb and ~15000 genes (Grauer and Li, 2000). Perhaps the answer could be found in the ancestor to the holothyrida and Ixodida sub-orders. Such a mite may be presumed to be a free-

living scavenger and would have needed its salivary glands to make the food source more accessible. It can be foreseen that matrix-degrading proteins, such as hyaluronidase and proteases, such as matrix metalloproteases may have been present, as this would have allowed the mite to enlarge its feeding site (Neitz and Vermeulen, 1987). A range of protease activities has been described in the SGE of *O. savignyi* (Mahlaku, Gaspar and Neitz, 2002). Serine protease inhibitors may have played a role to inhibit any protease activity present in the body fluids of the dead organisms it fed on. The ancestral lipocalins probably functioned in granule biogenesis, as this would have been an intrinsic property of the salivary gland as a secretory organ. Depending on the complexities of its food sources, it could be speculated that the salivary glands at the time of divergence between the holothyrida and ixodida, had already been differentiated organs. This means, that a certain subset of proteins were expressed in these glands and that the number targeted to the secretory pathway would have been limited to those used during their feeding process. Ticks may have originated with a limited set of proteins, from which new diversity had to be generated. This may account for the re-use of an existing protein fold. The state of this primitive salivary gland could also have influenced the protein repertoire of the ancestral tick. Proteins are not only expressed in the glands, but also need the signals necessary for secretion.

Question: Did ticks evolve anti-hemostatic strategies before or after divergence into the main tick families?

It has been suggested that hard and soft ticks adapted independently to a blood-feeding environment (Chapter 4). This was based on anti-hemostatic factors unique to hard and soft ticks. If the main tick families adapted independently to their new hemostatic environments, other features in their biology, that is also dependent on a blood-feeding lifestyle, should corroborate this. The feeding and reproductive strategies of hard and soft ticks differ quite remarkably. Adult female hard ticks feed once, secrete a salivary gland degenerating factor that causes the salivary gland to atrophy and proceeds to lay several thousands of eggs in one stage after which the tick dies. Adult soft ticks on the other hand, feed several times and lay several hundreds of eggs after each feeding period (Sonenshine, 1991). As these strategies are general throughout the Ixodidae and

Argasidae it can be assumed that these traits only evolved after the divergence of hard and soft ticks, probably at a stage when ticks were adapting to a blood-feeding environment.

Question: What was the driving force behind the evolution of hematophagy in ticks?

It was proposed that the divergence of ticks into their different families might have been triggered by the divergence of mammals and birds (Chapter 4). The divergence of mammals and birds could also have been a possible reason for the evolution of hematophagy in ticks. The ancestral holothyrid related tick probably fed on dead arthropods. The emergence of numerous new potential mammalian and avian hosts, with relatively thin epidermises that allows for the penetration and location of a fluid meal could have been a sufficient trigger that allowed a rapid adaptation to this new niche. This is probable when it is considered that ticks belong to the superorder Parasitiformes, which consists of the Holothyrida, Mesostigmata and Ixodida. Many Mesostigmata live as parasites on mammalian and avian hosts from where they feed on secretions obtained by penetrating the skin, causing blood and lymph fluid flow (Radovsky, 1985). An ancestral holothyrid-like mite could have made this transition from dead arthropods, to dead mammals and finally to live mammals, in the process starting to evolve components that can control its host's defense mechanisms.

Implications derived from this study for future research into the "tick genome"

It seems in retrospect that more questions were raised during this study than answered. While gene duplication events have been indicated for two protein families, the question of how many undiscovered members of both protein families exist in different tick species is now more pressing than before. More problematic even is the high level of divergence of these sequences and the indications that many functional proteins might only have acquired novel functions after the divergence of hard and soft ticks. This implies that even if the genome of a hard tick species is sequenced to serve as a model for tick genome studies, we might still miss some of the most important molecules involved in tick feeding from other species. The choice of a model tick or ticks for genome sequencing will remain a central problem. Choosing a tick closest to the ancestral tick (if

we can predict the more ancient lineages correctly) will allow us to study early evolutionary events although we will miss those proteins recently diverged. The most fruitful endeavor would be to sequence the genomes of representatives from both hard and soft ticks, as well as the Nuttallillidae. The latter is probably one of the most important targets, as it will provide us with an external reference point for the other tick families. As the Nuttallillidae is also the only monotypic family and occur only in Gondwanaland (the suggested cradle of tick origins), this tick might be the closest living fossil that we have to the ancestral tick. The scarcity of living specimens of this tick makes it a priority of study for tick biodiversity. If this tick species should be lost or become extinct we might lose one of the most valuable tick species still living for the study of tick evolution.

Future studies on the gene duplication mechanisms in argasid ticks

Gene duplication events for both the BPTI-like inhibitors and lipocalins can now be studied at chromosome level. Questions remaining to be answered are whether the duplicated genes are localized to the same chromosomes, in what order they are arranged on the chromosomes and what patterns of introns/exons they exhibit. Such knowledge has been fruitfully used to study mammalian lipocalin evolution (Salier, 2000). The known gene sequences can be utilized using *in situ* hybridization techniques and genomic libraries to answer these questions. If the genes from individual families are localized on the same chromosome, novel members of the different families could be identified, by limited chromosome sequencing. Studies into this field can allow the preliminary mapping of a tick genome, which could be important for future genome sequencing projects.

Future studies on the TSGPs

The expression of the TSGPs will allow the next step of characterization of these molecules. These include studies into the mechanisms of toxicity and the feasibility of their use as vaccine targets. While the TSGPs might not be a universal vaccine target that will provide cross-protection for all tick species, neutralization of the toxic activities alone would be a viable option to relieve the burden that these ticks place on their hosts.

Future studies on the BPTI-like hemostatic inhibitors

Expression of the different members of the BPTI-family should provide the means for further structural characterization in terms of mechanisms. An intriguing possibility that emerges from this study is the design of a chimeric protein with fXa, thrombin and platelet aggregation inhibitory capacities. Such a protein might be useful as a multi-functional agent to control thrombosis in a regulated manner and could also be used as a possible vaccine agent, to generate immune responses that could knock out more than one function necessary for tick feeding. The different evolutionary pathways proposed for the BPTI-like family can also be tested by a phylogenetic reconstruction of ancestral proteins and subsequent engineering of chimeric proteins (Chang and Donoghue, 2000). This could also allow the prediction of as yet undiscovered ancestral proteins from the same family.

Conclusion

Evolution as a biological phenomenon is multi-disciplinary. It can be considered on the level of the gene, the genome, protein function, cellular metabolic processes, individual cells, organs or whole organisms and populations. As such no individual study into any of the above categories can provide an accurate description of evolution if the other parts are not also considered. This study considered gene duplication and subsequent gain/loss of protein function, and its role during the adaptation of ticks to a blood-feeding environment. However, gene duplication implies multi-gene families and gain/loss of function and the existence of various distinct functions. To this end, studies into possible functions of several proteins have been conducted, which include inhibitors of platelet aggregation, blood clotting, granule biogenesis and toxins. It can be certain that not all functions of the proteins studied have yet been elucidated as some may be multi-functional and/or be in the process of evolving new functions. Preliminary studies into salivary gland biology has also been conducted as it was made clear that a study of the evolution of bio-active components secreted during feeding cannot fail to take into account the organ of origin. This study has shown that a holistic approach to evolution is necessary if we are to understand tick adaptation to a blood-feeding environment. The

results generated in this manner have left many avenues to be explored that will hopefully lead to a deeper understanding of ticks as highly adapted parasites. While a control method of ticks is envisaged at the end of the road, we hope that this study also shows ticks not only as villains but also as a part of a wonderful world of interaction at molecular level. Tick control after all is a necessity imposed by the drive of man to conquer this world. As always we should consider the possibility that in changing this world we might also lose the keys to its mysteries.

"The theory of evolution is quite rightly called the greatest unifying theory in biology. The diversity of organisms, similarities and differences between kinds of organisms, patterns of distribution and behavior, adaptation and interaction, all this was merely a bewildering chaos of facts until given meaning by the evolutionary theory"

Ernst Mayer, 1970

References

Adler M., Lazarus R.A., Dennis M.S. and Wagner G. 1991 Solution structure of kistrin, a potent platelet aggregation inhibitor and GP IIb-IIIa antagonist. *Science* **253**, 445-448.

Akerstrom B., Logdberg L., Berggard T., Osmark P. and Lindqvist A. 2000 Alpha (1)-Microglobulin: a yellow-brown lipocalin. *Biochim. Biophys. Acta* **1482**, 172-184.

Alger N.E. and Cabrera E.J. 1972 An increase in death rate of *Anopheles stephensi* fed on rabbits immunized with mosquito antigen. *J. Econ. Entomol.* **65**, 165-168.

Aljamali M., Bowman A.S., Dillwith J.W., Tucker J.S., Yates G.W., Essenberg R.C. and Sauer J.R. 2002 Identity and synthesis of prostaglandins in the lone star tick, *Amblyomma americanum* (L.), as assessed by radio-immunoassay and gas chromatography/mass spectrometry. *Insect Biochem. Mol. Biol.* **32**, 331-341.

Altschul S.F., Gish W., Miller W., Myers E.W. and Lipman D.J. 1990 Basic local alignment search tool. *J. Mol. Biol.* **215**, 403-410.

Anastopoulos P., Thurn M.J. and Broady K.W. 1991 Anticoagulant in the tick *Ixodes holocyclus*. *Aust. Vet. J.* **68**, 366-367.

Andrieux A., Hudry-Clergeon G., Ryckewaert J.J., Chapel A., Ginsberg M.H., Plow E.F. and Marguerie G. 1989 Amino acid sequences in fibrinogen mediating its interaction with its platelet receptor, GPIIbIIIa. *J. Biol. Chem.* **264**, 9258-9265.

Antuch W, Guntert P, Billeter M, Hawthorne T, Grossenbacher H, Wuthrich K. 1994 NMR solution structure of the recombinant tick anticoagulant protein (rTAP), a factor Xa inhibitor from the tick *Ornithodoros moubata*. *FEBS Lett.* 352, 251-257.

Arvan P. and Castle D. 1998 Sorting and storage during secretory granule biogenesis: looking backward and looking forward. *Biochem. J.* **15**, 593-610.

Astigarraga A., Oleaga-Péres A., Péres-Sánchez R. and Encinas-Grandes A. 1996 A study of the vaccinal value of various extracts of concealed antigens and salivary gland extracts against *Ornithodoros erraticus* and *Ornithodoros moubata*. *Vet. Parasitol.* **60**, 133-147.

Astigarraga A., Oleaga-Perez A., Perez-Sanchez R., Baranda J.A. and Encinas-Grandes A.1997 Host immune response evasion strategies in *Ornithodoros erraticus* and *O. moubata* and their relationship to the development of an antiargasid vaccine. *Parasite Immunol.* **19**, 401-410.

Aurora R. and Rose G.D. 1998 Helix capping. *Prot. Sci.* 7, 21-38.

Balashov Y.S. 1972 Bloodsucking Ticks (Ixodideae) - vectors of disease of man and animals. *Misc. Pub. Entomol. Soc. America*. **8**, 161-376.

Balashov Y.S. 1984 Interaction between blood-sucking arthropods and their hosts, and its influence on vector potential. *Annu. Rev. Entomol.* **29**, 137-56.

Balashov Y.S. 1989 Coevolution of ixodid ticks and terrestrial vertebrates. *Parazitologia* **23**, 427-467.

Balashov Y.S. 1994 Importance of continental drift in the distribution and evolution of ixodid ticks. *Entomol. Rev.* 73, 42-50.

Banerjee D.P., Momin R.R. and Samantaray S. 1990 Immunization of cattle (*Bos indicus* X *Bos taurus*) against *Hyalomma anatolicum anatolicum* using antigens derived from tick salivary gland extracts. *Int. J. Parasitol.* **20**, 969-972.

Baranda J.A., Pérez-Sánchez R., Oleaga A., Manzano R. and Encinas-Grandes A. 2000 Purification, N-terminal sequencing and diagnostic value of the major antigens of *Ornithodoros erraticus* and *O. moubata*. *Vet. Parasitol.* **87**, 193-206.

Bednar B., Condra C., Gould R.J. and Connolly T.M. 1995 Platelet aggregation monitored in a 96 well microplate reader is useful for evaluation of platelet agonists and antagonists. *Thromb. Res.* **77**, 453-463.

Beer J.H., Springer K.T. and Coller B.S. 1992 Immobilized Arg-Gly-Asp (RGD) peptides of varying lengths as structural probes of the platelet glycoprotein IIb/IIIa receptor. *Blood* **79**, 117-128.

Bell L.J. 1980 Organ culture of *Rhipicephalus appendiculatus* with maturation of *Theileria parva* in tick salivary glands in vitro. *Acta Trop.* **37**, 319-325.

Benton M.J. 1999 Early origins of modern birds and mammals: molecules vs. morphology. *BioEssays* **21**, 1043-1051.

Berman H.M., Westbrook J., Feng Z., Gilliland G., Bhat T.N., Weissig H., Shindyalov I.N. and Bourne P.E. 2000 The Protein Data Bank. *Nucl. Acids Res.* **28**, 235-242.

Bevers E.M., Comfrius P. and Zwaal R.F.A. 1993 Mechanisms involved in platelet procoagulant response. Mechanisms of platelet activation and control. *Adv. Exp. Med. Biol.* **344**, 195-208.

Bidlingmeyer B.A., Steven, A.C. and Tarvin T.L. 1984 Rapid analysis of amino acid using pre-column derivatization. *J. Chrom.* **336**, 93-104.

Binnington K.C. and Kemp D.H. 1980 Role of tick salivary glands in feeding and disease transmission. *Adv.Parasit.* **18**, 315-339.

Birk Y. 1987 In: Hydrolytic enzymes. (Editors: A. Neuberger and K. Brocklehurst), Elsevier, Amsterdam, 257-305.

Bjellqvist B., Hughes G.J., Pasquali Ch., Paquet N., Ravier F., Sanchez J.-Ch., Frutiger S. and Hochstrasser D.F. 1993 The focusing positions of polypeptides in immobilized pH gradients can be predicted from their amino acid sequences. *Electrophoresis* **14**, 1023-1031.

Black W.C. 4th, Klompen J.S. and Keirans J.E. 1997 Phylogenetic relationships among tick subfamilies (Ixodida: Ixodidae: Argasidae) based on the 18S nuclear rDNA gene. *Mol. Phylogenet. Evol.* **7**, 129-144.

Black W.C. and Piesman J. 1994 Phylogeny of hard- and soft-tick taxa (Acari: Ixodida) based on mitochondrial 16S rDNA sequences. *Proc. Natl. Acad. Sci. USA* **91**, 10034-1038.

Blazquez M. and Shennan K.I. 2000 Basic mechanisms of secretion: sorting into the regulated secretory pathway. *Biochem. Cell Biol.* **78**, 181-191.

Bloom A.L. and Thomas D.P. 1987 Thrombosis and Haemostasis. 2ed. Churchill Livingstone, Edinburgh London Melbourne and New York, 1-78, 90-101.

Bode W. and Huber R. 1992 Natural protein proteinase inhibitors and their interaction with proteinases. *Eur. J. Biochem.* **204**, 433-451.

Born G.V.R. and Cross M.J. 1963 The aggregation of blood platelets. *J. Physiol.* **168**, 178-195.

Bost F., Diarra-Mehrpour M. and Martin J.P. 1998 Inter-alpha-trypsin inhibitor proteoglycan family--a group of proteins binding and stabilizing the extracellular matrix. *Eur. J. Biochem.* **252**, 339-346.

Bowman A.S., Sauer J.R., Zhu K. and Dillwith J.W. 1995 Biosynthesis of salivary prostaglandins in the lone star tick, *Amblyomma americanum*. *Insect Biochem. Mol. Biol.* **25**, 735-741.

Bowman A.S., Coons L.B., Needham G.R. and Sauer J.R. 1997 Tick saliva: recent advances and implications for vector competence. *Med. Vet. Entomol.* **11**, 277-285.

Boyle J.S. and Lew A.M. 1995 An inexpensive alternative to glassmilk for DNA purification. *Trends Gen.* **11**, 1-8.

Bradford M. 1976 A rapid and sensitive method for the quantitation of microgram quantities of protein utilizing the principle of protein dye-binding. *Anal. Biochem.* **72**, 248-254.

Brandt W.F., Alk H., Chauhan M. and von Holt C. 1984 A simple modification converts the spinning cup protein sequencer into a vapour-phase sequencer. *FEBS Lett.* **174**, 228-232.

Burger D.B., Crause J.C., Spickett A.M. and Neitz A.W.H. 1991 A comparative study of proteins present in sweating-sickness-inducing and non-inducing strains of *Hyalomma truncatum* ticks. *Exp. Appl. Acarol.* **13**, 59-63.

Burgering M.J., Orbons L.P., van der Doelen A., Mulders J., Theunissen H.J., Grootenhuis P.D., Bode W., Huber R. and Stubbs M.T. 1997 The second Kunitz domain of human tissue factor pathway inhibitor: cloning, structure determination and interaction with factor Xa. *J. Mol. Biol.* **269**, 395-407.

Calvete J.J. 1994 Clues for understanding the structure and function of a prototypic human integrin: the platelet glycoprotein IIb/IIIa complex. *Thromb. Haemost.* **72**, 1-15.

Calvete J.J. 1995 On the structure and function of platelet integrin $\alpha_{IIb}\beta_3$, the fibrinogen receptor. *Proc. Soc. Exp. Biol. Med.* **208**, 346-360.

Chakrabartty A., Schellman J.A. and Baldwin R.L. 1991 Large differences in the helix propensities of alanine and glycine. *Nature* **351**, 586-588.

Champagne D.E., Nussenzvieg R.H. and Ribeiro J.M.C. 1995 Purification, partial characterization and cloning of nitric oxide-carrying heme proteins (nitrophorins) from salivary glands of the blood-sucking insect *Rhodnius prolixus*. *J. Biol. Chem.* **270**, 8691-8695.

Chang B.S. and Donoghue M.J. 2000 Recreating ancestral proteins. *Trends. Ecol. Evol.* **15**, 109-114.

Chase T. and Shaw E. 1967 p-Nitrophenyl-p'-guanodinobenzoate HCl: A new active site titrant for trypsin. *Biochem. Biophys. Res. Comm.* **29**, 508-514.

Chen C.S., Papayannopoulos I.A., Timmons S., Chou S.H. and Thiagarajan P. 1991 A modified Arg-Asp-Val (RDV) peptide derived during the synthesis of Arg-Glu-Asp-Val (REDV), a tetrapeptide derived from an alternatively spliced site in fibronectin, inhibits thebinding of fibrinogen, fibronectin, von Willebrand factor and vitronectin to activated platelets. *Biochim Biophys Acta.* **1075**, 237-247.

Chidgey M.A.J. 1993 Protein targeting to dense-core secretory granules. *BioEssays* **15**, 317-321.

Chothia C. and Lesk A.M. 1986 The relation between the divergence of sequence and structure in proteins. *EMBO J.* **5**, 823-826.

Chothia C. 1992 One thousand families for the molecular biologist. *Nature* **357**, 543-544.

Clark E.A., Shattil S.J., Ginsberg M.H., Bolen J. and Brugge J.S. 1994 Regulation of the protein tyrosine kinase pp72syk by platelet agonists and the integrin alpha IIb beta 3. *J. Biol. Chem.* **269**, 28859-28864.

Clemetson K.J. 1998 Introduction: integrins, dynamic cell receptors. *Cell. Mol. Life Sci.* **54**, 499-501.

Clermont Y., Rambourg A. and Hermo L. 1995 Trans-Golgi network (TGN) of different cell types: three-dimensional structural characteristics and variability. *Anat. Rec.* **242**, 289-301.

Colatsky, T.J., Spinelli, W. and Moubarak I.F. 1994 Block of myocardial potassium channels by antiarrythmic drugs: Dependence on Channel Gating. In: Ion channels in the cardiovascular system. Function and disfunction. (Ed. Spooner P.M., Brown A.M., Catterall W.A., Kaczorowski G.J. and Strauss H.C.) Futura Publishing Company, Inc, Armonk, New York, 415-424.

Colomer V., Kicska G.A. and Rindler M.J. 1996 Secretory granule content proteins and the luminal domains of granule membrane proteins aggregate in vitro at mildly acidic pH. *J. Biol. Chem.* **271**, 48-55.

Cooper B.J. and Spence I. 1976 Temperature-dependent inhibition of evoked acetylcholine release in tick paralysis. *Nature* **263**, 693-695.

Courtoy R. and Simar L.J. 1974 Importance of controls for the demonstration of carbohydrates in electron microscopy with the silver methanamine or the thiocarbohydrazide-silver proteinate methods. *J. Microsc.* **100**, 199-211.

Crampton A., McKay I. and Barker S.C. 1996 Phylogeny of ticks (Ixodida) inferred from nuclear ribosomal DNA. *Int. J. Parasitol.* **26**, 511-517.

Crause J.C., van Wyngaardt S., Gothe R. and Neitz A.W.H. 1994 A shared epitope found in the major paralysis inducing tick species of Africa. *Exp. Appl. Acarol.* **18**, 51-59.

Crause J.C., Verschoor J.A., Coetzee J., Hoppe H.C., Taljaard J.N., Gothe R. and Neitz A.W. 1993 The localization of a paralysis toxin in granules and nuclei of prefed female *Rhipicephalus evertsi evertsi* tick salivary gland cells. *Exp. Appl. Acarol.* **17**, 357-363.

Creighton T.E. 1978 Experimental studies of protein folding and unfolding. *Prog. Biophys. Mol. Biol.* **33**, 231-297.

Creighton T.E. 1992 Proteins. Structures and Molecular Properties. Second Edition. W.H. Freeman and Company, New York.

Dam-Mieras M.C.E. and Muller A.D. 1986 Blood coagulation as part of the haemostatic system. Blood Coagulation, *New Comp. Biochem.* **13**, 1-14.

de Castro J.J. and Newson R.M. 1993 Host resistance in cattle tick control. *Parasitol. Today* **9**, 13-17.

de Vos S., Zeinstra L., Taoufik O., Willadsen P. and Jongejan F. 2001 Evidence for the utility of the Bm86 antigen from *Boophilus microplus* in vaccination against other tick species. *Exp. Appl. Acarol.* **25**, 245-261.

Delfin J., Martinez I., Antuch W., Morera V., Gonzales Y., Rodriguez R., Marquez M., Sarovan A., Larionova N., Diaz J., Padron G. and Chavez M. 1996 Purification, characterization and immobilization of proteinase inhibitors from Stichodactyla helianthus. *Toxicon.* **34**, 1367-1376.

Dickinson R.G., O'Hagan J.E., Schotz M., Binnington K.C. and Hegarty M.P. 1976 Prostaglandin in the saliva of the cattle tick *Boophilus microplus*. *Aust. J. Exp. Biol. Med. Sci.* **54**, 475-486.

Dobson S.J. and Barker S.C. 1999 Phylogeny of the hard ticks (Ixodidae) inferred from 18S rRNA indicates that the genus *Aponomma* is paraphyletic. *Mol. Phylogenet. Evol.* **11**, 288-295.

Dobzhansky T. 1973 Nothing in biology makes sense except in the light of evolution. *Amer. Biol. Teacher* 35, 125-129.

Doolittle R.F. and Feng D.F. 1987 Reconstructing the evolution of vertebrate blood coagulation from a consideration of the amino acid sequences of clotting proteins. *Cold Spring Harbor Symp. Quant. Biol.* **LII**, 869-874.

D'Souza S.E., Haas T.A., Piotrowicz R.S., Byers-Ward V., McGrath D.E., Soule H.R., Cierniewski C., Plow E.F. and Smith J.W. 1994 Ligand and cation binding are dual functions of a discrete segment of the integrin beta 3 subunit: cation displacement is involved in ligand binding. *Cell* **79**, 659-667.

Dufton M.J. 1985 Proteinase inhibitors and dendrotoxins. Sequence classification, structural prediction and structure/activity. *Eur. J. Biochem.* **153**, 647-654.

Dunwiddie C.T., Neeper M.P., Nutt E.M., Waxman L., Smith D.E., Hofmann K.J., Lumma P.K., Garsky V.M. and Vlasuk G.P. 1992 Site-directed analysis of the functional domains in the factor Xa inhibitor tick anticoagulant peptide: identification of two distinct regions that constitute the enzyme recognition sites. *Biochemistry* **31**, 12126-12131.

Easteal S. 1999 Moecular evidence for the early divergence of placental mammals. *BioEssays* **12**, 1052-1058.

Echardt L., Haverkamp W. Borggrefe M. and Breithardt G. 1998 Experimental models of torsade de pointes. *Cardiovasc. Res.* **39**, 178-193.

El Shoura S.M. 1985 Ultrastructure of salivary glands of *Ornithodoros* (*Ornithodoros*) *moubata* (Ixodoidea: Argasidae). *J. Morph.* **186**, 45-52.

Ellis R.J. 2001a Macromolecular crowding: an important but neglected aspect of the intracellular environment. *Curr. Opin. Struct. Biol.* 11, 114-119.

Ellis R.J. 2001b Macromolecular crowding: obvious but underappreciated. *Trends Biochem. Sci.* 26, 597-604.

Emmons P. and McLennan H. 1980 Some observations on tick paralysis in marmots. *J. Exp. Biol.* 37, 355-362.

Escoubas P., Diochot S. and Corzo G. 2000 Structure and pharmacology of spider venom neurotoxins. *Biochimie* **82**, 893-907.

Esmon C.T. 1995 Cell mediated events that control blood coagulation and vascular injury. *Annu. Rev. Cell Biol.* 9, 1-26.

Evans G.O. 1992 Principles of Acarology. CAB International, Cambridge.

Fahey R.C, Hunt J.S. and Windham G.C. 1977 On the cysteine and cystine content of proteins. Differences between intracellular and extracellular proteins. *J. Mol. Evol.* **10**, 155-160.

Farrell R.E. Jr. 1993 In: "RNA methodologies. A laboratory guide for isolation and characterization". Academic Press, Harcourt Brace Jovanovich (Pub), San Diego, New York, Boston, London, Sydney, Tokyo, Toronto, 113-125.

Fawcett D.W., Binnington K. and Voigt W.P. 1986 The cell biology of the Ixodid tick salivary gland. In: Sauer J.R. and Hair J.A. (Eds) Morphology, Physiology and Behavioral Biology of Ticks, Ellis Horwood, Chichester, pp, 22-45.

Fawcett D.W., Doxsey S.J. and Büscher G. 1981 Salivary gland of the tick vector (*Rhipicephalus appendiculatus*) of East Coast fever. I. Ultrastructure of the type III acinus. *Tiss. Cell* **13**, 209-230.

Feldsman-Muhsam B. 1986 Observations on the mating behaviour of ticks. In: Sauer J.R. and Hair J.A. (Eds) Morphology, Physiology and Behavioral Biology of Ticks, Ellis Horwood, Chichester, pp, 217-232.

Felsenstein J. 1989 PHYLIP – Phylogeny inference package, Version 3.2 *Cladistics* **5**, 164-166.

Fersht A. 1999 Structure and mechanism in protein science. A guide to enzyme catalysis and protein folding. W.H. Freeman and Company, New York.

Filippova N.A. 1977 Ixodid ticks of the subfamily Ixodinae. *Leningrad: Izd. Nauka*, 393.

Fitch W.M. 2000 Homology, a personal view on some of the problems. *Trends Gen.* **16**, 227-231.

Flower D.R. 1996 The lipocalin protein family: structure and function. *Biochem. J.* **318**, 1-14.

Flower D.R. 2000 Beyond the superfamily: the lipocalins as receptors. *Biochim. Biophys. Acta* **1482**, 327-336.

Flower D.R., North C.T. and Sansom C.E. 2000 The lipocalin protein family: structural and sequence overview. *Biochim. Biophys. Acta* **1482**, 9-24.

Francischetti I.M.B., Ribeiro J.M.C., Champagne D. and Andersen J. 2000 Purification, cloning, expression and mechanism of action of a novel platelet aggregation inhibitor from the salivary glands of the blood-sucking bug, *Rhodnius prolixus*. *J. Biol. Chem.* 275, 12639-12650.

Fuentes-Prior P., Noeske-Jungblut C., Donner P., Schleuning W., Huber R. and Bode W. 1997 Structure of the thrombin complex with triabin, a lipocalin-like exosite-binding inhibitor derived from a triatomine bug. *Proc. Natl. Acad. Sci. USA* **94**, 11845-11850.

Gan Z.R., Gould R.J., Jacobs J.W., Friedman P.A. and Polokoff M.A. 1988. Echistatin. A potent platelet aggregation inhibitor from the venom of the viper, *Echis carinatus*. *J. Biol. Chem.* **263**, 19827-19832.

Ganfornina M.D., Gutierrez G., Bastiani M. and Sanchez D. 2000 A phylogenetic analysis of the lipocalin protein family. *Mol. Biol. Evol.* **17**, 114-126.

Gao X.D., Kaigorodov V. and Jigami Y. 1999 YND1, a homologue of GDA1, encodes membrane-bound apyrase required for Golgi N- and O-glycosylation in *Saccharomyces cerevisiae*. *J. Biol Chem.* **274**, 21450-21456.

Gaspar A.R., Crause J.C. and Neitz A.W. 1995 Identification of anticoagulant activities in the salivary glands of the soft tick, *Ornithodoros savignyi*. *Exp. Appl. Acarol.* **19**, 117-127.

Gaspar A.R.M.D., Joubert A.M., Crause J.C. and Neitz A.W.H. 1996 Isolation and characterization of an anticoagulant from the salivary glands of the tick, *Ornithodoros savignyi* (Acari: Argasidae). *Exp. Appl. Acarol.* **20**, 583-598.

Ghadially F.N. 1988 Ultrastructural pathology of the cell and matrix. A text and atlas of physiological and pathological alterations in the fine structure of cellular and extracellular components. Third edition. Vol. I. Butterworths, London, Boston, Singapore, Sydney, Toronto, Wellington, 354.

Gierasch L.M. 1989 Signal sequences. *Biochem.* **28**, 923-930.

Glick B.S. 2000 Organization of the Golgi apparatus. *Curr. Opin. Cell Biol.* **12**, 450-456.

Glombik M.M. and Gerdes H.H. 2000 Signal-mediated sorting of neuropeptides and prohormones: secretory granule biogenesis revisited. *Biochimie* **82**, 315-326.

Gogarten J.P. and Olendzenski L. 1999 Orthologs, paralogs and genome comparisons. *Curr. Opin. Gen. Dev.* **9**, 630-636.

Goldberger A.L. and Goldberger E. 1981 Clinical electrocardiography. (2 ed). The C.V. Mosby Company (St. Louis, Toronto, London).

Goldenberg D.P. and Creighton T.E. 1984 Gel electrophoresis in studies of protein conformation and folding. *Anal. Biochem.* **138**, 1-18.

Gordon J.R. and Allen J.R. 1991 Factor V and VII anticoagulant activities in the salivary glands of feeding *Dermacentor andersoni* ticks. *J. Parasitol.* **77**, 167-170.

Gothe R. 1983 Tick paralyses: Reasons for appearing during ixodid and argasid feeding. In Current topics in vector research, Vol. 2, K.F. Harris (ed.). Praeger Publishers, New York, pp. 199-223.

Gothe R. 1999 Zecken Toxikosen, Hieronyms, Munich.

Gothe R. and Kunze K. 1971 Stimulus conduction of efferent and afferent peripheral nerve fibers in fowl tick paralysis caused by *Argas (Persicargas) persicus* larvae. *Z. Tropenmed. Parasitol.* **22**, 292-296.

Gothe R. and Kunze K. 1982 Action potentials and conduction velocities of the tibial nerve in sheep paralysis caused by *Rhipicephalus evertsi evertsi*. *Zentralbl. Veterinarmed.B* 29, 186-192.

Gothe R. and Lämmler M. 1982 Sensitivity of laboratory animals to *Rhipicephalus evertsi evertsi* paralysis. *Zentralbl. Veterinarmed. B* 29, 249-252.

Gothe R. and Neitz A.W.H. 1991 Tick paralysis : pathogenises and etiology. *Adv. Dis. Vect. Res.* **8**, 177-204.

Gothe R., Hager H., Jehn E., Kunze K. and Thoenes W. 1971 Pathological-anatomical studies of peripheral nerves in fowl tick paralysis caused by *Argas (Persicargas) persicus* larvae. *Z. Tropenmed. Parasitol.* **22**, 285-291.

Gould R.J., Polokoff M.A., Friedman P.A., Huang T.F., Holt J.C., Cook J.J. and Niewiarowski S. 1990 Disintegrins: a family of integrin inhibitory proteins from viper venoms. *Proc. Soc. Exp. Biol. Med.* **195**, 168-171.

Grauer D. and Li W-H. 2000 Fundamentals of molecular evolution. 2ed. Sinauer Associates, Inc., Sunderland, Massachusetts.

Gregson J.D. 1943 The enigma of tick paralysis. *Proc. Entomol. Soc. B.C.* **40**, 19-23.

Gregson JD 1973 Tick paralysis: the appraisal of natural and experimental data. *Can. Dept. Agric. Monogr.* No. 9.

Grundy W.N. and Bailey T.L. 1999 Family pairwise search with embedded motif models. *Bioinformatics* **15**, 463-470.

Grütter M.G., Priestle J.P., Rahuel J., Grossenbacher H., Bode W., Hofsteenge J. and Stone S.R. 1990 Crystal structure of the thrombin-hirudin complex: a novel mode of serine protease inhibition. *EMBO J.* **9**, 2361-2365.

Guex N. and Peitsch M. C. 1997 SWISS-MODEL and the Swiss-PdbViewer: An environment for comparative protein modeling. *Electrophoresis* **18**, 2714-2723.

Guex, N., Diemand, A. and Peitsch, M.C. 1999 Protein modelling for all. *Trends Biochem. Sci.* **24**: 364-367.

Gutiérrez G., Ganfornina M.D. and Sánchez D. 2000 Evolution of the lipocalin family as inferred from a protein sequence phylogeny. *Biochim. Biophys. Acta* **1482**, 35-45.

Hanahan D., Jessee J. and Bloom F.R. 1991 Plasmid transformation of Escherichia coli and other bacteria. *Meth. Enzymol.* **204**, 63-113.

Hawiger J. 1989 Platelet secretory pathway's: an overview. *Meth. Enzymol.* **169**, 191-195.

Hawiger J. and Timmons S. 1992 Binding of fibrinogen and von Willebrands factor to platelets glycoprotein IIb-IIIa complex. *Meth. Enzymol.* 215, 228-242.

Hawiger, J. 1992. Repertoire of platelet receptors. *Meth. Enzymol.* 215, 131-136.

Hayashi T. and Nagai Y. 1980 The anomalous behavior of collagen peptides on sodium dodecyl sulfate-polyacrylamide gel electrophoresis is due to the low content of hydrophobic amino acid residues. *J. Biochem.* **87**, 803-808.

Helmy N. 2000 Seasonal abundance of *Ornithodoros (O.) savignyi* and prevalence of infection with *Borrelia* spirochetes in Egypt. *J. Egypt. Soc. Parasitol.* **30**, 607-619.

Hewick R.M., Hunkapiller M.W., Hood L.E. and Dreyer W.J. 1981 A gas-liquid solid phase peptide and protein sequenator. *J. Biol. Chem.* **256**, 7990-7997.

Hoffmann A., Walsmann P., Reisener G., Paintz M. and Markwardt F. 1991 Isolation and characterization of a thrombin inhibitor from the tick *Ixodes ricinus*. *Pharmazie* **46**, 209-212.

Hoogstraal H. 1956 African Ixodoidea. I. Ticks of the Sudan (with special reference to Equatoria Province and with preliminary reviews of the genera *Boophilus, Margaropus* and *Hyalomma*). Research Report NM 005 050.29.07, Department of the Navy, 1101.

Hoogstraal H. and Aeschlimann A. 1982 Tick host specificity. *Bull. Soc. Entomol. Suisse* **55**, 5-32.

Hoogstraal H. 1985 Argasid and Nuttalliellid ticks as parasites and vectors. *Adv. Parasitol.* **24**, 135-238.

Horn F., dos Santos P.C. and Termignoni C. 2000 *Boophilus microplus* anticoagulant protein: an antithrombin inhibitor isolated from the cattle tick saliva. *Arch. Biochem. Biophys.* 384, 68-73.

Howell C.J. 1966a Studies on karyotypes of South African Argasidae. I. *Ornithodoros savignyi* (Audouin) (1827). *Onderstepoort J. Vet. Res.* 33, 93-98.

Howell C.J. 1966b Collection of salivary gland secretion from the argasid *Ornithodoros savignyi* Audouin (1827) by the use of a pharmacological stimulant. *J. South Afr. Vet. Med. Ass.* 37, 236-239.

Howell C.J., Neitz A.W.H. and Potgieter D.J.J. 1975 Some toxic and chemical properties of the oral secretion of the sand tampan, *Ornithodoros savignyi* Audouin (1825). *Onderstepoort J. Vet. Res.* **43**, 99-102.

Huang T.F. 1998 What have snakes taught us about integrins? *Cell. Mol. Life S*

Hughes A.L. 1994 The evolution of functionally novel proteins after gene duplication. *Proc. R. Soc. Lond. B* **256**, 119-124.

Huttner W.B., Gerdes H.H. and Rosa P. 1991 The granin (chromogranin/secretogranin) family. *Trends Biochem. Sci.* **16**, 27-30.

Ibrahim M.A., Ghazy A.H., Maharem T.M. and Khalil M.I. 2001 Factor Xa (FXa) inhibitor from the nymphs of the camel tick *Hyalomma dromedarii*. *Comp. Biochem. Physiol. B Biochem. Mol. Biol.* **130**, 501-512.

Ikeo K., Takahashi K. and Gojobori T. 1992 Evolutionary origins of a Kunitz-type trypsin inhibitor domain inserted in the Amyloid β precursor protein of Alzheimer's disease. *J. Mol. Evol.* **34**, 536-543.

Instruction manual: Immobiline DryStip Kit for 2-D Electrophoresis with Immobiline DryStrip and ExcelGel SDS, Pharmacia Biotech No. 18-1038-63.

Jackson C.M. and Nemerson Y. 1980 Blood coagulation. *Annu. Rev. Biochem.* **49**, 765-811.

Jamaluddin M. 1991 New perspectives in blood platelet aggregation. *Curr. Sci.* **61**, 526-533.

Janse van Vuuren A.M., Crause J.C., Verschoor J.A., Spickett A.M. and Neitz A.W.H. 1992 The identification of a shared immunogen present in the salivary glands and gut of ixodid and argasid ticks. *Exp. Appl. Acarol.* **15**, 205-210.

Jeanmougin F., Thompson J.D., Gouy M., Higgins D.G. and Gibson TJ. 1998. Multiple sequence alignment with Clustal X. *Trends Biochem. Sci.* **23**, 403-405.

Jeffery C.J. 1999 Moonlighting proteins. *Trends Biochem Sci.* **24**, 8-11.

Johnson M.S., Sutcliffe M.J. and Blundell T.L. 1990 Molecular anatomy: phyletic relationships derived from three-dimensional structures of proteins. *J. Mol. Evol.* **30**, 43-59.

Jones S. and Thornton J.M. 1995 Protein-protein interactions: a review of protein dimmer structures. *Prog. Biophys. Molec. Biol.* **63**, 31-65.

Jordan S.P., Waxman L., Smith D.E. andVlasuk G.P. 1990 Tick anticoagulant peptide: kinetic analysis of the recombinant inhibitor with blood coagulation factor Xa. *Biochem.* **29**, 11095-11100.

Jordan S.P., Mao S.S., Lewis S.D. and Shafer J.A. 1992 Reaction pathways for inhibition of blood coagulation factor Xa by tick anticoagulant peptide. *Biochem.* **31**, 12126-12131.

Joubert A.M., Louw A.I., Joubert F., Neitz A.W.H. 1998 Cloning, nucleotide sequence and expression of the gene encoding factor Xa inhibitor from the salivary glands of the tick, *Ornithodoros savignyi*. *Exp. Appl. Acarol.* **22**, 603-619.

Joubert A.M., Crause J.C., Gaspar A.R., Clarke F.C., Spickett A.M. and Neitz AW. 1995 Isolation and characterization of an anticoagulant present in the salivary glands of the bont-legged tick, *Hyalomma truncatum*. *Exp. Appl. Acarol.* **19**, 79-92.

Kanost M.R. 1999 Serine proteinase inhibitors in arthropod immunity. *Dev. Comp. Immunol.* **23**, 291-301.

Karczewski J. and Connolly T.M. 1997 The interaction of disagregin with the platelet fibrinogen receptor, glycoprotein IIb-IIIa. *Biochem. Biophys, Res. Comm.* **241**, 744-748.

Karczewski J., Endris R. and Connolly T.M. 1994 Disagregin is a fibrinogen receptor antagonist lacking the Arg-Gly-Asp sequence from the tick, *Ornithodoros moubata*. *J. Biol. Chem.* **269**, 6702-6708.

Karczewski J., Waxman L., Endris R.G. and Connolly T.M. 1995 An inhibitor from the argasid tick *Ornithodoros moubata* of cell adhesion to collagen. *Biochem. Biophys. Res. Commun.* **208**,532-541.

Kaufman W. 1976 The influence of various factors on fluid secretion by in vitro salivary glands of ixodid ticks. *J. Exp. Biol.* **64**, 727-742.

Kaufman W. and Harris R.A. 1983 Neural pathways mediating salivary fluid secretion in the ixodid tick *Amblyomma hebraeum*. *Can. J. Zool.* 61, 1976-1980.

Kaufman W.R. 1977 The influence of adrenergic agonists and their antagonists on isolated salivary glands of ixodid ticks. *Eur. J. Pharm.* **45**, 61-68.

Kaufman W.R. 1989 Tick-Host interaction: a synthesis of current concepts. *Parasitol. Today* **5**, 47-56.

Keller P.M., Schultz L.D., Condra C., Karcsewksi J. and Connolly T.M. 1992 An inhibitor of collagen-stimulated platelet activation from the salivary glands of the *Haementeria officinalis* leech. II. Cloning of the cDNA and expression. *J. Biol. Chem.* **267**, 6899-6904.

Keller P.M., Waxman L., Arnold B.A., Schultz L.D., Condra C. and Connolly T.M. 1993 Cloning of the cDNA and expression of moubatin, an inhibitor of platelet aggregation. *J. Biol. Chem.* **268**, 5450-5456.

Kelley L.A., MacCallum R.M. and Sternberg M.J.E. 2000 Enhanced genome annotation using structural profiles in the program 3D-PSSM. *J. Mol. Biol.* **299**, 499-520.

Kelly R.B. 1985 Pathways of protein secretion in eukaryotes. *Science* **230**, 25-32.

Kemp D.H., Stone B.F. and Binnington K.C. 1982 Tick attachment and feeding: Role of the mouthparts, feeding apparatus, salivary gland secretions and host response. In: Obenchain F.D. and Galun R. (Eds), Physiology of Ticks, vol 1. Pergamon Press, Oxford, New York, Toronto, Sydney, Paris, Frankfurt, pp. 119-168.

Kimura M. 1983 The neutral theory of molecular evolution. Cambridge University Press.

Klompen H. and Grimaldi D. 2001 First Mesozoic record of a parasitiform mite: a larval argasid tick in Cretaceous amber (Acari: Ixodida: Argasidae). *Ann. Entomol. Soc. Am.* **94**, 10-15.

Klompen J.S.H., Black IV W.C., Keirans J.E. and Norris D.E. 2000 Systematics and biogeography of hard ticks, a total evidence approach. *Cladistics* **16**, 79-102.

Klompen J.S.H., Black IV W.C., Keirans J.E. and Oliver J.H. 1996 Evolution of ticks. *Annu. Rev. Entomol.* **41**, 141-161.

Kondrashov F.A., Rogozin I.B., Wolf Y.I. and Koonin E.V. 2002 Selection in the evolution of gene duplications. *Genome Biol.* 3, 0008.1-0008.9.

Kone K. 1948 Accidents mortels chez les zébus causés par des piqûres d'*Ornithodores*. *Bull. Serv. Elev. Ind. Anim. A.O.F.* 2, 25-26.

Kordiš D. and Gubenšek F. 2000 Adaptive evolution of animal toxin multigene families. *Gene* **261**, 43-52.

Krezel A.M., Wagner G., Seymour-Ulmer J. and Lazarus R.A. 1994 Structure of the RGD protein decorsin: conserved motif and distinct function in leech proteins that affect blood clotting. *Science* **264**, 1944-1947.

Kumar S., Tamura K. and Nei M. 1994 MEGA: Molecular Evolutionary Genetics Analysis software for microcomputers. *Comp. Appl. Biosci.* **10**, 189-191.

Kunitani M. and Johnson D. 1986 Model of protein conformation in the reversed-phase separation of interleukin-2 muteins. *J. Chrom.* **371**, 313-333.

Kunze K. and Gothe R. 1971 Tick paralysis in chickens caused by *Argas (Persicargas) persicus*-larvae. 3. Neurophysiological investigations. *Z. Parasitenkd.* **36**, 251-264.

Laemmli U.K. 1970 Cleavage of structural proteins during the assembly of the head of bacteriophage T4. *Nature* **227**, 680-685.

Lane R.S. and Poinar, G.O. 1986 First fossil tick (Acari: Ixodidae) in New World Amber. *Int. J. Acarol.* **12**, 75-78.

Laskowski M. Jr. and Kato I. 1980 Protein inhibitors of proteinases. *Ann. Rev. Biochem.* **49**, 593-626.

Laskowski R.A., Rullmannn J.A., MacArthur M.W., Kaptein R. and Thornton J.M. 1996 AQUA and PROCHECK-NMR: programs for checking the quality of protein structures solved by NMR. *J. Biomol. NMR* **8**, 477-486.

Law J.H., Ribeiro J.M.C. and Wells M.A. 1992 Biochemical insights derived from insect diversity. *Ann. Rev. Biochem.* **64**, 87-111.

Lehmann T. 1993 Ectoparasites : direct impact on host fitness. *Parasitol. Today*. **9**, 8-13.

Li W.H., Gu Z., Wang H. and Nekrutenko A. 2001 Evolutionary analyses of the human genome. *Nature* **409**, 847-849.

Limo MK, Voigt WP, Tumbo-Oeri AG, Njogu RM, ole-MoiYoi OK. 1991 Purification and characterization of an anticoagulant from the salivary glands of the ixodid tick *Rhipicephalus appendiculatus*. *Exp. Parasitol.* **72**, 418-429.

Lindquist E.E. 1984 Current theories on the evolution of major groups of Acari and on their relationships with other groups of Arachnida, with consequent implications for their classification. In: Acarology VI (Volume 1), D.A. Griffiths and C.E. Bowman (eds), John Wiley & Sons, New York, pp. 28-62.

Liu C.Z., Wang Y.W., Shen M.C. and Huang T.F. 1994 Analysis of human platelet glycoprotein IIb-IIIa by fluorescein isothiocyanate-conjugated disintegrins with flow cytometry. *Thromb. Haemost.* **72**, 919-925.

Longhurst C.M. and Jennings L.K. 1998 Integrin-mediated signal transduction. *Cell. Mol. Life Sci.* **54**, 514-526.

Lynch M. and Conery J.S. 2000 The evolutionary fate and consequences of duplicate genes. *Science* **290**, 1151-1155.

Madsen O., Scally M., Douady C.J., Kao D.J., DeBry R.W., Adkins R., Amrine H.M., Stanhope M.J., de Jong W.W. and Springer M.S. 2001 Parallel adaptive radiations in two major clades of placental mammals. *Nature* **409**, 610-614.

Maeda N. and Smithies O. 1986 The evolution of multigene families: human haptoglobulin genes. *Ann. Rev. Genet.* **20**, 81-108.

Mahlaku M.M., Gaspar A.R.M. and Neitz A.W.H. Characterization of the proteolytic activity present in the salivary glands of the tick, *Ornithodoros savignyi*. IUBMB/SASBMB special meeting on: The biochemical and molecular basis of disease, Cape Town, South Africa, 19-23 November 2001, P230.

Mans B.J. 1997 Biochemical properties of a platelet aggregation inhibitor of the tick, *Ornithodoros savignyi*. MSc. Dissertation.

Mans B.J., Louw A.I. Gaspar A.R.M.D. and Neitz A.W.H. 1998a Apyrase activity and platelet aggregation inhibitors in the tick *Ornithodoros savignyi*. *Exp. Appl. Acarol.* 22, 353-366.

Mans B.J., Louw A.I. Gaspar A.R.M.D. and Neitz A.W.H. 1998b Purification and characterization of apyrase from the tick, *Ornithodoros savignyi*. *Comp. Biochem. Physiol. B* **120**, 617-624.

Mans B.J., Coetzee J., Louw A.I., Gaspar A.R.M. and Neitz A.W.H. 2000 Disaggregation of aggregated platelets by apyrase from the tick, *Ornithodoros savignyi* (Acari: Argasidae). *Exp. Appl. Acarol.* **24**, 271-282.

Mans B.J., Venter J.D., Vrey P.J. Louw A.I. and Neitz A.W.H. 2001 Identification of putative proteins involved in granule biogenesis of tick salivary glands. *Electrophoresis* 22, 1739-1746.

Mans B.J., Louw A.I. and Neitz A.W.H. 2002a Amino acid sequence and structure modeling of savignin, a thrombin inhibitor from the tick, *Ornithodoros savignyi*. *Insect Biochem. Mol. Biol.* 32, 821-828.

Mans B.J., Louw A.I. and Neitz A.W.H. 2002b Savignygrin, a platelet aggregation inhibitor from the soft tick, *Ornithodoros savignyi*, presents the RGD integrin recognition motif on the Kunitz-BPTI fold. *J. Biol. Chem.* (in press).

Mans B.J., Louw A.I. and Neitz A.W.H. 2002c Evolution of Hematophagy in Ticks: Common Origins for Blood Coagulation and Platelet Aggregation Inhibitors from Soft Ticks of the Genus *Ornithodoros*. *Mol. Biol. Evol.* (in press).

Mans B.J., Steinmann C.M., Venter J.D., Louw A.I. and Neitz A.W.H. 2002 Pathogenic mechanisms of sand tampan toxicoses induced by the tick, *Ornithodoros savignyi*. *Toxicon* (in press).

Mäntyjärvi R., Rautiainen J. and Virtanen T. 2000 Lipocalins as allergens. *Biochim. Biophys. Acta* 1482, 308-317.

Maritz C. 1999 Microscale isolation and neurophathogenic properties of the paralysis toxin of the tick, *Argas (Persicargas) walkerae*. MSc. Dissertation, University of Pretoria, Pretoria, South Africa.

Maritz C., Louw A.I., Gothe R. and Neitz A.W. 2000 Detection and micro-scale isolation of a low molecular mass paralysis toxin from the tick, *Argas (Persicargas) walkerae*. *Exp. Appl. Acarol.* 24, 615-630.

Maritz C., Louw A.I., Gothe R. and Neitz A.W. 2001 Neuropathogenic properties of *Argas (Persicargas) walkerae* larval homogenates. *Comp. Biochem. Physiol A Mol. Integr. Physiol.* 128, 233-239.

Markwardt F. 1994 Coagulation inhibitors from blood-sucking animals. A new line of developing antithrombotic drugs. *Pharmazie* 49, 313-316.

Masina S. and Broady K.W. 1999 Tick paralysis: development of a vaccine. *Int. J. Parasitol.* 29, 535-541.

Mason P.J., Jones M.B., Elkington J.A. and Williams J.G. 1985 Polyad[illegible] l globin mRNA at a downstream minor site in the absence of the major site and utilization of an AAUACA polyadenylation signal. *EMBO J.* 4, 205-211.

Matthews B.W., Remington S.J., Grutter M.G. and Anderson W.F. 1981 Relation between hen egg white lysozyme and bacteriophage T4 lysozyme: evolutionary implications. *J. Mol. Biol.* 147, 545-558.

Mayer E. 1970 Populations, Species, and Evolution, Cambridge, Harvard University Press.

McDowell R.S., Dennis M.S., Louie A., Shuster M., Mulkerrin M.G. and Lazarus R.A. 1992 Mambin, a potent glycoprotein IIb-IIIa antagonist and platelet aggregation inhibitor structurally related to short neurotoxins. *Biochem.* 31, 4766-4772.

McGregor J.L., Brochier J., Wild F., Follea G., Trzeciak M.C., James E., Dechavanne M., McGregor L. and Clemetson K.J. 1983 Monoclonal antibodies against platelet membrane glycoproteins. Characterization and effect on platelet function. *Eur. J. Biochem.* 131, 427-436.

McLaghlan A.D. 1982 Rapid comparison of protein structures. *Acta Crys. A* 38, 871-873.

McSwain J.L., Essenberg R.C. and Sauer J.R. 1992 Oral secretion elicited by effectors of signal transduction pathways in the salivary glands of *Amblyomma americanum* (Acari: Ixodidae). *J. Med. Entomol.* 29, 41-48.

Ménez A. 1998 Functional architectures of animal toxins: a clue to drug design? *Toxicon* 36, 1557-7152.

Minagawa S., Ishida M., Shimakura K., Nagashima Y. and Shiomi K. 1997 Isolation and amino acid sequences of two Kunitz-type protease inhibitors from the sea anemone Anthopleura aff. xanthogrammica. *Comp. Biochem. Physiol. B* 118, 381-386.

Minton A.P. 1997 Influence of excluded volume upon macromolecular structure and associations in 'crowded' media. *Curr. Opin. Biotechnol.* 8, 65-69.

Minton A.P. 2000 Implications of macromolecular crowding for protein assembly. *Curr. Opin. Struct. Biol.* 10, 34-39.

Minton A.P. 2001 The influence of macromolecular crowding and macromolecular confinement on biochemical reactions in physiological media. *J. Biol. Chem.* 276, 10577-10580.

Montford W.R., Weichsel A. and Andersen J.F. 2000 Nitrophorins and related antihemostatic lipocalins from *Rhodnius prolixus* and other blood-sucking arthropods. *Biochim. Biophys. Acta* 1482, 110-118.

Moses E. and Hinz H.J. 1983 Basic pancreatic trypsin inhibitor has unusual thermodynamic stability parameters. *J. Mol. Biol.* 170, 765-776.

Munderloh U.G. and Kurtti T.J. 1995 Cellular and molecular interrelationships between ticks and prokariotic tick-borne pathogens. *Annu. Rev. Entomol.* 40, 221-243.

Murphy W.J., Eizirik E., Johnson W.E., Zhang Y.P., Ryder O.A. and O'Brien S.J. 2001 Molecular phylogenetics and the origin of placental mammals. *Nature* 409, 614-618.

Murzin A. G., Brenner S. E., Hubbard T. and Chothia C. 1995 SCOP: a structural classification of proteins database for the investigation of sequences and structures. *J. Mol. Biol.* 247, 536-540.

Murzin A.G. 1998 How far divergent evolution goes in proteins. *Curr. Opin. Struct. Biol.* 8, 380-387.

Needham G.R. and Teel P.D. 1986 Water balance by ticks between bloodmeals. In: Morphology, physiology and behavioral biology of ticks. Editors. John R. Sauer and J. Alexander Hair. Ellis Horwood Limited, Chichester, John Wiley and Sons, New York, Chichester, Brisbane, Toronto, 100-151.

Neeper M.P., Waxman L., Smith D.E., Schulman C.A., Sardana M., Ellis R.W., Schaffer L.W., Siegl P.K., Vlasuk G.P. 1990 Characterization of recombinant tick anticoagulant peptide. A highly selective inhibitor of blood coagulation factor Xa. *J. Biol. Chem.* **265**, 17746-11752.

Nei M. and Kumar S. 2000 Molecular evolution and phylogenetics. Oxford University Press Inc., New York.

Neitz A.W. and Vermeulen NM. 1987 Biochemical studies on the salivary glands and haemolymph of *Amblyomma hebraeum*. *Onderstepoort J Vet. Res.* **54**, 443-450.

Neitz A.W., Prozesky L., Bezuidenhout J.D., Putterill J.F. and Potgieter D.J.1981 An investigation into the toxic principle in eggs of the tick Amblyomma hebraeum. *Onderstepoort J. Vet. Res.* **48**, 109-117.

Neitz A.W.H. 1976 Biochemical investigation into the toxic salivary secretion of the tick *Ornithodoros savignyi*. D.Sc.(Agric)-thesis, University of Pretoria, South Africa.

Neitz A.W.H., Bezuidenhout J.D., Vermeulen N.M.J., Potgieter D.J.J. and Howell C.J. 1983 In search of the causal agents of tick toxicoses. *Toxicon* **S3**, 317-320.

Neitz A.W.H., Howell, C.J. and Potgieter, D.J.J. 1969 Purification of the toxic component in the oral secretion of the sand tampan *Ornithodoros savignyi* Audouin (1827). *J. S.A. Chem. Ind.* **22**, 142-149.

Neitz A.W. and Gothe R. 1986 Changes in the protein pattern in the salivary glands of paralysis inducing female *Rhipicephalus evertsi evertsi* during infestation. *J. Vet. Med. B* 33, 213-220.

Neitz W.O. 1959 Sweating sickness: the present state of our knowledge. *Onderstepoort J. Vet. Res.* **23**, 3-20.

Neitz W.O. 1962 Second meeting FAO/OIE expert panel on tick-borne diseases of livestock. Cairo, UAR: FAO/OIE. December, Working Paper nr. 2.

Nevill E.M. 1964 The role of carbon dioxide as stimulant and attractant to the sand tampan, *Ornithodoros savignyi* (AUDOUIN) *Onderstepoort J. Vet. Res.* **31**, 59-68.

Nicholls A., Sharp K.A. and Honig B. 1991 Protein folding and association: insights from the interfacial and thermodynamic properties of hydrocarbons. *Proteins* **11**, 281-296.

Nielsen H., Engelbrecht J., Brunak S. and von Heijne G. 1997 Identification of prokaryotic and eukaryotic signal peptides and prediction of their cleavage sites. *Prot. Eng.* **10**, 1-6.

Nienaber J., Gaspar A.R.M.D. and Neitz A.W.H. 1999 Savignin, a potent thrombin inhibitor isolated from the salivary glands of the tick, *Ornithodoros savignyi* (Acari:Argasidae). *Exp. Parasitol.* **93**, 82-91.

Nilsson T. and Warren G. 1994 Retention and retrieval in the endoplasmic reticulum and the Golgi apparatus. *Curr. Opin. Cell Biol.* **6**, 517-521.

Noeske-Jungblut C., Haendler B., Donner P., Alagon A., Possani L. and Schleuning W.D. 1995 Triabin, a highly potent exosite inhibitor of thrombin. *J. Biol. Chem.* **270**, 28629-28634.

Noeske-Jungblut C., Kratzschmar J., Haendler B., Alagon A., Possani L., Verhallen P, Donner P. and Schleuning W.D. 1994 An inhibitor of collagen-induced platelet aggregation from the saliva of *Triatoma pallidipennis*. *J. Biol. Chem.* **269**, 5050-5053.

Ogawa M., Herai Y., Koizumi N., Kusano T. and Sano H. 2001 7-Methylxanthine methyltransferase of coffee plants. Gene isolation and enzymatic properties. *J. Biol. Chem.* **276**, 8213-8218.

Ohno S. 1970 Evolution by gene duplication. New York, Springer.

Oliver J.H. 1989 Biology and systematics of ticks (Acari: Ixodida). *Annu. Rev. Ecol. Syst.* **20**, 397-430.

Opdebeeck J.P. 1994 Vaccines against blood-sucking arthropods. *Vet. Parasitol.* 54, 205-222.

Opdebeeck J.P., Wong J.Y.M., Jackson L.A. and Dobson C. 1988 Vaccines to protect Hereford cattle against the cattle tick, *Boophilus microplus*. *Immunol.* **63**, 363-367.

Orengo C.A., Jones D.T. and Thornton J.M. 1994 Protein superfamilies and domain superfolds. *Nature* **372**, 631-634.

Paesen G.C., Adams P.L., Harlos K., Nuttall P.A. and Stuart D.I. 1999 Tick histamine-binding proteins: isolation, cloning, and three-dimensional structure. *Mol. Cell.* **3**, 661-671.

Paesen G.C., Adams P.L., Nuttall P.A. and Stuart D.L. 2000 Tick histamine-binding proteins: lipocalins with a second binding cavity. *Biochim. Biophys. Acta* **1482**, 92-101.

Page R.D. and Holmes E.C. 2000 Molecular evolution. A phylogenetic approach. Blackwell Science.

Papayannopoulos I.A. and Biemann,K. 1992 Amino acid sequence of a protease inhibitor isolated from *Sarcophaga bullata* determined by mass spectrometry. *Protein Sci.* **1**, 278-288.

Parsons P.A. and Bodmer W.F. 1961 The evolution of overdominance: natural selection and heterozygote advantage. *Nature* **190**, 7-12.

Paton W.S. 1929 Insects, ticks, mites & venomous animals of medical and veterinary importance. Part 1. H.R. Grubb LTD. Croydon. Great Britain.

Patthy L. 1999 Protein evolution. Blackwell Science.

Peculis B.A. 1997 The sequence of the 5' end of the U8 small nucleolar RNA is critical for 5.8S and 28S rRNA maturation. *Mol. Cell Biol.* **17**, 3702-3713.

Peitsch M.C. 1995 Protein modeling by E-mail. *Bio/Technology* **13**, 658-660.

Peitsch M.C. 1996 ProMod and Swiss-Model: Internet-based tools for automated comparative protein modeling. *Biochem. Soc. Trans.* **24**, 274-279.

Perona J.J. and Craik C.S. 1997 Evolutionary divergence of substrate specificity within the chymotrypsin-like serine protease fold. *J. Biol. Chem.* 272, 29987-22990.

Pervaiz S. and Brew K. 1987 Homology and structure-function correlations between alpha 1-acid glycoprotein and serum retinol-binding protein and its relatives. *FASEB J.* **1**, 209-214.

Phoeling H.M. and Neuhoff V. 1981 Visualization of proteins with silver "stain": A critical analysis. *Electrophoresis* 2, 141-147.

Pitt-Rivers R. and Impiombato F.S. 1968 The binding of sodium dodecyl sulphate to various proteins. *Biochem. J.* **109**, 825-830.

Plow E.F., Cierniewski C.S., Xiao Z., Haas T.A. and Byzova T.V. 2001 AlphaIIbbeta3 and its antagonism at the new millennium. *Thromb. Haemost.* **86**, 34-40.

Plow E.F., Haas T.A., Zhang L., Loftus J. and Smith J.W. 2000 Ligand binding to integrins. *J. Biol. Chem.* **275**, 21785-21788.

Poinar G.O. 1995 First fossil soft ticks, Ornithodoros antiquus n. sp. (Acari: Argasidae) in Dominican amber with evidence of their mammalian host. *Experentia Basel* **51**, 384-387.

Prager E.M. and Wilson A.C. 1993 Information content of immunological distances. *Meth. Enzymol.* **224**, 140-152.

Pritchard L. and Dufton M.J. 1999 Evolutionary trace analysis of the Kunitz/BPTI family of proteins: functional divergence may have been based on conformational adjustment. *J. Mol. Biol.* **285**, 1589-1607.

Qian Y., Essenberg R.C., Dillwith J.W., Bowman A.S. and Sauer J.R. 1997 A specific prostaglandin E2 receptor and its role in modulating salivary secretion in the female tick, *Amblyomma americanum* (L.). *Insect Biochem. Mol. Biol.* **27**, 387-895.

Qian Y., Yuan J., Essenberg R.C., Bowman A.S., Shook A.L., Dillwith J.W. and Sauer J.R. 1998 Prostaglandin E2 in the salivary glands of the female tick, *Amblyomma americanum* (L.): calcium mobilization and exocytosis. *Insect Biochem. Mol. Biol.* **28**, 221-228.

Radovsky F.J. 1985 Evolution of mammalian mesotigmate mites. Coevolution of parasitic arthropods and mammals. Ed. Ke Chung Kim, John Wiley and Sons, Inc. 441-503.

Ralston G.B. 1990 Effects of "crowding" in protein solutions. *J. Chem Edu.* **67**, 857-860.

Rash L.D. and Hodgson W.C. 2002 Pharmacology and biochemistry of spider venoms. *Toxicon* **40**, 225-254.

Reed J., Hull W.E., von der Lieth C., Kubler D., Suhai S. and Kinzel V. 1988 Secondary structure of Arg-Gly-Asp recognition site in proteins involved in cell-surface adhesion. Evidence for the occurrence of nested b-bends in the model hexapeptide GRGDSP. *Eur. J. Biochem.* **178**, 141-154.

Ribeiro J.M.C., Makoul G., Levine J., Robinson D. and Spielman A. 1985 Antihemostatic, autoinflammatory and immunosuppressive properties of the saliva of a tick *Ixodes dammini*. *J. Exp. Med.* **161**, 332-344.

Ribeiro J. M. C. 1987 Role of saliva in blood-feeding by arthropods. *Ann. Rev. Entom.* **32**, 463-478.

Ribeiro J.M., Makoul G.T., Robinson D.R. 1988 *Ixodes dammini*: evidence for salivary prostacyclin secretion. *J. Parasitol.* **74**, 1068-1069.

Ribeiro J.M.C. 1989 Role of saliva in tick/host interactions. *Exp. Appl. Acarol.* **7**, 15-20.

Ribeiro J.M.C., Endris T.M. and Endris R. 1991 Saliva of the soft tick *Ornithodoros moubata* contains anti-platelet and apyrase activity. *Comp. Biochem. Physiol. A* **100**, 109-112.

Ribeiro J.M., Evans P.M., MacSwain J.L. and Sauer J. 1992 *Amblyomma americanum*: characterization of salivary prostaglandins E2 and F2 alpha by RP-HPLC/bioassay and gas chromatography-mass spectrometry. *Exp. Parasitol.* **74**, 112-116.

Ribeiro J.M. 1995 Blood-feeding arthropods: live syringes or invertebrate ph *Dis.* **4**, 143-152 .

Ribeiro J.M., Schneider M. and Guimaraes J.A. 1995 Purification and characterization of prolixin S (nitrophorin 2), the salivary anticoagulant of the blood-sucking bug *Rhodnius prolixus*. *Biochem. J.* **308**, 243-249.

Ribeiro J.M. and Mather T.N. 1998 *Ixodes scapularis*: salivary kininase activity is a metallo dipeptidyl carboxypeptidase. *Exp. Parasitol.* **89**, 213-221.

Riek R.F. 1957 Studies on the reactions of animals to infestation with ticks. *Aust. J.Agric. Res.* **8**, 215-223.

Roshdy M.A. 1972 The subgenus *Persicargas* (Ixodoidea, Argasidae, *Argas*). 15. Histology and histochemistry of the salivary glands of *A. (P.) persicus (Oken)*. *J. Med. Entomol.* **9**, 143-148.

Roshdy M.A. and Coons L.B. 1975 The subgenus Persicargas (Ixodoidea: Argasidae: *Argas*). 23. Fine structure of the salivary glands of unfed *A. (P.) Arboreus* Kaiser, Hoogstraal, and Kohls. *J. Parasitol.* **61**, 743-752.

Rost B. 1997 Protein structures sustain evolutionary drift. *Fold. Des.* **2**, S19-S24.

Rost B. 1999 Twilight zone of protein sequence alignments. *Prot. Eng.* **12**, 85-94

Rousselot R. 1956 Meeting report No. 1956/18. Report of the joint FAO/OIE meeting on the control of tick-borne diseases of lifestock, Rome, 83.

Rubin G.M. and other authors. 2000 Comparative genomics of the eukaryotes. *Science* **287**, 2204-2215.

Ruoslahti E. and Pierschbacher M.D. 1987 New perspectives in cell adhesion: RGD and integrins. *Science* **238**,491-497.

Russouw P.S., Farrant J., Brandt W., Maeder D. and Lindsey G.G. 1995 Isolation and characterization of a heat-soluble protein from pea (*Pisum sativum*) embryos. *Seed Sci. Res.* **5**, 137-144.

Rychlik W. and Rhoades R.E. 1989 A computer program for choosing optimal oligonucleotides for filter hybridization, sequencing and in vitro amplification of DNA. *Nucl. Acid. Res.* **17**, 8543-8551.

Rydel T.J., Ravichandran K.G., Tulinsky A., Bode W., Huber R., Roitsch C. and Fenton J.W. 2d. 1990 The structure of a complex of recombinant hirudin and human alpha-thrombin. *Science* **249**, 277-280.

Sali A. and Blundell T.L. 1993 Comparative protein modelling by satisfaction of spatial restraints. *J. Mol. Biol.* **234**, 779-815.

Sali A., Potterton L., Yuan F., van Vlijmen H. and Karplus M. 1995 Evaluation of comparative protein modeling by MODELLER. *Proteins* **23**, 318-326.

Salier J.P. 2000 Chromosomal location, exon/intron organization and evolution of lipocalin genes. *Biochim Biophys Acta*. **1482**, 25-34.

Sambrook J., Fritsch E.F. and Maniatis T. 1989 In: Molecular cloning: A laboratory manual. Cold Spring Harbour, Cold Spring Harbour Laboratory Press.

Sanchez J.C., Rouge V., Pisteur M., Ravier F., Tonella L., Moosmayer M., Wilkins M.R. and Hochstrasser D.F. 1997 Improved and simplified in-gel sample application using reswelling of dry immobilized pH gradients. *Electrophoresis* **18**, 324-327.

Sardana M., Sardana V., Rodkey J., Wood T., Ng A., Vlasuk G.P. and Waxman L. 1991 Determination of disulfide bond pairs and stability in recombinant tick anticoagulant peptide. *J. Biol. Chem.* **266**, 13560-13563.

Sasaki T. 1984 Amino acid sequence of a novel Kunitz-type chymotrypsin inhibitor from hemolymph of silkworm larvae, *Bombyx mori FEBS Lett.* **168**, 227-230.

Sasaki T. 1988 Amino-acid sequences of two basic chymotrypsin inhibitors from silkworm larval hemolymph. *Biol. Chem. Hoppe-Seyler* **369**, 1235-1241.

Saudek V., Atkinson R.A. and Pelton J.T. 1991 Three-dimensional structure of echistatin, the smallest active RGD protein. *Biochem.* **30**, 7369-7372.

Sauer J.R., Essenberg R.C. and Bowman A.S. 2000 Salivary glands in ixodid ticks: control and mechanism of secretion. *J. Insect Physiol.* **46**, 1069-1078.

Sauer J.R., Mane S.D., Schmidt S.P. and Essenberg R.C. 1986 Molecular basis for salivary gland secretion in ixodid ticks. In: Sauer J.R. and Hair J.A. (Eds) Morphology, Physiology and Behavioral Biology of Ticks, Ellis Horwood, Chichester, pp. 55-74.

Sauer J.R., McSwain J.L. Bowman A.S., and Essenberg R.C. 1995 Tick salivary gland physiology. *Ann. Rev. Entomol.* **40**, 245-267.

Scarborough R.M., Rose J.W., Hsu M.A., Phillips D.R., Fried V.A., Campbell A.M., Nannizzi L. and Charo I.F. 1991 Barbourin. A GPIIb-IIIa-specific integrin antagonist from the venom of *Sistrurus m. barbouri. J. Biol. Chem.* **266**, 9359-9362.

Scarborough R.M., Rose J.W., Naughton M.A., Phillips D.R., Nannizzi L., Arfsten A., Campbell A.M. and Charo I.F. 1993 Characterization of the integrin specificities of disintegrins isolated from american pit viper venoms. *J. Biol. Chem.* **268**, 1058-1065.

Schägger H. and von Jagow G. 1987 Tricine-Sodium-Dodecyl Sulphate-Polyacrylamide Gel Electrophoresis for the separation of proteins in the range from 1 to 100 kDa. *Anal. Biochem.* **166**, 368-379.

Schechter I. and Berger A. 1967 On the size of the active site in proteases. I. Papain. *Biochem. Biophys. Res. Commun.* **27**, 157-162.

Schweitz H., Bruhn T., Guillemare E., Moinier D., Lancelin J.M., Beress L. and Lazdunski M. 1995 Kalicludines and kaliseptine. Two different classes of sea anemone toxins for voltage sensitive K+ channels. *J. Biol. Chem.* 270, 25121-25126.

Scudder S.H. 1885 A contribution to our knowledge of Paleozoic Arachnides. *Proc. Am. Acad. Sci. Ser.* 2, 12.

Sculley M.J., Morrison J.F. and Cleland W.W. 1996. Slow-binding inhibition: the general case. *Biochim. Biophys. Acta* **1298**, 78-86.

Senn H. and Klaus W. 1993 The nuclear magnetic resonance solution structure of flavoridin, an antagonist of the platelet GP IIb-IIIa receptor. *J. Mol. Biol.* **232**, 907-25.

Seymour J.L., Henzel W.J., Nevins B., Stults J.T. and Lazarus R.A. 1990 Decorsin. A potent glycoprotein IIb-IIIa antagonist and platelet aggregation inhibitor from the leech *Macrobdella decora. J. Biol. Chem.* **265**, 10143-10147.

Shapiro S.Z., Buscher G. and Dobbelaere D.A.E. 1987 Acquired *appendiculatus* (Acari: Ixodidae): identification of an antigen eliciting resistance in rabbits. *J. Med. Entomol.* **24**, 147-154.

Shattil S.J., Gao, J. and Kashiwagi, H. 1997 Not just another pretty face: regulation of platelet function at the cytoplasmic face of integrin $\alpha_{IIb}\beta_3$. *Thromb. Haemost.* **78**, 220-225.

Shultz J.W. 1990 Evolutionary morphology and phylogeny of Arachnida. *Cladistics* **6**, 1-38.

Skerra A. 2000 Lipocalins as a scaffold. *Biochim. Biophys. Acta* **1482**, 337-350.

Sonenshine D.E. 1991 Biology of Ticks, vol. 1and 2, Oxford University Press, New York, Oxford.

Spiess E.B. 1989 Genes in populations. Second edition. John Wiley and Sons, New York, Chichester, Brisbane, Toronto, Singapore.

St Charles R., Padmanabhan K., Arni R.V., Padmanabhan K.P. and Tulinsky A. 2000 Structure of tick anticoagulant peptide at 1.6 A resolution complexed with bovine pancreatic trypsin inhibitor. *Prot. Sci.* **9**, 265-272.

Stone B.F. and Binnington K.C. 1986 The paralyzing toxin and other immunogens of the tick *I. holocyclus* and the role of the salivary glands in their biosyntheses. In: Morphology, Physiology and Behavioral Biology of Ticks (ed. Sauer, J.R. and Hair, J.A.), pp. 75-99. Chichester: Ellis Horwood.

Stone B.F., Binnington K.C., Gauci M. and Aylward J.H. 1989 Tick/host interactions for *Ixodes holocyclus*: role, effects, biosynthesis and nature of its toxic and allergenic oral secretions. *Exp. Appl. Acarol.* 7, 59-69.

Stone B.F., Doube B.F. and Binnington K.C. 1979 Toxins of the Australian paralysis tick *Ixodes holocyclus*. *Rec. Adv. Acarol.* **1**, 347-356.

Stubbs M.T. and Bode W. 1993 A player of many parts: the spotlight falls on thrombin's structure. *Thromb. Res.* **69**, 1-58.

Stubbs M.T. and Bode W. 1995 The clot thickens: clues provided by thrombin structure. *Trends Biochem. Sci.* **20**, 23-28.

Stuiver I., Ruggeri Z. and Smith J.W. 1996 Divalent cations regulate the organization of integrins alpha v beta 3 and alpha v beta 5 on the cell surface. *J. Cell. Physiol.* **168**, 521-531.

Sutcliffe M.J., Jaseja M., Hyde E.I., Lu X., Williams J.A. 1994 Three-dimensional structure of the RGD-containing neurotoxin homologue dendroaspin. *Nat. Struct. Biol.* **11**, 802-807.

Tanaka A.S., Andreotti R., Gomes A., Torquato R.J., Sampaio M.U. and Sampaio C.A. 1999 A double headed serine proteinase inhibitor-human plasma kallikrein and elastase inhibitor from *Boophilus microplus* larvae. *Immunopharm.* **45**, 171-177.

Tanaka K. and Fukudome H.1991 Three-dimensional organization of the Golgi complex observed by scanning electron microscopy. *J. Electron. Microsc. Tech.* **17**, 15-23.

Tans G. and Rosing J. 1986 Multicomponent enzyme complexes of blood coagulation. Blood Coagulation, *New Comp. Biochem.* **13**, 59-86.

Telemo E., Westrom B.R., Ekstrom G. and Karlsson B.W. 1987 Intestinal macromolecular transmission in the young rat: influence of protease inhibitors during development. *Biol. Neonate* **52**, 141-148.

Thornton J.M. 1981 Disulphide bridges in globular proteins. *J. Mol. Biol.* **151**, 261-287.

Thurn M.J., Gooley A. and Broady K.W. 1992 Identification of the neurotoxin from the paralysis tick, *Ixodes holocyclus*. In: Gopalakrishnakone P., Tan C.K., editors. Recent advances in toxicology research, 2. Singapore: Venom and Toxin Research Group, National University of Singapore, 243-256.

Todd A.E., Orengo C.A. and Thornton J.M. 1999 Evolution of protein function, from a structural perspective. *Curr. Opin. Chem. Biol.* **3**, 548-556.

Tomalski M.D. and Miller LK. 1991 Insect paralysis by baculovirus-mediated expression of a mite neurotoxin gene. *Nature* **352**, 82-75.

Tomalski M.D., Hutchinson K., Todd J. and Miller L.K. 1993 Identification and characterization of tox21A: a mite cDNA encoding a paralytic neurotoxin related to TxP-I. *Toxicon* **31**, 319-326.

Tooze S. 1998 Biogenesis of secretory granules in the trans-Golgi network of neuroendocrine and endocrine cells. *Biochim. Biophys. Acta* **1404**, 231-244.

Torquato S, Truskett TM, Debenedetti PG. 2000 Is random close packing of spheres well defined? *Phys. Rev. Lett.* **84**, 2064-2067.

Trager W. 1939 Acquired immunity to ticks. *J. Parasitol.* **25**, 57-81.

Urbé S., Tooze S.A. and Barr F.A. 1997 Formation of secretory vesicles in the biosynthetic pathway. *Biochim. Biophys. Acta* **1358**, 6-22.

Valenzuela J.G., Charlab R., Mather T.N., Ribeiro J.M. 2000 Purification, cloning, and expression of a novel salivary anticomplement protein from the tick, *Ixodes scapularis*. *J. Biol. Chem.* 275, 18717-18723.

van de Locht A., Stubbs M.T., Bode W., Friedrich T., Bollschweiler C., Hoffken W. and Huber R. 1996 The ornithodorin-thrombin crystal structure, a key to the TAP enigma? *EMBO J.* **15**, 6011-6017.

Van Regenmortel M.H.V., Joisson C. and Wetter C. 1993 Comparative immunological methods. *Meth. Enzymol.* 224, 130-139.

Van Waarde A. 1987 What is the function of protein carboxyl methylation? *Comp. Biochem. Physiol. B* 86, 423-438.

Viljoen G.J., Bezuidenhout J.D., Oberem P.T., Vermeulen N.M., Visser L., Gothe R. and Neitz A.W. 1986 Isolation of a neurotoxin from the salivary glands of female *Rhipicephalus evertsi evertsi*. *J. Parasitol.* 72, 865-874.

Viljoen G.J., Neitz A.W.H., Prozesky L., Bezuidenhout J.D. and Vermeulen N.M.J. 1985 Purification and properties of tick egg toxic proteins. *Insect Biochem.* 15, 475-482.

Viljoen G.J., Van Wyngaardt S., Gothe R., Visser L., Bezuidenhout J.D. and Neitz A.W. 1990 The detection and isolation of a paralysis toxin present in *Argas (Persicargas) walkerae*. *Onderstepoort J. Vet. Res.* 57, 163-168.

von Heijne G. 1990 The signal peptide. *J. Memb. Biol.* **115**, 195-201.

Vriend G. 1990 WHAT IF: A molecular modeling and drug design program. *J.Mol. Graph.* 8, 52-56.

Vulliet R. 1996 Improved technique for the preparation of water-in-oil emulsions containing protein antigens. *BioTechniques* **20**, 797-800.

Wallace A.C., Laskowski R.A. and Thornton J.M. 1995 LIGPLOT: a program to generate schematic diagrams of protein-ligand interactions. *Prot. Eng.* **8**, 127-134.

Walter D.E. and Proctor H.C. 1998 Feeding behaviour and phylogeny: observations on early derivative Acari. *Exp. Appl. Acarol.* 22, 39-50.

Wang X., Coon L.B., Taylor D.B., Stevens S.E. and Gartner T.K. 1996 Variabilin, a novel RGD-containing antagonist of glycoprotein IIb-IIIa and platelet aggregation inhibitor from the hard tick *Dermacentor variabilis*. *J. Biol. Chem.* **271**, 17785-17790.

Waxman L. and Connolly T.M. 1993 Isolation of an inhibitor selective for collagen-stimulated platelet aggregation from the soft tick *Ornithodoros moubata*. *J. Biol. Chem.* **268**, 5445-5449.

Waxman L., Smith D.E., Arcuri K.E. and Vlasuk G.P. 1990 Tick anticoagulant peptide (TAP) is a novel inhibitor of blood coagulation factor Xa. *Science* **248**, 593-596.

Wei A., Alexander R.S., Duke J., Ross H., Rosenfeld S.A. and Chang C.H. 1998 Unexpected binding mode of tick anticoagulant peptide complexed to bovine factor Xa. *J. Mol. Biol.* **283**, 147-154.

Weidner H. 1964 Eine Zecke, Ixodes succineus sp. n., im baltischen Bernstein. *Veroff. Uberseemus. Bremen* 3, 143-151.

Whale E. 1992 The end of the message: 3'-End processing leading to polyadenylated messenger RNA. *BioEssays* **14**, 113-118.

Wikel S.K. 1996 Host immunity to ticks. *Annu. Rev. Entomol.* **41**, 1-22.

Wilkins M.R., Williams K.L., Appel R.D. and Hochstrasser D.F. (Eds) 1997 Proteome research: new frontiers in functional genomics. Springer-Verlag, Berlin, Heidelberg, New York.

Willadsen P. 2001 The molecular revolution in the development of vaccines against ectoparasites. *Vet. Parasitol.* **101**, 353-368.

Willadsen P., Bird P., Cobon G.S. and Hungerford J. 1995 Commercialisation of a recombinant vaccine against *Boophilus microplus*. *Parasitol.* 110, S43-S50.

Wilson A.C., Carlson S.S. and White T.J. 1977 Biochemical evolution. *Annu. Rev. Biochem.* **46**, 573-639.

Xu Y., Carr P. D., Guss J. M. and Ollis D. L. 1998 The crystal structure of bikunin from the inter-alpha-inhibitor complex: a serine protease inhibitor with two Kunitz domains. *J. Mol. Biol.* **276**, 955-966.

Yuan Y.P., Eulenstein, O., Vingron, M. & Bork, P. 1998 Towards detection of orthologues in sequence databases. *Bioinformatics* **14**, 285-289

Zhang Y., Ribeiro J.M.C., Guimaraes J.A. and Walsh P.N. 1998 Nitrophorin-2: a novel mixed-type reversible specific inhibitor of the intrinsic factor-X activating complex. *Biochem.* **37**, 10681-10690.

Zhong X. and Guidotti G. 1999 A yeast Golgi E-type ATPase with an unusual membrane topology. *J. Biol. Chem.* 274, 32704-32711.

Zhu K., Bowman A.S., Brigham D.L., Essenberg R.C., Dillwith J.W. and Sauer J.R. 1997 Isolation and characterization of americanin, a specific inhibitor of thrombin, from the salivary glands of the lone star tick *Amblyomma americanum* (L.). *Exp. Parasitol.* **87**, 30-38.

Zimmerman S.B. 1993 Macromolecular crowding effects on macromolecular interactions: some implications for genome structure and function. *Biochim. Biophys. Acta.* **1216**, 175-185.

Zwaal R.F.A., Bevers E.M. and Comfrius P. 1986 Platelets and coagulation. *Blood Coagulation. New Comp. Biochem.* **13**, 141-170.